

# Geographia Technica



Technical Geography  
an International Journal for the Progress of Scientific Geography

**Volume 16, Geographia Technica No. 2/2021**

[www.technicalgeography.org](http://www.technicalgeography.org)

**Cluj University Press**

## Editorial Board

Okke **Batelaan**, Flinders University Adelaide, Australia  
Yazidhi **Bamutaze**, Makerere University, Kampala, Uganda  
Valerio **Baiocchi**, Sapienza University of Rome, Italy  
Gabriela **Biali**, "Gh. Asachi" University of Iasi, Romania  
Habib **Ben Boubaker**, University of Manouba, Tunisia  
Gino **Dardanelli**, University of Palermo, Italy  
Qingyun **Du**, Wuhan University, China  
Renata **Dulias**, University of Silesia, Poland  
Massimiliano **Fazzini**, University of Ferrara, Italy  
Edward **Jackiewicz**, California State University, Northridge CA, USA  
Shadrack **Kithiia**, University of Nairobi, Kenya  
Jaromir **Kolejka**, Masaryk University Brno, Czech Republic  
František **Križan**, Comenius University in Bratislava, Slovakia  
Muh Aris **Marfai**, Universitas Gadjah Mada, Yogyakarta, Indonesia  
Béla **Márkus**, University of West Hungary Szekesfehervar, Hungary  
Jean-Luc **Mercier**, Université de Strasbourg, France  
Igor **Patrakeyev**, Kyiv University of Construction and Architecture, Ukraine  
Cristian Valeriu **Patriche**, Romanian Academy, Iasi, Romania  
Dušan **Petrovič**, University of Ljubljana, Slovenia  
Hervé **Quénot**, Université de Rennes 2 et CNRS, France  
Sanda **Roșca**, Babes-Bolyai University of Cluj-Napoca, Romania  
José J. de **Sanjosé Blasco**, University of Extremadura, Spain  
Richard R. **Shaker**, Reyson University, Toronto, Canada  
Sarintip **Tantane**, Naresuan University, Phitsanulok, Thailand  
Gábor **Timár**, Eötvös University Budapest, Hungary  
Kinga **Temerdek-Ivan**, Babes-Bolyai University of Cluj-Napoca, Romania  
Yuri **Tuchkovenko**, Odessa State Environmental University, Ukraine  
Eugen **Ursu**, Université de Bordeaux, France  
Changshan **Wu**, University of Wisconsin-Milwaukee, USA  
Chong-yu **Xu**, University of Oslo, Norway

## Editor-in-chief

Ionel **Haidu**, University of Lorraine, France

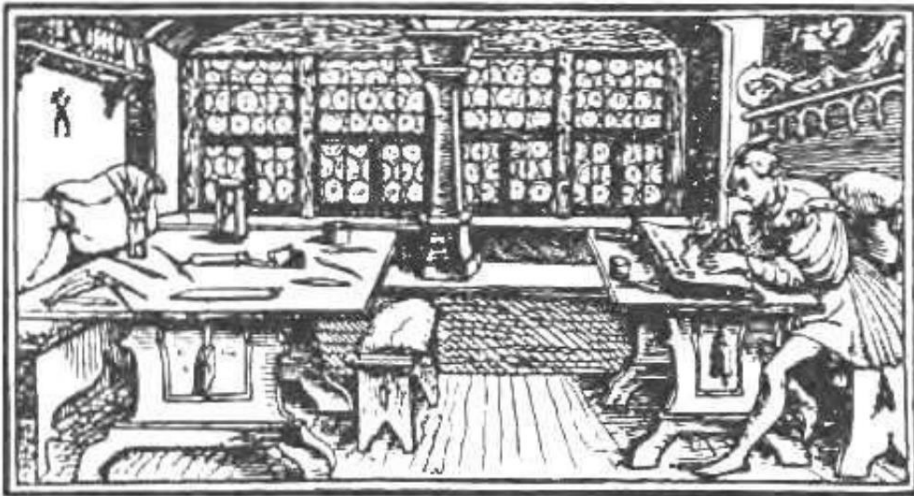
## Editorial Secretary

Marcel Mateescu, Airbus Group Toulouse, France  
George Costea, Yardi Systemes, Cluj-Napoca, Romania

## Online Publishing

Magyari-Sáska Zsolt, "Babes-Bolyai" University of Cluj-Napoca, Romania

# **Geographia Technica**



**Technical Geography**

**an International Journal for the Progress of Scientific Geography**

**2021 – No. 2**

**Cluj University Press**

**ISSN: 1842 - 5135 (Printed version)**

**ISSN: 2065 - 4421 (Online version)**

© 2021. All rights reserved. No part of this publication may be reproduced or transmitted in any form or by any means, electronic or mechanical, including photocopy, recording or any information storage and retrieval system, without permission from the editor.

Babeş-Bolyai University  
Cluj University Press  
Director: Codruța Săcelean  
Str. Hașdeu nr. 51  
400371 Cluj-Napoca, România  
Tel./fax: (+40)-264-597.401  
E-mail: [editura@editura.ubbcluj.ro](mailto:editura@editura.ubbcluj.ro)  
<http://www.editura.ubbcluj.ro/>

Asociatia Geographia Technica  
2, Prunilor Street  
400334 Cluj-Napoca, România  
Tel. +40 744 238093  
[editorial-secretary@technicalgeography.org](mailto:editorial-secretary@technicalgeography.org)  
<http://technicalgeography.org/>

Cluj University Press and Asociatia Geographia Technica  
assume no responsibility for material, manuscript, photographs or artwork.



# Contents

## *Geographia Technica*

Volume 16, Issue 2, autumn 2021

*An International Journal of Technical Geography*

ISSN 2065-4421 (Online); ISSN 1842-5135 (printed)

**ASSESSMENT OF POTENTIAL IMPACTS OF CLIMATE AND SOCIO-ECONOMIC CHANGES ON FUTURE WATER SECURITY IN THE HIMALAYAS, INDIA**

Quan V. DAU & Kittiwet KUNTIYAWICHAI (UK & Thailand) ..... 1  
DOI: 10.21163/GT\_2021.162.01

**ASSESSMENT OF THE BLACK SEA SHELF ECOSYSTEM SUSTAINABILITY WITH MATHEMATICAL SIMULATION METHOD**

Viktor KOMORIN (Ukraine) ..... 19  
DOI: 10.21163/GT\_2021.162.02

**SPECIFIC TYPES AND CATEGORIZATIONS OF BROWNFIELDS: SYNTHESIS OF INDIVIDUAL APPROACHES**

Kamila TURECKOVA (Czech Republic) ..... 29  
DOI: 10.21163/GT\_2021.162.03

**USING BIG GLOBAL DATABASE TO ANALYSE IMPACT OF WEB NEWS TO TOURIST VISITS DUE TO THE 2017 ERUPTION OF AGUNG VOLCANO, BALI, INDONESIA**

Putu Perdana Kusuma WIGUNA (Indonesia) ..... 40  
DOI: 10.21163/GT\_2021.162.04

**ROCK MASS RATING AND FEASIBILITY ASSESSMENT OF KARST CAVE GEO-ECOTOURISM IN TANJUNGSARI DISTRICT, GUNUNGKIDUL REGENCY, YOGYAKARTA SPECIAL REGION, INDONESIA**

Sari Bahagiarti KUSUMAYUDHA, Banbang PRASTISTHO, Muhammad Faizal ZAKARIA, Istiana RAHATMAWATI & Tuti SETYANINGRUM (Indonesia) ..... 53  
DOI : 10.21163/GT\_2021.162.05

**LONG-TERM WATER DEMAND ASSESSMENT USING WEAP 21: CASE OF THE GUELMA REGION, MIDDLE SEYBOUSE (NORTHEAST ALGERIA)**

Essia BOUDJEBIEUR, Lassaad GHRIEB, Ammar MAOUI, Hicham CHAFFAI & Zine Labidine CHINI (Algeria) ..... 69  
DOI : 10.21163/GT\_2021.162.06

**APPLICATION OF GIS IN THE ASSESSMENT OF FLOOD RISK IN THE REGION ZENICA - DOBOJ CANTON**

Aida KORJENIĆ, Edin HRELJA, Amina SIVAC & Amra BANDA (Bosnia and Herzegovina) ..... 80  
DOI: 10.21163/GT\_2021.162.07

**SENTINEL 2 IMAGERY AND BURN RATIOS FOR ASSESSING THE JULY 5, 2021 WILDFIRES SEVERITY IN THE REGION OF KHENCHELA (NORTHEAST ALGERIA)**

Nouar BOULGHOBRA (Algeria) ..... 95  
DOI: 10.21163/GT\_2021.162.08

**FLASH FLOOD HAZARD MAPPING USING SATELLITE IMAGES AND GIS INTEGRATION METHOD: A CASE STUDY OF LAI CHAU PROVINCE, VIETNAM**

Quoc Lap KIEU (Vietnam) ..... 105  
DOI: 10.21163/GT\_2021.162.09

**GEOGRAPHIC INFORMATION SYSTEM FOR FLOOD MANAGEMENT BY CASCADE MODEL PREDICTIVE CONTROL (MPC)**

Kajwis KLAHAN, Suwatana CHITTALADAKORN & Sitang PILAILAR (Thailand) ..... 116  
DOI : 10.21163/GT\_2021.162.10

**APPLICABILITY OF TOOLS FOR BROWNFIELD REGENERATION IN THE CZECH REPUBLIC: A REGIONAL PERSPECTIVE**

Jaroslav ŠKRABAL, Petra CHMIELOVÁ, Kamila TUREČKOVÁ & Jan NEVIMA (Czech Republic) ..... 132  
DOI: 10.21163/GT\_2021.162.11

**ARTIFICIAL NEURAL NETWORKS FOR THE CLASSIFICATION OF SHRIMP FARM FROM SATELLITE IMAGERY**

Ilada AROONSRI & Satith SANGPRADID (Thailand) ..... 149  
DOI: 10.21163/GT\_2021.162.12

**FUNCTIONAL LAND AND EMOTIONAL LANDSCAPE. DRY STONE CONSTRUCTIONS IN LA GARRIGA D'EMPORDÀ IN THE 19TH CENTURY**

Ramon RIPOLL, Jordi GOMIS, Carlos TURÓN, Gabi BARBETA & Miquel-Àngel CHAMORRO (Spain) ..... 160  
DOI: 10.21163/GT\_2021.162.13

**FLOOD RECONSTRUCTION OF 1ST JANUARY 2020 STORM IN AN URBAN HOUSING AREA OF TANGERANG SELATAN, INDONESIA**

Marelianda AL DIANTY, Frederik J. PUTUHENA, Darrien Y.S. MAH, Rosmina A. BUSTAMI & Fachrian KANAFANI (Indonesia & Malaysia) 171  
DOI: 10.21163/GT\_2021.162.14

**BUILDING AND EXPLORING NETWORK DATA MODEL FOR A SEASON LEVEL CLIMATE CHANGE STUDY FOR FIVE LARGE CITIES IN HUNGARY**

Zsolt MAGYARI-SÁSKA (Romania) ..... 183  
DOI: 10.21163/GT\_2021.162.15

**USING WEB GIS FOR MARKETING HISTORICAL DESTINATION CAIRO, EGYPT**

Reda Alkot MOHAMED, Zakaria Yehia ABD EL GAWAD & Mihai VODA (Egypt & Romania) ..... 193  
DOI: 10.21163/GT\_2021.162.16

# ASSESSMENT OF POTENTIAL IMPACTS OF CLIMATE AND SOCIO-ECONOMIC CHANGES ON FUTURE WATER SECURITY IN THE HIMALAYAS, INDIA

Quan V. DAU<sup>1</sup>, Kittiwet KUNTIYAWICHAI<sup>2\*</sup>

DOI: 10.21163/GT\_2021.162.01

## ABSTRACT:

The shifts in socio-economic development and climate conditions currently become the challenge for water resources system security in the Himalayan region. The aforesaid concern was found pertinent to the main objective of this study, which is to evaluate the combined impacts of climate and socio-economic changes on likely future water security in the Himalayan basin, India. The future climate was projected by Multi-model Ensembles under the Representative Concentration Pathway (RCP) 4.5 scenario. Land use projection under the Shared Socioeconomic Pathway (SSP) 1 scenario was performed using Markov Chain, whose transition probabilities were derived using multi-layer perceptron neural networks. The results showed that future annual precipitation and temperature at the downstream part will increase from baseline by 5% – 10% and 1.0°C – 1.55°C, respectively. The land use projections showed that irrigated areas will decrease for Punjab by 10% – 30% and Haryana by 5% – 10% due to the increase in urbanisation, whereas it will be increased in Rajasthan by 12% – 18%. Consequently, the annual irrigation water demand was found to be decreased by 10% for Punjab and 5% for Haryana, while it will be increased by 13% for Rajasthan. Eventually, the obtained findings will be beneficial for planning strategies to ensure water security in the Himalayan region, in particular the Beas-Sutlej basin.

**Key-words:** *climate change, multi-model ensembles, global climate models, land use change, reservoir management*

## 1. INTRODUCTION

The Himalayas contain one of the largest freshwater resources in the world. The region is a source of ten major river systems that include the Indus and Ganges providing water for irrigation, hydropower generation, and domestic consumption for more than 20% of the world's population (Mukherji et al., 2015). However, climate change and rapid socio-economic growth are threatening the quality and quantity of the region's water resources (Dau and Kuntiyawichai, 2020).

For India, the continued population growth is increasingly noticeable which may significantly affect the water security in the country. For instance, India is currently the world's second most populous country but is expected to surpass China within the next few decades (Samir et al., 2018). Goyal and Surampalli (2018) stated that current 1.2 billion Indian population have experienced tremendous economic growth in the last 20 years with only 4% and 9% of the world's water resources and arable land, respectively. Such a phenomenal growth of the population can only lead to higher domestic, industrial and agricultural water demands (Dau et al., 2021a).

---

<sup>1</sup> Institute for Infrastructure and Environment, Heriot-Watt University, Edinburgh EH14 4AS, UK, [infohqvan@gmail.com](mailto:infohqvan@gmail.com)

<sup>2\*</sup> Sustainable Infrastructure Research and Development Centre, Department of Civil Engineering, Faculty of Engineering, Khon Kaen University, Khon Kaen, 40002, Thailand. Corresponding author: [kkitti@kku.ac.th](mailto:kkitti@kku.ac.th)

The total cultivated land in India is approximately 183 M-ha (million hectares), which is about 55% of the total area of the country (FAO, 2015). As per the Central Water Commission, water consumption in Indian agriculture accounted for 85.3% of the total withdrawal in 2000 with industry, energy, domestic, and other sectors accounting for 1.2%, 0.3%, 6.6%, and 6.4%, respectively (Mirza and Ahmad, 2005). It is obvious that water demand for agriculture is the sector with the highest water demand, which requires most attention to help if struggling in high demand, is of utmost importance and would consider to be the main focus of this study. Every year, India receives about 4,000 BCM (billion cubic meters) from precipitation including snowfall, with only 48% of this entering the surface and groundwater bodies, while the remaining 52% is lost as evapotranspiration (Dhawan, 2017). However, due to lack of adequate infrastructure and inappropriate water management, there is only 20% out of 48% of the precipitation is actually used (Dhawan, 2017). The total annual utilizable water resources in the country are 1,123 BCM, whereof, 690 BCM is surface water and 433 BCM is groundwater (IRES, 2020). Groundwater withdrawal is estimated to be 231 BCM annually of which about 90% is used for irrigation, a much higher proportion than the global average of 40% (Siebert et al., 2010). In particular, this is a major problem in the northern region of India where groundwater level has fallen at the rate of 2 cm per year between 2002 and 2013 due to over extraction and poor recharge facility (Asoka et al., 2017).

Climate change is also the main concern for India as shown in several recent studies that average temperatures in the Himalayas have already increased by 0.74°C in the past 100 years (Li et al., 2016, Du et al., 2004). This is due to its location in tropical latitudes where relatively high temperatures occur more frequently than in other regions of the world (Manish et al., 2016). Increasing temperatures will result in glacier losses and alteration of the hydrologic balance in the basin as stated by Kulkarni and Karyakarte (2014) that a vast loss in glacier mass from  $-9 \pm 4 \text{ Gt}\cdot\text{year}^{-1}$  (1975 – 1985) to  $-20 \pm 4 \text{ Gt}\cdot\text{year}^{-1}$  (2000 – 2010). These are significant losses for the major rivers in the region for which glacier currently contributes about 70% of their runoff (Singh and Bengtsson, 2004).

Referring to the importance of the abovementioned issues, the objective of this study was to assess the possible impacts of climate and socio-economic changes on future water security in the Himalayan basin, India. To achieve its main objective, a more robust methodology for impact assessment was as follows: a statistical downscaling method called “Delta Change” was firstly applied to produce a watershed scale multi-model ensemble projections. The Markov chain modeling was also applied to monitor and predict the future land use pattern of the study area. Thereafter, both changes in climate and land use were then simulated by the WEAP water allocation model to enhance the understanding of future water security trend. For a better understanding of how the future climate will impact the surface water resources in the Himalayan basin, the Multi-model Ensembles (MME) of the Coupled Model Intercomparison Project phase 5 (CMIP5) global climate models, forced with the Representative Concentration Pathway (RCP) 4.5, and the Shared Socioeconomic Pathway (SSP) 1 scenario – were considered. The selection of RCP 4.5 was due to the reduction of fossil fuel consumption, which can minimise a large amount of the carbon dioxide emission. In addition, the feedbacks from stakeholders, i.e. scientists from 3 different projects (CHANSE, UPSCAPE, and SusHi-Wat), policy-makers, and farmers, also suggested the SSP1 scenario since India has set a target to increase its renewable energy capacity of 175 GW by mid-century (Chaturvedi et al., 2020). The MME is a promising way to reduce uncertainties in present-day simulations and to improve confidence in some aspects of future climate projections (Wang et al., 2018). The approach was used for this study because it shows the uncertainty across models in simulating the climate (Tebaldi and Knutti, 2007), which can be more reliable than using a single model (Dong et al., 2015). It is a matter of fact that the selected climate models operate at very coarse spatial scales, a technique called statistical downscaling was then used to derive climate information at finer spatial resolution from coarser spatial resolution GCM output by combining climate model projections with local/regional observations (Dau et al., 2017) (Note: this research used the statistical downscaling technique due to its efficient diagnostics to assess the GCMs reliability (Benestad and Haugen, 2007), with reasonable results comparable to dynamical downscaling (Penalba et al., 2014).

## 2. STUDY AREA

The study area is the Beas-Sutlej basin, in the Western Himalayas, India, where about 2,673 km<sup>2</sup> (12% of the basin area) is covered by permanent snowfields and glacier (Singh and Bengtsson, 2004) (**Fig. 1**). The Beas basin lies entirely in India with a total area of 12,569 km<sup>2</sup> of which 780 km<sup>2</sup> is situated in the upper part under permanent snow (Jain et al., 2007). The Sutlej basin covers an area of 56,860 km<sup>2</sup> with 22,275 km<sup>2</sup> of this lying in India. There are two main reservoirs, i.e. the Pong and the Bhakra, that serve domestic, irrigation, hydropower generation, and flood control purposes (Adeloye et al., 2019). Climatologically, the basin is mostly influenced by tropical monsoon in which four seasons can be distinguished, i.e. winter (December – February), summer (March – May), rainy (June – August), and autumn (September – November). The mean annual precipitation is estimated between 1,200 mm and 1,800 mm, whereas the average temperature ranges from -10°C to +10°C depending on the altitude varying from 100 to 7,000 meters above mean sea level (MSL). There are large-scale schemes located in the irrigated lands or the so-called “command areas” in the States of Punjab, Haryana and Rajasthan (see **Fig. 1**). According to the information from Dhawan (2017), it can be summarized that rice, wheat and sugarcane are the largest India’s crop production with the proportion of 90% of country-wide production, in which they are considered to be the most water consuming crops.

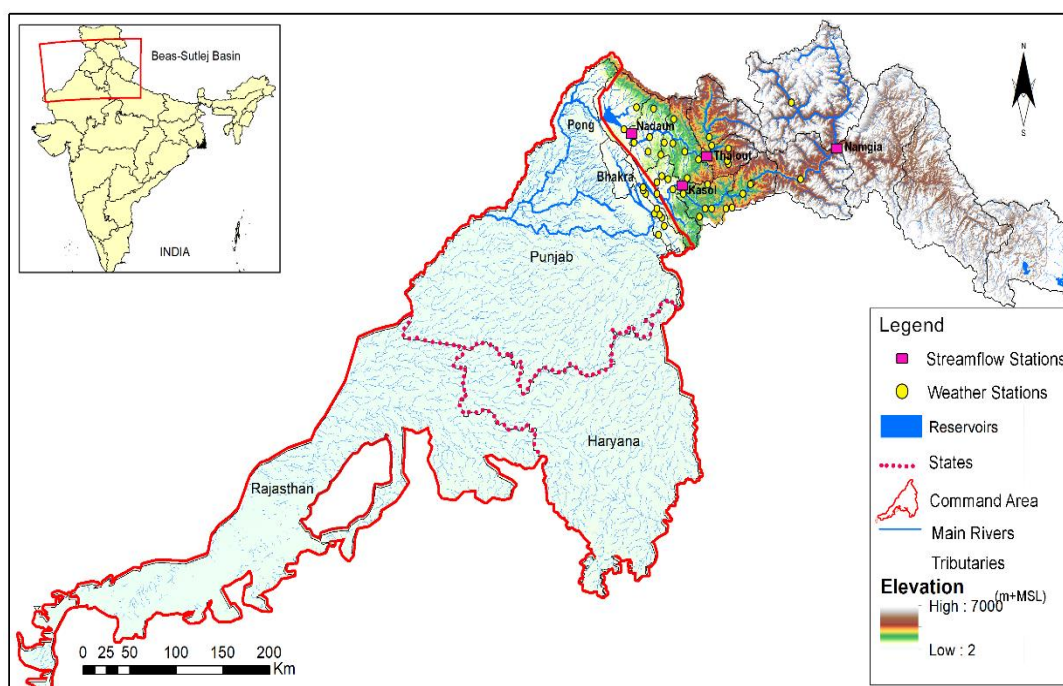


**Fig. 1** The Beas-Sutlej River Basin.

## 3. DATA AND METHODS

It is of paramount importance to provide detailed information about the potential impacts of climate and socio-economic changes in order to enhance preparedness and adaptation strategies in the Himalayan basin, India, where the information about climate projections and hydro-climatic impacts is somehow questionable. To make it clear, **Fig. 2** shows the workflow of this study, in which each component was described in the following sub-sections.

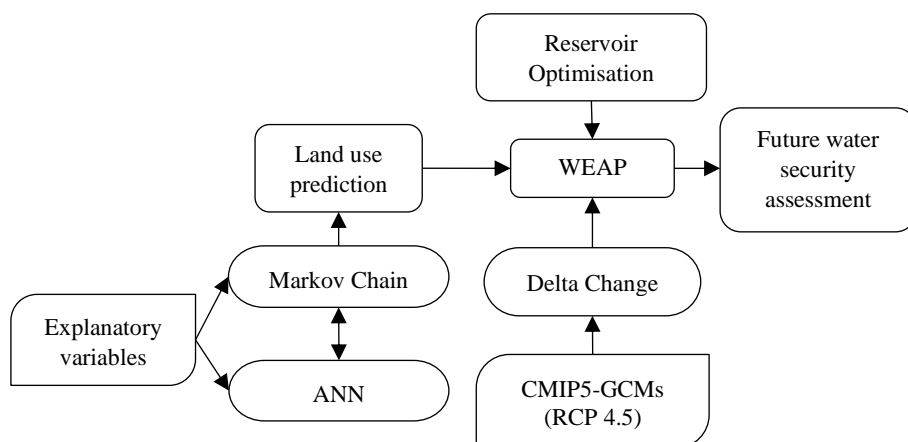


**Fig. 2** The workflow for assessing the climate and socio-economic change impacts on future water security in the Himalayan basin, India

### 3.1 Data collection

The ERA-Interim historical reanalysis data over 1990 to 2007 (baseline) used in this study were dynamically downscaled to 5 km x 5 km using the Weather Research and Forecasting (WRF) model forced with atmospheric initial and boundary conditions for selected CMIP5 GCMs (Taylor et al., 2012) as a baseline. **Table 1** summarises all the CMIP5 GCM models used in this study, including the grid resolutions which represent the distance between adjacent grid points in degrees.

**CMIP5 models and their grid resolutions**

**Table 1.**

No.	Model acronym	Atmospheric grid (°)		No.	Model acronym	Atmospheric grid (°)	
		Latitude	Longitude			Latitude	Longitude
1	ACCESS1.0	1.2500	1.8750	19	GISS-E2-H-CC	2.0000	2.5000
2	ACCESS1.3	1.2500	1.8750	20	GISS-E2-HP1	2.0000	2.5000
3	BCC-CSM1.1	2.7906	2.8125	21	GISS-E2-R-CC	2.0000	2.5000
4	BCC-CSM1.1(m)	2.7906	2.8125	22	HadGEM2-AO	1.2500	1.8750
5	BNU-ESM	2.7906	2.8125	23	HadGEM2-CC	1.2500	1.8750
6	CanESM2	2.7906	2.8125	24	HadGEM2-ES	1.2500	1.8750
7	CCSM4	0.9424	1.2500	25	INM-CM4	1.5000	2.0000
8	CESM1(BGC)	0.9424	1.2500	26	IPSL-CM5A-LR	1.8947	3.7500
9	CESM1(CAM5)	0.9424	1.2500	27	IPSL-CM5A-MR	1.2676	2.5000
10	CMCC-CM	0.7484	0.7500	28	IPSL-CM5B-LR	1.8947	3.7500
11	CMCC-CMS	3.7111	3.7500	29	MIROC-ESM	2.7906	2.8125
12	CNRM-CM5	1.4008	1.40625	30	MIROC-ESM-CHEM	2.7906	2.8125
13	CSIRO-Mk3.6.0	1.8653	1.8750	31	MIROC5	1.4008	1.4063
14	EC-EARTH	1.1215	1.1250	32	MPI-ESM-LR	1.8653	1.8750
15	FGOALS-g2	2.7906	2.8125	33	MPI-ESM-MR	1.8653	1.8750
16	GFDL-CM3	2.0000	2.5000	34	MRI-CGCM3	1.1215	1.1250
17	GFDL-ESM2G	2.0225	2.0000	35	NorESM1-M	1.8947	2.5000
18	GFDL-ESM2M	2.0225	2.5000	36	NorESM1-ME	1.8947	2.5000

The observed discharges and reservoir data, i.e. bathymetry, inflow/outflow, and hydropower capacity, were gathered from the Bhakra and Beas Management Board (BBMB) and relevant agencies. Land cover maps at 300 m resolution for the years 2000, 2005, and 2010 provided by the European Space Agency Climate Change Initiative (ESA-CCI) were utilized for explaining the variations of land use and vegetation due to social-economic changes.

Domestic water demand was estimated from historical population in 2000 obtained from the Census of India and projected population (1-km grid cells) re-downscaled by Gao (2017) under SSPs. The SSPs (O'Neill et al., 2014) under five different pathways, i.e. sustainability-SSP1, middle of the road-SSP2, regional rivalry-SSP3, inequality-SSP4, and fossil-fuelled development-SSP5, were used for describing broad socio-economic trends that could shape future society. Accordingly, projected population under SSP1 scenario was used for this study.

### 3.2 Global climate downscaling under RCP 4.5 using Delta Change approach

A widely used technique called Delta Change suggested by (Lenderink et al., 2007) was chosen to correct the biases associated with the downscaled future projection data produced by a high resolution (5 km) WRF simulation obtained from (Bannister et al., 2019). The WRF model was forced by 18 baseline years of ERA-Interim historical reanalysis climate data (1990 – 2007) (Note: more details related to WRF model can be seen in (Bannister et al., 2019). For each GCM, the future projected climate data for each time horizon, e.g. mid-century (2033 – 2050), end-century (2083 – 2100), etc., was carried out in order to obtain monthly delta changes in precipitation ( $\Delta P_m^{GCM}$ ) and temperature ( $\Delta T_m^{GCM}$ ) (Note: the selected time horizons were chosen in order to take into account the medium- and long-term effects of climate change on glacier melting, as suggested by previous studies (Nepal, 2016, Dau and Adeloye, 2021, Maurer et al., 2019). These changes were then applied to the WRF baseline (1990 – 2007) for providing the corresponding high-resolution future climate projection as shown in Eqs. (1) and (2).

$$P_{m,y}^F = P_{m,y}^{H,WRF} \times \Delta P_m^{GCM} \tag{1}$$

$$T_{m,y}^F = T_{m,y}^{H,WRF} + \Delta T_m^{GCM} \tag{2}$$

where,  $P$  and  $T$  are the downscaled precipitation and temperature in month  $m$  and year  $y$ , respectively;  $F$  and  $H$  refer to a future time slice and historical period, respectively;  $\Delta P_m^{GCM}$  and  $\Delta T_m^{GCM}$  are changes between the future and baseline periods for each CMIP5 GCM which can be calculated as follows.

$$\Delta P_m^{GCM} = \left( \frac{P_m^{F,GCM}}{P_m^{H,GCM}} \right) \tag{3}$$

$$\Delta T_m^{GCM} = \left( T_m^{F,GCM} - T_m^{H,GCM} \right) \tag{4}$$

A simple statistical test was further carried out as given in Eq. (5). Skew coefficient ( $G$ ) was then compared with the approximate 95% confidence limits for zero skew between the  $-1.96SE$  and  $+1.96SE$  interval, where  $SE$  is standard error of estimate of sample skew coefficient, approximately equal to  $\sqrt{\frac{6}{n}}$ . If the skew coefficient falls within the 95% confident limits, then the null hypothesis that the skew is zero is not rejected (symmetrical distribution); otherwise, they are asymmetrical distribution.

$$G = \frac{n \sum_{i=1}^n (y_i - \mu_y)^3}{(n-1)(n-2)\sigma_y^3} \tag{5}$$

where,  $G$  is skew coefficient;  $n$  is sample size;  $\mu_y$  and  $\sigma_y$  are mean and standard deviation of  $y$ , respectively

### 3.3. Land use change projection

The projection of land use changes was performed with the spatial model coupling Markov Chains proposed by (Marko et al., 2016). The Markov Chain model contains two main processes: the transition probability matrix ( $\tau$ ) describes the probability of land cover changes from one period to another (Eq. (6)); and a projection phase to determine the future land change patterns based on the information given in the first stage (Eq. (7)):

$$\tau = \begin{pmatrix} \tau_{11} & \cdots & \tau_{1n} \\ \vdots & \ddots & \vdots \\ \tau_{n1} & \cdots & \tau_{nn} \end{pmatrix} \quad \begin{matrix} \sum_{j=1}^n \tau_{ij}=1; & i, j \in N \\ 0 \leq \tau_{ij} \leq 1 \end{matrix} \quad (6)$$

$$\theta_{(t+1)} = \tau \times \theta_t \quad (7)$$

where,  $\tau$  is the transition probability matrix;  $\tau_{ij}$  represents the probability of the system transitioning from land use type  $i$  to  $j$ ;  $n$  is the total number of land use types; and  $\theta_t$  and  $\theta_{t+1}$  are land use maps at time  $t$ , and  $t+1$ .

The determination of transition probability matrix requires relationship between land use patterns and factors known to influence them. Explanatory variables such as topographic conditions (elevation, slope, distance to urban, rivers, roads), and human interaction (population) were used to explain potential transition changes in land use. These driving factors were initially validated to determine the associations with each of classes in land use map using the Cramer's  $V$  statistic (Cramér, 1946) in Eq. (8).

$$V = \sqrt{\frac{\chi^2/n}{\min(k-1, r-1)}} \quad (8)$$

where  $\chi$  is chi-squared;  $n$  is the total of observations; and  $k$  and  $r$  are number of column and row in land use maps.

The transition probability can be predicted using multi-layer perceptron (MLP) in neural network (Park and Lek, 2016). In the neural network architecture, explanatory variables were defined as nodes of the input layer, while land change pattern map between 2000 and 2005 was analysed to determine the observed potential transition probability that forms the nodes in the output layer. The study used 50% of the sample size for training and the remaining 50% for testing. Land cover maps for the years 2000 and 2005 were used for the training and testing and that for 2010 was used for validation. Numbers of hidden layer were determined based on the traditional trial and error approach.

The model performance was assessed using  $R^2$ . The Kappa Index of Agreements (Pontius, 2002) were also used to compare the observed "proportion correction" to the expected "proportion correction" due to chance for land use maps in 2010, in which a Kappa value greater than 0.75 is considered as very good to excellent agreement (Landis and Koch, 1977).

### 3.4 Integrated reservoir operating and management

In this study, a reservoir operation simulation program in WEAP (Water Evaluation And Planning) model, which was developed by the Stockholm Environment Institute (Sieber and Purkey, 2011) and has been widely used in many regional water allocation problems (Dau et al., 2021a, Dau et al., 2018), was applied for determining optimal water allocation for each monthly time step based on demand priorities and supply preference. The optimal rule curves were developed based on Genetic Algorithm (GA), for a multiple purpose and combined within a single objective function (Eq. (9)), covering of irrigation water supply, hydropower, and flood control. As a result, the Upper Rule Curve (URC) and Lower Rule Curve (LRC) can be specified based on 24 decision variables for the design of reservoir release policies.



$$f = \min \sum_{i=1}^2 \sum_{t=1}^T \left[ \left( \frac{D_t^i - R_t^i}{D_t^i} \right)^2 + \left( \frac{P_{max}^i - P_t^i}{P_{max}^i} \right)^2 + \left( \frac{\max Z_t^i - Z(LRC_m^i)}{Z(URC_m^i) - Z(LRC_m^i)} \right)^2 \right] \quad (9)$$

subject to the constraints:

*Water balance:*

$$S_{t+1} = S_t + Q_t - R_t - EV_t \quad (10)$$

*Hydropower generation:*

$$P_{min} \leq P_t \leq P_{max} \quad (11)$$

$$P_t = \min(\eta g \rho R_t \bar{H}_t, P_{max}) \quad (12)$$

*Flood control:*

$$Z_t(LRC_m) \leq Z(t) \leq Z_t(URC_m) \quad (13)$$

$$\max Z = \min[(a \times S_t^3) + (b \times S_t^2) + (c \times S_t) + d, Z(URC_m)] \quad (14)$$

*Irrigation water supply:*

$$\text{If } \begin{cases} WA_t \geq URC_m, & R_t = S_t + Q_t - EV_t - URC_m \text{ \& } ER_t = R_t - D_t \\ URC_m \geq WA_t > LRC_m, & R_t = D_t \text{ \& } ER_t = 0 \\ \text{else,} & R_t = 0 \end{cases} \quad (15)$$

where  $D_t^i$  and  $R_t^i$  are respectively allocated demand and actual release during time  $t$  of the reservoir  $i$ ;  $P_t$  is hydropower generation at period  $t$ ;  $P_{min}$  and  $P_{max}$  are minimum and maximum plant power capacities;  $\max Z_t$  is maximum reservoir water level at period  $t$ ;  $LRC_m$  and  $URC_m$  are upper and lower limits of rule curves in month  $m$ ;  $S_t$  and  $S_{t+1}$  are respectively initial and final storage;  $Q_t$  is inflow;  $\eta$  is overall efficiency factor;  $g$  is acceleration of gravity;  $\rho$  is water density;  $\bar{H}_t$  is hydraulic head of dam;  $EV_t$  is net evaporation in volume unit;  $WA_t$  water availability at the beginning of time ( $WA_t = S_t + Q_t$ );  $ER_t$  is excess release;  $a, b, c, d$  are the constant coefficients obtained from the storage – elevation curve for each reservoir given at the Pong (Eq. (16)) and Bhakra reservoirs (Eq. (17)):

$$Z_{t,Pong} = (3^{-10} \times S_t^3) + (5^{-6} \times S_t^2) + (0.031 \times S_t) + 349.14 \quad (16)$$

$$Z_{t,Bhakra} = (9^{-11} \times S_t^3) + (2^{-6} \times S_t^2) + (0.0263 \times S_t) + 393.5 \quad (17)$$

### 3.5 Simulation of water resources

For examining water allocation and demand in the study area, the WEAP model was applied. In addition, the optimised rule curves, which define the top of conservation storage zones and the top of buffer storage zones, were also considered in the WEAP to estimate water allocation in the basin.

Regarding the runoff volume calculation for the upstream mountainous area, the Rainfall-Runoff Soil Moisture (RRSM) method, which relies on empirical functions for describing evapotranspiration, surface and sub-surface runoffs, and deep percolation for a watershed unit, was used (Note: groundwater component was ignored in the simulation). This method considers two soil layers: the upper compartment that simulates surface runoff when forced with rainfall and evapotranspiration; and the lower soil layer where baseflow routing to the river and soil moisture changes are simulated (Yates et al., 2005).

In terms of mass balance of glacial systems, by considering the accumulation of glacier to be uniform, the glacier volume was then calculated by multiplying the ice depth with the sub-basin area covering by snow and ice (Sieber and Purkey, 2011). The projected glacier area was obtained from a recent study by (Prasad et al., 2019) for measuring ice and snow melt at basin scale.

For the downstream irrigated command area, the MABIA (MAitrise des Besoins d'Irrigation en Agriculture) method was employed for estimating irrigation demands (Sieber and Purkey, 2011). The MABIA determines the actual evapotranspiration ( $ET_c$ ) from the reference crop evapotranspiration ( $ET_0$ ) using "dual"  $K_c$  method (see Eq. (18)), where  $K_{cb}$  is basal crop coefficient,  $K_e$  is evaporation from the soil surface.

$$ET_c = (K_{cb} + K_e)ET_0 \quad (18)$$

## 4. RESULTS AND DISCUSSIONS

### 4.1 Probability density distribution function for climate data

Based on the skew coefficient (G), it is possible to determine the distributions of precipitation and temperature revealed by the multi-model ensemble (MME) dataset. The statistical weather parameter reveals that future monthly precipitation in the Himalayan region would dominate by symmetrical and asymmetrical distributions varying from month to month. It was found that the monthly precipitation has a symmetrical distribution for the months of Feb, Mar, Jun, Aug, Nov, and Dec, which represents a distribution with a shape similar to a normal distribution, while the months of Jan, Apr, May, Jul, Sep, and Oct with an asymmetrical appearance is more closely fitted to the log-normal distribution. In case of annual time-scale, referring to **Fig. 3**, the precipitation distribution appears as a left-leaning curve, which is positive asymmetry or the so-called right-skewed distribution, for both the mid- and end-century periods. In comparison to the precipitation, the temperature is more symmetrically distributed, and it can accurately be described by a normal distribution.

### 4.2 Climate projection for upstream of the basin

As shown in **Fig. 3**, the projected mean annual precipitation indicates a rising pattern between 15% to 20% across the GCMs, in which the highest occurrence indicated by the BNU-ESM model and lowest intensity represented by the GFDL-ESM2G model. The precipitation seems to be increased during the monsoon season, with the average rainfall of approximately 300 mm in July. In comparison to the baseline period, the average annual temperature shows the increase between 3.5°C and 5.0°C in the future across the GCMs, with the highest rise indicated by the GFDL-CM3 model projection by 7.0°C. Interestingly, the obtained finding corresponds to the recent studies conducted by (Krishnan et al., 2019, Rajbhandari et al., 2018), which concluded that the future annual temperature would reach up to 5°C in the Himalayan basin.

The increase in temperature could probably reduce glacier volume in the Himalayan upstream as it was found that the mean annual glacier volume could reduce from approximately 1,403 BCM (baseline) to be 1,197 BCM in the mid-century (reduce by -14.5%) and 876 BCM in the end-century (reduce by -37.5%). In contrast, the glacier melting would increase the runoff volume that enters the Pong and Bhakra reservoirs. As a consequence, the mean annual runoff in the Beas River would increase to 10.00 BCM in comparison to the baseline (8.77 BCM), whereas the Sutlej River would also increase to 23.00 BCM compared to its baseline (21.71 BCM) across the GCMs projection.

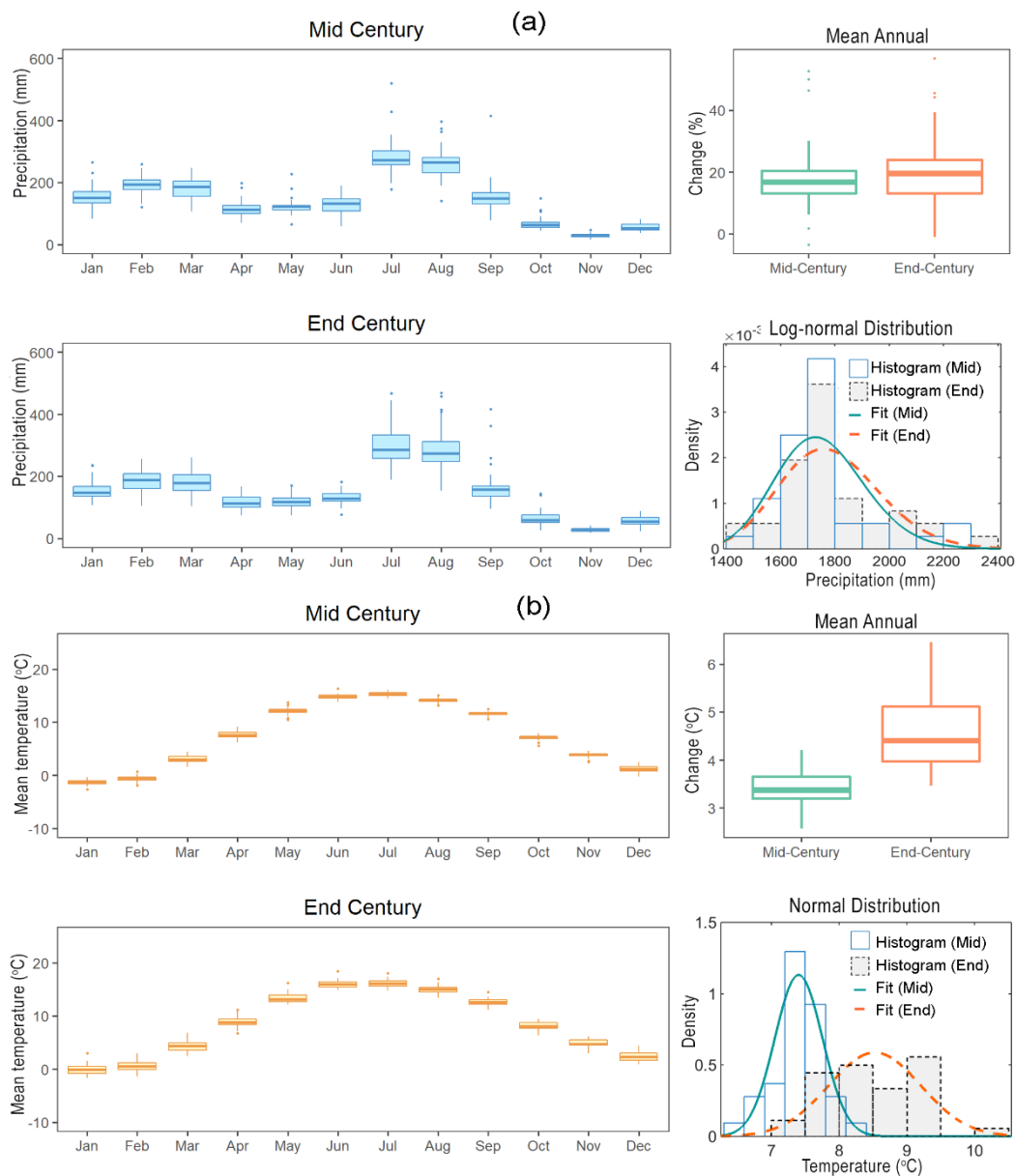


**Fig. 3** The mean monthly climate data, annual changes, and annual probability density function for (a) precipitation and (b) temperature at the upstream

### 4.3 Climate projection for downstream of the basin

The climate projections were averaged across the GCM models and presented for each state in the command area. Referring to the downscaled results, it was revealed that the downstream would experience a warmer future climate, in which the mean annual precipitation would increase between 5% and 10% in the mid- and end-centuries in comparison to the baseline, with high intensity during the monsoon season. By considering both mid- and end-centuries (**Fig. 4**), the result suggests that future monthly precipitation will increase from its baseline, i.e. in Punjab from 180 mm to 200 mm, in Haryana from 130 mm to 150 mm, and in Rajasthan from 70 mm to 80 mm.

In addition, the maximum temperature will also increase from its baseline, i.e. in Rajasthan from 23.89°C to 25.44°C, in Punjab from 22.84°C to 24.39°C, and in Haryana from 22.87°C to 24.53°C. The aforesaid finding expresses the potential severe impacts for the future water resources in Rajasthan State, which would affect the extensive agricultural plots due to lacking of rainfall and surface water availability.

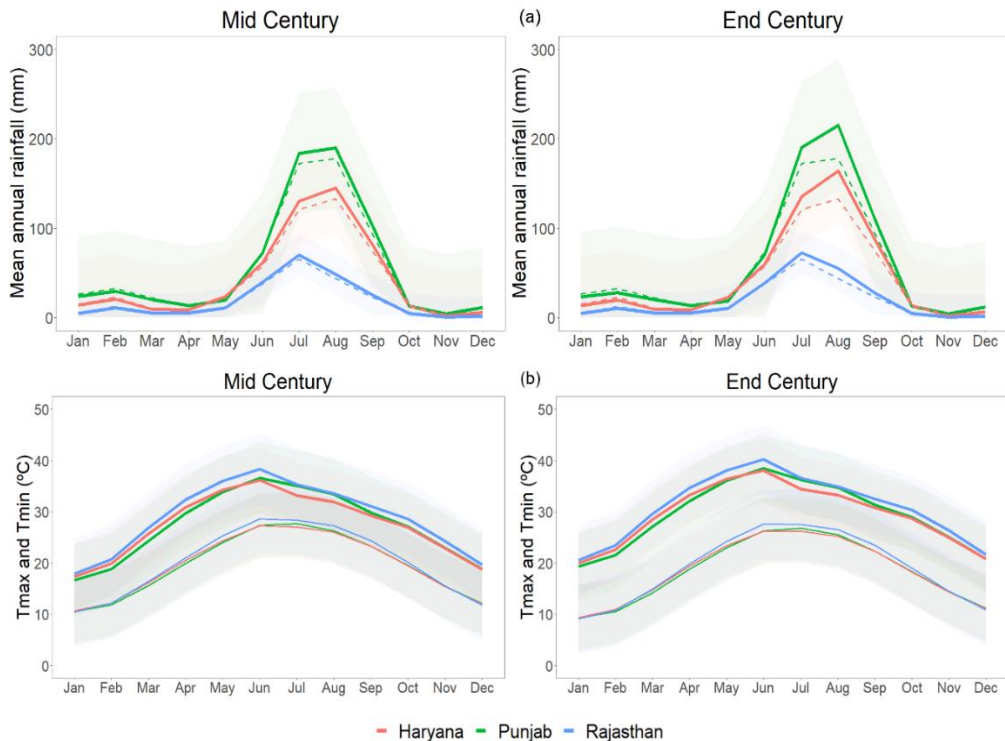


**Fig. 4** Ensemble mean of monthly (a) rainfall (dotted lines are the baseline) and (b) maximum & minimum temperature in irrigated areas

#### 4.4 Projections for socio-economic and land use changes

The projected population under SSP1 scenario for the Beas-Sutlej basin expresses a rapid growth in the mid-century between 35% and 45% but it would be decreased by the end-century between 10% and 20% compared to the baseline (year 2000). Based on the analysis, the population density was expected to expand significantly at the downstream. Obviously, the ratio between rural and urban population in Punjab, Haryana, and Rajasthan States was found to be changed remarkably from 66/34, 71/29, and 77/23, respectively in 2001 to 63/37, 65/35, and 75/25, respectively in 2011 (CensusInfo, 2011). It can be said that the rapid increase in population together with changes in migration consequences could potentially increase the demand for downstream domestic water consumption.

Regarding future land use changes, there are several drivers used for land use projections. In details, the road network was found to be one of the main direct drivers since it provides the access to previous remote areas and also promotes anthropogenic disturbance near roadways. Secondly, the urban center was also the main contributor to urban population growth, which might lead to be more susceptible to land use change. Moreover, environmental gradients such as changing temperature and precipitation with altitude, was also found to be a good predictor to the area suitable for agriculture and vulnerable to conversion to agricultural land.

Lastly, the slope is also of paramount importance to determine the land useful for human development, for instance, agriculture and building require a fairly gentle slope. As a result, the V statistic test results indicated that elevation (0.375), population (0.260), slope (0.247) and distance to cities (0.199) are a very strong correlation with the land use change, while distance to rivers (0.134) and roads (0.089) showed moderate and weak correlations, respectively. Thereafter, these explanatory variables were modeled with the “static” role in model structure, which is a function of certain fixed (unchanging) driving factors for expressing aspects of basic suitability for the transition under consideration. The transition probability prediction revealed a good performance in the neural network, i.e.  $R^2$  index greater than 0.83 and the Kappa index of agreement of 98% when compared the projected to its observed land use map in 2010 (**Fig. 5**).

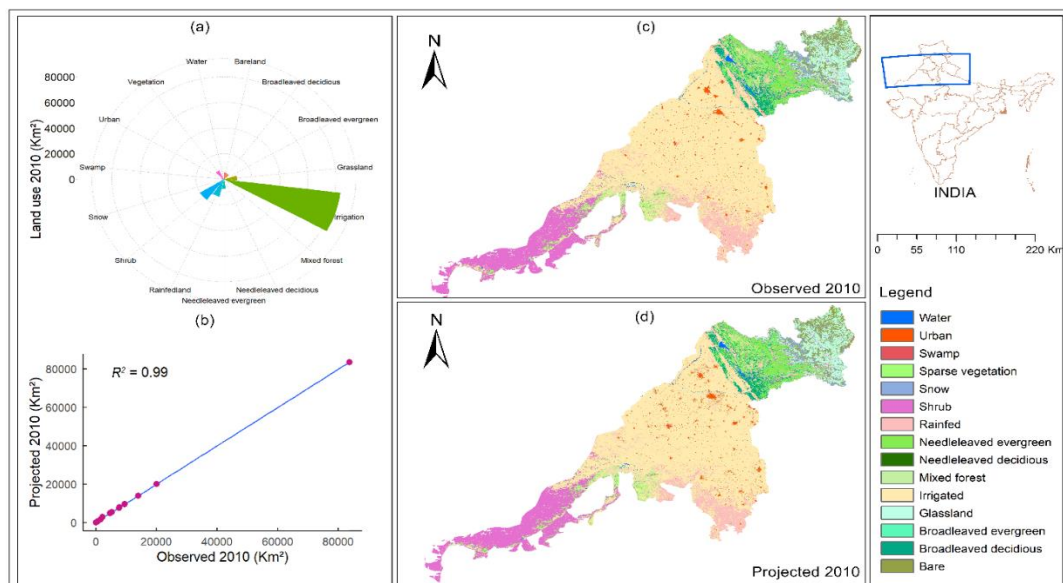


**Fig. 5** Detailed information about (a) land use types, (b) correlation between 2010 observed and projected areas, (c) 2010 observed land use map, and (d) 2010 projected land use map.

It was found that the irrigated land would likely be decreased in the future and switched to urban areas. In details, Punjab and Haryana irrigated lands would decrease by 15% to 30% and 5% to 10%, respectively, compared to the baseline. Conversely, irrigated land in Rajasthan is expected to expand by about 12% to 18% in the future in comparison to the baseline period, as can clearly be seen from the historical data during 1995 to 2010 that the expansion of arable land was mainly at the expense of shrub vegetation. Importantly, the insights gained from this land use change study is somehow in consistent with the findings of (Naikoo et al., 2020) who revealed that the major change from agriculture to urban areas also occurred in New Delhi located at the downstream of Haryana and Punjab States, which experienced the decrease from 12% to 32% during the period of 1990 to 2018. Correspondingly, Meer and Mishra (2020) also found a similar trend in land use change during 1979 to 2018 in Northern India where the urban coverage expanded significantly over the region possibly due to increased population, while the agricultural areas decreased by 55%.

#### 4.5 Future projection for water resources system

Prior to further WEAP model simulations for water demands and supplies and water storage and releases from the reservoirs, the calibration and validation processes were executed by comparing the monthly simulated and observed discharge and reservoir inflow at four available streamflow stations and two reservoir sites, respectively (see **Fig. 1** for their locations).

Referring to **Fig. 6**, it is apparent that the simulated data is consistent with the observed values for the entire simulation periods. In addition to graphical technique, statistical indicators, i.e. Pearson's correlation coefficient ( $r$ ) (Pearson, 1895) and Nash-Sutcliffe Efficiency (NSE) (Nash and Sutcliffe, 1970) were also used to evaluate the WEAP model performance.

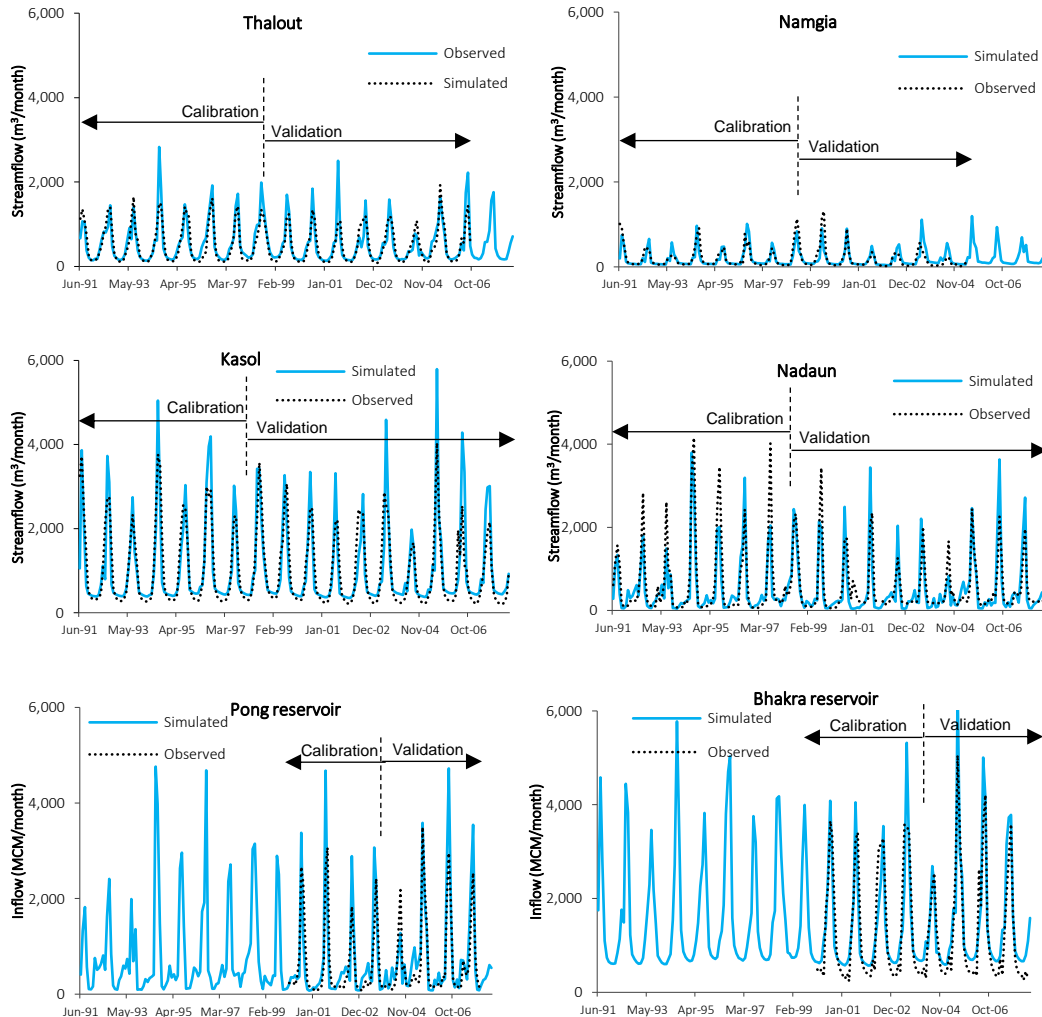


**Fig. 6** Monthly simulated and observed streamflow during calibration and validation at different monitoring stations.

With respect to **Table 2**, based on Moriasi et al. (2007), the WEAP showed acceptable results with the values of  $r$  and  $NSE > 0.50$  for both calibration and validation. Therefore, it can be said that the WEAP model is well calibrated and can be used to evaluate water allocation in the study area according to different scenarios. Thereafter, the WEAP model in association with the optimal rule curves for Pong and Bhakra reservoirs under joint operation, was applied for water allocation simulations. In this case, the reservoir management zone called conservation zone (the space between LRC and URC) was defined to freely release the water from the conservation pool to fully meet downstream requirements, in which when the reservoir storage level falls inside the buffer zone (the space between dead storage and LRC), the flow release rate is limited using a buffer coefficient ( $\alpha$ ) with the value between zero and one to limit the amount of water available for each month at critical

conditions in the reservoir. In this study, the value of  $\alpha$  of 0.1 was defined for the Pong and Bhakra reservoirs, which indicates that the reservoir release will be reduced by 10% if the storage level falls into the buffer zone.

**Table 2.**

**Calibration and validation results of WEAP model**

Station	Process	Period	Fitness criterion	
			r	NSE
Thalout	Calibration	1991 – 1998	0.89	0.74
	Validation	1999 – 2005	0.88	0.61
Namgia	Calibration	1991 – 1998	0.76	0.56
	Validation	1999 – 2004	0.70	0.50
Kasol	Calibration	1991 – 1999	0.89	0.77
	Validation	2000 – 2007	0.84	0.53
Nadaun	Calibration	1991 – 1999	0.90	0.80
	Validation	2000 – 2007	0.84	0.50
Pong	Calibration	2000 – 2004	0.83	0.68
	Validation	2005 – 2007	0.81	0.55
Bhakra	Calibration	2000 – 2004	0.87	0.77
	Validation	2005 – 2007	0.84	0.57

Regarding the increase of future precipitation, glacier melt, and reduction in cultivated land, the mean annual runoff is expected to increase in the Sutlej River (in the range of 3.6% to 4.67%) and Beas River (by 4.73% to 7.82%) in comparison to the baseline. Referring to **Fig. 7**, the mean monthly runoff in the Beas and Sutlej Rivers is likely to increase from pre-monsoon to monsoon periods.

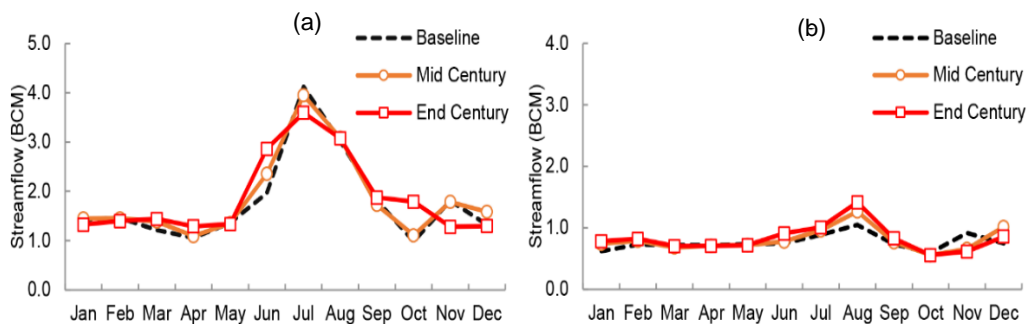


**Fig. 7** The projected streamflow for the (a) Sutlej and (b) Beas Rivers during the mid and end century periods

The runoff in the Sutlej River is much higher than in the Beas River, as stated by NAPCC (2011) that about 25% of the inflow from the Beas River was diverted to the Sutlej River through a Beas-Sutlej Link. It was found that, at the end of the century, the flow in the Sutlej River will be slightly different than the mid-century. Furthermore, the glacier melting was also found to contribute to some portion of flow in the Sutlej and Beas Rivers by about 59% and 35% of the total runoff, respectively.

Depending on the GCM models, the moderate reduction in irrigation water demand was found at Punjab State by the average of 10% and Haryana State by 5% (compared to the baseline). In contrast, the irrigation water demand in Rajasthan State was found to be increased by about 10% (compared to the baseline) (see **Fig. 8** for more details). Interestingly, the abovementioned changes were found to be in line with the changes in land use, which corresponds to in the previous study conducted by (Dau et al., 2021b) using the GFLD-CM3 model under RCP 8.5 scenario and SSP 1 pathway.

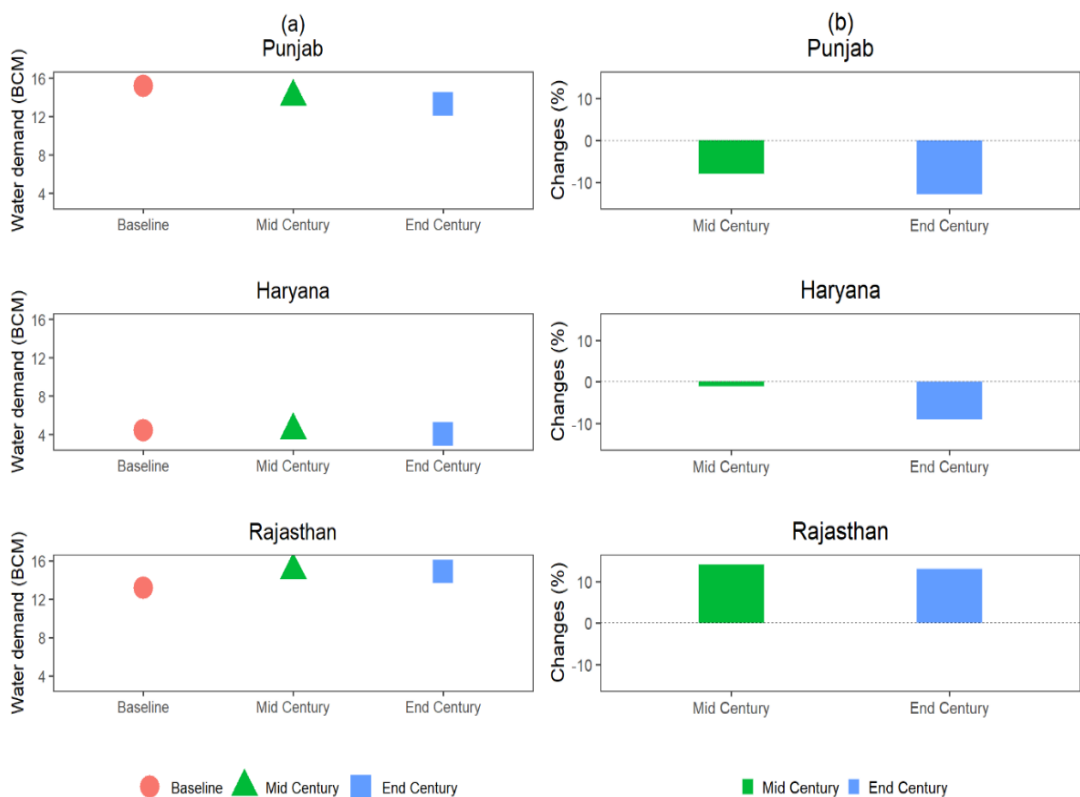


**Fig. 8** The mean irrigation water demand in the cases of (a) annual requirements and (b) changes in the future across the GCM models

Based on the obtained findings from this study, compared to the baseline, the relationship among projected precipitation, projected irrigated command areas, and projected irrigation water demand of each state under future climate and socio-economic conditions is illustrated in simplified **Fig. 9** (Note: the figure is not drawn to scale). As seen in **Fig. 9a**, the states of Punjab, Haryana, and Rajasthan are likely to increase in precipitation, however, the irrigated areas in Punjab and Haryana are expected to decrease and is likely to increase in Rajasthan. In **Fig. 9b**, it can be noticed that due to the decrease of irrigated areas in Punjab and Haryana, and the increase in Rajasthan, the decrease in irrigation water demand is then clearly seen for both states and is potentially to increase in Rajasthan.



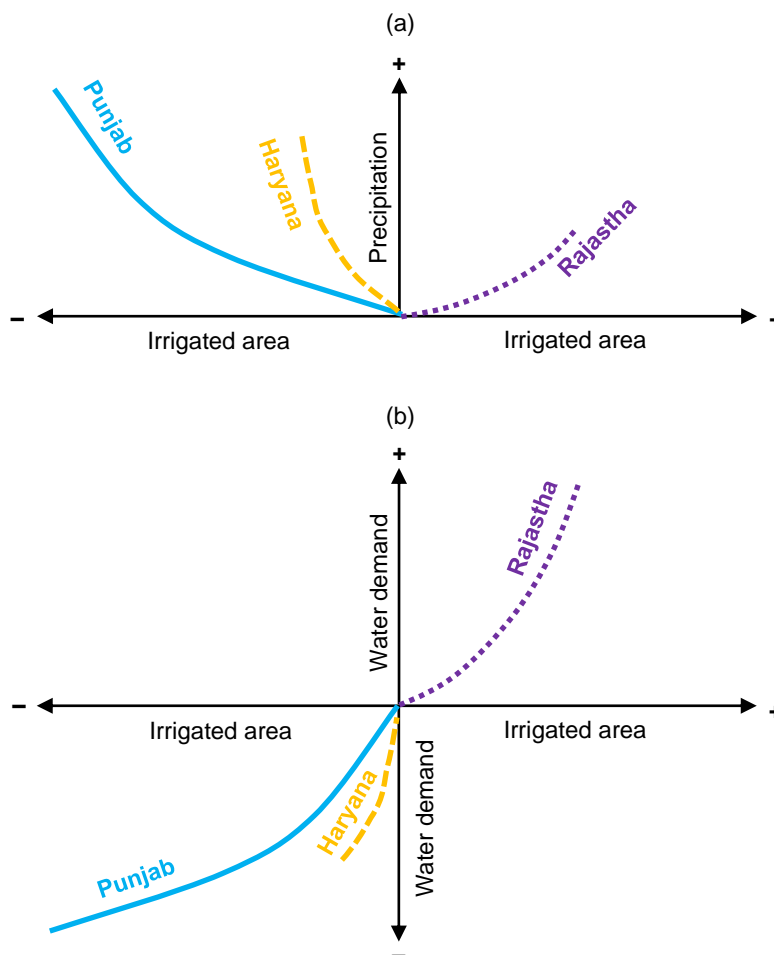


**Fig. 9** The relationship between (a) the projected precipitation and the projected irrigated command areas and (b) the projected irrigation water demand and the irrigated command areas of each state under future climate and socio-economic conditions

In line with the population growth under SSP1 scenario, the results expressed a slight shortage for domestic water consumption by 1% during the mid-century, which is meaningless in comparison to the whole system. Given the increase for future runoff as the consequences of rising in precipitation (5% to 10% at the downstream part) and the reduction on irrigation water demand as mentioned previously, efficient water managements such as couple human-natural system, water reuse, or demand-side management, etc. would possibly eliminate water shortage issue for domestic uses. As a conclusion, domestic water consumption will not a huge challenge in this study area.

## 5. CONCLUSIONS

The assessment of the effects of global climate and socio-economic changes on water resources system in the Sutlej-Beas was carried out. The results indicated that future annual precipitation and temperature will increase from baseline, in which high runoffs are likely to occur over the pre-monsoon to monsoon seasons, as a consequence of glacier melting and heavy rainfall. Based on the land use projections, future irrigated areas in Punjab and Haryana is found to be decreased due to the

expansion of urban areas, whereas a slight increase is found in Rajasthan. The main findings also suggested that the annual irrigation water demand is expected to increase in Rajasthan State, while it will be decreased in Punjab and Haryana States, as a consequence of climate and land use changes.

The study is certainly not without limitations, some of which are discussed below and will be the purpose of future work. The application of the Delta scaling approach for climate change was justified but it would be better to implement with other methods like the statistical and dynamical downscaling approaches. In addition, relying on only RCP 4.5 and SSP1 scenarios could probably be insufficient to represent all the important aspects of both climate and socio-economic changes. Therefore, applying different RCP and SSP scenarios would minimise the uncertainties in climate model projections.

The outcomes of this study are expected to be beneficial for the Bhakra and Beas Management Board (BBMB) and other relevant agencies in managing the main infrastructures for irrigation water supply, hydropower production, and flood relief, situated in the Beas-Sutlej system.

## ACKNOWLEDGEMENTS

The work reported herein was funded by the UK-NERC (grant numbers NE/N016394/1 and NE/N015541/1) – “Sustaining Himalaya Water Resources in a Changing Climate (SusHi-Wat)” – as part of the UK-India Newton-Bhabha Sustainable Water Resources (SWR) thematic Programme.

## REFERENCES

- Adeloye, A. J., Wuni, I. Y., Dau, Q. V., Soundharajan, B.-S. & Kasiviswanathan, K. S. (2019). Height–Area–Storage functional models for evaporation-loss inclusion in reservoir-planning analysis. *Water*, 11, 1413.
- Asoka, A., Gleeson, T., Wada, Y. & Mishra, V. (2017). Relative contribution of monsoon precipitation and pumping to changes in groundwater storage in India. *Nature Geoscience*, 10, 109-117.
- Bannister, D., Orr, A., Jain, S. K., Holman, I. P., Momblanch, A., Phillips, T., Adeloye, A. J., Snapir, B., Waite, T. W., Hosking, J. S. & Allen-Sader, C. (2019). Bias correction of high-resolution regional climate model precipitation output gives the best estimates of precipitation in Himalayan catchments. *Journal of Geophysical Research: Atmospheres*, 124, 14220-14239.
- Benestad, R. & Haugen, J. (2007). On complex extremes: Flood hazards and combined high spring-time precipitation and temperature in Norway. *Climatic Change*, 85, 381-406.
- Censusinfo. (2011). *CensusInfo India 2011 - Final population totals* [Online]. India. Available: [http://dataforall.org/dashboard/censusinfoindia\\_pca](http://dataforall.org/dashboard/censusinfoindia_pca) [Accessed May 01 2020].
- Chaturvedi, V., Koti, P. N., Sugam, R., Neog, K. & Hejazi, M. (2020). Cooperation or rivalry? Impact of alternative development pathways on India’s long-term electricity generation and associated water demands. *Energy*, 192, 116708.
- Cramér, H. (1946). *Mathematical Methods of Statistics (PMS-9)*, Princeton, Princeton University Press.
- Dau, Q. V. & Adeloye, A. J. (2021). Water security implications of climate and socio-economic stressors for river basin management. *Hydrological Sciences Journal*.
- Dau, Q. V. & Kuntiyawichai, K. (2020). Identifying adaptive reservoir operation for future climate change scenarios: A case study in Central Vietnam. *Water Resources*, 47, 189-199.
- Dau, Q. V., Kuntiyawichai, K. & Adeloye, A. J. (2021a). Future changes in water availability due to climate change projections for Huong basin, Vietnam. *Environmental Processes*, 8, 77-98.
- Dau, Q. V., Kuntiyawichai, K. & Plermkamon, V. (2017). Quantification of flood damage under potential climate change impacts in Central Vietnam. *Irrigation and Drainage*, 66, 842-853.
- Dau, Q. V., Kuntiyawichai, K. & Suryadi, F. X. (2018). Drought severity assessment in the lower Nam Phong River Basin, Thailand. *Songklanakarin J. Sci. Technol.*, 40, 985-992.
- Dau, Q. V., Momblanch, A. & Adeloye, A. J. (2021b). Adaptation in a Himalayan water resources system under a sustainable socio-economic pathway in a high-emission context. *Journal of Hydrologic Engineering*, 26.

Dhawan, V. (2017). *Water and Agriculture in India: Background Paper for the South Asia Expert Panel During the Global Forum for Food and Agriculture (GFFA) 2017*, OAV - German Asia-Pacific Business Association.

Dong, S., Xu, Y., Zhou, B. & Shi, Y. (2015). Assessment of indices of temperature extremes simulated by multiple CMIP5 models over China. *Advances in Atmospheric Sciences*, 32, 1077-1091.

Du, M., Kawashima, S., Yonemura, S., Zhang, X. & Chen, S. (2004). Mutual influence between human activities and climate change in the Tibetan Plateau during recent years. *Global and Planetary Change*, 41, 241-249.

Fao (2015). FAO AQUASTAT Country profile - India. Italy: Food and Agriculture Organisation of the United Nations.

Gao, J. (2017). Downscaling global spatial population projections from 1/8-degree to 1-km grid cells. *NCAR Technical Note NCAR/TN-537+STR*.

Goyal, M. K. & Surampalli, R. Y. (2018). Impact of climate change on water resources in India. *Journal of Environmental Engineering*, 144, 04018054.

Ires. (2020). *India's water resources* [Online]. India: Indian Water Resources Society. Available: <http://iwrs.org.in/indias-water-resources> [Accessed 03 November 2020].

Jain, S., K. Agarwal, P. & Singh, V. (2007). *Hydrology and water resources of India*, Springer, Dordrecht.

Krishnan, R., Shrestha, A. B., Ren, G., Rajbhandari, R., Saeed, S., Sanjay, J., Syed, M. A., Vellore, R., Xu, Y., You, Q. & Ren, Y. (2019). Unravelling climate change in the Hindu Kush Himalaya: rapid warming in the mountains and increasing extremes. In: WESTER, P., MISHRA, A., MUKHERJI, A. & SHRESTHA, A. B. (eds.) *The Hindu Kush Himalaya Assessment: Mountains, Climate Change, Sustainability and People*. Cham: Springer International Publishing.

Kulkarni, A. & Karyakarte, Y. (2014). Observed changes in Himalayan glaciers. *Current science*, 106, 237-244.

Landis, J. R. & Koch, G. G. (1977). The measurement of observer agreement for categorical data. *Biometrics*, 33, 159-174.

Lenderink, G., Buishand, A. & Van Deursen, W. (2007). Estimates of future discharges of the river Rhine using two scenario methodologies: direct versus delta approach. *Hydrol. Earth Syst. Sci.*, 11, 1145-1159.

Li, H., Xu, C.-Y., Beldring, S., Tallaksen, L. M. & Jain, S. K. (2016). Water resources under climate change in Himalayan basins. *Water Resources Management*, 30, 843-859.

Manish, K., Telwala, Y., Nautiyal, D. C. & Pandit, M. K. (2016). Modelling the impacts of future climate change on plant communities in the Himalaya: a case study from Eastern Himalaya, India. *Modeling Earth Systems and Environment*, 2, 92.

Marko, K., Zulkarnain, F. & Kusratmoko, E. (2016). Coupling of Markov chains and cellular automata spatial models to predict land cover changes (case study: upper Ci Leungsi catchment area). *IOP Conference Series: Earth and Environmental Science*, 47, 012032.

Maurer, J. M., Schaefer, J. M., Rupper, S. & Corley, A. (2019). Acceleration of ice loss across the Himalayas over the past 40 years. 5, eaav7266.

Meer, M. S. & Mishra, A. K. (2020). Land Use/Land Cover Changes over a District in Northern India using Remote Sensing and GIS and their Impact on Society and Environment. *Journal of the Geological Society of India*, 95, 179-182.

Mirza, M. M. Q. & Ahmad, Q. K. (2005). *Climate change and water resources in South Asia*, USA, CRC Press.

Moriasi, D. N., Arnold, J. G., Van Liew, M. W., Bingner, R. L., Harmel, R. D. & Veith, T. L. (2007). Model Evaluation Guidelines for Systematic Quantification of Accuracy in Watershed Simulations. *Transactions of the ASABE*, 50, 885-900.

Mukherji, A., Molden, D., Nepal, S., Rasul, G. & Wagnon, P. (2015). Himalayan waters at the crossroads: issues and challenges. *International Journal of Water Resources Development*, 31, 151-160.

Naikoo, M. W., Rihan, M., Ishtiaque, M. & Shahfahad (2020). Analyses of land use land cover (LULC) change and built-up expansion in the suburb of a metropolitan city: Spatio-temporal analysis of Delhi NCR using landsat datasets. *Journal of Urban Management*, 9, 347-359.

Napcc (2011). Appendix 2 Lower Sutlej sub-basin. *TA 7417- IND: Support for the national action plan on climate change support to the National water mission*. India.

Nash, J. E. & Sutcliffe, J. V. (1970). River flow forecasting through conceptual models part I — A discussion of principles. *Journal of Hydrology*, 10, 282-290.

Nepal, S. (2016). Impacts of climate change on the hydrological regime of the Koshi river basin in the Himalayan region. *Journal of Hydro-environment Research*, 10, 76-89.

- O'Neill, B. C., Kriegler, E., Riahi, K., Ebi, K. L., Hallegatte, S., Carter, T. R., Mathur, R. & Van Vuuren, D. P. (2014). A new scenario framework for climate change research: the concept of shared socioeconomic pathways. *Climatic Change*, 122, 387-400.
- Park, Y. S. & Lek, S. (2016). Chapter 7 - Artificial Neural Networks: multilayer perceptron for ecological modeling. In: JØRGENSEN, S. E. (ed.) *Developments in Environmental Modelling*. Elsevier.
- Pearson, K. (1895). Note on regression and inheritance in the case of two parents. *Proceedings of the Royal Society of London Series I*.
- Penalba, L. M., Elazegui, D. D., Soukhly, O., Amit, M. G. C., Lansigan, F. P. & Faderogao, F. J. F. (2014). Climate change impacts on food security and livelihoods: case studies from Lao PDR and the Philippines. In: LEBEL, L., HOANH, C. T., KRITTASUDTHACHEEWA, C. & DANIEL, R. (eds.) *Climate risks, regional integration and sustainability in the Mekong region. Petaling Jaya, Malaysia: Strategic Information and Research Development Centre (SIRDC)*. Sweden: Stockholm Environment Institute (SEI).
- Pontius, R. (2002). Statistical methods to partition effects of quantity and location during comparison of categorical maps at multiple resolutions. *Photogrammetric Engineering and Remote Sensing*, 68, 1041-1050.
- Prasad, V., Kulkarni, A. V., Pradeep, S., Pratibha, S., Tawde, S. A., Shirsat, T., Arya, A. R., Orr, A. & Bannister, D. (2019). Large losses in glacier area and water availability by the end of the twenty-first century under high emission scenario, Satluj basin, Himalaya. 116, 1721-1730.
- Rajbhandari, R., Shrestha, A., Nepal, S. & Wahid, S. (2018). Projection of future precipitation and temperature change over the transboundary Koshi River basin using Regional Climate Model PRECIS. *Atmospheric and Climate Sciences*, 8, 163-191.
- Samir, K., Marcus, W., Markus, S. & Wolfgang, L. (2018). Future population and human capital in heterogeneous India. *Proceedings of the National Academy of Sciences*, 115, 8328-8333.
- Sieber, J. & Purkey, D. (2011). WEAP, water evaluation and planning system. U.S. Center, Somerville, USA: Stockholm Environment Institute.
- Siebert, S., Burke, J., Faures, J. M., Frenken, K., Hoogeveen, J., Döll, P. & Portmann, F. T. (2010). Groundwater use for irrigation – a global inventory. *Hydrol. Earth Syst. Sci.*, 14, 1863-1880.
- Singh, P. & Bengtsson, L. (2004). Hydrological sensitivity of a large Himalayan basin to climate change. *Hydrol. Process.*, 18, 2363-2385.
- Taylor, K. E., Stouffer, R. J. & Meehl, G. A. (2012). An overview of CMIP5 and the experiment design. *Bulletin of the American Meteorological Society*, 93, 485-498.
- Tebaldi, C. & Knutti, R. (2007). The use of the multi-model ensemble in probabilistic climate projections. *Phil. Trans. R. Soc. A.*, 365, 2053-2075.
- Wang, B., Zheng, L., Liu, D. L., Ji, F., Clark, A. & Yu, Q. (2018). Using multi-model ensembles of CMIP5 global climate models to reproduce observed monthly rainfall and temperature with machine learning methods in Australia. *International Journal of Climatology*, 38, 4891-4902.
- Yates, D., Purkey, D., Sieber, J., Huber-Lee, A. & Galbraith, H. (2005). WEAP21—A demand-, priority-, and preference-driven water planning model. *Water International*, 30, 501-512.

## ASSESSMENT OF THE BLACK SEA SHELF ECOSYSTEM SUSTAINABILITY WITH MATHEMATICAL SIMULATION METHOD

Viktor KOMORIN<sup>1</sup> 

DOI: 10.21163/GT\_2020.162.02

### ABSTRACT:

The system analysis approach has been used for assessment of the sustainability of the marine shelf ecosystem with the method of mathematical modeling on the example of the north-western shelf of the Black Sea, as the most vulnerable part of the sea to the influence of natural and anthropogenic factors. Based on numerical experiments, an analysis of ecosystem risk in dynamic phase space was performed. Results have shown that the ecosystem risk of the Black Sea shelf zone has fluctuated around baseline value over the last decade under the existing influences of natural and anthropogenic factors, but the system approaches an unstable state with an increase of the combined effects of natural and anthropogenic factors.

**Key-words:** *system analysis, ecosystem risk, marine ecosystem, mathematical modeling, ecosystem stability, Black Sea.*

### 1. INTRODUCTION

The Black Sea is a unique body of water, eighty-seven percent of which is hydrogen sulfide. The upper layer of water remains suitable for the life of oxygen organisms, the thickness of which has been decreasing over the last decades. It may be about 60 meters in the central regions of the sea (Slobodnik J. et al.2020a). Any sufficiently powerful external influence, whether anthropogenic or natural ones can affect the stability of marine ecosystems. Anthropogenic problems of the Black Sea are formed and most acutely manifested in the coastal and shelf zone of the seas. Here there are a high level of economic activity and so many marine sources of pollution. The most significant impact of human activities on marine ecosystems exercise regulation of river flow, the activity of ports including works of dredging in the port waters and approach channels, dumping soil, exploration, and production of hydrocarbon resources, environmentally unjustified intensification of resource and service sectors in the marine and coastal waters, including fishing and other seafood, uncontrolled industrialization, chemicals, urbanization coast. These activities led to an unacceptable increase in marine pollution domestic, industrial, agricultural and other waste containing hazardous and harmful substances and pathogens.

The Northwestern Black Sea shelf is the most environmentally sensitive area of the Black Sea (Slobodnik et al., 2020b, 2020c). This was indicated with assessment data of the ecosystem of the Black Sea to 8 descriptors MSFD (Directive 2008/56 / EC of the European Parliament and of the Council of 17 June 2008 establishing a framework for community action in the field of marine environmental policy (Marine Strategy Framework Directive) presented in reports Draft EU / UNDP Project: Improving Environmental Monitoring in the Black Sea - Phase II (EMBLAS-II) ENPI / 2013 / 313-169 (Slobodnik et al., 2020a, 2020b, 2020c). A typical illustration of the assessment is represented in **Fig. 1** for BEAST (Slobodnik et al. 2020c). The biggest problems of the Black Sea are eutrophication, biodiversity loss, toxic pollution, etc. (BS EEA, 2015). This paper examines the impact of electrification, exacerbated by climate change, on the resilience of the marine shelf ecosystem in the field of ecological, economic, social systems.

---

<sup>1</sup> *Research Institution "Ukrainian Scientific Centre of Ecology of the Sea", Odesa, 65009, Ukraine, vkomorin@gmail.com*

This concept combines the human-nature systems and their components through ecosystem services and the factors of influence. It's arising from the direct use of services, as the indirect influence through human activities in general (Maes et al., 2016). Ecosystem function is defined as the capacity to provide ecosystem services (De Groot, 2010). Ecosystem services, in turn, derive from ecosystem functions and represent flows of services for which there is demand. For this concept, ecosystem services also cover products derived from these ecosystems (Edward and Barbier, 2017). Ecosystem services of the sea and coastal zones are considered within the issues of biodiversity conservation, use of water resources, conservation/ restoration of marine ecosystems, climate regulation, agriculture (Liquete et al., 2013).

The ability to provide ecosystem services regularly is depended on the stability of the system and its vulnerability to the effects. This can be analyzed through mathematical modeling of ecosystem risk within the theory of dynamical systems. The history of the use of ecological models goes back to the main work of Robert May (May, 1974). Historically, the use of mathematical models in ecology has been based on the use of tools that require fewer data and are easier to use in management decisions. Modern methods allow the use of models describing ecosystem components in more detail (Fulford, Heymans and Wei Wu, 2020).

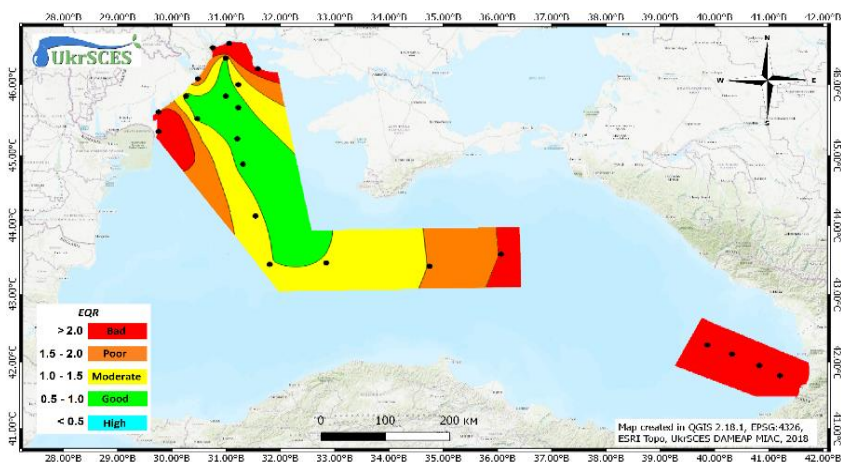


**Fig. 1.** Indicative assessment of environmental and ecological status of the Black Sea areas investigated during the JOSS 2019 based on eutrophication indicator BEAST index EQR (Slobodnik et al. 2020c, URL: [http://emblasproject.org/wp-content/uploads/2019/07/EMBLAS-II\\_NPMS\\_JOSS\\_2017\\_ScReport\\_FinDraft2.pdf](http://emblasproject.org/wp-content/uploads/2019/07/EMBLAS-II_NPMS_JOSS_2017_ScReport_FinDraft2.pdf)).

Objective scientifically-based forecasting of ecological consequences of the impact on the marine environment of functioning and planned economic objects, estimation of efficiency of various administrative decisions in the field of rational use, protection, and restoration of resources of a shelf zone of the sea are impossible without the use of mathematical models of the formation of quality of waters of marine ecosystems (Addison et al., 2018). Creation and verification of such models, for their application as a tool of ecological forecasting in the course of scenario modeling of natural processes, is one of the main tasks of environmental monitoring of coastal marine waters. Examples of the application of mathematical models for solving diagnostic and prognostic problems of the marine ecosystem and its components for the shelf areas of the Black Sea can be found in the following works (Tuchkovenko et al., 2005; Komorin and Tuchkovenko, 2002; Komorin et al., 2008; Komorin et al., 2017; Orlova I. et al., 2005). One of the models that allow analyzing changes in aquatic ecosystems under the influence of anthropogenic factors is AQUATOX (AQUATOX, 2018). This model has been successfully used to measure human impact on the Black Sea, for example, in the work specified in the references (Şimşek et al., 2019). There are several groups of requirements for

biological systems according to the definition of "sustainability" (Svirezhev, 1974; Odum, Eugene P., 1953). First, the time invariance of a geographic area or landscape. The region can include a wide variety of biocenosis, the total ecosystem of the region, poorly connected. The main processes that determine the dynamics of the region indicators will not change the number of species inhabiting its individual and global biogeochemical cycles.

The second group of requirements is the preservation of the number of species in a biological community. The biological community is the higher level of organization of living matter than the population. It should be defined as a set of populations that inhabits the area and forms the structure of food (trophic) links and metabolism. The concept of the biological community reflects that populations of living organisms are not randomly scattered across the Earth as independent groups, but form organized systems. A community is sustainable if the number of its constituent species does not change over time. This ecological definition is the closest to the various definitions of sustainability.

The third group of requirements applies to individual populations rather than communities. It is considered that a community is stable or stable if the numbers of its constituent populations do not fluctuate sharply. In thermodynamics, a system is stable if there are small probabilities of large fluctuations that can take it far from equilibrium and even destroy it.

On the other hand, there is a developed mathematical theory of stability, in which the definition of stability is given exhaustively (Polderman and Willems, 1998). But this theory does not work with the real objects, but with their mathematical models. Therefore, if we have a sufficiently "good" (in the sense of adequacy and completeness of description) mathematical model of a biological community or ecosystem (for example, in terms of differential or difference equations), then the question of the stability of a real community can be answered by examining our model stability. In mathematical theory, there are several concepts of stability of motion: Lyapunov stability, asymptotic stability, orbital stability, Poisson stability, Lagrange stability. One of the main ones is Lyapunov's resilience. For sustainable movement on Lyapunov the small initial shift increases. If the small initial shift not only increases, and eventually goes to zero, the movement has robust property of asymptotic stability.

The concept of orbital stability does not consider the distance between the points of the original and perturbed trajectories at the same time, and the minimum distance from the depicting point of the perturbed trajectory to the orbit corresponding to the original motion. Orbitally stable motion may not be stable according to Lyapunov. Non-stationary states of the system are possible, i.e. those in which the equilibrium state does not have time to be established. Increasing nonlinearity in the system beyond some critical value again leads the system to bifurcation: macroscopic consistency is replaced by the inconsistency of random fluctuations, which leads to ambiguous results: a small change in the initial condition over time leads to arbitrarily large changes in system dynamics. In this situation, the system is characterized by instability with its initial parameters (Lyapunov instability) and an exponential tendency to divergence. This behavior of systems was assigned the term dynamic.

Unambiguous characteristics of signal chaos are the spectrum of Lyapunov parameters. The positive maximum Lyapunov index is a measure of chaotic dynamics, zero Lyapunov exponents indicate the maximum limit cycle or quasi-periodic orbit and the negative maximum Lyapunov exponent is a fixed point. The system of dimension  $n$  has  $n$  Lyapunov exponents:  $\lambda_1, \lambda_2, \dots, \lambda_n$ , ordered in descending order. Dynamic systems for which the  $n$ -dimensional phase volume decreases are called dissipative. If the phase volume is maintained, then such systems are called conservative. Conservative system always has at least one conservation law. The existence of the conservation law often leads to the existence of a corresponding Lyapunov zero. For dissipative dynamical systems, the sum of Lyapunov exponents is always negative. In dissipative systems, Lyapunov indices are invariant under all initial conditions. The attractor is the most important concept that captures the specifics of dissipative structures. In fact, attractor can be considered as a factor of order (the order parameter for the system in the process of self-organization) (Nikolis and Prigogine, 1989). In terms of Lyapunov much can be said about the dynamic system, as there is a mode of attractor dimension if any, and the entropy of a dynamical system. Dynamic chaos instability corresponds to each



trajectory, i.e. the presence of at least one positive Lyapunov exponent. Attraction to the attractor requires that large-volume phase volumes be compressed, as reflected in the Lyapunov spectrum. Knowledge of Lyapunov parameters allows us to estimate the fractal dimension of the attractor.

The purpose of this study is to evaluate the stability of the dynamics of the marine ecosystem of the Black Sea under the influence of natural and anthropogenic factors on ecosystem-based analysis of the dynamics of risk in dynamic phase space using models AQUATOX. The objects of research are the ecosystem of coastal waters of the Black Sea and natural and anthropogenic factors of influence. The subject of the study is indicators of the state of the marine ecosystem and indicators of influencing factors. The research methods are comparative analysis and the method of mathematical modeling of the dynamics of the marine ecosystem.

## 2. MATERIALS AND METHODS

Assessing the impact of natural and anthropogenic factors on the quality of coastal waters of the Black Sea held with the model AQUATOX, which is well suited for the analysis of causes and occurrence of eutrophication (Park and Clough, 2003). Possible applications include consideration of water quality criteria for organic matter and analysis of management alternatives. AQUATOX simulates many interrelated variables important in the dynamics of dissolved oxygen, and their impact on the aquatic environment: nitrogen (total, nitrate, ammonia ions, and compounds); phosphorus (total amount, phosphates); dissolved oxygen; algal biomass, chlorophyll; periphyton biomass; macrophytes; transparency. **Table 1** shows the main types of organisms that are included in the model.

**Table 1.**

**The main species of organisms taken into account in the mathematical model of the ecosystem of the Black Sea Coastal Zone (BSCZ)**

Organism	The name of the organism characteristic BSCZ	The name of the organism, or its analogues in the AQUATOX library
Phytoplankton	Diatom	Diatom
	Green algae	Greens
	Blue-green algae	Bl-Greens
	Dinophytic algae	Dinoflagellate
	Golden algae	Chrysophyta
Zooplankton	Paddlefish	Copepoda
	Branchiopoda	Cladocera
	Rotifers	Rotifera
	Predatory zooplankton	Predatory Zooplankton
Benthos	Polychaetes	Polychaete
	Amphipods	Amphipod
	Mussels	Mussel
	Gastropods	Gastropod
Fishes	Anchovy	Anchovy (Hamsa)
	Sprat	Sprats
	Horse mackerel	Horse-mackerel
	Goby	Goby

Characteristics of phytoplankton and zooplankton, input data of temperature, salinity, nutrients in AQUATOX was set according to data of the Ukrainian Scientific Center of Ecology of the Sea (UkrSCES) (see **Fig. 2**), which are presented in the reports on the website of the institution <http://www.sea.gov.ua/?p=1215>.



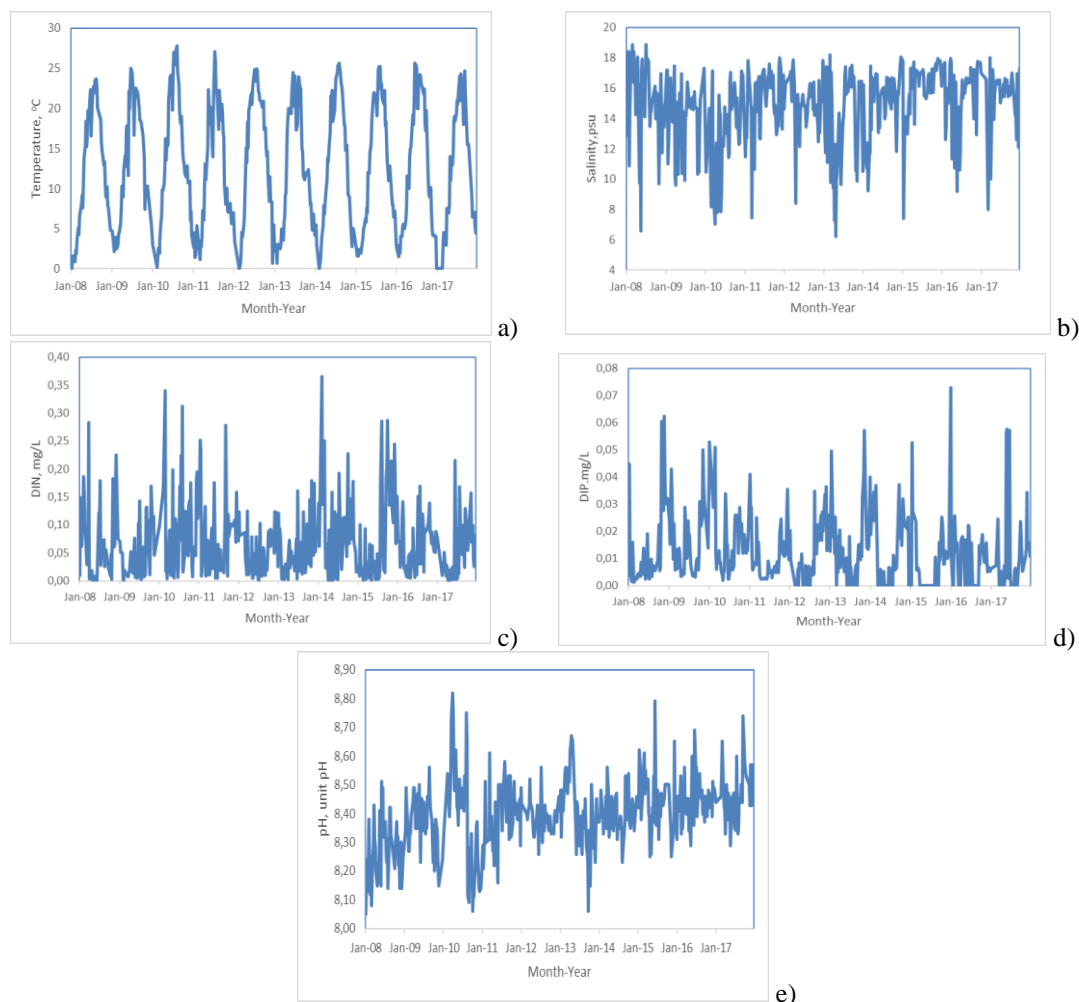


**Fig. 2.** Long-term changes in temperature - (a), salinity - (b), concentration of the mineral forms of phosphorus (DIP) - (c) and nitrogen (DIN) - (d) and pH - (e), (2008 – 2018, UkrSCES).

The quality of model calculations is evaluated based on the ratio  $S/\sigma$ , where  $\sigma$  - is the standard deviation, which is determined for the analyzed series of values of the concentration of the substance by the formula:

$$\sigma = \sqrt{\frac{\sum(C_j)^2 - \frac{(\sum C_j)^2}{n}}{n-1}}, \quad (1)$$

$S$  - mean-square error of test results calculated values of concentration of the substance found in the regression equation, which is defined by the formula:

$$S = \sqrt{\frac{\sum(C_j - C_m)^2}{n-2}}, \quad (2)$$

where  $C_m$  - is the value of the concentration of the substance obtained from the equation of the model according to the data of water flow in the watercourse, at which  $C_j$  was recorded.

### 3. CALCULATION

Using the model was assessed the stability of the dynamics of the marine ecosystem of the Black Sea carried out for the period from 2008 to 2018 in this UkrSCES. To quantify the impact of natural and anthropogenic factors on the state of marine shelf ecosystems, we use the ecosystem risk, which can be expressed as a function of the relationship of influencing factors with ecosystem status parameters in Euclidean space used in (Komorin et al. 2015):

$$R = \sqrt{E^2 + C^2}, \quad (3)$$

where  $E$  – is an integral factor of influence;

$C$  – is an integral indicator of the state of the ecosystem.

In general, the integral factor of influence is determined by:

$$E = \frac{\sum_i^N e_i}{N}, \quad (4)$$

where  $e_i$  – is an indicator of the  $i$ -th factor of influence, which is the normalized value of the deviation of the factor from the norm to the maximum amplitude of oscillations;  
 $N$  - the number of influencing factors.

The integrated state indicator is calculated with a similar formula. Modeling coastal ecosystems of the Black Sea held in diagnostic mode. At the same time, the factors influencing the state of the ecosystem were determined during the period of 2008 - 2018 every week by UkrSCES in Odessa Bay (Malyi Fontan). The main indicator of Lyapunov characterizes the degree of exponential divergence of close trajectories. The presence of a positive exponent of Lyapunov in the system indicates that any two close trajectories diverge rapidly over time, i.e. there is a sensitivity to the values of the initial conditions. Therefore, the definition of the exponent Lyapunov allows us to identify a dynamic system in terms of the presence of chaotic behavior. Lyapunov indicators were calculated to study the stability of the marine biocenosis. The TISEAN system was used for calculations (TISEAN 3.0.1, 2018).

### 4. RESULTS AND DISCUSSION

In **Table 2** according to the results of (Komorin et al., 2015) the results of the quality assessment of model calculations are given. As factors of influence were considered indicators that depend more on natural factors of influence - the temperature and salinity of seawater; anthropogenic - concentrations of nutrients and pH. The temporal dynamics of ecosystem risk are presented in **Fig. 3**. The upper limit of the confidence interval for the arithmetic mean of the ecosystem risk during 2008 - 2018 was taken as a critical value (arithmetic mean plus standard deviation). The results of the calculation of ecosystem risk according to formula (3) in the plane of the dependence of the ecosystem on the factors of influence are presented in **Fig. 4**. The values of risk, which are located in the red zone are critical.

Table 2.

Parameters for assessing the quality of model calculations

Indicators	S/σ
Nitrates	0.21
Salinity	0.22
Phosphates	0.23
Oxygen	0.24
Ammonium nitrogen	0.25
Dinophytes	0.35
Greens	0.56
Blue-Green	0.60
Diatoms	0.70
Total zooplankton	0.71

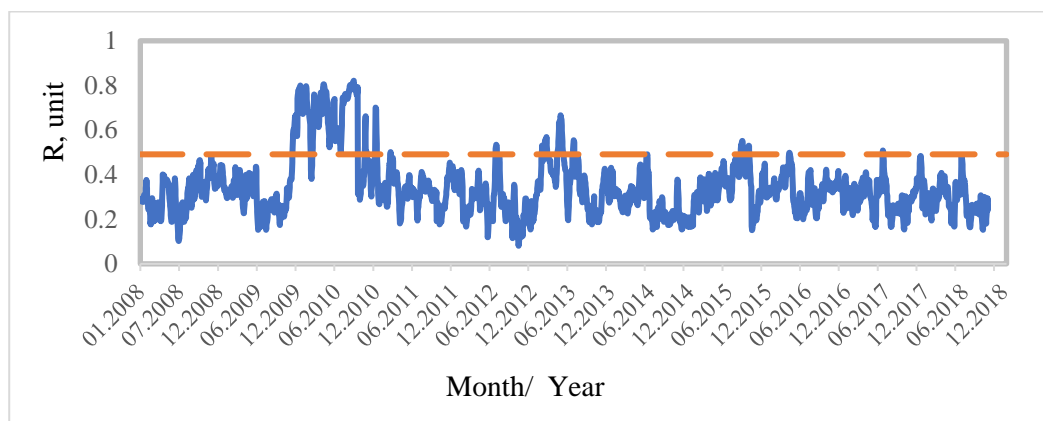


Fig. 3. Temporal dynamics of ecosystem risk (R) for the period 2008-2018.

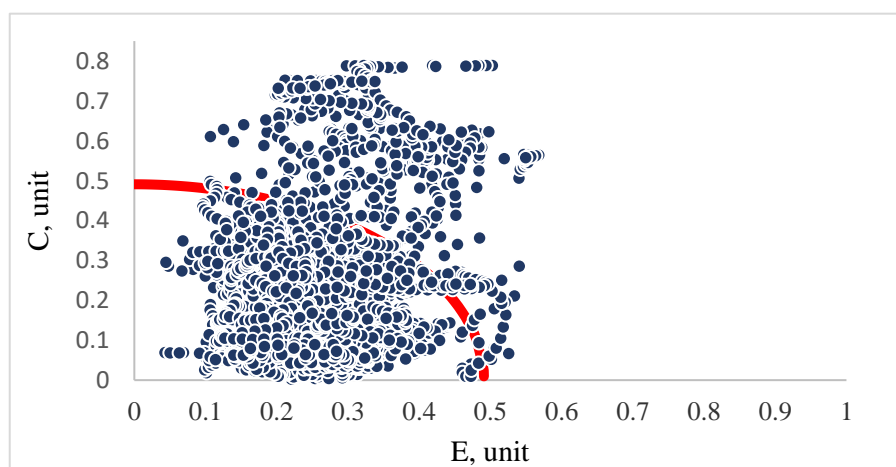
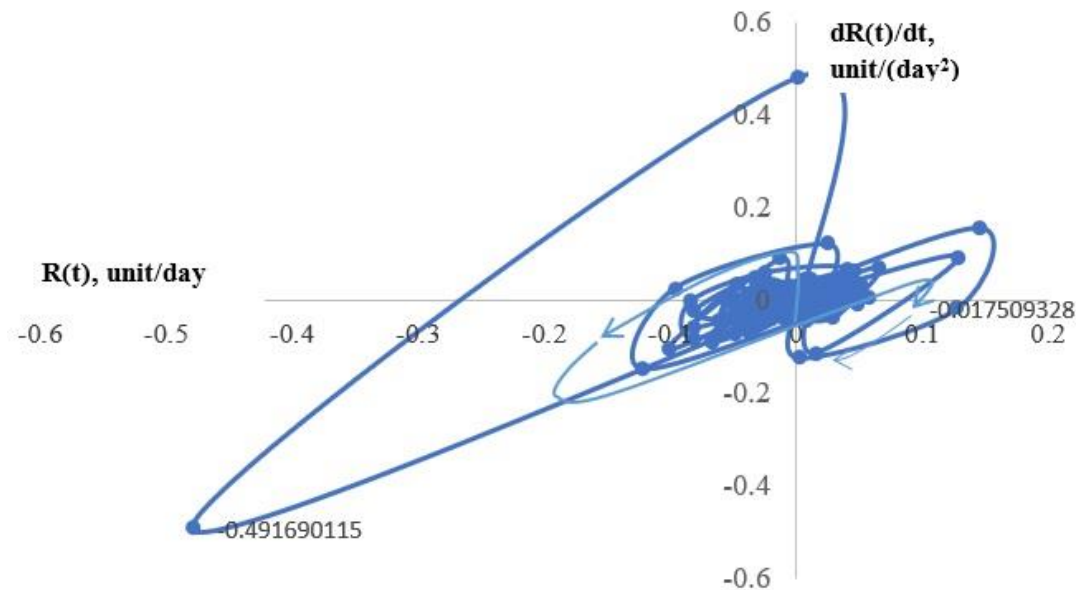


Fig. 4. Estimated values of ecosystem risk in the planes and the dependence of the state of the ecosystem (C) on the sum of factors (E).

As can be seen from **Fig. 3** and **Fig. 4**, points corresponding to the spring period have entered the zone beyond the red line of critical risk. Thus, the results obtained for the last ten years show that the marine ecosystem of Odessa Bay was in crisis at the end of winter and in summer. Analysis of the dynamics of ecosystem risk in the dynamic phase space shows that the ecosystem after external influence seeks to maintain the initial values (see **Fig. 5**). In other words, changes in the biotic structure of the ecosystem and the intensity of changes in biomass in response to changes in environmental conditions are aimed at maintaining the optimal balance in the new conditions.



**Fig. 5.** Dynamics of ecosystem risk ( $R$ ) in phase space:  $R(t)$  and  $dR(t)/dt$  ( $t$  – time in days).

Estimation of the maximum Lyapunov exponent  $\lambda$ , which characterizes the velocity of divergence of close trajectories of dynamics in the phase space, allows us to conclude the stability of the ecosystem under the influence of certain factors. A positive value of the indicator is usually taken as an indicator of system instability. The analysis showed that the system approaches an unstable state with an increase in nutrients 5 times the norm, as well as a result of the combined effects of natural (changes in temperature and salinity of seawater) and anthropogenic factors (increase in nutrients at least 2 times). For the period from 2008 to 2018, the Lyapunov index  $\lambda$  varies from  $(-0.04)$  to  $(-0.001)$ . Since  $\lambda < 0$ , this means that such a system does not show signs of instability.

## 5. CONCLUSIONS

A system analysis approach has been used for a comprehensive assessment of the impact of natural and anthropogenic factors on the resilience of coastal ecosystems of the Black Sea was conducted with the ecosystem risk and mathematical modeling on the AQUATOX. Modeling of the Black Sea coastal water ecosystem was carried out in diagnostic mode. The factors influencing on the state of the ecosystem were determined during the period 2008 - 2018 based on weekly measurements of the UkrSCES in Odessa Bay (Maly Fontan). The ecosystem risk indicator was used to quantify the impact of natural and anthropogenic factors on the state of marine shelf ecosystems. It was represented as a function of the relationship of influencing factors with ecosystem status parameters in Euclidean space.

As indicators reflecting the effect of environmental factors impact on the marine ecosystem considered the temperature and salinity of seawater, anthropogenic - nutrients, and pH. In the plane

of distribution of ecosystem risk by factors of condition and impact in the critical risk zone, some points correspond to the winter-spring and summer periods of the year. The paper identifies indicators of the sustainability of the ecological system over ten years.

Analysis of the dynamics of ecosystem risk in the dynamic phase space shows that the ecosystem afterward external influence seeks to maintain its original values. In other words, the change in the biological structure of the ecosystem and the intensity of changes in the state of the ecosystem in response to changes in environmental conditions are aimed at maintaining the optimal balance in the existing conditions. The largest changes in ecosystem risk correspond to the same winter-spring and summer periods of the year.

Estimation of the maximum Lyapunov exponent  $\lambda$ , which characterizes the velocity of divergence of close trajectories of dynamics in the phase space, allowed us to conclude the stability of the ecosystem under the influence of certain factors. The analysis showed that the system approaches an unstable state with an increase in nutrients 5 times the norm, as well as a result of the combined effects of natural (changes in temperature and salinity of seawater) and anthropogenic factors (increase in nutrients at least 2 times). For the model diagnostic period from 2008 to 2018, the Lyapunov index  $\lambda$  varies from (-0.04) to (-0.001), i.e. it is less than zero, which means that the system is in a stable state.

## REFERENCES

- AQUATOX. (2018) Linking water quality and aquatic life. [Online] Available from: <https://www.epa.gov/ceam/aquatox>. [Accessed 19<sup>th</sup> August 2019]
- BS EEA. (2015) Black Sea region briefing - The European environment — state and outlook 2015. [Online] Available from: <https://www.eea.europa.eu/soer/2015/countries/black-sea>. [Accessed 11th May 2020]
- De Groot, R.S. (2010) Challenges in integrating the concept of ecosystem services and values in landscape planning, management and decision making // *Ecol. Complex.* – 2010. – Vol. 7. – P. 260-272
- Edward, B., Barbier. (2017) Marine ecosystem services // *Current Biology*, Volume 27, Issue 11, 5 June 2017, Pages R507-R510
- Komorin V. 2015. Development of scenarios for improving the quality of coastal waters of the Gulf of Odessa on the basis of mathematical modeling: report on the SR / UkrSCES; Odesa. 97.
- Komorin, V. M., Pavlenko, M. Yu., Verlan, V. A., Denga, Yu. M., Dudnik, D.S., Krasota, L. L., Melnik, Ye. A., Orlova, I. G., Popov, Yu. S., Rachinska, O. V., Terenko, G. V., Ukrainskiy, V.V. (2017) Ukrainian Lower Danube water assessment/ Technical report "Inventory, Assessment and Remediation of Anthropogenic Sources of Pollution in the Lower Danube Region of Ukraine, Romania and the Republic of Moldova", UkrSCES. – Odesa, 2017. 282.
- Komorin, V., Popov Yu., Ukrainskiy, V. (2008) Assessment of variability of hydrodynamic characteristics of the north-western shelf of the Black Sea // *Bulletin of Odesa State Ecological University*. № 5. 188 – 201.
- Komorin, V., Tuchkovenko, Yu. (2002) Using a numerical hydrodynamic model to predict sea level fluctuations in the ports of the northwest shelf of the Black Sea. *Meteorology, climatology, hydrology*, 46. 324-331.
- Liquete, C., Piroddi, C., Drakou, E. G., Gurney, L., Katsanevakis, S., Charef, A., Egoh, S. (2013) Current Status and Future Prospects for the Assessment of Marine and Coastal Ecosystem Services: A Systematic Review // *Review of Marine and Coastal Ecosystem Services*. – July 2013. – Vol. 8, Is. 7. – 15 p.
- Maes, J., Liquete, G., Teller, A., Erhard, M., Paracchini, M.-L., Barredo, C. J. I., Grizzetti, B., Cardoso, A., Somma F., Petersen J.-E., Meiner, A., Gelabert, E., Zal, N., Kristensen, P., Bastrup-Birk, A., Biala, K., Piroddi, C., Egoh, B. N., Degeorges, P., Fiorina, C., Santos-Martín F., Naruševičius, V., Verboven, J., Pereira, H. M., Bengtsson, J., Gocheva, K., Marta-Pedroso C., Snäll, T., Estreguil, C., San-Miguel-Ayanz, J., Perez-Soba, M., Grêt-Regamey, A., Lillebo A., Malak, D. A., Condé, S., Moen, J., Czúcz, B., Drakou, E., Zulian, G., Lavalle, C. (2016) An indicator framework for assessing ecosystem services in support of the EU Biodiversity Strategy to 2020/ *Ecosystem Services* 17 (2016). P. 14-23: <http://creativecommons.org/licenses/by/4.0>. – 10.09.2018.
- May, R. M. (1974) Patterns of species abundance—Mathematical aspects of dynamics of populations. *SIAM Review*, 16, 585–585.

- Nikolis, G., Prigogine, I. (1989) *Exploring Complexity: An Introduction*. W. H. Freeman and Company, New York. 352
- Odum, Eugene P. (1953) *Fundamentals of ecology*. Philadelphia: W. B. Saunders Company, 1953. 383.
- Orlova, I, Pavlenko, N., Ukrainyi, V., Popov, Y., Matsokin, L., Komorin, V., Gavrilova, T., Lisovskiy, R., Baryshevskaya, G. (2005) Hydrological and hydrochemical indicators of the state of the northwest shelf of the Black Sea: reference book /- Odesa: UkrSCES, 2005. 616.
- Addison, P. F. E., Collins, D. J. R., Trebilco, Howe, S., Bax, N., Hedge, P., Jones, G., Miloslavich, P., Roelfsema, C., Sams, M., Stuart-Smith, R. D., Scanes, P., Baumgarten P., McQuatters-Gollop A. (2018) A new wave of marine evidence-based management: emerging challenges and solutions to transform monitoring, evaluating, and reporting ICES *Journal of Marine Science*, Volume 75, Issue 3, May-June 2018, Pages 941–952, <https://doi.org/10.1093/icesjms/fsx216>
- Park, R.A., Clough, J.S. (2003) AQUATOX for Windows: A Modular Fate and Effects Model for Aquatic Ecosystems: Perfluoroalkylated Surfactant and Estuarine Versions, Addendum to Release 2 Technical Documentation. EPA 823-R-04-001, U.S. Environmental Protection Agency, Washington, DC.
- Polderman, J.W., Willems, J.C. (1998) *Stability Theory*. In: *Introduction to Mathematical Systems Theory*. Texts in Applied Mathematics, vol 26. Springer, New York, NY. [https://doi.org/10.1007/978-1-4757-2953-5\\_7](https://doi.org/10.1007/978-1-4757-2953-5_7)
- Fulford, R. S., Heymans, S. J. J., Wei, Wu. (2020) *Mathematical Modeling for Ecosystem-Based Management (EBM) and Ecosystem Goods and Services (EGS) Assessment // Ecosystem-Based Management, Ecosystem Services and Aquatic Biodiversity* pp 275-289
- Şimşek, A., Küçük, K., Bakan, G. (2019) Applying AQUATOX for the ecological risk assessment coastal of Black Sea at small industries around Samsun, Turkey // *International Journal of Environmental Science and Technology*. -2019. Volume 16, p. 5229 –5236
- Slobodnik, J., Alexandrov, B., Komorin, V., Mikaelyan, A., Guchmanidze, A., Arabidze, M., Korshenko, A., Moncheva, S. (2020a) *National Pilot Monitoring Studies and Joint Open Sea Surveys in Georgia, Russian Federation and Ukraine, 2016: Final Scientific Report / J. Slobodnik, B. Alexandrov, V. Komorin, A. Mikaelyan, A. Guchmanidze, M. Arabidze6 A. Korshenko, S. Moncheva. – Dnipro: Seredniak T.K. [Online] Available from: [http://emblasproject.org/wp-content/uploads/2018/08/EMBLAS-II\\_NPMS\\_JOSS\\_2016\\_ScReport\\_Final3.pdf](http://emblasproject.org/wp-content/uploads/2018/08/EMBLAS-II_NPMS_JOSS_2016_ScReport_Final3.pdf)*
- Slobodnik, J., Medinets, V., Alexandrov, B., Komorin, V., Mikaelyan, A., Guchmanidze, A., Arabidze, M., Korshenko, A. (2020b). *12-Months National Pilot Monitoring Studies in Georgia, Russian Federation and Ukraine, 2016-2017: Final Scientific Report/ J. Slobodnik, V. Medinets, B. Alexandrov, V. Komorin, A. Mikaelyan, A. Guchmanidze, M. Arabidze, A. Korshenko. – Dnipro: Seredniak T.K. [Online] Available from: [http://emblasproject.org/wp-content/uploads/2019/07/EMBLAS-II\\_NPMS\\_12\\_months-2016\\_2017\\_FinDraft2.pdf](http://emblasproject.org/wp-content/uploads/2019/07/EMBLAS-II_NPMS_12_months-2016_2017_FinDraft2.pdf)*
- Slobodnik, J., Alexandrov, B., Komorin, V., Mikaelyan, A., Guchmanidze, A., Arabidze, M., Korshenko, A. (2020c) *National Pilot Monitoring Studies and Joint Open Sea Surveys in Georgia, Russian Federation and Ukraine, 2017: Final Scientific Report / J. Slobodnik, B. Alexandrov, V. Komorin, A. Mikaelyan, A. Guchmanidze, M. Arabidze6 A. Korshenko. – Dni pro: Seredniak T.K. [Online] Available from: [http://emblasproject.org/wp-content/uploads/2019/07/EMBLAS-II\\_NPMS\\_JOSS\\_2017\\_ScReport\\_FinDraft2.pdf](http://emblasproject.org/wp-content/uploads/2019/07/EMBLAS-II_NPMS_JOSS_2017_ScReport_FinDraft2.pdf)*
- Svirezhev, Yu. (1974) Possible ways to generalize the fundamental theorem of natural selection by R. Fischer // *Journal of General Biology*. – 1974. – T. 35, № 4. 590-601
- TISEAN 3.0.1. (2018) *Nonlinear Time Series Analysis*. [Online] [http://www.mpiikpks-dresden.mpg.de/~tisean/Tisean\\_3.0.1/index.html](http://www.mpiikpks-dresden.mpg.de/~tisean/Tisean_3.0.1/index.html). – 12.11.18.
- Tuchkovenko, Yu., Ilyushin V., Komorin, V. (2005) Simulation of the transport of sediments in the Kerch Strait. *Meteorology, climatology, hydrology*, 49. 446-459.

## SPECIFIC TYPES AND CATEGORIZATIONS OF BROWNFIELDS: SYNTHESIS OF INDIVIDUAL APPROACHES

Kamila TUREČKOVÁ<sup>1</sup> 

DOI: 10.21163/GT\_2021.162.03

### ABSTRACT:

The issue of brownfields, abandoned and unused sites and buildings, is repeatedly accentuated by the experts with respect to the predominant contemporary urbanistic, environmental, economic or social approaches. Despite the fact that the issue of brownfields was scientifically discussed from various points of view, there are still some general findings that have not been fully covered and processed. One of them is the basic typology of brownfields. The aim of the paper is thus to synthesize the heterogeneous typology of brownfields into a logical and comprehensive framework that would reflect its content and classification comprehensiveness. Such synthesis of typological schemes and their objective categorization into standard classes and groups reflects the general requirements regarding the characteristics of brownfields and enables to define the individual brownfields according to a uniform method and analyze them using the standardized categories. The presented categorization of brownfields is based on the already used classification which is then extended with new groups that are unified in terms of their content. The next part of the paper is the definition of specific types of brownfields such as, for example, blackfield, bluefield or goldfield and others.

**Key-words:** *Bluefield, Blackfield, Greyfield, Goldfield, Whitefield, Brownfield categorization.*

### 1. INTRODUCTION

Brownfields, the reasons for their development, the effects of their existence, resulting issues and suggestions how to deal with them are all current topics both for professional and non-professional discussion across public and private subjects and institutions interested in this issue. Brownfields, withing the current (modern) approach and concerning the economic development and current dynamic enhancement of life quality, are perceived to be a significant, yet a specific feature of regional development and spatial arrangement of the environment in which we live (Turečková et al., 2021). Nowadays, brownfields represent urban specifics of human origin that include abandoned properties that do not serve their original function and are fully or partially unutilized. Alker et al. (2000) or Yount (2003) define brownfield as a property that is underused, neglected, or possibly contaminated, and is the remains of industrial, agricultural, residential, military or other activities. Ferber et al. (2006) define brownfields as the properties that are impacted by their former utilization, are abandoned or unutilized, have potential contamination issues and are usually located in built-up areas (in the vicinity of the settlement areas) and in order to be meaningfully utilized they require active (private or public) intervention. Such properties may be the remains of industrial, agricultural, military, transport, religious, housing and other activities (e.g. community facilities) be it either in the form of land or buildings (sites) that are located anywhere within the cadastral area of the cities and municipalities (Krzystofik, Kantor-Pietraga & Spórna, 2013 or Turečková et al., 2019).

---

<sup>1</sup> School of Business Administration in Karvina, Silesian University in Opava, Univerzitní Nam. 1934/3, 733 40 Karvina, Czech Republic, [tureckova@opf.slu.cz](mailto:tureckova@opf.slu.cz)

Brownfields were researched from various points of view, for example in relation to sustainable development (Vráblík, 2009; Martinát et al., 2016 or Heatherington et al., 2019), urbanism and city planning (Vojvodíková, 2014; Kirschner, 2006; Bergatt Jackson and Votoček, 2010; Navrátil et al., 2018 or Turečková et al., 2018); environmental and geographical aspects (Klusáček et al., 2011; Duží and Jakubínský, 2013; Frantál, 2015; Martinát et al., 2015). A range of studies are dealing with the impact of brownfields on the values of the residential properties in their vicinity (De Sousa, 2000; Mihaescu and vom Hofe, 2012; Sun and Jones, 2013 or Turečková et al., 2017), on the development limits of residential housing in relation to brownfields (Spilková and Šefrna, 2010) or the impact on the existence of brownfields regarding the utilization of unbuilt empty sites in the open countryside (Bartke a Schwarze, 2015).

The list of other implications of the existence of brownfields for other research objects is quite extensive and it is not the purpose of this article to follow this topic. We can conclude that the majority of the papers focusing on the issue of brownfields encourage the process of their regeneration. Abandoned and unused buildings and sites are both objectively and subjectively related to a wide range of undesirable environmental, social and economic effects and impacts that become more urgent with the delay of their regeneration (Turečková and Chmielová, 2018). There are many reasons to get involved in reusing brownfields. Among the key ones are the fact that brownfield regeneration contributes to sustainable urban development (Vráblík, 2009), reduces the negative effects of suburbanization with urban sprawl (Jackson, 2002) and preserves the local, temporal and urban continuity of residential, social and social and environmental structures of the landscape. Reflecting all the above-mentioned the regeneration of brownfields is socially desirable and appropriate (Schädler et al., 2011).

As it was mentioned above, the issue of abandoned and unused buildings and sites is relatively well-known yet it still offers some space for further investigation and scientific research. This paper is focusing on one such overlooked issue related to the existence of brownfields. The paper is not intended to be purely research-focused yet its objective is to synthesise the more or less fragmented typology of brownfields into a uniform, logical and comprehensive framework while maintaining completeness in terms of the content and classification. At this point, however, it is necessary to add that the categorization of brownfields itself is subject to a number of spatial and temporal constraints. Such a synthesis of typological patterns supplemented with definitions of specific types of brownfields has not yet been published (based on the bibliographic search of the domestic and foreign resources) and so it creates a large space for future use. The categories of brownfields created are based on the already used categorization that is extended if necessary and unified in terms of their content. The categorization of specific types of brownfields on „one spot“ including blackfield, greyfield, goldfield, bluefield and whitefield is unique. The above mentioned reflects the motivation why this paper was written.

The paper is divided into five parts. The introductory part is followed by the chapter presenting the applied methodology and introducing the authors who in their concepts of the typology of brownfields created areas that were indirectly adopted or modified by the author of this paper. The third part called Special types of brownfields defines the individual alternative terms used for the concrete types of brownfields such as blackfields, greyfields, bluefields, goldfields and whitefield. The fourth chapter refers to the general categorization of brownfields and suggests ten basic classification areas that can be applied when doing a standard categorization of brownfields. The last part, the Conclusion, closes the paper with a summary of the presented text and states the objective with which the paper was composed.

## **2. METHODOLOGY**

The presented paper is entirely theoretical and it aims to unite, synthesize and categorize brownfields by researching the expert resources of scientific nature, both Czech and foreign, and comparing them according to their most frequently used characteristics, properties and features. The current non-uniform classification as well as the terminological disunity of objectively used types of



brownfields leaves space for unintentional confusion of some of the types of the classification schemes. The unification of the typology of brownfields on „one spot“ will also enable to define the selected brownfield according to the categorization that has not been available up to now to such extent that will be presented in the following chapters of this paper.

The first chapter focusing on the specific types of brownfields is based on the concrete search of authors who provided their expert comments on the given type of brownfield. This traditional scientific approach is combined with information that is specific for these types of brownfields yet represents general knowledge.

The sphere of categorization and classification of brownfields according to various criteria is rather extensive and often overlaps semantically. The traditional classification quoted in the Czech texts mostly comes from the domestic authors such as Kadeřábková and Piecha (2009), Šilhánková et al., (2006) and Dvořáková Lišková, Vojvodíková and Majstríková (2016). And also the following authors like Vráblík (2009), Jankových-Kirschner (2005), Doležalová (2015) or Jackson et al., (2004). Selected categories of brownfields are also specified in the National Brownfield Regeneration Strategy or in Brownfields Handbook (2006), or are mentioned in other documents (e.g. in the individual strategies for brownfield reuse in the regions of the Czech Republic). As far as foreign resources are concerned, the categorization according to the CABERBET project from 2006 is frequently quoted (also termed as ABC model). The presented synthesis of brownfield typology is also based on information from the classification and categorization of brownfields by the selected foreign authors (Norrman et al., 2015; Pizzol et al., 2016; Ferber et al., 2006; Bakker, 2016; Yakhlef and Abed, 2019 or Naveed et al., 2018). It needs to be said that the Czech authors mentioned above also reflect the foreign brownfield typology in their approach as far as the classification of brownfields is concerned which in no way differs from the international concept.

The brownfield categorization stated below was created by a synthesis of three approaches: (1) it applies the already used classification but makes it more specific or partly adjusts it and supplements it; (2) it unifies in terms of terminology and content the objectively identical classification that is used differently by various authors and lastly (3) the author supplements the classification with her own categories that she considers essential as far as the determination of factors and description of individual brownfields are concerned, in particular in the case of analytical work and empirical research focused on brownfields. The categorization scheme presented in **Table 1** (Chapter 4) was compiled through a synthesis of adopted (to a certain extent, yet not fully) brownfield typology from authors and resources mentioned above and own author's invention.

### 3. SPECIAL TYPES OF BROWNFIELDS

To reflect the need to specify brownfields according to their significant characteristics, derived terms that could be used with the word „-field“ were created. Thus the expressions like blackfields, bluefields and others started to be used. These terms represent abandoned and underused sites or buildings (brownfield) with a specific particularity that is directly and immediately specified by using the given „word derivative“. So far we recognize four specific types of brownfields. They are (1) blackfield; (2) greyfield; (3) bluefield; and lastly (4) goldfield (the use of the term „whitefield“ is ambiguous). By contrast, we need to clearly distinguish greenfield (greenfield site) which is the very opposite to brownfield from the urban viewpoint and it represents unoccupied site (undeveloped, unused) with agricultural or farmland (Kibert, 2008) or former natural areas, which after the amendment of the spatial plan was defined as a developing area intended for residential, commercial or industrial development (Institute for Ecopolitics, 2006). Specific types are the so-called derelict greenfields that are represented by abandoned agricultural areas (former gardens, plantations, planted fields, etc.) that were formerly actively used for agriculture but now lie fallow. These areas are the most suitable ones as far as functional transformation is concerned (Krzystofik, Kantor-Pietraga & Spórna, 2013).

By blackfields we understand abandoned areas with an extreme ecological burden that restricts their new use to a significant degree and which considerably increases the costs and/or prolongs the

regeneration process. The ecological burden is characterized mainly by contamination of soil, groundwater and subsurface water or other segments of the environment, as blackfields are mostly of industrial, mining or military origin. Extreme contamination of these sites by toxic or poisonous substances poses a significant risk to the environment and human health, which requires potential immediate intervention and such dangerous and undesirable situation needs to be eliminated. According to Krzystofik, Kantor-Pietraga and Spórna (2013), blackfields are represented by all types of landfills, post-flotation reservoirs, post-mining sites (of coal, some selected minerals or oil) that are chemically or radioactively contaminated, etc. Other sites defined as blackfields are abandoned reservoirs or sites that are heavily contaminated by pesticides or other chemicals used in agriculture, or sites with service or laboratory buildings where undesirable chemicals were used. Blackfield thus represents the worst type of brownfield (**Fig. 1**).

The term greyfield refers to brownfields that surround vast areas of asphalt concrete used as large car parks and transport infrastructure for the nearby sites and buildings (Moeller, 2011). It can be deduced that greyfields are abandoned and malfunctioning sites of public services (especially retail and commercial shopping centres, office buildings or compact residential areas). The reason why they emerged was the relocation of commercial and shopping activities to bigger, more modern shopping areas, and office and housing services to more lucrative areas within the developer projects, mainly in the suburbia. Greyfields do not show a high degree of contamination, do not require costly rehabilitation and thus can be used for new investment without any needless costs. The benefit of greyfields is that they generally have the basic infrastructure (water supply, electricity, heating, gas supply, the site is connected to the sewage system, and another technical and non-technical infrastructure is available) and they are located in the vicinity of the city centres and municipalities. The topicality of greyfield regeneration, especially if supported by the public sector, may reflect the undesirable manifestation of the so-called urban sprawl.



**Fig. 1.** Blackfield Petroleum lagoon in Ostrava, Czech Republic (Source: *idnes.cz; petrol.cz*).

Note: The lagoons were one of the biggest environmental burdens in the Czech Republic. It was a landfill for waste from a refinery and a chemical plant that processed mineral oils. All sludges from oil lagoons have already been mined and the site has been stabilized with lime.

Bluefield is a type of brownfield that is located near the water source and its former function was closely related to the use of water or its regulation (mainly flood control). In this context, Pinch and Munt (2002) emphasise that bluefields are underused buildings located between the mainland and „water space“ (river, lake, sea, etc.). Thus, old ports and quays, piers, docks, shipyards, embankments, slipways, barrages, fishpond drains, clogged raceways and others can be also classified as bluefields. The regeneration of bluefields has its specifics that are reflected in the special water source conservation, in the expanding number of people involved (e.g. Water Stream Management, The Ministry of Agriculture and others are involved in the regeneration process) or in their importance for the infrastructure and transport.

The last type of brownfield, which is the least known yet widely used, is the so-called goldfield. Its potential regeneration presents an extremely profitable investment with a high rate of return. Goldfield is originally a standard brownfield (i.e. it is not goldfield at the very beginning) and it is transformed into goldfield due to an exogenous „change“. This can be a change in spatial planning, in consumers´ behaviour particularly in response to fashion trends or social responsibility, investment incentives and targeted subsidies for companies, newly established effects of urban sprawl, and others. The area of the former Karolina mine near Ostrava city centre is an example of goldfield (**Fig. 2**), which at the same time used to be a typical blackfield due to its high soil contamination (more in Suchacek, 2019). This site became interesting for the investors after its redevelopment had been finished and an urbanistic competition for its reuse was announced. An attractive project in terms of investments resulted in building „a new centre“ of Ostrava that gradually interconnected the Forum shopping centre Nová Karolina, office buildings in Nová Karolina Park and residential houses in Residence Nová Karolina. The site of Nová Karolina presently generates additional income for the investors and at the same time, the locality contributed to the economic development of the region and boosted the attractiveness of the city.



**Fig. 2.** Goldfield Nová Karolina in Ostrava, Czech Republic

(Source: *ostrava.cz; cizp.cz; gemo.cz; fabriky.cz*).

From time to time, the use of the term „whitefield“ can be noticed. The international expert resources do not mention this term, in the Czech scientific environment it is defined by Kadeřábková and Piecha (2009). They define whitefield as a brownfield that will be taken care of by the market itself due to its extremely favourable location. If we establish our definition of whitefield as being the counterpoint to blackfield and broaden it with the above-mentioned feature, we can characterise whitefield as a brownfield that is not contaminated, doesn´t require any involvement of the public sector in its regeneration process, is located in an interesting and desirable locality and is attractive to be reused by the private sector. Unlike goldfield, its financial rate of return and investment attractiveness is much higher. There is another viewpoint that depicts whitefield as a brownfield that was entirely removed and its existence is not apparent at all at present. It can be said that it is the so-called „non-original“ greenfield.

#### 4. CLASSIFICATION OF BROWNFIELDS; STANDARDIZED CATEGORIZATION SCHEME OF BROWNFIELDS

As it was mentioned in the introduction, this part of the paper will be focused on the synthesis of the categorization scheme of brownfields. We aim to unify the diverse typology of brownfields into one complex framework that will reflect the basic characteristics of brownfields that are routinely determined with brownfields. The listing of ten categories in which brownfields can be divided is certainly not comprehensive: there are more aspects according which the brownfields can be classified, yet they are not very frequently used and are regionally specific. This means that they are not uniform and do not meet the requirement that the category is universally accepted.

The basic categorization of brownfields thus refers to (1) their original function including the categorization according to the (economic) sectoral classification; (2) area; (3) location; (4) ownership; (5) contamination and ecological burden. Another categorization takes into consideration the perspective of the potential regeneration and within this homogenous group brownfields can be categorized according to (6) the development point of view (class); (7) development potential; (8) the participant of the potential regeneration; (9) type of financing of the potential regeneration and lastly (10) according to the financial attractiveness of the regenerated brownfield, and these individual categories are logically and factually interconnected, both vertically and horizontally. The individual categories will be specified in more detail further in the text (see **Table 1** or **Fig. 3**).

Based on the economic sector, brownfields are traditionally categorized into three groups that reflect the specific functions that were performed by the original site or building, i.e. which type of activity was carried out there and what had been its purpose before it turned into brownfield (concrete subdivision into individual sectors is based on the standardized international categorization of economic activities NACE Rev. 2, for more e.g. Turečková, 2014). The primary sector refers to the activities related to agricultural production (crop or animal) or raw material extraction (underground or surface). The secondary sector includes mainly the brownfields formerly used for industrial production, transport and distribution services, construction and others. Brownfields that are part of the tertiary sector include abandoned and unused buildings formerly functioning as public facilities (education facilities, hospitals, commercial and cultural centres, buildings for business and tourism, restaurant facilities and others), administrative facilities (logistic and commercial), formerly used for services, residential (flats, housing) and others. The last subgroup (not categorized within the sectors) are military brownfields, former chateaus and religious buildings (monasteries, abandoned cemeteries, churches) that refer to their specific type of ownership rather than their former functionality (these specific brownfields were more or less multifunctional).

Based on the area that they occupy, brownfields can be divided into small (up to 1 ha), middle-sized (1-10 ha), large (10-100 ha) and extensive ones (with an area of more than 1 km<sup>2</sup>). Brownfields can be both found in the urban zones as well as rural zones. To better specify the localization of brownfields within the urban zone, we can divide them according to their location in (1) the central parts of cities (inner city zones), (2) in the suburban zones or within the areas of (3) the countryside settlements (smaller municipalities). Abandoned and unused buildings and sites can also be located (4) outside urban areas (i.e. in the rural zones). We can also classify brownfields based on their ownership, i.e. who is the owner of the specific building or site and is entitled to handle the property. We can differentiate between public ownership (the owner of the property is the state, self-governing unit, other public company or public institution, and others.), private ownership, mixed ownership (not honest) and there may occur a situation when the proprietary rights are not solved at the given moment and the owner is unknown. As contamination and ecological burden are both considered as far as „terminology“ is concerned the identical property of brownfields, we can thus define brownfields (1) without ecological burden – not contaminated, (2) with ecological burden – contaminated, when the level of contamination is specified in more detail and (3) brownfields in which we are not simply aware of any objective ecological burden and we do not know whether the property is contaminated or not; then these buildings and sites may be defined as having „an unknown degree of ecological burden – unknown degree of contamination“.

The description of the second part of the categorization scheme concerning the development potential resulting from the subsequent brownfield regeneration will be directed across the defined groups (horizontally) as such description will reflect more appropriately both the content and factual interconnection of individual types of brownfields: (1) if we consider the building or the site of the present brownfield highly (economically) attractive for its further use that will generate profit after the regeneration or renovation, its development potential is high due to its attractiveness for the private sector which will use private sources (investment) for its regeneration. Such a brownfield may be termed as self-developing as its regeneration results from the activation of its inner potential in response to the requirements of the neighbourhood.

Table 1.

Categorization scheme of brownfields, subdivision and typology.

<b>Brownfields according to the economic sector and former function</b>		<i>primary sector</i>		agricultural mining and extractive	
		<i>secondary sector</i>		industrial and construction transport and infrastructure	
		<i>tertiary sector</i>		logistic, commercial and administrative facilities former public facilities residential and housing facilities others	
		<i>others</i>		religious buildings military former chateaus	
<b>Brownfields according to area</b>	<i>small</i>	up to 1 ha	<b>Brownfields according to location</b>	in the central parts of cities	
	<i>middle-sized</i>	1 – 10 ha		in the suburban areas	
	<i>large</i>	10 – 100 ha		in the countryside settlements	
	<i>extensive</i>	over 100 ha		outside urban area	
<b>Brownfields according to ownership</b>	private ownership		<b>Brownfields according to contamination and ecological burden</b>	without ecological burden	without contamination
	public ownership			with ecological burden	contaminated
	mixed ownership			unknown degree of ecological burden	unknown degree of contamination
	unsettled ownership rights				
↑					
<b>BROWNFIELDS</b>			<b>blackfield greyfield bluefield goldfield</b>		
↓					
<i>prospects of potential regeneration</i>					
↓					
<b>Brownfields according to the development potential</b>					
<i>development class</i>	<i>development potential</i>	<i>active actor</i>	<i>type of funding</i>	<i>project plan (financial attractiveness)</i>	
self-developing	high	private sector	private investment	profitable	
partially developing	medium	collaboration of public and private sector	co-financing of public and private sector	profitable with public support	
passively developing	low	public sector	public sources	noncommercial, socially desirable	
non-developing	none	none	not possible to fund	without plan	

Source: own

The next type (2) represent partially developing brownfields with a medium development potential, which will not be attractive for the private sector, both economically and socially, unless they get „moderate“ (financial and procedural) support from the public sector. For example, the decontamination costs or technical and transport infrastructure expenses will be covered by the public budget – in this way, the brownfield will become potentially more attractive for private investors and at the same time the private sector will allow for lower costs when regenerating this property. The third category (3) are brownfields that are unattractive for the private sector as they would not be able to generate any profit for this sector even in the long run. Here, the public sector should take responsibility, especially on the level of self-governing units, for the regeneration of these brownfields at its own expense provided it is socially desirable and in the public interest. The development potential of these brownfields is low and these properties are passively developing. The last group (4) are brownfields without development potential, the so-called non-developing. Society is indifferent to its existence and there are no undesirable implications for society as a whole. The regeneration of such brownfield is not necessary (is without a plan), not even by the intervention of the public sector.

## 5. CONCLUSION

Brownfields are frequently the subjects of research and it is essential to categorize or divide these abandoned and unused buildings and sites according to the required perspectives for the purposes of further research. Only appropriate and uniform classification of brownfields may predict their appropriate comparability and guarantee their meaningful analysis.

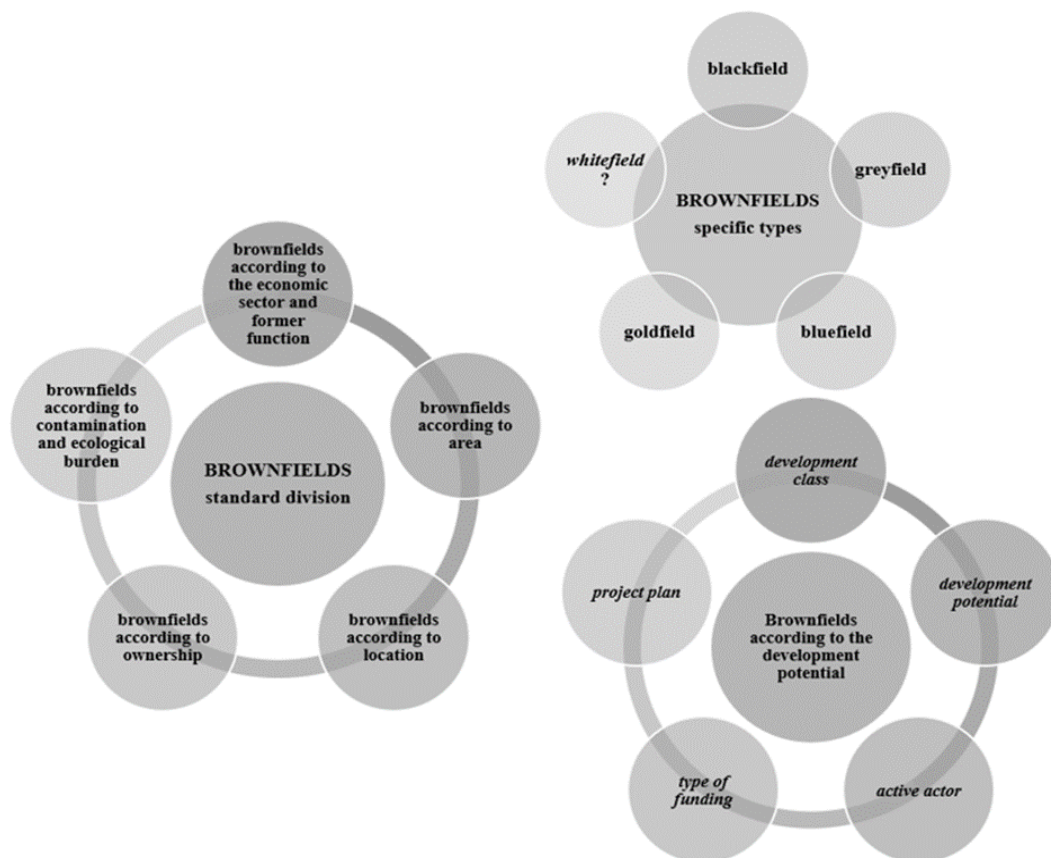


Fig. 3. Scheme of division and typology of brownfields.

Based on a search of relevant resources this paper aimed to synthesize the heterogenous typology of brownfields into a complex and unified scheme that reflects both the content as well as the classification comprehensiveness and the logical interconnectedness of the selected classification of brownfields. This classification concerns the basic categories of brownfields and is subject to spatial, time and functional changes, in particular in the context of quantitative research. The presented categorization scheme defines ten typological groups of brownfields. Such performed synthesis of typological schemes and their objective categorization into standard classes and groups reflects the general requirements regarding the characteristics of brownfields and enables to define the individual brownfields according to a uniform method and further analyse them using the standardized categories.

At the same time, specific types of abandoned and unused buildings and sites were defined and a specific term was used for each of them representing the individual qualities of the individual brownfield. One of them is blackfield that is typical for its high level of concentration of ecological burden, followed by greyfield which is surrounded by vast grey areas of concrete and asphalt formerly used as a car park. Bluefield refers to the interconnection of water areas and sources, and goldfield, which is profitable and attractive for private investors once it has been regenerated as it is supposed to generate substantial profit in the future. These specific types of brownfields were supplemented with whitefield representing the least frequent type of brownfield and its existence is still controversial among the experts. Such comprehensive categorization of brownfields has never been published so far. In the field of further research, the specified categorization of brownfields can be used in the creation of databases, time and spatial comparison or in combination with other quantitative-statistical methods (cluster, factor, correspondence analysis, etc.).

In conclusion, it is essential to say that the categorization of brownfields may be approached from a broader perspective and they can be defined based on viewpoints that reflect the local needs or the needs of the concrete research plans. Their variability and quantity are extensive and it was not the aim of this paper to mention it here. The criterium for the selection of the above-mentioned classification scheme was uniformity, general applicability and the requirement to be the most frequently quoted brownfield classification among the relevant expert resources.

## ACKNOWLEDGMENT

This paper was supported by the project SGF/7/2020 „The measures of the public sector for the strengthening of the regeneration potential of brownfields in the area of the Czech Republic“.

## REFERENCES

- Alker, S., Joy, V., Roberts, P. & Smith, N. (2000) The definition of brownfield. *Journal of Environmental Planning and Management*, 43 (1), 49-69. ISSN: 0964-0568. DOI 10.1080/09640560010766
- Bartke, S. & Schwarze, R. (2015) No perfect tools: Trade-offs of sustainability principles and user requirements in designing support tools for land-use decisions between greenfields and brownfields. *Journal of environmental management*, 153, 11-24.
- Bergatt Jackson, J. & Votoček, J. (2010) Metodika inventarizace brownfieldů v úrovni ORP. Available from: <http://www.usti-nadlabem.cz/files/Metodika.pdf> [Accessed February 2021].
- Brownfields příručka, (2006) Brownfields příručka. Available from: [http://fast10.vsb.cz/lepob/index2/handbook\\_cz\\_screen.pdf](http://fast10.vsb.cz/lepob/index2/handbook_cz_screen.pdf) [Accessed February 2021].
- De Sousa, C. A. (2003) Turning brownfields into green space in the City of Toronto. *Landscape and urban planning*, 62 (4), 181-198.
- Duží, B. & Jakubínský, J. (2013) Dilemma of Brownfields Redevelopment in Post-Communist Cities. The Case Study of Ostrava: the Czech Republic. *Human Geographies*, 7 (2), 53-64. ISSN 1843-6587
- Dvořáková Lišková, Z., Vojvodíková, B. & Majstříková, T. (2016) *Základy brownfieldů v ekonomických souvislostech*. Praha: Jihočeská univerzita v Českých Budějovicích.
- Ferber et al. (2006) Sustainable brownfield regeneration: CABERNET network report. Nottingham: University of Nottingham.

- Frantál, B. (2015) Have local government and public expectations of wind energy project benefits been met? Implications for repowering schemes. *Journal of Environmental Policy & Planning*, 17 (2), 217-236.
- Heatherington, C., Jorgensen, A. & Walker, S. (2019) Understanding landscape change in a former brownfield site. *Landscape research*, 44, (1), 19-34. DOI: 10.1080/01426397.2017.1374359
- Jackson, J. B. et al. (2004) Brownfields snadno a lehce: Příručka zejména pro pracovníky a zastupitele obcí. IURS – Institut pro udržitelný rozvoj sídel o. s.
- Jankových-Kirschner, V. (2005) Klasifikace brownfields: Studie k disertační práci regenerace brownfields. Praha: České vysoké učení technické. Fakulta Architektury.
- Kadeřábková, B. & Piecha, M. (2009) Brownfields: jak vznikají a co s nimi. Praha: C. H. Beck.
- Doležalová, L. (2015) Regenerace brownfieldů: vývoj politik a příklady realizací. Praha: IREAS, Institut pro strukturální politiku.
- Kibert, Ch. J. (2008) Sustainable Construction: Green Building Design and Delivery. Hoboken: John Wiley & Sons. ISBN978-0-470-11421-6
- Kirschner, V. (2006) Regenerace brownfields jako odpověď na zastavování krajiny kolem měst. *Urbanismus a územní rozvoj*, 9 (2), 34–39. ISSN 1212-0855
- Klusáček, P., Krejčí, T., Kunc, J., Martinát, S. & Nováková, E. (2011) The post-industrial landscape in relation to local self-government in the Czech Republic. *Moravian Geographical Reports*, 19 (4), 8-28. ISSN 1210–8812
- Krzystofik, R., Kantor-Pietraga, I. & Spórna, T. (2013) A Dynamic Approach to the Typology of Functional Derelict Areas (Sosnowiec, Poland). *Moravian Geographical Reports*, 21 (2), 20-35.
- Martinát, S. et al. (2015) Spatial relations and perception of brownfields in old industrial region: case study of Svinov (Ostrava, Czech Republic). *Organization and Environment*, 27 (2), 181-201. ISSN: 1086-0266
- Martinát, S., Dvořák, P., Frantál, B., Klusáček, P., Kunc, J., Navrátil, J., Turečková, K. & Reed, M., (2016) Sustainable urban development in a city affected by heavy industry and mining? Case study of brownfields in Karvina, Czech Republic. *Journal of Cleaner Production*, 118 (1), 78–87.
- Mihaescu, O. & vom Hofe, R. (2012) The impact of brownfields on residential property values in Cincinnati, Ohio: A spatial hedonic approach. *Journal of Regional Analysis & Policy*, 42 (3), 223-236.
- Moeller, D. W. (2011) Environmental Health. 4th ed. London: Harvard College. ISBN 978-06-74047-40-2
- Naveed, A., Zhu, Y., Ibrahim, M., Waqas, M. & Waheed, A. (2018) Development of a Standard Brownfield Definition, Guidelines, and Evaluation Index System for Brownfield Redevelopment in Developing Countries: The Case of Pakistan. *Sustainability*, 10 (4347).
- Navrátil, J., Picha, K., Martinát, S., Nathanail, P. C. Turečková, K. & Holešínská, A. (2018) Resident's preferences for urban brownfield revitalization: Insights from two Czech cities. *Land Use Policy*, 76 (1), 224-234. ISSN: 0264-8377. DOI: 10.1016/j.landusepol.2018.05.013.
- Pinch, P. & Munt, I. (2002) Blue Belts: An Agenda for 'Waterspace' Planning in the UK. *Planning Practice and Research*, 17 (2), 159-174.
- Pizzol, L., Zabeo, A., Klusáček, P., Giubilato, E., Critto, A., Frantál, B., Martinát, S., Kunc, J., Osman, R. & Bartke, S. (2016) Timbre brownfield prioritization tool to support effective brownfield regeneration. *Journal of Environmental Management*, 166, 178-192.
- Schädler, S., Morio, M., Bartke, S., Rohr-Zänker, R. & Finkel, M. (2011) Designing Sustainable and Economically Attractive Brownfield Revitalization Options Using an Integrated Assessment Model. *Journal of Environmental Management*, 92 (3), 827-837.
- Spilková, J. & Šefrna, L. (2010) Uncoordinated new retail development and its impact on land use and soils: A pilot study on the urban fringe of Prague, Czech Republic. *Landscape and Urban Planning*, 94 (2), 141-148.
- Sun, W. & Jones, B. (2013) Using multi-scale spatial and statistical analysis to assess the effects of brownfield redevelopment on surrounding residential property values in Milwaukee County, USA. *Moravian Geographical Reports*, (2), 56-64.
- Šilhánková, V. et al. (2006) Rekonverze vojenských brownfields. Pardubice: Univerzita Pardubice.
- Turečková, K. (2014) Quaternary sector as a source of growth and competitiveness in the EU. In: Proceedings of the 2nd International Conference on European Integration 2014. Ostrava: VŠB-TU Ostrava, 723-730.
- Turečková, K. & Chmielová, P. (2018) Brownfieldy v regionálním rozvoji a v externalitní teorii. In: XXI. mezinárodní kolokvium o regionálních vědách. Brno: MU ESF Brno, 302-308. ISBN 978-80-210-8969-3



- Turečková, K., Martinát, S., Škrabal, J., Chmielová, P. & Nevima, J. (2017) How local population perceive impact of brownfields on the residential property values: some remarks from post-industrial areas in the Czech Republic. *Geographia Technica*, 12 (2), 150-164.
- Turečková, K., Nevima, J., Škrabal, J. & Martinát, S. (2018) Uncovering patterns of location of brownfields to facilitate their regeneration: Some remarks from the Czech Republic. *Sustainability*, 10 (6), 224-234.
- Turečková, K., Nevima, J., Škrabal, J. & Tuleja, P. (2019) Categorization of Impact of the Selected Variables for Potential Brownfield Regeneration in the Czech Republic by Means of Correspondence Analysis. *Geographia Technica*, 14 (2), 120-130.
- Ústav pro ekopolitiku, o. p. s. (2006) Revitalizace „brownfields“v ČR. Available from: <http://www.ekopolitika.cz/cs/brownfields/revitalizace-brownfields-v-cr.html> [Accessed January 2020].
- Vojvodíková, B. et al. (2014) *Brownfieldy – a co s nimi souvisí*. Praha: European Science and Art Publishing. ISBN 978-80-87504-23-9
- Vráblík, P. et al. (2009) Metodika revitalizace území pro hospodářský, sociální a environmentální rozvoj v postižených regionech. Available from: [http://fzp.ujep.cz/projekty/wd-44-07-1/dokumenty/dc03/DC003\\_Metodika\\_revitalizace\\_uzemi.pdf](http://fzp.ujep.cz/projekty/wd-44-07-1/dokumenty/dc03/DC003_Metodika_revitalizace_uzemi.pdf) [Accessed February 2019].
- Yakhlef, M. & Abed, A. (2019) Identification of Brownfield Sites, Classification and Typologies Case Study of Amman, Jordan. *Journal of Engineering and Applied Sciences*, 14 (10), 3144-3149.
- Yount, K. R. (2003) What are brownfields? Finding a conceptual definition. *Environmental Practice*, 5 (1), 25-33.
- Suchacek J. (2019) The Benefit of Failure: On the Development of Ostrava's Culture. *Sustainability*, 11 (9), 2592. <https://doi.org/10.3390/su11092592>
- Turečková, K., Nevima, J., Duda, D. & Tuleja, P. (2021) Latent Structures of Brownfield Regeneration: A Case Study of Regions of the Czech Republic. *Journal of Cleaner Production*, 311(127478). DOI: <https://doi.org/10.1016/j.jclepro.2021.127478>.
- Jackson, J. (2002) Urban Sprawl. *Urbanismus a území rozvoj*, 5 (6), 21-28.
- Norrman, J. et al. (2015) BALANCE 4P: Balancing decisions for urban brownfield redevelopment. Available from: [https://publications.lib.chalmers.se/records/fulltext/231843/local\\_231843.pdf](https://publications.lib.chalmers.se/records/fulltext/231843/local_231843.pdf) [Accessed May 2021].
- Bakker, J., Frangopol, D. M. & van Breugel, K. (2016) Life-Cycle of Engineering Systems: Emphasis on Sustainable Civil Infrastructure. In: *Proceedings of the Fifth International Symposium on Life-Cycle Civil Engineering (IALCCE 2016)*, 2016. Delft, The Netherlands.

## USING BIG GLOBAL DATABASE TO ANALYSE IMPACT OF WEB NEWS TO TOURIST VISITS DUE TO THE 2017 ERUPTION OF AGUNG VOLCANO, BALI, INDONESIA

Putu Perdana Kusuma WIGUNA<sup>1</sup>

DOI: 10.21163/GT\_2021.162.04

### ABSTRACT:

Bali Island, well known as The Island of The Gods, is a top tourist destination. In 2017, Agung Volcano eruption causes lots of tourist canceled their visits to Bali due to excessive news about the danger to travel to Bali. This was the first research conducted to analyses impact of volcanic disaster to tourist visits using big data in Bali, Indonesia. This research uses big global database or big data to analyses the impact of web news to tourist visits to Bali due to Agung volcano eruption. Big data is a term that describes the large volume of data, both spatial and non-spatial that inundates the world on a day-to-day basis. Big data in this research were processed from The Global Database of Events, Language, and Tone (GDELT) Project. GDELT project monitors the world's broadcast, print, and web news from nearly every corner of every country creating a free open platform for computing on the entire world. The purpose of this research is to analyses the impact of Agung Volcano eruption to tourist visits to Bali in 2017. Every news data sets from every country, filtered, calculated and spatially analyzed to discover the timeline and impact of Agung Volcano eruption on tourist visits to Bali in 2017. Geographic Information Systems (GIS) were used for calculation and spatial analysis. The result shows that the number of tourist visits were declining in October and November 2017 but raised again in December. November has the highest number of news related to the eruption. After the eruption in December, the number of tourist visits start to rising due to the operational of the airport. The declining caused by shutdown of Bali airport and travel warning policy from foreign country for their citizen to not to travel to Bali. Even though the number of tourists is declining in October and November, number of tourists visit on the same period in 2017 were higher than 2016.

**Key-words:** *Agung Volcano eruption, tourist visits, big data*

### 1. INTRODUCTION

In the last few years big data has getting great prominence at international arena and gaining momentum at academies, industries and other institutions. The concept of big data emerged in the scientific fraternity in the mid-1990s and become the focal point during 2008-2010. Big data including geospatial big data has so much to offer to the society in meteorology, diagnostics, disaster management, logistics, and so on (Kamali & Augasta, 2017). As per the available data 80% of the same is geo referenced i.e., which shows the importance of geospatial big data handling. Geospatial data or spatial data is nothing but the information of a physical object, defined by values in a coordinate system. In common man's language, geospatial represents the location, size and shape of an object on earth such as a country, rivers, towns or skyscrapers (Shu, 2016).

Geospatial data collection is shifting from a data sparse to a data rich paradigm. Whereas some years back geospatial data capture was based on technically demanding, accurate, expensive and complicated devices, where the measurement process was itself sometimes an art, we are now facing a situation where geospatial data acquisition is a commodity implemented in everyday devices such as smartphones used by many people. These devices are capable of acquiring environmental geospatial information at an unprecedented level with respect to greatly improved geometric accuracy, temporal resolution and thematic granularity. They are small, easy to handle, and able to acquire data even unconsciously (Li, et al., 2016).

---

<sup>1</sup> Udayana University, Faculty of Agriculture, Indonesia, [wiguna@unud.ac.id](mailto:wiguna@unud.ac.id)

This data capture paradigm is similar to the situation in topographic data collection for digital terrain models by capturing significant topographic points with morphological characteristics on the one hand ( “qualified” points, i.e., points with semantics) - as opposed to the collection of point clouds using LiDAR sensors or stereo matching, leading to masses of “unqualified” points. The first approach requires manual selection and measurement and guarantees that the topographic reality can be interpolated from the sparse measurements. The second approach assumes that the topographic reality is captured by the dense measurements and can be reconstructed from them - thus the object formation and identification are shifted to the analysis process (Li, et al., 2016).

Another important feature of big data that makes it prevalent is that it provides extraordinary fine-grained detailed data in terms of analysis units, spatial, and temporal resolution. For instance, smart card and mobile phone data are collected at the individual level (Richardson, et al, 2013). Such data can be observed at short intervals, for example, on a per-hour basis. Data with fine analysis units offer a significant chance for rigorous and accurate research because researchers can examine the causal relationship in a small analysis unit and avoid ecological fallacy and the other issues caused by data aggregation (Robinson, 2009). The rapid growing flood of big data, originating from the many different types of sensors, messaging systems and social networks in addition to more traditional measurement and observation systems, have already invaded many aspects of our everyday existence. Big data, including geospatial big data, has great potential to benefit many societal applications such as climate change, disease surveillance, disaster response, monitoring critical infrastructures, transportation and so on (Li, et al., 2016).

Big data generated from geo-informatics and remote sensing platforms can contribute to early warning systems for disasters. Geographical Information Systems (GIS), Global Positioning Systems (GPS) and environmental monitoring sensors with cloud services have a potential to predict disasters such as snowmelt floods and earthquakes (Fang, et al., 2015, Buribayeva, et al., 2015). Geo-informatics information along with transportation network data can benefit to understand human mobility patterns during disasters (Song et al., 2015). Whereas, social media (e.g., twitter) offers autonomously distribution of disaster awareness and can provides near to real time information of the occurrence of disasters (Cen, et al., 2011, Grolinger, et al., 2013, Choi & Bae, 2015).

Big data has a significant role in all phases of disaster management. Big data from sensor networks, social media, and from other sources are available and shows its usefulness in disaster management already. These big data help policy makers and first responders to come with quick and concrete decision on the number of people affected, type and nature of the damage and where to allocate the resource (Rahman et al., 2017). In recent years, the literature on disaster management mostly focused on the potential that lies in using specific kinds of data for natural disaster management (Cinnamon, et al., 2016, Erdelj, & Natalizio, 2016, Dos Santos Rocha, 2016)

One of big data platform that provides free data related to news and event around the globe is GDELT Project. GDELT or Global Data on Events, Language, and Tone is one such source where data is aggregated from various newspaper sources around the globe. GDELT database is updated with more than 30,000 events a day; hence it remains current with respect to the important events in the world on daily basis. One of the important events that aggregated at GDELT database is disaster occurrence around the globe (Leetaru, & Schrodt. 2013, Keertipati et al., 2014).

One of major disaster event in 2017 is Agung Volcano eruption in Bali Island, Indonesia. Bali Island, despite having one of the active volcanos in Indonesia, also well-known as the best tourist island in the world. Bali has been crowned the world's favourite destination by Trip Advisor (Paris, 2017, Nurhayati, 2017, Christo, 2017). The threat of Agung Volcano eruption has provided a direct example of how natural disasters shock Bali tourism. Thousands of tourists were affected by the eruption due to airport closing, flight cancelation and travel warning (Rahmawati et al, 2019). Overall, the eruption had an impact on many tourists cancel their visit to Bali. This research on using big global database to analyze disasters was the first research and it has never been conducted in Bali. Using the GDELT database, this research aims to filters news on the Agung Volcano eruption and try to understand the effect of news of the eruption to the number of tourist visits to Bali, Indonesia.

## **2. LITERATURE REVIEW**

### **2.1. Agung Volcano**

Agung volcano is Bali's highest and most sacred mountain, towers over the eastern end of the island, in Karangasem Regency. The Agung volcano, whose name means "Paramount," rises above the SE caldera rim of neighboring Batur volcano, and the northern and southern flanks extend to the coast. The summit area extends 1.5 km E-W, with the high point on the W and a steep-walled 800-m-wide crater on the E. The Pawon cone was located low on the SE flank. Only a few eruptions dating back to the early 19th century have been recorded in historical time. The 1963-64 eruption, one of the largest in the 20th century, produced voluminous ashfall along with devastating pyroclastic flows and lahars that caused extensive damage and many fatalities (Global Volcanism Program, 2018).

Increases in seismic activity were first noted at Agung Volcano during mid-August 2017. Exponential increases in the rate of events during the middle of September led PVMBG to incrementally raise the Alert Level from I to IV (lowest to highest) between 14 and 22 September. Steam-and-gas emissions were intermittently observed 50-500 m above the summit crater from the end of September through October, with occasional bursts as high as 1,500 m. Seismicity dropped off almost as quickly as it rose, beginning on 20 October, and then continued a more gradual decrease through the end of the month and into November. The number and intensity of hot spots observed within the summit crater increased during September, then levelled off during October. Ash emissions first appeared on 21<sup>st</sup> of November, rising to 700 m above the summit. Ash density and heights of plumes increased several times during the rest of November to about 3,000 m. Ashfall as deep as 5 mm affected neighboring communities, and was reported several hundred kilometers from the summit; the international airport about 60 km SW was forced to close for a few days at the end of the month. Thermal data indicated effusion of lava into the summit crater at the end of November. After 30 November, emissions continued, primarily comprised of steam and gas, with intermittent plumes of dense ash, rising up to 2.5 km above the summit throughout December (Global Volcanism Program, 2018).

### **2.2. Bali Tourism**

Bali tourism has become a world-famous tourist destination all over the world. It is proven that the visit of foreign tourists and domestic tourists to Bali from year to year is increasing (Antara & Sumarniasih, 2017, Anom, et al., 2020). However, it is not only tourist visits for vacation that cause the development factor of tourist visits to Bali to increase, but the frequent holding of international events is also one of the development factors for the increase in visits.

The attraction of Bali tourism is not only found in the arts and culture of the Balinese people, but also in the natural beauty such as white sand beaches, sunset views and mountain views (Arismayanti, 2017). Bali's natural tourism with the beautiful natural scenery such as in Kuta Beach, Jimbaran, Uluwatu, Kintamani, Lake Batur and towering Mount Batur, Gitgit Waterfall Tourism Object, Natural Hot Springs, is the main attraction for most tourists, for a vacation to the island of Bali.

Bali also has uniqueness in culture that become a very interesting tourist attraction (Wesnawa, 2017, Pratiwi, et al., 2019). Local traditional village or ancient Bali village such as Tenganan, Trunyan, Penglipuran and others has uniqueness that are different from another traditional village in the world.

For nature lovers, adventure tourism in Bali is one of the best. Climbing to the top of the highest volcano in Bali, Agung Volcano will provide many valuable experiences. This activity is indeed favored by foreign and domestic tourists. Ascent to the highest mountain in Bali with a start point at the cultural location of Pasar Agung Temple or from Besakih Temple and then climb to peak to enjoy sunrise. Tours to Agung Volcano, the active volcano in Bali, which located in Rendang District, Karangasem Regency, are certainly a special moment for tourists. Agung volcano is also believed to be a sacred mountain in Bali (Mudana, et al., 2018).

Beside adventure tourism, the nearby popular tourist location are Besakih Mother Temple, Pasar Agung Temple, Sidemen village and recreational rafting on the Telaga Waja river. Tourists who take part in group tours can also take the time to stop by to some of these attractions and feel the unique nature beauty and village life.

### **2.3. Global Data on Events, Language, and Tone (GDELТ) Database**

GDELТ Data is the largest, most comprehensive, and highest resolution open database ever created. Just 2015 data alone has recorded nearly three-quarters of a trillion snapshots and over 1.5 billion location references, making it one of the largest spatial-temporal data sets in existence and encouraging studies using freely available big data. GDELТ's Global Knowledge Graph (GKG) connects the people, organizations, locations, themes, numbers, images and emotions into one holistic network across the planet. Each GKG record is a pairing of a set of names, events, counts, actors, locations, themes, and tones (GDELТ, 2019, Hopp, et al., 2019).

The GDELТ project is an ongoing effort to monitor print, broadcast and web news in more than 100 languages from around the world and to keep them updated. GDELТ is moving beyond the focus of Western media towards a much more global perspective on what is happening in the world. The GDELТ project created by Kalev Leetaru of Georgetown University in collaboration with Google, BBC Monitoring, National Academies Keck Futures Program, LexisNexis Group, JSTOR, DTIC, and the Internet Archive (GDELТ Project, 2019).

The GDELТ Events Database records more than 300 categories of activity worldwide, from riots and protests to peace calls and diplomatic exchanges. The existing database consists of more than 2.5 TB of available information per year with more than a quarter of a billion records. The platform covers data from 1979 to the present, and is updated every 15 minutes, meaning that there is a continuous stream of records being entered into the database. (GDELТ Project, 2019).

### **2.4. Previous Research**

So far, only a few scholars have conducted research in utilizing GDELТ to make predictions about disaster. Previous research showed that GDELТ database has used to analyses natural disasters, as demonstrated for Nepal earthquake (Yu, et al., 2016) and hurricanes (Owuor, et al., 2020). Yu, et al., (2016) was using GDELТ to show the dynamics of people's attention to Nepal earthquake. In addition, also using other datasets to analyses funds and donation related to the earthquake reconstructions process. Available dataset and surveys from citizens in affected areas along with the reconstruction dataset help capture and explain the efforts that the international and local organizations and governments have put on the post-earthquake relief, and its effectiveness. Owuor et al., (2020) was comparing GDELТ data and geo-tagged tweets related to hurricane in Dorian in South-Eastern USA and then statistically analyzed the distance between daily GDELТ events, tweets, and the hurricane center in different days. It assesses the potential role of geographic coverage in the hurricane prediction map on the level of event related news and tweeting activities.

Tourism is shaped by a wide range of factors and forces, including exogenous ones that have no direct link with the tourism sector. Natural disasters and unexpected events are prime examples of such determining factors, as they have profound effects on tourism flows considerably. A volcanic disaster can affect tourism for obvious reasons because there is a very close link between tourism and natural disasters. In the event of a natural disaster tourism is significantly disrupted and in many cases the industry is destroyed, requiring redevelopment and adjustment (Gaudru, 2014, Rosello et al., 2020). GDELТ database has never been used for volcanic disaster analysis, especially related to volcanic eruption and the effect on tourism in Bali. The news about volcanic eruptions may affects tourist to cancel their arrivals to Bali. It is interesting to analyzed whether the news were able to influence tourists to cancel their visit to Bali which lead to reducing number of tourist visits.

### 3. STUDY AREA

Area of study is Bali Province, Republic of Indonesia; with the capital city is Denpasar City. Bali Province is an island which famously known as The Island of the Gods (Tallon, 2013, Parimartha et al., 2016). Bali is a small island around 5,636.66 Km<sup>2</sup> which divide into 8 Regency and one Municipality. Total population from 2017 about 3,890,757 inhabitants. Its major potential economic development are emphasized on tourism and agriculture (Center Bureau of Statistics of Bali Province, 2017). **Fig 1.** shows the map of Bali Province.



**Fig. 1.** Map of Bali Island on OSM Basemap.

### 4. DATA AND METHODS

The research materials were GDELT Project's GDELT 1.0 Global Knowledge Graph (GKG) data of 2017 (The GDELT Project, 2017) and tourist visits data of 2016 and 2017 from Centre Bureau of Statistics (BPS) of Bali Province. The research tool is computer with office tool and GIS software.

GKG dataset offers various fields to describe the characteristics of natural and man-made disasters, such as the type of a disaster, the number of news articles reporting the disaster, the number of victims, and the location where the disaster occurred (Kwak and An, 2014). GDELT Project's daily GDELT 1.0 Global Knowledge Graph (GKG) data of 2017 which available to download freely then sorted out to find the related news about Agung Volcano eruption from all around the world. This data then visualized and analyzed to find the relation between the Agung Volcano eruption news and tourist visits to Bali province. Before data visualization process, news extraction carried out to prevent hoax news by ascertaining the source of the news and its author as well as tracing the sources cited in the news. Hoax news related to disasters will be different from other news in terms of themes and content.

The extraction started by identifying all GKG records falling under the “AGUNG” and “ERUPTION” theme. Based on this theme, the Event mentions table was searched for AGUNG ERUPTION related articles during the study period. GDELТ entries in the Events table were filtered to WORLDCITY and WORLDSTATE. Each location in the GKG comes with a latitude/longitude pair which represents the centroid of the location (Owuor, et al., 2020).

Data analysis including creation of spatial analysis and non-spatial analysis including Attribute Query, Spatial Query and Generation of new data sets from the original database. Attribute query including creation of new non-spatial attribute from the GKG data, spatial query including creation of point data of the location distribution of news source related to Agung volcano eruption and generation of new data sets from the spatial query and non-spatial query.

Data on tourist visits before and during the eruption of Agung Volcano, in 2016 and 2017, was obtained through the news portal from the Central Bureau of Statistics (BPS) of the Province of Bali and information from the Tourism Office of the Province of Bali. Monthly tourist visit data will be matched with the amount of news about the eruption of Agung Volcano to find out whether news about the eruption of Agung Volcano affects the number of tourist visits to Bali.

## 5. RESULTS AND DISCUSSIONS

There were 9492 news related to Agung Volcano eruption from 231 countries in 2017. As much as 1014 news (10.6%) were came from top 10 countries of Indonesia, Japan, United Kingdom, Australia, China, Italy, India, France, Russia and Canada. **Fig. 2** shows the spatial distribution of news related to Agung Volcano Eruption.

Using heatmap analysis, the most news were coming from Indonesia, with other were distributed in South East Asia, South Asia, Europe, North America and Australia. Africa and South America were less contributed to the news to Agung Volcano eruption. **Fig. 3** shows the heap map of news distribution related to Agung Volcano Eruption. The news related to Agung Volcano eruption started in 14<sup>th</sup> of September 2017. The news mainly about the raised alert level for the Agung Volcano in Bali following an increase in seismic activities and volcanic earthquakes.

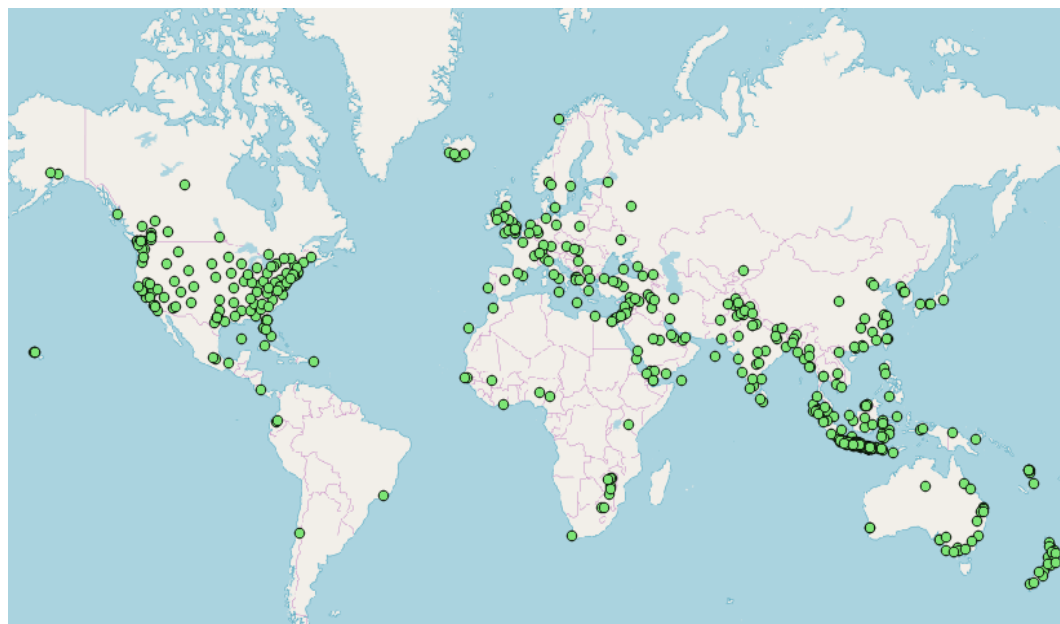


**Fig. 2.** Spatial Distribution of News Related to Agung Volcano Eruption.



The National Disaster Mitigation Agency said the alert has been raised and recommends villagers to stay further than 6 kilometers (3.8 miles) from the mountain's crater (Chosunilbo & Chosun, 2017, Phys.org, 2017, The Daily Mail, 2017, The Hindu, 2017, The Washington Times, 2017, Marboen, 2017). The highest number of news posted in September started from 22<sup>nd</sup> until 30<sup>th</sup> with the highest number of news was on the 26<sup>th</sup> with total of 320 news. The news mainly focused on Indonesian Government that raised the alert level for a volcano to the highest level with more than 11,000 villagers have left their homes around the mountain and more evacuations were expected (Astro Awani, 2017, Belfast Telegraph, 2017, Calgary Herald, 2017, Whiteside, 2017).

In October, from the 1<sup>st</sup> until 6<sup>th</sup> the news the news related to Agung Volcano generally focused on the evacuees who live outside the immediate danger zone to return home. The status of Agung Volcano was lowered on the 29<sup>th</sup> of October. A statement by the Indonesian National Agency for Disaster Management said evacuated residents within the designated hazard should stay put, but villagers outside the hazard zone could safely go home but should not venture close to the crater, which was still emitting smoke (Arkansas Online, 2017, Fox News, 2017, Humanitarian News, 2017, Mail Online, 2017, Relief Web, 2017, The Denver Post, 2017).

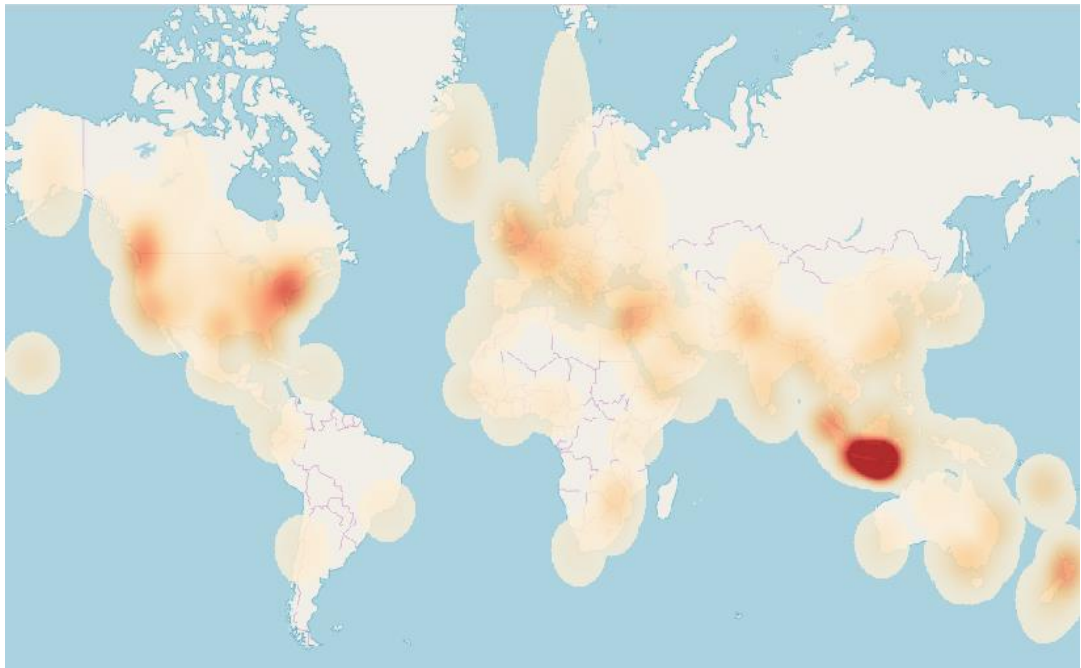


**Fig. 3.** The Heap Map of News Related to Agung Volcano Eruption.

In November, the news related to Agung Volcano eruption started from the 21<sup>st</sup> until 30<sup>th</sup> and peaked at 27<sup>th</sup> with 1646 news. The first three weeks of November there were no significant activity of Agung Volcano. At 21<sup>st</sup> of November the first ash emission was appeared, rising to 700 m above the summit (Global Volcanism Program, 2018). The news from 21<sup>st</sup> until 26<sup>th</sup> of November mainly about the eruption of Agung Volcano which releasing ash and smokes from crater producing imminent heavy ash rain. Volcanologists say the eruption was caused by magma heating water, or phreatic eruption, rather than a generally more dangerous eruption of magma itself. The Energy and Mineral Resources Ministry's Volcanology and Geological Hazard Mitigation Center (PVMBG) reported that Agung Volcano has erupted, releasing volcanic ashes and smoke from the crater. The eruption occurred at 5.05 p.m. local time, with grey smoke rising about 700 meters from the crater. From 27<sup>th</sup> until 30<sup>th</sup> of November, the world pays attention on the Agung Volcano eruption and the shuts down Bali and Lombok airport. The volcano has shifted from steam-based eruptions to



magmatic eruptions. Indonesian authorities raised the alert for a rumbling volcano to the highest level on Monday and closed the international airport including international airport on the neighboring island of Lombok. At 30<sup>th</sup> of November, the airport re-opens even though Agung Volcano still erupted. The exclusion zone around the crater was widened to 10 kilometers (6 miles). Previously it ranged between 6 kilometers and 7.5 kilometers (ABC 57 News, 2017, France 24, 2017, Oman Daily Observer, 2017, The Indian Express, 2017, The Star Online, 2017, World Buletin, 2017).

The news of Agung Volcano eruptions in December began with 318 news on the 1<sup>st</sup> day and declining until reached 45 news on the 8<sup>th</sup>. The news in December were mainly about the Agung volcano was calm, emitting only a thin column of sulfuric steam. The volcano’s alert remains at the highest level but Bali is safe except for the 10-kilometre exclusion zone. Bali international airport was operating normally. From the second week of December the news were mainly about the European Union support to Agung Volcano eruptions victim and the effect of the disaster to tourism in Bali. Indonesia Coordinating Minister for Maritime Affairs Luhut Pandjaitan said that Bali was safe for those spending yearend holiday as volcanic impacts from Agung Volcano will not affect tourism spots (Asia Pasific Daily, 2017, European Council, 2017, Fresh News Asia, 2017).

November has the highest number of news related to agung Volcano eruption. As much as 5852 news (61.65%) from around the world were posted in November, followed by September with 2057 news (21.67%) and December with total of 1125 news (11.85%). The lowest number of news were in October with total of 458 news related to Agung Volcano eruption **Table 1** shows the number of news related to Agung Volcano eruption. **Fig. 4** shows daily number of news related to Agung Volcano eruptions.

**Table 1.**

**Number of News Related to Agung Volcano Eruption.**

Month	Number of News	% of News
...	0	0
Sep	2057	21.67
Oct	458	4.82
Nov	5852	61.65
Dec	1125	11.85
<b>TOTAL</b>	<b>9492</b>	<b>100</b>

Agung Volcano eruption last for 4 months from September until December 2017. Many news agencies have reported the development of the eruptions and analyses the impact to tourist visits to Bali. Travel warning, airport closed and flights were several factors that might affect the tourist visits to Bali especially on the holiday seasons in December. Based on data of tourist visits to Bali from Center Bureau of Statistics of Bali Province and Tourism Office of Bali Province, at the peak of Agung Volcano eruptions in November, total tourists visit to Bali was 741,649 compared to 655,962 tourists in November 2016. In December, total tourist visits were 939,048 compared to 882,026 in December 2016. This number was smaller compared to September 2017 with total tourist visits reached 832,026. Total 8,643,680 tourist was visiting Bali in 2016 and total 8,735,633 was visiting Bali in 2017. This indicates that the number of tourists that visiting Bali was increasing. Table 2 shows the number of tourists visit to Bali in 2016 and 2017 compared to the number of news related to Agung Volcano eruption. At the start of the news about Agung Volcano at 14<sup>th</sup> of September, there were no significant decline in tourist visits. This is because tourists were already in Bali. During the closing of the Airport lot of tourists were unable to come back to their country of origin. At the peak of Agung Volcano eruption in November 2017, the number of tourists was declining as the news of Agung Volcano eruptions were increasing.

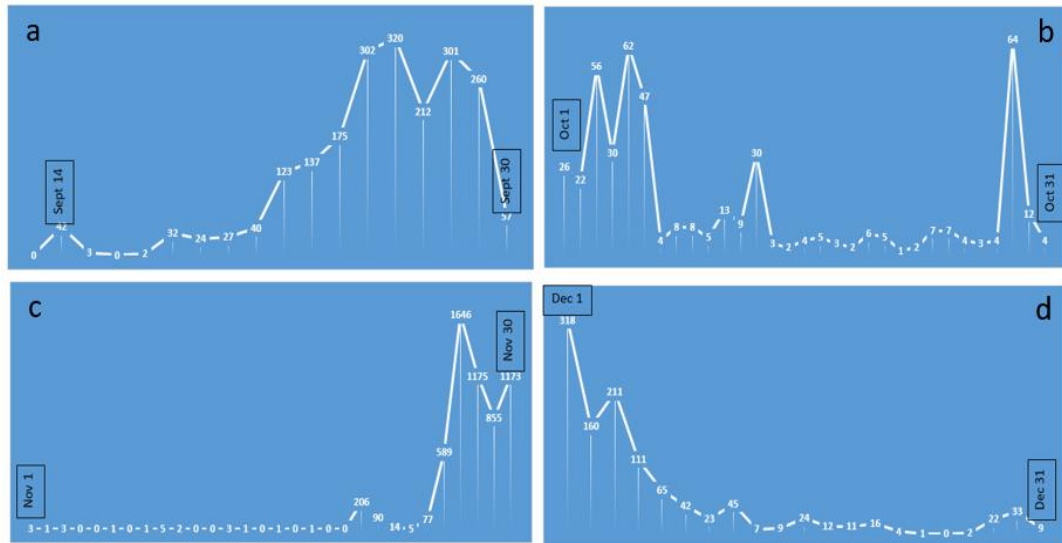


**Fig. 4.** Number of Daily News of Agung Volcano Eruptions; (a) September; (b) October; (c) November; (d) December.

After the eruption, the number of tourist visits start to rise in December due to the operational of the airport. The declining was caused by shutdown of Bali Airport and travel warning policy from foreign country to their citizen to not travel to Bali. Even though the number of tourists were declining in October and November 2017, total number of tourist visits in September until December 2017 were higher than September until December 2016. **Fig. 5** shows the monthly number of tourists visit to Bali in 2016 and 2017 compared to the number of news related to Agung Volcano eruption.

**Table 2.**

**The number of tourists visit to Bali in 2016 and 2017 compared to the number of news related to Agung volcano eruption.**

Month	2016	2017	News
Jan	597558	658308	0
Feb	513852	520462	0
Mar	576438	618834	0
Apr	534395	705710	0
May	647790	646467	0
Jun	1035563	659718	0
Jul	1084950	890368	0
Aug	704662	790323	0
Sep	725240	832026	2057
Oct	685244	732720	458
Nov	655962	741649	5852
Dec	882026	939048	1125
<b>TOTAL</b>	<b>8643680</b>	<b>8735633</b>	<b>9492</b>

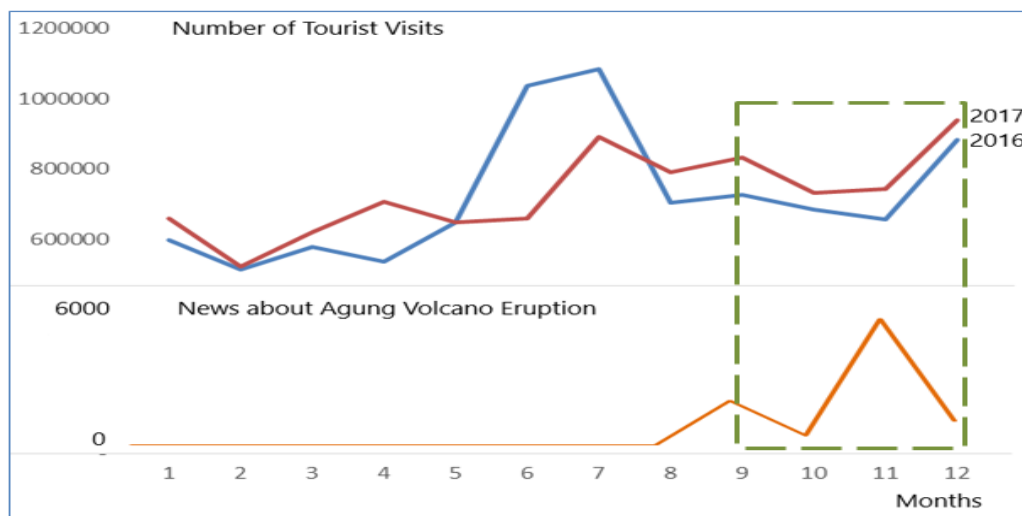


Fig. 5. The monthly number of tourists visit to Bali in 2016 and 2017, compared to the number of news related to Agung volcano eruption.

## 5. CONCLUSIONS

The news about Agung Volcano eruption started at 14th of September 2017 until the end of December which indicates that the eruption process was taking a long time. The news in September mainly about Indonesian Government that raised the alert level for a volcano to the highest level with more evacuations are expected. In October about the status of Agung Volcano was lowered and the evacuees who live outside the immediate danger zone to return home. In November the news mainly about Agung Volcano eruptions which triggered the shutdown of Bali and Lombok airport. In December the news was mainly about the Agung volcano was calm, even though volcano's alert remains at the highest level but Bali is safe except for the 10-kilometre exclusion zone. Bali's international airport was operating normally.

Total tourists visit to Bali at the peak of Agung Volcano eruptions in November was 741,649 compared to 655,962 tourists in November 2016. In December, total tourist visits was 939,048 compared to 882,026 in December 2016. The number of tourists is declining in October and November but rising again in December. November has the highest number of news related to the eruption. After the eruption in December, the number of tourist visits start to rising due to the operational of the airport. The declining caused by shutdown of Bali airport and travel warning policy from foreign country to their citizen to not to travel to Bali. Even though the number of tourists is declining in October and November, number of tourists' visit in September until December 2016 were higher than September until December 2016.

## REFERENCES

- ABC 57 News. 2017. *Bali Volcano Shuts Downs Flights, Sends Residents Scurrying To Safety*. WBND. Last access on September 2020. <http://www.abc57.com/news/bali-volcano-shuts-downs-flights-sends-residents-scurrying-to-safety>.
- Anom, I.P., Mahagangga, I.G.O., Suryawan, I.B., Koesbardiati, T. & Wulandari, I.G.A. 2020. Case study of Balinese tourism: Myth as cultural capital. *Utopia y Praxis Latinoamericana*, 25(6), 122-133. doi: 10.5281/zenodo.3987586
- Antara, M & Sumarniasih, M.S. 2017. Role of Tourism in Economy of Bali and Indonesia. *Journal of Tourism and Hospitality Management*, 5(2), 34-44. doi: 10.15640/jthm.v5n2a4.





- Astro Awani. 2017. *Volcano On Indonesia's Bali Island At Highest Alert Level, Thousands Evacuated*. Astro Awani Network Sdn. Bhd. Last access on November 2020. <https://calgaryherald.com/pmn/news-pmn/nearly-10000-leave-homes-around-active-bali-volcano/wcm/467a9fcf-fb59-48a5-8ab0-cd9546fb3d88>
- Arkansas Online. 2017. *Some Who Fled Volcano Can Go Home*. Arkansas Democrat-Gazette, Inc. Last access on November 2020. <https://www.arkansasonline.com/news/2017/oct/01/some-who-fled-volcano-can-go-home-20171/>
- Arimsayanti, N.K. 2017. Branding Strategy of Tourism in Bali Based on Cultures and Heritage. *8<sup>th</sup> International Science, Social Science, Engineering and Energy Conference*, 1-14.
- Asia Pasific Daily. 2017. *Indonesia Declares Bali Returns to Normal, Airport Closure Unlikely*. Asia Pasific Daily. Last access on September 2020. <https://www.apdnews.com/e-world/807317.html>.
- Buribayeva, G., T. Miyachi, A. Y. and Y. Mikami. 2015. An Autonomous Emergency Warning System Based on Cloud Servers and SNS. *Procedia Computer Science* 60, 722-729.
- Belfast Telegraph. 2017. *11,000 Evacuated As Indonesia Raises Volcano Alert On Bali*. Belfast Telegraph Ireland. Last access on November 2020. <https://www.belfasttelegraph.co.uk/news/world-news/11000-evacuated-as-indonesia-raises-volcano-alert-on-bali-36158999.html>
- Calgary Herald. 2017. *Nearly 10,000 Leave Homes around Active Bali Volcano*. Associated Press. Last access on November 2020. <https://calgaryherald.com/pmn/news-pmn/nearly-10000-leave-homes-around-active-bali-volcano/wcm/467a9fcf-fb59-48a5-8ab0-cd9546fb3d88>
- Cinnamon, J., S.K. Jones, and Adger, W.N. 2016. Evidence and Future Potential of Mobile Phone Data for Disease Disaster Management. *Geoforum* 2016, 75, 253–264.
- Cen, J., T.Yu, Z. Li, S. Jin and S. Liu 2011. Developing A Disaster Surveillance System Based On Wireless Sensor Network And Cloud Platform. *IET International Conference on Communication Technology and Application (ICCTA)*.
- Center Bureau of Statistics (BPS) of Bali Province. 2017. Bali in Figure. Denpasar: Center Bureau of Statistics (BPS) of Bali Province.
- Channel News Asia. 2017. *Indonesia's Mount Agung Erupts For a Second Time*. Mediacorp. Last access on November 2020. <https://www.channelnewsasia.com/news/asia/indonesia-s-mount-agung-erupts-for-a-second-time-bali-9440086>
- Choi, S & Bae, B. 2015. The Real-Time Monitoring System of Social Big Data for Disaster Management. *Computer Science and its Applications*, pp. 809-815, Springer Berlin Heidelberg.
- Chosunilbo & Chosun. 2017. *Indonesia Raises Alert Level for Bali Volcano*. Digital Chosun Inc. Last access on November 2020. [http://english.chosun.com/site/data/html\\_dir/2017/09/15/2017091500541.html](http://english.chosun.com/site/data/html_dir/2017/09/15/2017091500541.html)
- Christo, J.P. 2017. *Bali named TripAdvisor's Best Destination in the World*. Tempo Inti Media TBK. Last access on November 2020. <https://en.tempco.co/read/news/2018/03/07/199916400/Bali-named-TripAdvisors-Best-Destination-in-the-World>
- Dos Santos Rocha, R., A. Widera, R.P. van den Berg, J.P. de Albuquerque, B., Helingrath. 2016. Improving the Involvement of Digital Volunteers in Disaster Management. *Proceedings of the International Conference on Information Technology in Disaster Risk Reduction, Sofia, Bulgaria, 16–18 November 2016*; Murayama, Y., Velez, D., Zlateva, P., Gonzalez, J.J., Eds.; Springer: Cham, Switzerland, 2016; 214–224.
- Erdelj, M. and E.Natalizio. 2016. UAV-assisted disaster management: Applications and open issues. *Proceedings of the 2016 International Conference on Computing, Networking and Communications (ICNC 2016), Kauai, HI, USA, 15–18 February 2016*; IEEE: Piscataway, NJ, USA; 1–5.
- European Council. 2017. *Victims of Mount Agung Eruptions in Bali Receive EU Support*. European Council. Last access on September 2020. [https://ec.europa.eu/echo/news/victims-mount-agung-eruptions-bali-receive-eu-support\\_en](https://ec.europa.eu/echo/news/victims-mount-agung-eruptions-bali-receive-eu-support_en)
- Fang, S., X.Lida, Z. Yunqiang, Y. Liu, Z. Liu, H. Pei, J. Yan and Huifang Zhang. 2015 An integrated Information System For Snowmelt Flood Early-Warning Based on Internet of Things. *Frontiers*, 17 (2), 321-335.
- France 24. 2017. *Bali Closes Airport As Up To 100,000 Set To Evacuate*. France 24. Last access on September 2020. <https://www.france24.com/en/20171126-bali-volcano-eruption-disrupts-international-flights-mount-agung>
- Fresh News Asia. 2017. *Indonesia Declares Bali Returns to Normal, Airport Closure Unlikely*. Fresh News Asia. Last access on September 2020. <http://m.en.freshnewsasia.com/index.php/en/6432-indonesia-declares-bali-returns-to-normal-airport-closure-unlikely.html>
- Fox News. 2017. *Bali Volcano's Alert Status Lowered after Decreased Activity*. Fox Media Group. Last access on November 2020. <https://wtop.com/asia/2017/10/bali-volcanos-alert-status-lowered-after-decreased-activity/>

- Gaudru, H. 2014. Volcano Tourism: The Effect of Eruptions and Disasters. In: Erfurt-Cooper P. (eds) *Volcanic Tourist Destinations. Geoheritage, Geoparks and Geotourism (Conservation and Management Series)*. Springer, Berlin, Heidelberg. doi:10.1007/978-3-642-16191-9\_26
- Global Volcanism Program, 2018. Agung (264020) in *Volcanoes of the World*, v. 4.7.3. Venzke, E (ed.). Smithsonian Institution. Last access on November 2020, <https://volcano.si.edu/volcano.cfm?vn=264020>
- Grolinger, K., M. A. Capretz, E. Mezghani and E. Exposito. 2013. Knowledge as a Service Framework For Disaster Data Management. *IEEE 22nd International Workshop on Enabling Technologies: Infrastructure for Collaborative Enterprises (WETICE)*, 2013, 313-318.
- Humanitarian News. 2017. *Indonesia: Half of Volcano Evacuees on Bali Are Asked to Go Home*. Humanitarian News. Last access on November 2020. <http://humanitariannews.org/2017/1001/indonesia-half-volcano-evacuees-bali-are-asked-go-home>
- Hopp, F. R., Schaffer, J., Fisher, J. T., & Weber, R. 2019. iCoRe: The GDELT interface for the advancement of communication research. *Computational Communication Research*, 1(1), 13–44. doi:10.31235/osf.io/smjwb.
- Kamali, C. & Augasta, M.G. 2017. Geo-Spatial Big Data Analysis: An Overview. *International Journal of Trend in Research and Development (IJTRD)*, ISSN: 2394-9333.
- Keertipati, S., M. K. Purvis and B. T. R. Savarimuthu. 2014. *Multi-level Analysis of Peace and Conflict Data in GDELT*. doi: 10.1145/2689746.2689750.
- Kwak, H. & An, J. 2014. Understanding News Geography and Major Determinants of Global News Coverage of Disasters. *Computation+Journalism Symposium*, New York USA, 1-7.
- Li, S., Dragicevic, S., Anton, F., Sester, M., Winter, S., Coltekin, A., ... Cheng, T. 2016. Geospatial Big Data Handling Theory and Methods: A Review and Research Challenges. *I S P R S Journal of Photogrammetry and Remote Sensing*, 115, 119-133. doi: 10.1016/j.isprs.2015.10.012
- Leetaru, K. and P. Schrodt. 2013. *GDELT: Global Data on Events, Language, and Tone, 1979-2012*. International Studies Association Annual Conference. San Diego, CA.
- Mail Online. 2017. *Bali Volcano Evacuees Outside Danger Zone Told To Go Home*. Associated Newspapers Ltd. Part of the Daily Mail, The Mail on Sunday & Metro Media Group. Last access on November 2020. <https://www.dailymail.co.uk/wires/afp/article-4935564/Bali-volcano-evacuees-outside-danger-zone-told-home.html>
- Marboen, A.P (ed). 2017. *Volcanic Activity Of Mount Agung In Bali Increasing*. Antara News. Last access on November 2020. <https://en.antaranews.com/news/112675/volcanic-activity-of-mount-agung-in-bali-increasing>.
- Mudana, I.G., Sutarna, Ketut & Widhari, C.I.S. 2018. Local Community Entrepreneurship in Mount Agung Trekking. *Journal of Physics: Conference Series*, 953(1), 1-9. doi:10.1088/1742-6596/953/1/012107.
- Nurhayati, D. 2017. *Bali is world's top destination for 2017, says TripAdvisor*. SPH Digital News/ Asiaone Group. Last access on November 2020, <http://www.asiaone.com/travel/bali-worlds-top-destination-2017-says-tripadvisor>
- Oman Daily Observer. 2017. *Some Bali Flights Resume After Mount Agung Volcano Interrupts Travel*. Oman Establishment for Press, Publication and Advertising (OEPPA). Last access on September 2020. <http://www.omanobserver.om/bali-volcano-appears-calm/>
- Owuor, I., Hochmair, H. & Cvetojevic, S. 2020. Tracking Hurricane Dorian in GDELT and Twitter. *AGILE: GIScience Series*, 1, 2020, full paper Proceedings of the 23rd AGILE Conference on Geographic Information Science, 1-18. doi:10.5194/agile-giss-1-19-2020.
- Paris, N. 2017. *Bali Named Greatest Destination on Earth by TripAdvisor*. Fairfax Media. Last access on November 2020, <http://www.traveller.com.au/bali-named-greatest-destination-on-earth-by-tripadvisor-gvd0eo>.
- Parimartha, I.G., Gde Putra, I.B., Ririen, L. P. K. & AAGN Ari Dwipayana (ed). 2016. *Crescent On The Island Of Gods, Traces Of Islamic Village In Kusamba-Bali*. Al-Albab. 5. 265. doi:10.24260/alalbab.v5i2.746.
- Phys.org. 2017. *Indonesia Raises Alert Level for Bali Volcano*. Associated Newspapers Ltd. Last access on November 2020. <https://phys.org/news/2017-09-indonesia-bali-volcano.html>
- Pratiwi, D.P.E., Sulatra, I.K. & Candra, K.D.P. 2019. Bali Tourism Advertisements: A Linguistic Analysis. *International Journal of Linguistics, Literature and Culture*, 5(1), 43-53. doi:10.21744/ijllc.v5n1.582
- Rahman, M. S. L., Di and M. Esraz-UI-Zannat .2017. The Role of Big Data in Disaster Management. *Proceedings, International Conference on Disaster Risk Mitigation, Dhaka, Bangladesh*.
- Rahmawati, P.I., Trianasari & Martin, A.A.N.Y. 2019. The Economic Impact of Mount Agung Eruption on Bali Tourism. *Advances in Economics, Business and Management Research*, 69, 3<sup>rd</sup> International Conference on

- Tourism, Economics, Accounting, Management, and Social Science, 98-107. doi: 10.2991/teams-18.2019.18.
- Richardson, D.B., Volkow, N.D., Kwan, M.-P., Kaplan, R.M., Goodchild, M.F., Croyle, R.T., 2013. Spatial Turn in Health Research. *Science* 339, 1390.
- Relief Web. 2017. *Half of Volcano Evacuees on Bali Are Asked to Go Home*. ReliefWeb. Last access on November 2017. <https://reliefweb.int/report/indonesia/half-volcano-evacuees-bali-are-asked-go-home>
- Republika Online. 2017. *Mt Agung Erupts, Releases Volcanic Ash And Smoke*. Republika.Co.Id. Last access on November 2020. <https://www.republika.co.id/berita/en/national-politics/17/11/21/ozrwc4414-mt-agung-erupts-releases-volcanic-ash-and-smoke>.
- Robinson, W.S., 2009. Ecological Correlations and the Behavior of Individuals. *International Journal of Epidemiology*. 38, 337–341.
- Rosselló J., Becken S. & Santana-Gallego M. 2020. The effects of natural disasters on international tourism: A global analysis. *Tourism Management*, 79, 1-11. doi: 10.1016/j.tourman.2020.104080.
- Shu, H. 2016. Big Data Analytics: Six Techniques. *Geo-spatial Information Science*, 19(2), 119-128, doi: 10.1080/10095020.2016.1182307.
- Su, Y., Lan, Z., Lin, Y., Comfort, L.K. & Joshi, J. 2016. Tracking Disaster Response and Relief Following the 2015 Nepal Earthquake. *IEEE 2nd International Conference on Collaboration and Internet Computing (CIC)*, Pittsburgh, PA, 495-499. doi:10.1109/CIC.2016.075.
- Song, X., Q. Zhang, Y. Sekimoto, R. Shibasaki, N. Jing Yuan and Xing Xie. 2015. A Simulator of Human Emergency Mobility Following Disasters: Knowledge Transfer from Big Disaster Data. *AAAI, 2015*, 730-736.
- Tallon, M. 2013. Reflections from Bali: The Island of God. Oath Inc. Last access on November 2020. Retrieve from [https://www.huffingtonpost.com/monique-svazlian-cpcc-acc/bali-travel\\_b\\_4019409.html](https://www.huffingtonpost.com/monique-svazlian-cpcc-acc/bali-travel_b_4019409.html).
- The Daily Mail. 2017. *Indonesia Raises Alert Level for Bali Volcano*. Associated Newspapers Ltd. Last access on November 2020. <https://www.dailymail.co.uk/wires/ap/article-4884234/Indonesia-raises-alert-level-Bali-volcano.html>
- The Denver Post. 2017. *Bali Authorities Urge Many Who Fled Volcano to Return Home*. Digital First Media. Last access on November 2020. <https://www.denverpost.com/2017/09/30/mount-agung-volcano-bali-people-fleeing/>
- The GDELT Project. 2019. A global database of society. Last access on November 2020, <https://www.gdeltproject.org>
- The Hindu. 2017. *Indonesia Raises Alert Level for Bali Volcano*. The Hindu. Last access on November 2020. <https://www.thehindu.com/news/international/indonesia-raises-alert-level-for-bali-volcano/article19684655.ece>
- The Indian Express. 2017. *Some Bali Flights Resume After Mount Agung Volcano Interrupts Travel*. The Indian Express. Last access on November 2020. <https://indianexpress.com/article/world/some-bali-flights-resume-after-mount-agung-volcano-interrupts-travel-4954922/>
- The Star Online. 2017. *Dozens of Flights Cancelled As Bali Volcano Continues To Spew Smoke*. Star Media Group Berhad (ROC 10894D). Last access on November 2020. <https://www.thestar.com.my/news/regional/2017/11/26/dozens-of-flights-cancelled-as-bali-volcano-continues-to-spew-smoke/>
- The Washington Times. 2017. *Indonesia Raises Alert Level for Bali Volcano*. The Washington Times, LLC. Last access on November 2020. <https://www.washingtontimes.com/news/2017/sep/14/indonesia-raises-alert-level-for-bali-volcano/>
- Wesnawa, I.G.A. 2017. Sustainable Tourism Development Potential in the Improvement of Economic and Social Life Community Corridor in Bali. *International Research Journal of Management, IT & Social Sciences*, 4(3), 1-12. <https://sloap.org/journals/index.php/irjmis/article/view/391>
- Whiteside, D. 2017. *Volcano On Indonesia's Bali Island At Highest Alert Level, Thousands Evacuated*. Reuters. Last access on November 2020. <https://uk.reuters.com/article/uk-usa-nuclear-russia/u-s-would-destroy-banned-russian-warheads-if-necessary-nato-envoy-idUKKCNIMC1J2>
- World Buletin. 2017. *Flights Resume as Bali's Volcano-Hit Airport*. World Buletin. Last access on November 2020. <https://www.worldbulletin.net/asia-pacific/flights-resume-as-balis-volcano-hit-airport-h196420.html>
- Xinhua News. 2017. *Indonesia's Mount Agung Volcano Erupts*. Xinhuanet. Last access on November 2020. [http://www.xinhuanet.com/english/2017-11/21/c\\_136769370.html](http://www.xinhuanet.com/english/2017-11/21/c_136769370.html)



# ROCK MASS RATING AND FEASIBILITY ASSESSMENT OF KARST CAVE GEO-ECOTOURISM IN TANJUNGSARI DISTRICT, GUNUNGKIDUL REGENCY, YOGYAKARTA SPECIAL REGION, INDONESIA

*Sari Bahagiarti KUSUMAYUDHA<sup>1\*</sup>* , *Bambang PRASTISTHO<sup>1</sup>*, *Muhammad Faizal ZAKARIA<sup>2</sup>* , *Istiana RAHATMAWATI<sup>3</sup>* , *Tuti SETYANINGRUM<sup>4</sup>* 

DOI: 10.21163/GT\_2021.162.05

## ABSTRACT:

Tanjungsari district, Gunungkidul Regency, Yogyakarta Special Territory, is located in the karst geopark area of Gunungsewu, Indonesia. The area is geologically constituted of cavernous limestones, characterized by the existence of subsurface drainage. Since the Gunungsewu area was declared as one of the Unesco Global Geoparks in 2015, the tourism sector of this region has propagated rapidly. Tanjungsari district does not like to be left behind in developing the tourism sector. There are several caves in the district that have the potential to be developed for cave tourism, including Bentar Cave, Cabe Cave, Grengseng Cave, Pakubon Cave, and Tritis Cave, which have their uniqueness and attractiveness in terms of exokarst, endokarst, and legends. The development of these potential sites is expected able to improve the economic sector and welfare of the surrounding community. For the caves in Tanjungsari district competitive, the concept of development must be different from that of other places, it is cave geo-ecotourism. In connection with the matters mentioned above, studies and assessments applying engineering geological, social-economical, and agricultural investigations were conducted to explore the potential and feasibility of cave geo-ecotourism in the Tanjungsari area. Based on the application of cave rock mass rating (CRMR), Bentar Cave has a total score of 69 (Fair), Cabe Cave = 75 (Good), Grengseng Cave = 47 (Poor), Pakubon Cave = 81 (Good), and Tritis Cave = 79 (Good). The results of this study indicate that Bentar Cave has a value of 63.3%, Cabe Cave 50%, Grengseng Cave 66.7%, Pakubon Cave 63.3%, and Tritis Cave 73.3% feasibility or readiness if it will be developed as a geo-eco-cave tourism.

**Key-words:** karst, geo eco-tourism, cave, rock mass rating

## 1. INTRODUCTION

Tanjungsari district, Gunungkidul Regency, Yogyakarta Special Territory, is located in the karst geopark area of Gunungsewu, Indonesia. The area is geologically constituted of cavernous limestones, characterized by the existence of subsurface drainage. Since the Gunungsewu area was declared as one of the Unesco Global Geoparks in 2015, the tourism Tanjungsari District belongs to the Gunungkidul Regency, Yogyakarta Special Territory, Indonesia (**Fig. 1**), with an area of 71.63 square kilometers. The landform shows karst topography, apart of the Gunungsewu mountains, sloping varies from 5% to more than 40%, and at an altitude between 100 - 300 meters above sea level. Karst landscape of Tanjungsari area is characterized by subsurface drainage bringing about it subjected to water shortage. In the year 2015, the Gunungsewu has been designated as one of the Global Geopark areas by UNESCO (Kusumayudha, 2018). Since Gunungsewu pointed as Unesco Global Geopark (UGG), the tourism sector is growing rapidly everywhere.

<sup>1</sup>Geological Engineering Dept., Univ. Pembangunan Nasional Veteran Yogyakarta, [saribk@upnyk.ac.id](mailto:saribk@upnyk.ac.id) \*, [Bambang.prastistho@gmail.com](mailto:Bambang.prastistho@gmail.com)

<sup>2</sup>Geophysical Engineering Dept., Univ. Pembangunan Nasional Veteran Yogyakarta, [mfaizal@upnyk.ac.id](mailto:mfaizal@upnyk.ac.id)

<sup>3</sup>Management Dept., Univ. Pembangunan Nasional Veteran Yogyakarta, [rahاتمawati@gmail.com](mailto:rahاتمawati@gmail.com)

<sup>4</sup>Agrotechnology Dept., Univ. Pembangunan Nasional Veteran Yogyakarta, [Setyaningrumtuti@gmail.com](mailto:Setyaningrumtuti@gmail.com)

Realizing this condition, Tanjungsari District doesn't want to be left behind, it likes to improve its natural potential to be optimally made use for tourism development (Kusumayudha, et.al, 2020). There are five caves in the Tanjungsari district, that expected can be developed as tourist destinations, namely Bentar Cave, Cabe Cave, Grengseng Cave, Pakubon Cave, and Tritis Cave. These caves have unique ornaments, including stalactites and stalagmites, as well as interesting legends, but have not been well exploited and invented yet (Anoname, 2018). In order to develop cave tourism that can be used as a mainstay and superior area for the region, it is necessary to explore and inventory its uniqueness which is different from those of other places, so that they are able to compete with other cave tourism objects that have already developed (Puspitasari & Rahatmawati, 2017).

Related to the plan of tourism development, there is a relatively new concept of tourism, called geotourism, a model of tourism which emphasizes on geology and geomorphology as the basis of fostering sustainable tourism development (Dowling, 2013). It differs from ecotourism, that is described as about uniting conservation, communities, and sustainable travel (Ruda, 2016). This means that those who implement, participate in and market ecotourism activities should considering some principles, they are minimizing physical, social, behavioral, and psychological impacts, and developing environmental, cultural awareness and respect (<https://notaclueadventures.com/2015/03/blog/ecotourism-vs-geotourism/>). In terms of Geo-ecotourism, of course it is the combination of the two concepts. Tanjungsari is assumed to have the potency of adopting these concepts in developing its tourism (Kusumayudha, et.al., 2020). In order to develop the area to be a different and sophisticated tourism destination, Tanjungsari needs to apply geo-ecotourism. Based on the backgrounds mentioned above, it is necessary to conduct a research with the objectives to assess the potential and feasibility of karst cave geo-ecotourism in Tanjungsari district based on engineering geological assessments, including geomorphological and lithological mapping, rock mass rating to determine the cave bearing capacity, and social-economical-agricultural evaluation.



**Fig. 1.** Location of the Study Area ([www.mapsofworld.com/indonesia/provinces/jawa-tengah.html](http://www.mapsofworld.com/indonesia/provinces/jawa-tengah.html)).



## 2. STUDY AREA

### 2.1. Geology

Physiographically, Tanjungsari district is situated in the Gunungsewu sub-zone of the Southern Mountains of Central Java - East Java (Van Bemmelen, 1949). The Gunungsewu sub-zone is characterized by karst topography with conical and sigmoid hills, showing axis orientation of west-east, with a height difference of 10 m - 100 m, comprises about 45,000 small and large hills of 50 m - 300 m diameter (Kusumayudha, 2005).



Fig. 2. Reef limestone (left) and bedded limestone (right) (Kusumayudha, et.al, 2020).

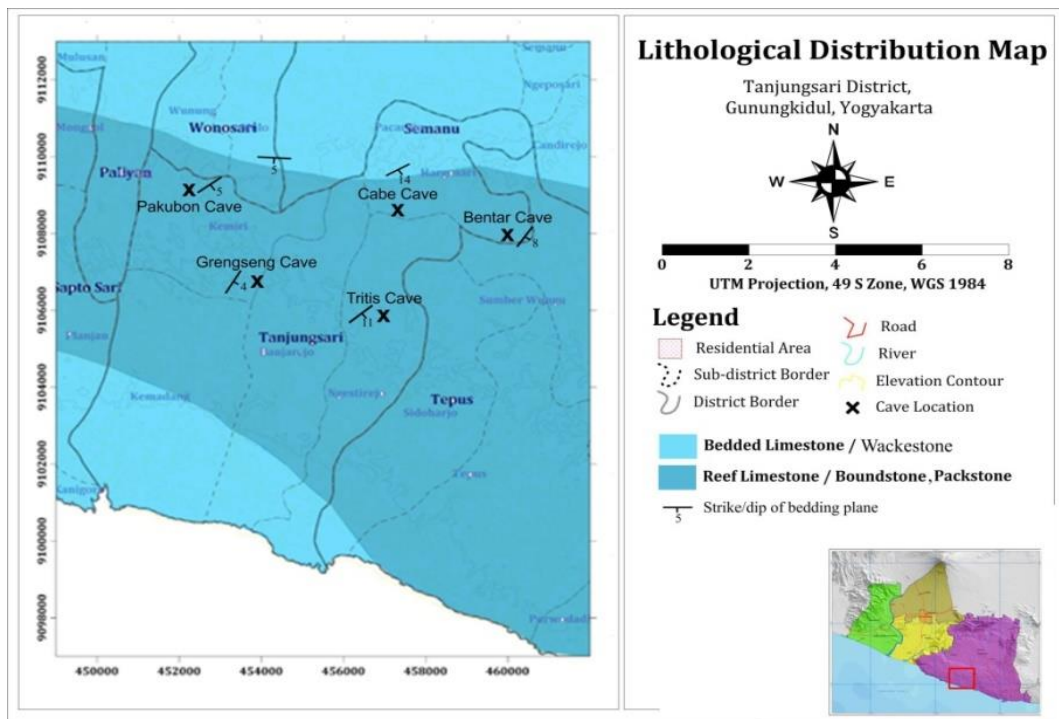


Fig. 3. Lithological distribution of the Tanjungsari and surrounding area (Kusumayudha, et.al, 2020, updated).

The Gunungsewu karst area is mainly occupied by limestones of the Wonosari Formation, which is generally presenting karstification, and in some places showing calichification (Kusumayudha, 2002). In the basement of Wonosari Formation there exist some lithologic units, from the oldest to the youngest are tuffaceous sandstones of Semilir Formation, volcanic rock consisting of breccias, and lava of Nglanggran Formation, marl of the Sambipitu Formation, and sandy-tuff limestones of the Oyo Formation. Gunungsewu limestone was deposited in the middle Miocene to late Miocene (Suyoto, 1994).

Geomorphologically, the study area displays a hilly karst topography, with a height difference of 10 m - 30 m, and the hills diameter ranges from 50 m - 200 m. Macro karst is found in the form of conical to dome-shaped hills, dolines, uvalas, and locvas, while micro karst and lapies which classified as exokarst are also found in the study area.

Lithology in the study area predominantly comprises limestones of the Wonosari Formation, deposited from the middle Miocene to the late Miocene epoch. There are two (2) lithofacieses of the limestone included in *boundstone* and *packstone* of reef limestone, and *wackestone* of bedded limestone (Fig. 2).

The limestones have undergone karstification, entering in the maturity stage, marked by the intensiveness of the carbonate dissolution process, resulting in caves with various ornaments such as stalactites, stalagmites, cinterflags, and flowstones. The distribution of the lithofacies is relatively northwest - southeast, with geological structure shows a homoclinic with an inclination of less than 15°, to the south and southwest (Fig. 3).

## 2.2. Caves, Underground Flows, and Hydrogeology

In the Gunungsewu area, around 460 karst caves were identified, 5 (five) of which are located in the study area, including Bentar Cave, Cabe Cave, Grengseng Cave, Pakubon Cave, and Tritis Cave. Many of the caves are fed by underground rivers, as the main drainage of the Gunungsewu area, and generally discharge to the Indian Ocean. The flow direction of the underground channels is influenced by the pattern of crack structures, and the dip slope of the limestone beddings (Kusumayudha & Santoso, 1998). One of the main subsurface rivers in the Gunungsewu area is River Bribin (Kusumayudha, 2002).

River Bribin is located in the northern part of the study area, with a flow rate reaching 900 l/sec (Kusumayudha, 2002, 2005). The catchment area of River Bribin is in the Ponjong district, Bedoyo district, and surrounding areas. The streams that were originally on the surface, submerge underground through the Songgilap Cave (Kusumayudha, 2002, 2005). The Bribin flow discharges to the Baron Bay through a karst spring with the rate of 20,000 l/sec in the peak of the rainy season (Kusumayudha, 2005).

The study area hydrogeologically includes in the Wonosari – Baron subsystem, which is characterized by surface runoff that turns into subsurface flow, the presence of free aquifers and perched aquifer with a thickness of 100 - 400 m, discharge through an underground river estuary with an average discharge of 7900 l / sec (Kusumayudha, 2002, 2005).

## 2.3. Culture, Agriculture, and Economics Values

Culture is one of the characteristics that can distinguish one area from another. Tanjungsari which includes in the Gunungsewu karst area has a unique, rare culture and needs to be preserved. This area has various kinds of cultural heritage, including historical heritages in some caves. The caves have proven to be the center of past activities. In these caves are found relics of the past, and therefore they are called Archeological Caves (Kusumayudha, et.al, 2020). Caves of Tanjungsari that included in archaeological caves are Grengseng Cave and Pakubon Cave. The cultural potential also involves traditional dancing, called *jathilan*, which expressing heroic soldiers of riding horse. The horce in this dancing is made of woven bamboo, or cow scalp.

From an agricultural aspect, in the study area, especially of surrounding the caves, there are very potential for *empon-empon* plants (spice plants, including ginger, turmeric, gatangal, and curcuma). *Empon-empon* are good plants commodity to be cultivated because people always need it for various purposes. They are rhizomes used as traditional ingredients, and commonly consumed for conventional medicine and cooking spices. Some of the benefits of *empon-empon* include: as raw material for medicines and herbal medicine, food and beverage industry cooking ingredients, traditional body care ingredients, cosmetics for beauty care, dyes, and for their essential oils. (Cahyadi, 2017). The price is quite high. By cultivating *empon-empon*, it is hoped that people in the Tanjungsari sub-district can support their economics, by selling *empon-empon* products either in fresh or processed form.

Another agricultural potential of the Tanjungsari district is cassava plants. In this area, cassava is produced in quantity that exceeds the needs of the local community. Therefore, it is necessary to diversify the handling of cassava so that it can be processed into various snack foods. The local community has processed cassava into various crispies, crackers, chips, and also cassava flour (*mokaf*). With this *mokaf* they create a variety of culinary variations, including brownies, *fried shrimp with mokaf*, and *cendol* (colourful shaved-ice desserts).

### 3. DATA AND METHODS

The research was applying analytical, descriptive and surveys of engineering geological investigation methods, utilized two kinds of data, both secondary includes a variety of information from the results of existing research and studies, and primary data that were obtained through surveys, investigations, and field mapping. Activities have been done including geomorphological mapping, lithological - stratigraphical identifications, and geologic structural analyses. While cave tracking had been done to map and inventory the distribution of cave passages, uniqueness, and speleothems. Rock sampling was also carried out for petrological assessment, as well as for rock properties testing. The method used to determine the strength of the rock is unconfined compressive strength (UCS). Cultural and agricultural surveys were also done to complete the study.

In order to assess the significance of the geological and geomorphological sites for cave geotourism targets, the concept of geomorphosites is appropriate to be applied (Kubalíkova, 2013). Some assessment was carried out for geotourism purposes, from several perspectives, with an emphasis on using scientific, cultural and economics parameters (**Table 1**). The results of the assessment can serve as a basis for appropriate use of geoheritage, its management, and identification of geotourism potential of the study area (Kubalíkova, 2013).

**Table 1.**

**Assessment criteria according to Reynard, et al. (2007), (Kubalíkova, 2013), modified.**

Value	Criteria
scientific values	integrity; representativeness; paleogeographical value; rareness
ecological values	ecological impact; protected species
aesthetic values	number of viewpoints; landscape/scenic beauty
cultural values	religious importance; historical importance; artistic importance
social-economic values	economic products; human resource support, agricultural support

To evaluate the mentioned geomorphosite assessment methods in terms of suitability for geotourism purposes, each of the criteria related to the parameters is then given a value. The value is =1, when the method considers the criterion, 0.5 if the method partly considers the criterion, and 0, for the method does not consider the criterion (Kubalíkova, 2013). This study was also completed with a geomechanical assessment for the limestone comprising the cave, mentioned RMR (Rock

Mass Rating), roof thickness, and source of vibration. In this case, the cave is assumed to be a tunnel, to be invented their bearing capacity for tourism.

RMR was developed by Bieniawski in 1973 (Franklin & Dussault, 1989), utilizes the following six rock mass parameters: 1) Uniaxial compressive strength (UCS) of intact rock material; 2) Rock quality designation (RQD); 3) Spacing of discontinuities; 4) Condition of discontinuities, given as 4a Length, persistence 4b Separation 4c Smoothness 4d Infilling 4e Alteration/weathering; 5) Groundwater conditions (Table 2). The classification of RQD is using Table 2. After an assessment was carried out based on Table 3, the classification of the rock mass quality was then determined using Table 4.

**Table 2.**

**RQD Classification.**

RQD	< 25%	25 - 50%	51 - 75%	76 - 90%
Rock Mass Classification	Very poor	Poor	Fair	Good

**Table 3.**

**Parameters and values of RMR (Bieniawski, 1973 vide Franklin & Dussault, 1989).**

Parameter		Range of Values								
Compressive strength (Mpa)	Values	>250	100-250	50-100	25-50	10-25	3-10	<3		
	Rating	15	12	7	4	2	1	0		
RQD (%)	Values	90 – 100	75 – 90	50 - 75	25 - 50	<25				
	Rating	20	17	13	8	3				
Joint Density	Values	>2	0.6 – 2	0.2 – 0.6	0.06 – 0.2	<0.006				
	Rating	20	15	10	8	5				
Joint Condition	Values	Very rough surfaces	Slightly rough surfaces	Slightly rough surfaces	Slickensided surfaces or Gouge <5 mm thick, or Separation 1 – 5 mm	Soft gouge >5 mm thick, or Separation > 5 mm				
		Not continuous	Separation <1 mm	Separation <1 mm	Continuous	Continuous				
		Unweathered wall rock	Slightly weathered walls	Highly weathered walls	Continuous					
		Rating	30	25	20	10	0			
		Ground-water Condition	Values	Completely dry	Damp	Wet	Dripping	Flowing		
			Rating	15	10	7	4	0		

**Table 4.**

**Geomechanics Classification of Rock Masses (Bieniawski, 1973, vide Franklin & Dussault, 1989).**

Class	Description of Rock Mass	RMR (Sum of Rating Increments)
I	Very Good Rock	81 – 100
II	Good Rock	61 – 80
III	Fair Rock	41 – 60
IV	Poor Rock	21 - 40
V	Very Poor Rock	>20

In this study the Bieniawski RMR method was modified by adding 2 other parameters, namely 1) the thickness of the cave roof, and 2) the source of vibrations/shocks. This method is then used to study the feasibility of the cave, especially in relation to the carrying capacity of the cave if it is developed as a tourist visit, and the risk of cave collapse, from a geotechnical aspect. The values for the two additional parameters are as follows (Table 5):

**Table 5.**

**Addition Parameters and their Values and Rating.**

Parameter	Range of Values					
Cave roof thickness (m)	Values	<1	1 - 5	5-10	10-20	>20
	Rating	0	5	10	15	20
Distance to the source of vibration (m)	Values	< 50	50-100	100-200	200-500	> 500
	Rating	0	5	10	15	20

After being modified, the scoring for cave rock mass rating (CRMR) to be as follows (**Table 6**):

**Table 6.**

**Geotechnical Classification of the Cave Feasibility for Tourism.**

Class	Description of Rock Mass	Sum of Rating Increments		Geotechnical Feasibility
		RMR	CRMR	
I	Very Good Rock	81 – 100	91 - 120	Very Good
II	Good Rock	61 – 80	71 - 90	Good
III	Fair Rock	41 – 60	51 - 70	Fair
IV	Poor Rock	21 - 40	31 - 50	Poor
V	Very Poor Rock	< 20	< 30	Very Poor

This method was then used to assess the feasibility of the cave when they are intended to be used for tourism destination from the engineering geological point of view.

**4. RESULTS AND DISCUSSIONS**

**4.1. Cave Geo-Ecotourism Feasability of Tanjungsari Area**

Based on potencies investigation and assessment on the caves of Tanjungsari District for geo eco-tourism, it can be described as the following.

**a. Bentar Cave**

The Bentar Cave is located in Jrahah hamlet, Hargosari village, easily accessible, the road to the cave has been adequately constructed by the local community. It has an extraordinarily beautiful charm, although its morphology can be classified as a vertical cave (**Fig. 4**).



**Fig. 4.** Vertical shaft (left) and the window of the light (right) of the Bentar Cave (Kusumayudha, et.al, 2020).



The cave exists due to the control of fractures dissected the limestone, which then interacts with meteoric water to form a vertical shaft. Inside the cave, there is a natural window on the roof of the cave, causing light from outside to be able to penetrate the cave. This place is very interesting as a means of photography to display breakthrough images of light (**Fig. 4**).

This cave is interesting and challenging, especially for adventure-loving tourists, because of the vertical passageways. Young tourists have often visited to enjoy the challenges in the cave. However, for general tourists, it needs to be facilitated with artificial stairs, so that they are helped when they want to enter and explore the Bentar Cave. This cave is divided into several rooms, namely the left side room, the living room, and the right-side room. The left side room is about 20 meters from the living room, then go down the stairs about 8 meters. This space is 30 meters in diameter with a height of 50 meters and there is an air hole above. In this room their live bats, frogs, and grasshoppers. Stalactites and stalagmites of the cave are still active.

From an engineering geological point of view, Bentar Cave has a fairly good feasibility, due to the thickness of the cave roof is quite thick, the depth of the cave reaches  $> 10$  m from the surface, joint spacing in general is  $> 2$  and is cemented with calcite and is overgrown with cave speleothems. Thus, the risk of collapse is small. To support the construction of Bentar Cave as a tourist attraction, tracing the cave has been carried out with the results as shown in **Fig. 5**.

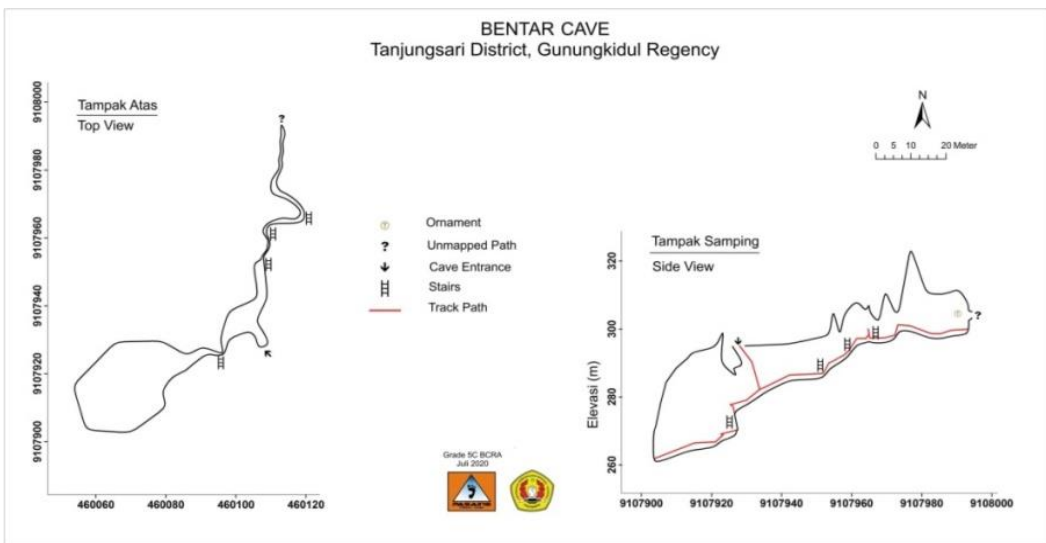


**Fig. 5.** Situation map of Cave Bentar (Kusumayudha, et.al, 2020).

Preparations made by the local community for the development of cave tourism include forming a management forum of tourism conscious community, namely *Pokdarwis Swargaloka*. The group has built 20-meter-high stairs for visitors. The community also tries to support the development of the cave with culinary delights made from local ingredients, such as cassava, papaya leaves, and *empon-empon*. Plants that grow around the cave are perennials, cassava, and *empon-empon* plants that still need an arrangement.

## b. Cabe Cave

Cabe Cave is located in Timunsari hamlet, Hargosari village, situated on a hill. The accessibility of this cave is still inadequate to open immediately as a tourist attraction, because to reach it, visitors have to walk hike up more than 500 m through rocky paths. The mouth of the cave is relatively narrow, only sufficient for one person to enter. However, in the cave, there is a wide enough hallway and space. Inside the cave, there are ornaments in the form of stalactites, stalagmites, and pillars (**Fig. 6**).

The Cabe Cave belongs to cultural heritage, because there a historical inscription has been found in this cave, called Nganjatan I and II inscriptions. They are bronze inscriptions with a length of 48 cm, a width of 18 cm, and a thickness of 0.2 cm with ancient Javanese script consisting of 12 lines of writing. By the way, this cave has not been well explored because the local people still protect it, considering that this cave has historical recollections, even though this cave actually has a beautiful charm of stalactites and stalagmites. It is hoped that this cave can be developed as a cultural heritage cave.

From the feasibility aspect of engineering geology, it is estimated that this cave has a small risk of collapse, because the roof of the cave is quite thick, with a solid density of 0.6 m, the fractures are generally open but filled with recrystallization of calcite. On the other hand, the plants that grow around the cave are generally wild plants, yams, and nuts. There has been no adequate arrangement from the aspect of agriculture, human resource support is still minimal. *Pokdarwis* (tourism conscious community) has been formed, but it has not worked optimally.



**Fig 6.** Environmental situation of cave Cabe (left), the mouth of Cave Cabe (right).

### c. Grengseng Cave

The Grengseng Cave is located in Kelor Lor hamlet, Kemadang village. The cave entrance is close to a preliminary school, residential area, and very close to an inter-village road. The cave inside is quite wide, there are various ornaments of stalactites and stalagmites, and pillars (**Fig. 7**). According to residents around this cave, the passage of the cave may penetrate to residential areas.

Grengseng Cave has three interconnected entrances. The first entrance is 3,2m wide, the second entrance wide: 4,5m and the third entrance is 2m in width. Unfortunately, the roof thickness of the area of surrounding the first entrance only ranges 2 m – 3 m, there are many opened cracks and joints, with joint density of about 0.28 – 0.57 m. The depth of the cave cannot be ascertained yet, but the depth for the oxygen safe reach is approximately 137m. There are more than 15 rooms in the cave with active stalactites and stalagmites. Inside the cave can be found various animals such as bats, squats, crickets, and worms. According to local history, Grengseng cave had been visited by king Brawijaya (Bhre Kertabumi), the last king of the Majapahit Kingdom, in the 14th century, for meditation (Setyaningrum, et.al., 2020). The situation map is displayed in **Fig. 8**.

There are various traditional events that routine to be done in Grengseng Cave, namely *Sadranan* and *Rasulan*. The events are held once every 35 days, on Friday night, which is believed to be a good day to face the planting period, and harvesting period. The activities are about cleaning the environment of the hamlet.

A series of tourism potentials are offered at Grengseng Cave and its surroundings. It consists of enjoying the sunrise and sunset on the top of Bei hill, exploring the Grengseng cave, visiting a *karawitan* (Javanis traditional music) studio which at the same time we can play directly with the traditional musicians, visiting *mokaf* (cassava flour) making, and trying to make *mokaf* yourself accompanied by a group team, calling on the natural *batik*-making process and trying to do it, entering the vertical Banteng cave, tracking Banteng Cave, going to *Watu Kodok* beach, and enjoying the atmosphere at the Bamboo Hill (Setyaningrum, et.al, 2020). The support of human

resources in this area is good, *Pokdarwis* has worked enthusiastically, efforts to organize agricultural aspects have started to be made by the local community.



**Fig. 7.** In side of the Grengseng cave and its ornaments (Kusumayudha, et.al, 2020)

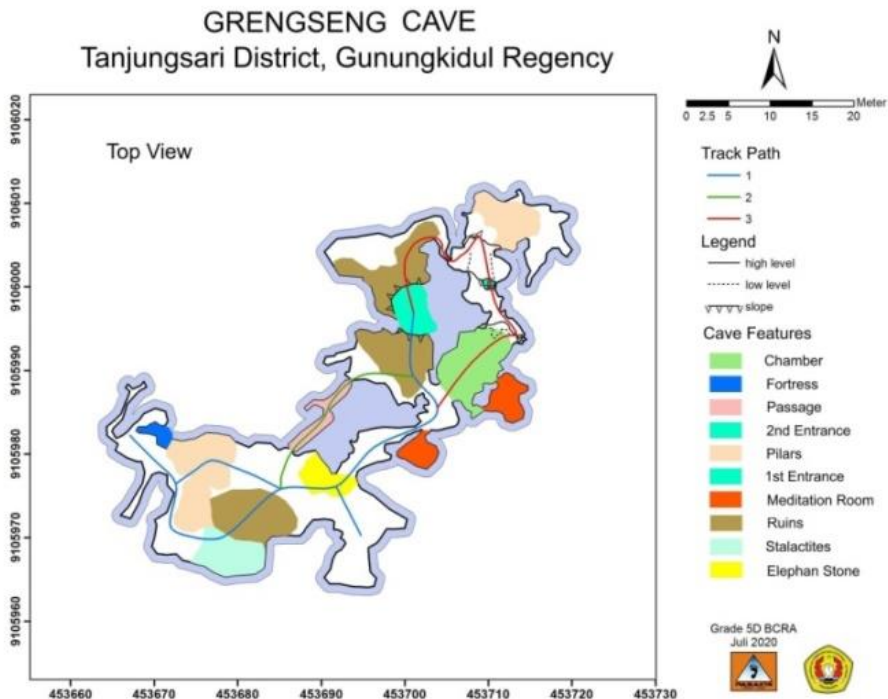


**Fig. 8.** Situation map of the Grengseng Cave (Kusumayudha, et.al, 2020).

#### d. Pakubon Cave

The Pakubon Cave is located at Ngasem hamlet, Kemiri village. To access the cave is very easy, it is close to the Baron beach, about 1 km distance. With an adequate wide enough road. Although it is intended to be opened as a new tourist destination, but the facilities around the cave are still minimal, including the parking area, and the way to entrance and exit the cave. There is an area for a camping ground or out bond activities, in front of the cave. A relatively large room can be found inside, on the roof, there are stalactites, some of which are relatively big in size and unique in shape, like crystal chandeliers (**Fig. 9**). There are no stalagmites. This indicates that Pakubon Cave is often traversed by water flows. The situation map of Pakubon Cave is shown in **Fig. 10**.





**Fig. 9.** Inside of the Pakubon Cave, there is a unique form of stalactite: crystal chandelier like (Kusumayudha, et.al, 2020).

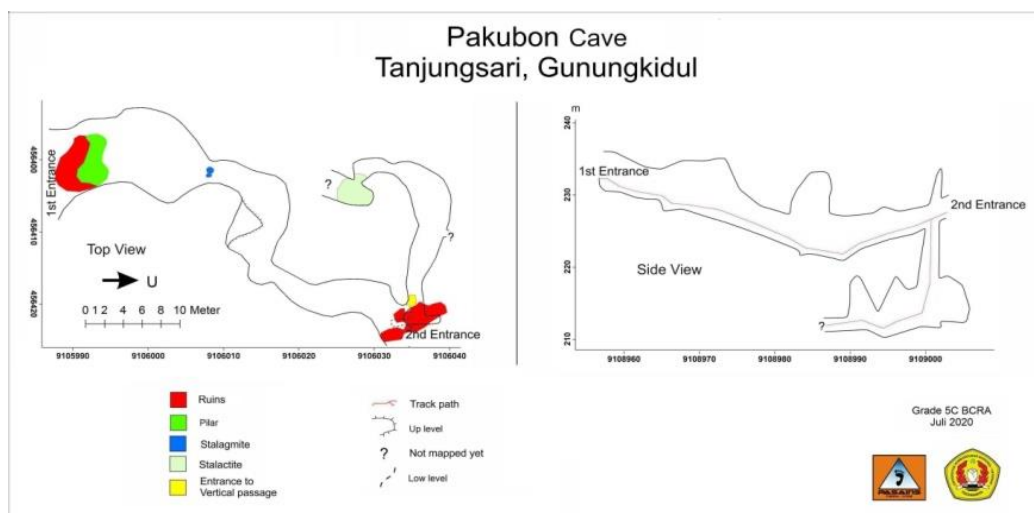


**Fig. 10.** Situation map of the Pakubon cave. (Kusumayudha, et.al, 2020).

To support Pakubon Cave tours, Ngasem hamlet also contains a cultural, historical, and educational wealth. The cultural wealth has been preserved until today, such as cleaning the lake and the apostles. Inside the Pakubon cave, there are many active stalactites and an interesting panoramic view of the cave walls. The panorama and beauty of Pakubon Cave are also complemented by the presence of calcite crystals, as well as decorative flowstones, cinterflags, some that resemble flowers, and stone carvings. Pakubon Cave can be developed as a natural, cultural and educational tourism object. Although this cave is potential to be developed as geo-eco-tourism, but human resource support of this area is not optimal yet. Actually, there is agricultural potential, because various kinds of plants can be cultivated in this area, including teak, cashew, cassava, *empon-empon*, nuts, and horticulture trees.

### e. Tritis Cave

The Tritis Cave is located in Jaten hamlet, Ngestirejo village. Inside the cave, there are stalagmites and stalactites. This cave is also often used for a ritual or meditation place. There is a lake in front of the cave. The bottom of the lake is covered by sediments with the composition of clay at the top, volcanic ash and silt, and sandy silt at the bottom.

Based on some residents' information, sediments at the bottom of the lake have ever been dredged, intended to make the lake's capacity greater, and the lake's water is expected to be

increased. Unfortunately, sediment dredging at the bottom of the lake resulted in the lake leaking. Based on infiltration testing using a double ring infiltrometer, the infiltration rate of the sediment that is predominantly composed of silt on the lake ranges 10 – 13 cm/hour. This indicates that the relatively water-resistant layer has been lost due to dredging, leaving a relatively permeable layer. Another uniqueness of the Tritis Cave is the discovery of volcanic ash deposit layers near the mouth of the cave (**Fig.11**).



**Fig. 11.** Cave Tritis entrance (left) and volcanic ash deposit (right) (Kusumayudha, et.al, 2020).

The scenery on the porch of Tritis cave has its own beauty. To support Tritis Cave geotourism, the community has planted various decorative plants and local fruits, as well as the presentation of various processed agricultural products. Around the Tritis Cave, cassava is the main commodity developed in the area. Various kinds of processed products can be used as a complement to culinary tours. Planting local fruit, especially *srikaya* around the tourist area, besides complementing the beauty of the scenery, it also adds to the completeness of biodiversity and can be enjoyed by the fruit. Likewise, planting sunflowers and various other attractive plants increases the beauty of the view on the cave porch.

#### **4.2. Rock Mass Rating and Feasibility Assessment for Caves Geo Eco-tourism.**

Cave RMR (CRMR) has been carried out to acquire information and indicators about the carrying capacity and safety of the cave if it is developed for tourist visits. The components used in conducting this method are based on the value of RQD (Rock Quality Designation), rock strength, discontinuity spacing, joint conditions, groundwater conditions around the caves, roof thickness, and distance to the source of vibration. The result is as follows (**Table 7**)

Based on the assessment on the rock masses make up the five caves, using CRMR, the total score of Bentar Cave = 69 is fair rock category, Cabe Cave = 75, including in good rock, Grengseng Cave = 47 classified as poor rock, Cave Pakubon = 81 categorized as good rock, and Tritis Cave = 79 belongs to good rock as well. Thus, from a geotechnical aspect, the feasibility of Bentar Cave can be categorized as adequate, Grengseng Cave is not feasible, while Cabe Cave, Pakubon Cave, and Tritis Cave are suitable to be developed as tourism objects. With a thin roof and a lot of joints, Grengseng Cave is at risk of collapse.

With this risk, if Grengseng Cave is intended to be developed as a tourist attraction, it is necessary to safeguard the cave, to reduce the risk of collapse, namely by grouting the cracks of the cave roof. However, it is necessary to select cracks to be grouted, in order not significantly to affect speleothem formation and growth.

After finishing the CRMR, an assessment using the method promoted by Kubalikova (2013) was carried out on the five caves of the study area. The assessment was done to find out how much potential and feasibility they would be if they were developed as a karst cave geo eco-tourism. The results of this study can be seen in **Table 8**.

**Table 7.**

**Cave Rock Mass Rating of the Study Area.**

Cave Name	Parameter	Discription	Rating	Total Score & CRMR Class
Bentar	UCS (Mpa)	43.12	4	69 (Fair)
	RQD (%)	60 - 70	13	
	Joint Density	0.5	10	
	Joint Condition	Rough surface, aperture > 10 mm, <i>hard wall rock</i>	15	
	Groundwater Condition	Wet	7	
	Cave roof Thickness	10 m – 20 m	15	
	Source of Vibration	Distance to the road 50 - 100 m	5	
Cabe	UCS (Mpa)	60.27	5	75 (Good)
	RQD (%)	70 - 90	13	
	Joint Density	0.6	10	
	Joint Condition	Rough surface, aperture > 10 mm, joints are filled with calcite, <i>hard wall rock</i>	15	
	Groundwater Condition	Wet	7	
	Cave roof Thickness	5 m – 10 m	10	
	Source of Vibration	Distance to the road 200 – 500 m	15	
Grengseng	UCS (Mpa)	37.68	3	47 (Poor)
	RQD (%)	40; 52; 62; 94	13	
	Joint Density	0.28 – 0.57	7	
	Joint Condition	Opened joint, filled with soil, 5 mm - 100 mm	15	
	Groundwater Condition	Wet, and dripping	4	
	Cave roof Thickness	3 - 5 m	5	
	Source of Vibration	Distance to the road < 50 m	0	
Pakubon	UCS (Mpa)	46.76	4	81 (Good)
	RQD (%)	80 - 85	17	
	Joint Density	0.8	13	
	Joint Condition	Rough surface, aperture > 10 mm, parts of which are filled with calcite, <i>hard wall rock</i>	15	
	Groundwater Condition	Wet	7	
	Cave roof Thickness	5 m – 10 m	10	
	Source of Vibration	Distance to the road 200 – 500 m	15	
Tritis	UCS (Mpa)	36.11	3	79 (Good)
	RQD (%)	70 - 80	16	
	Joint Density	0.55 – 0.56	10	
	Joint Condition	Opened joint, filled with calcite, 10 mm - 100 mm thick	15	
	Groundwater Condition	Damp	10	
	Cave roof Thickness	5 m – 10 m	10	
	Source of Vibration	Distance to the road 200 – 500 m	15	

**Table 8.**

**The whole feasibility assessment of cave geo-ecotourism are as follows.**

Parameter	Criteria	Assessment and Valuation of the Cave				
		Bentar	Cabe	Grengseng	Pakubon	Tritis
geotechnical value	Cave Rock Mass Rating (CRMR)	0.5	1.0	0.0	1.0	1.0
	integrity	0.5	0.5	1.0	1.0	1.0
scientific and educational value	representativeness	0.5	0.5	1.0	1.0	1.0
	paleogeographical value	0.5	0.5	0.5	0.5	1.0
	rareness	1.0	0.5	0.5	0.5	0.5
ecological value	ecological impact	0.5	0.5	0.5	0.5	0.5
	protected species	1.0	0.5	1.0	0.5	0.5
aesthetic values	number of viewpoints	1.0	0.5	1.0	1.0	0.5
	landscape/scenic beauty	0.5	0.5	0.5	0.5	1
	religious importance	0	0	0	0	0
cultural value	historical importance	0.5	1.0	1.0	0.5	0.5
	artistic importance	0.5	0.5	0.5	1.0	1.0
social-economics value	economic products	1.0	0.0	1.0	0.5	1.0
	human resource support	1.0	0.5	1.0	0.5	1.0
	agricultural support	0.5	0.5	0.5	0.5	0.5
<b>Total Scores</b>		<b>9.5</b>	<b>7.5</b>	<b>10</b>	<b>9.5</b>	<b>11</b>
<b>% of Feassibility</b>		<b>63.3%</b>	<b>50.0%</b>	<b>66.7%</b>	<b>63.3%</b>	<b>73.3%</b>

Based on the above study, the results show that Bentar Cave has a value of 63.3%, Cabe Cave 50.0%, Grengseng Cave 66.7%, Pakubon Cave 63.3%, and Tritis Cave 73.3% feasibility or readiness when they will be developed as cave geo eco-tourism. The five caves have their respective strengths and weaknesses. For this reason, in the future research, it is recommended to conduct a SWOT analysis in order to determine the solutions and to take further action of developing them.

The things that need to be considered at this time for each of the 5 caves are as follows: Bentar Cave is necessary to provide more facilities, Cabe Cave needs to be more open, environmental arrangement, and adds more adequate facilities, Grengseng Cave needs to geotechnical support for the roof of the cave in particular which is around the mouth of the cave, Pakubon Cave needs to improve its facilities and environmental arrangements, while Tritis Cave needs better management, promotion, and creating tourism flow modelling, to identify the fluctuation of tourism stream and its cartographic representation for transport companies (Nistor & Nicula, 2021).

## 5. CONCLUSIONS

1. In the Tanjungsari area that is geomorphologically forms a karst topography, composed of reef limestone classified into *boundstone* and *packstone* and bedded limestone of wackestone, there are 5 (five) caves with their uniqueness in term of ornaments and history, identified able to be developed to become geo eco-tourism, namely Bentar Cave, Cabe Cave, Grengseng Cave, Pakubon Cave, and Tritis Cave.
2. Based on the application of Cave RMR, Bentar Cave has a total score of 69 (Fair), Cabe Cave total score = 75 (Good), Grengseng Cave total score = 47 (Poor), Pakubon Cave total score = 81 (Good), and Tritis Cave total score = 79 (Good).
3. Referring to the feasibility assessment using parameters of geotechnical, scientific-educational, ecological, aesthetic, cultural, and social-economic values, Bentar Cave has a total score of 63.3%, Cabe Cave 50.0%, Grengseng Cave 66.7%, Pakubon Cave 63.3%, and Tritis Cave 73.3% feasibility or readiness for being developed as cave geo eco-tourism destinations.
4. In general, the 5 caves are potential to be developed as karst cave geo-ecotourism with their own strength and weakness, however, they need to be built, organized, and managed based on the integrated concept of geo-ecotourism which is considering geological and geotechnical, scientific-educational, ecological, aesthetics, cultural, and social-economical values.

## ACKNOWLEDGEMENT

This study was held with funding from the Institute of Research and Community Service of Universitas Pembangunan Nasional Veteran Yogyakarta. In relation to that, the authors express a high appreciation and deep gratitude to the institution for its support in the operation of this study.

## REFERENCES

- Anoname (2018) *The statistics of Gunungkidul*, Central Statistics Agency of Gunungkidul Regency
- Cahyadi, A. (2017) Land resources of the Gunungsewu Karst Area, [https://www.researchgate.net/publication/326114734\\_Sumberdaya\\_Lahan\\_Kawasan\\_Karst\\_Gunungsewu](https://www.researchgate.net/publication/326114734_Sumberdaya_Lahan_Kawasan_Karst_Gunungsewu)
- Dowling, R.K. (2013) Global Geotourism – An Emerging Form of Sustainable Tourism. *Czech Journal of Tourism*, 2(2), 59-79. DOI: 10.2478/cjot-2013-0004.
- Franklin, J.A. & Dusseault, M.B. (1989) *Rock Engineering*, McGraw Hill Publishing Company, New York.
- Kubalikova, L. (2013) Geomorphosite assessment for geotourism purposes. *Czech Journal of Tourism*, 2(2), 80-104. DOI: 10.2478/cjot-2013-0005.
- Kusumayudha, S.B. Zakaria, M.F., Prastistho, B., Rahatmawati, I., Setyaningrum T. (2020) The Potencies of Cave Geo-Ecotourism Development in Tanjungsari District, Gunungkidul Regency, Yogyakarta Special Region, *LPPM UPN "Veteran" Yogyakarta Conference Series Proceeding on Political and Social Science (PSS)*, Volume 1 Number 1 (2020): 309-322, <http://proceeding.researchsynergypress.com/index.php/pss/article/view/208>
- Kusumayudha, S.B. (2018) *Mengenal Hidrogeologi Karst (Introduction to Karst Hydrogeology)*, penerbit Pohon Cahaya, Yogyakarta
- Kusumayudha, S.B. (2005) *Karst Hydrogeology and Fractal Geometry of the Gunungsewu Area*, Adicita Publisher, Yogyakarta
- Kusumayudha, S.B. (2002) The Gunungsewu Hydrogeologic System, Book: *Sumberdaya Geologi Daerah Istimewa Yogyakarta dan Jawa Tengah, IAGI*, Pengda DIY-Jateng, 128 – 139
- Kusumayudha, S.B. & Santoso, A. (1998) Daerah Aliran Sungai Bawah Tanah di Gunungsewu Berdasarkan Peta Anomali Gravitasi dan Pola Struktur Geologi, Proc PIT HAGI XXIII: 66- 72

- Nistor, M.M. & Nicula A.S. (2021) Application of GIS Technology for Tourism Flow Modelling in the United Kingdom, *Geographia Technica*, Vol. 16, Issue 1, 2021, pp 1 to 12, DOI: 10.21163/GT\_2021.161.01
- Puspitasari, P., Rahatmawati, I. (2017) Mapping Potensi Wisata dalam Upaya Tata Kelola Green Ecotourism di Kabupaten Kaimana, Provinsi Papua Barat, Indonesia, *Proc. Seminar Nasional & Call for Paper in conjunction with 59 years of the faculty of Economics and Business*, UPN "Veteran" Yogyakarta
- Rahatmawati, I., Kusumayudha, S.B., Prastistho, B., Setyaningrum, T., Zakaria, M.F., Priyandhita, N. (2020) The Intention to Repeat Visit Tourist Visits on The Geotourism Object of Cave Bentar, Tanjungsari, Gunungkidul, Yogyakarta, Indonesia, *Journal of Environmental Management and Tourism*, Vol 11 No 8, pp 1931-1937, doi: [https://doi.org/10.14505/jemt.v11.8\(48\).00](https://doi.org/10.14505/jemt.v11.8(48).00)
- Ruda, A. (2016) Exploring Tourism Possibilities using GIS-Based Spatial Association Methods, *Geographia Technica*, Vol. 11, Issue 2, 2016, pp 87 to 101, DOI: 10.21163/GT\_2016.112.09
- Setyaningrum, T., Rahatmawati, I., Kusumayudha, S.B., Prastistho, B., Zakaria, M.F. (2020) *Geo Eko-wisata Gua Tanjungsari (Cave Geo Eco-tourism of Tanjungasri)*, LPPM UPN "Veteran" Yogyakarta
- Suyoto (1994) Sekuen Stratigrafi Karbonat Gunungsewu, *Proc IAGI Annual Meeting XXIII*, Vol I: 67-76
- Van Bemmelen, R..W., (1949). *The Geology of Indonesia*, Vol. IA, Gov. Print. Office, The Hague Martinus Nijhoff.
- <https://notaclueadventures.com/2015/03/blog/ecotourism-vs-geotourism>

## LONG-TERM WATER DEMAND ASSESSMENT USING WEAP 21: CASE OF THE GUELMA REGION, MIDDLE SEYBOUSE (NORTHEAST ALGERIA)

Essia BOUDJEBIEUR<sup>1\*</sup>, Lassaad GHRIEB<sup>2</sup>, Ammar MAOUI<sup>3</sup>,  
Hicham CHAFFAI<sup>1</sup>, Zine Labidine CHINI<sup>4</sup>

DOI: 10.21163/GT\_2021.162.06

### ABSTRACT:

The Guelma sub-basin, an integral part of the Middle Seybouse basin, covers a surface area of 818 km<sup>2</sup>, subject to subhumid climate. The main surface water reservoir is the Bouhamdane dam with a regulated volume of 55 hm<sup>3</sup>. The main underground reservoirs are found in the aquifer systems of the Guelma plain, the Bouchegouf plain, the H'lia water table and the Heliopolis karst. To enable the rational use of water resources in the study region, integrated management of these resources remains essential. In this work we used WEAP 21 software (Water Evaluation and Planning), for the modeling of water resources, considering the year 2017 as the reference year for 2020-2050, with a base scenario «water demand». The results of the simulation show a significant water shortage of around 50.5 hm<sup>3</sup>, marking a scarcity of the resource, noticed from the reference year 2017, because of the unfavorable climatic conditions which significantly impacted the water reserve in the municipalities of the watershed. This shortage will decrease to a volume of 31 hm<sup>3</sup> in 2024, and 104.20 hm<sup>3</sup> in 2050.

**Key-words:** water resources, integrated management, Middle Seybouse basin, climate change, WEAP21, water demand

### 1. INTRODUCTION

The discussion of aspects of the integrated water resources management is one of the major problematics raised in Algeria today. It is becoming an absolute necessity for a good management of water resources allocation in order to equitably satisfy the drinking water needs of the population and the economic sectors. (Zerkaoui et al., 2018, Al-Shutayri, et Al-Juaidi, 2019, Alemu et Dioha, 2020, Ali et al., 2014).

It is a vital necessity to maintain water resources in the face of increasing demands in agricultural, industrial and municipal uses. Production of crops and livestock is water consuming; agriculture alone accounts for 70% of all water consumption (www.unesco.gr). The world will need 50% more food supply for the population estimated at 9.5 billion for 2050 (Singh, 2014). It is estimated that the water consumption for both rainfed and irrigated agriculture will increase by approximately 19% by 2050. About 30% of fresh water on earth is stored in aquifers (Shiklomanov and Rodda 2003).

---

<sup>1\*</sup> University Badji Mokhtar, Water Resource Lab. & Sustainable Development, 23000 Annaba, Algeria, [a.boudjebieur@yahoo.fr](mailto:a.boudjebieur@yahoo.fr), [hichamchaffai@yahoo.fr](mailto:hichamchaffai@yahoo.fr)

<sup>2</sup> University 8 May 1945, Water Resource Lab. & Sustainable Development, 24000 Guelma, Algeria, [ghrieblassaad@yahoo.fr](mailto:ghrieblassaad@yahoo.fr)

<sup>3</sup> University 8 May 1945, Civil Engineering and Hydraulic Laboratory, 24000, Guelma, Algeria, [maoui\\_ammam@yahoo.fr](mailto:maoui_ammam@yahoo.fr)

<sup>4</sup> University of Saad Dahlab Blida 1, Algeria, [chini\\_zine@yahoo.fr](mailto:chini_zine@yahoo.fr)

Since the late 1970s the occurrence of drought years increases in North Africa is presenting a major constraint to the future development of these regions. According to the IPCC conventions, a general decrease in rainfall together with a prominent surface heating can be expected for sub-Saharan Africa and north of the Sahara until 2050, resulting in further decreasing fresh water availability (Klose et al., 2008).

In Algeria, the multiplication of water needs linked mainly to the demographic expansion, the irrational exploitation of resources and the development of economic and agricultural activities has significantly increased the demand for water. (Kiniouar et al., 2017, Hamlat et al., 2013, Kahlerras et al., 2018).

Models are among the most useful devices in water supply management, and especially multi-objective modeling tools that involve stakeholders and facilitate decision making. They can be utilized in gathering data and improving the process of planning and managing the water supply systems (Sulis et Sechi, 2013, Shahraki, et al., 2016, Léville et al., 2003, Saadoun et al., 2014), combining physical and socioeconomic parameters. In the WEAP (Water Evaluation and Planning System) model (Stockholm Environment Institute 2005) standard linear programming is used for the water allocation problems.

Using WEAP a water planner can analyse a full range of water issues through a scenario-based approach. Scenarios could include climate variability and change, watershed condition and changes, anticipated demands, ecosystem needs, the regulatory environment, operational objectives and available infrastructure (Yates et al., 2005 Husain et Rhyme, 2021).

The software, developed by the Stockholm Environment Institute, has shown its performance in many cases in terms of simulation for the choice of scenarios of development and management of the water resource in the medium and long term and decision-making which are needed (SEI 2008). This model is a decision support system (DSS) and provides a complete analysis of water supply and demand at present and estimation for the process in the future (Yazdanpanah, et al., 2008 Höllermann et al., 2010). This software is used when there is multipurpose and competitive demand and allows the analysis of different management patterns (Seiber, et al., 2005 Husain et Rhyme 2021, Xue et al., 2015).

The main objective of this study is to assess the impact of additional water demand in the Guelma region, Middle Seybouse, in long-term, using the Water Evaluation and Planning system (WEAP).

## 2. MATERIALS AND METHODS

### 2.1. Description of the study area

#### 2.1.1. Geographic location

Covering an area of approximately 818 km<sup>2</sup>, the sub-catchment area of the middle Seybouse is located northeast of Algeria, 60 km south of the Annaba city between latitudes 36°14' and 36 ° 35' north and longitudes 7 ° 16' and 7 ° 44 'east, drained by the main stream which is the Seybouse which flows from west to east over a distance of 55.30 km (**Fig.1**).

The population was estimated at the end of 2017 at around 355,250 inhabitants, with a density of 334 inhabitants / km<sup>2</sup> (Algerian national statistics office 2008). The basin of the middle Seybouse is subject to a Mediterranean climate, rainy and cold in winter and hot and dry in summer. The mean annual rainfall for a 30-year observation period is of the order of 615.8 mm, with a mean annual temperature of around 18.26 ° C.

From a hydrogeological point of view, this is a collapsing zone filled with very permeable alluvial deposits, which contains a significant water table supplied by infiltration water and by lateral contributions from the Seybouse watershed (**Fig. 2**).



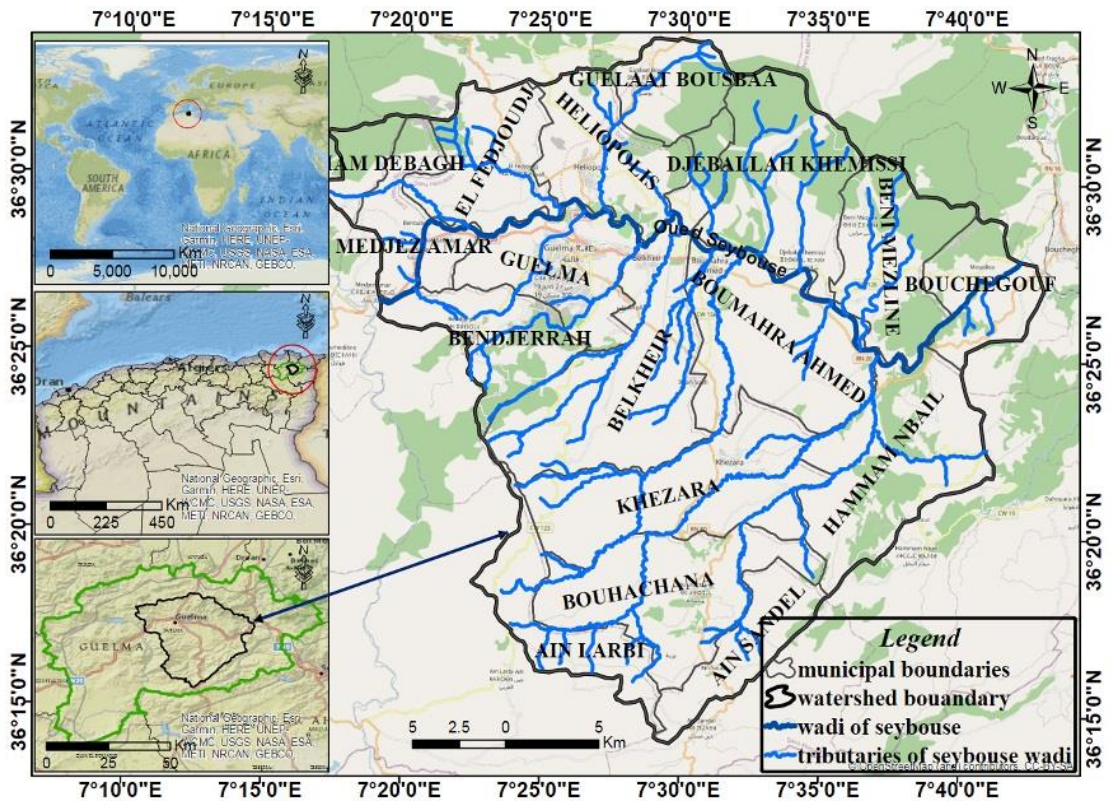


Fig. 1. Location map of the study area.

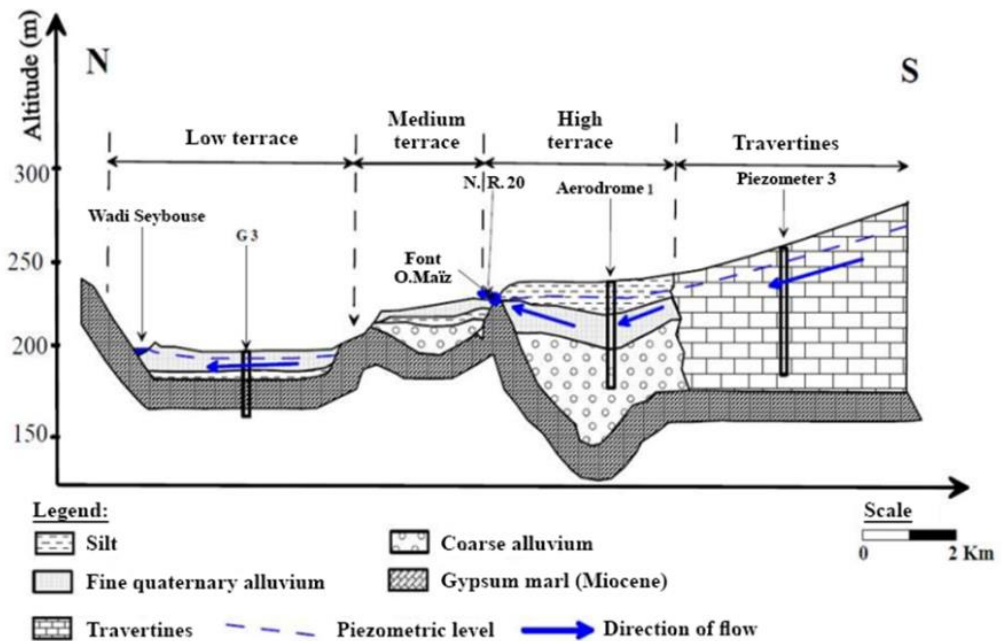


Fig. 2. Hydrogeological cross-section in the study area (B. Gaud ,1974).

### 2.1.2. Distribution of water resources

The population is supplied with drinking, irrigation and industrial water in the middle Seybouse basin, provided by groundwater extracted from the catchment areas of Héliopolis, OuedH'lia, the plains of Guelma and Bouchegouf with an estimated volume of  $17 \text{ hm}^3/\text{year}$ , as well as treated water from the Bouhamdane dam, with a volume of more than  $63 \text{ hm}^3/\text{year}$ , including  $18 \text{ hm}^3/\text{year}$  for drinking water supply (four municipalities out of seventeen), and more than  $45 \text{ hm}^3/\text{year}$  for the large irrigation scheme (Guelma-Bouchegouf) (Water Resources Department, 2018).

The distribution of drinking water in our study area encounters difficulties which make the management of these resources difficult (Fig. 3).

We can cite:

- the distribution time slots are insufficient in relation to the volume distributed;
- the delivery pipes are very old and generate a loss of more than 30% compared to the volume produced and distributed;
- the endowment is low compared to the Algerian standard.

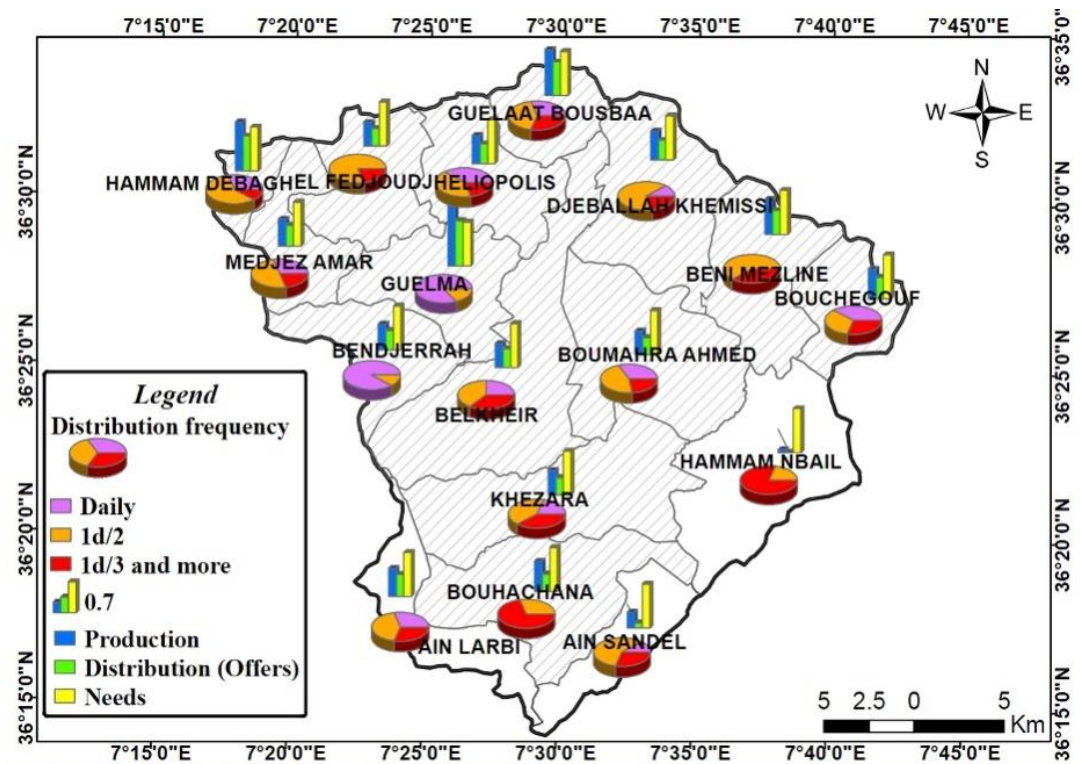


Fig. 3. Map of the production and distribution frequencies of water drinking water in the study area.

The irrigated perimeter, covering a surface area of 9,250 ha, also encountered several problems, mainly due to the mixed distribution network, which plays the dual role of backflow and distribution. The breakdown and dilapidation of this network in addition to frequent power cuts at pumping stations have reduced the volume allocated to irrigation to more than 35%. The 2017 season irrigation campaign at the Guelma-Bouchegouf perimeter took place under exceptional conditions, given the drop in the water level of the Hammam Debagh dam, the main source of power for the perimeter which was deprived of power for the year 2017-2018.

## 2.2. Methodology

The Water Assessment and Planning System (WEAP21) (<http://www.weap21.org/>), is a modeling and planning tool, developed by the Stockholm Environment Institute. It has enough flexibility to adopt different levels of data availability with a friendly graphical user interface. It is a useful tool for water resources management, which includes both water supply and demand issues, in addition to water quality and ecosystem preservation, such as required by an integrated approach to watershed management (Agarwal et al., 2019, Górska, 2020, Omar and Moussa,2016, Mostafa and Sarjoughian,2021). **Fig. 4** summarizes the steps followed for the realization of the model.

Data for 2017 are used in our study for all water resources and water demand by municipality as a unit. For this purpose, we have on the one hand for each municipality a drinking water demand site, a farming water demand site and an industrial water demand site if it exists, considering evaporation as a demand for water, and on the other hand water supply elements such as groundwater extracted from aquifers and surface water from the dam and hill reservoirs and finally rainfall and runoff in the sub-basin (**Fig.4**).The database of the study area which allows the application of the model is collected from many administrations, such as Hydrographic Basin Agency, National Agency for Hydraulic Resources, National Meteorological Office, Directorate of Agricultural Services, National Statistics Office, National Office for Irrigation Perimeters, Algerian Water and the two existing meteorological stations in the middle Seybouse sub-basin Hammam Debagh and Belkhier stations for hydrological data.

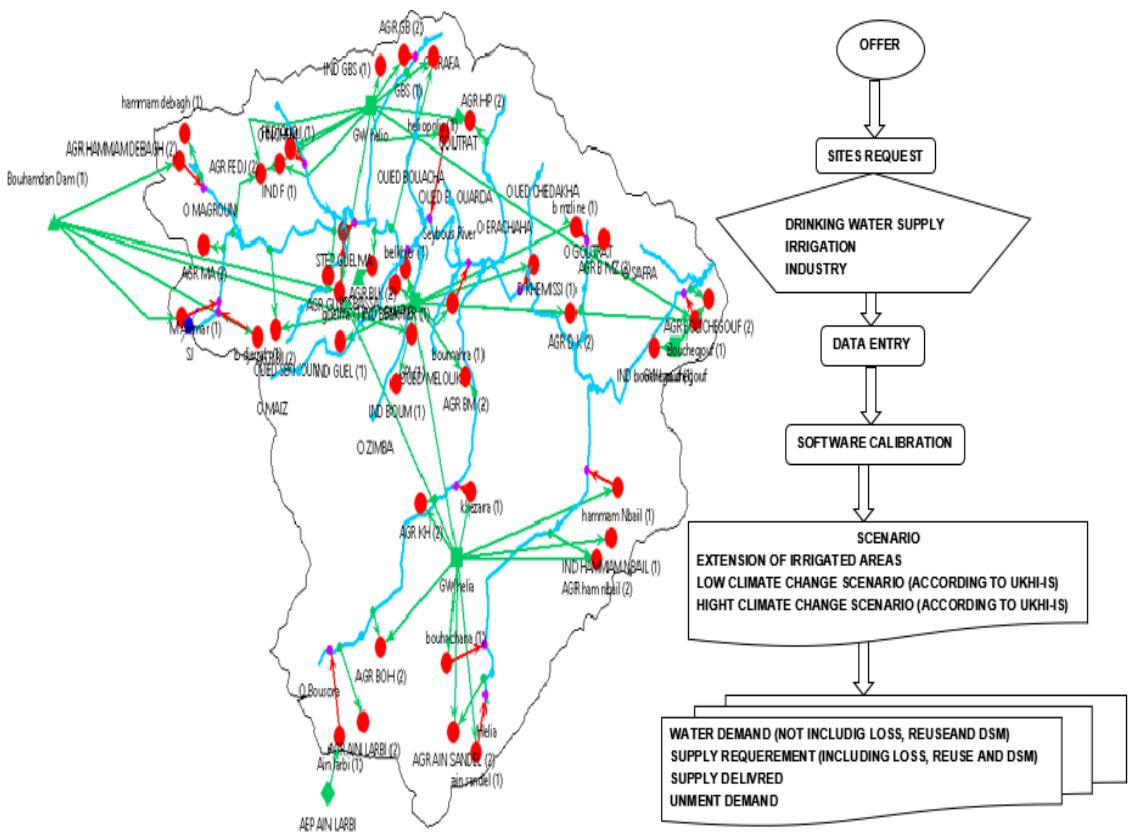


**Fig. 4.** Conceptual model of water resources distribution.

In this part, the time parameters should be resolved. Create a year of current accounts for the project. for that, we have chosen the year 2017 as the reference year for all information on the system:

demand sites, supply data, consumption, transmission link. The baseline scenario is established from the current account, in which all data base are introduced, to simulate the same system evolution without intervention (SEI,2008). For our study, the reference scenario covers the period (2020 - 2050), It translates simply a projection of trends current without major changes, and serves as a point of comparison for others Scenarios in which changes in system data can be realized. To carry out our work well, we have adopted the scenarios: climate change with its two hypotheses (high and low) and extension of irrigated areas. The study duration is from the year 2020 until 2050.

### 2.3. Climate change scenarios (CCS)

According to the results of the national project ALG / 98 / G31, northeastern Algeria is subject to the consequences of global warming with reduced inputs and increased temperature (Abdelguerfi, 2003). According to the UKHI (United Kingdom Meteorological Office High Resolution). model, the IPCC “IS92a” scenario with the two high and low assumptions was adopted (**Table 1**).

**Table 1.**  
**The GIEC “IS92a” scenario with the two high and low hypotheses.**

Season	Climatic parameters	2020		2050	
		Low	High	Low	High
Autumn	T° C (+)	0.8	1.1	1.2	2.2
	P % (-)	6	8	10	15
Winter	T° C (+)	0.65	0.8	0.95	1.6
	P % (-)	10	10	16	16
Spring	T° C (+)	0.85	0.95	1.25	1.9
	P % (-)	5	9	10	20
Summer	T° C (+)	0.85	1.05	1.25	2.1
	P % (-)	8	13	15	22

In this study, the statistical downscaling model LARS-WG 6.0, which is a stochastic generator of meteorological conditions based on observed data (Semenov et al. 1998), was used to extract future precipitation and temperatures at the local scale from the MCGs of CMIP5 under two scenarios RCP 4.5 and RCP 8.5. It should be noted that all climate model outputs are in general biased due to the systematic errors that occur after the discretization and the spatial averaging in grid cells and due to the imperfect conceptualization of the models themselves (Teutschbein and Seibert 2012). Using the models’ outputs as they are can lead to significant errors in impact evaluations. Thus, it is necessary to apply bias correction to the models’ outputs before their use in impact analyzes (Teutschbein and Seibert 2012). The version 6.0 of LARS-WG (Semenov & Stratonovitch, 2015)) provides for a chain of measurement allowing the correction of the bias of the GCM outputs at the time of the extraction and the generation of climate data from the CMIP5 models.

## 3. RESULTS AND DISCUSSION

### 3.1. Irrigated land extension scenario (ILES)

Due to the low use of irrigated land in relation to useful agricultural land (UAA), the agricultural services of the Guelma province, foresees an increase rate of 50% every 10 years in these irrigated lands. (Five- years project 2014-2019 (WRD, 2017).



In the three scenarios adopted and for the seventeen municipalities of the watershed, the number of inhabitants increases from 346,342 in 2017 to 688,091 inhabitants in 2050, i.e., an increase of 50.33% and the surface area of irrigated land jumps from 14,302.5 ha (i.e. 18.65% of UAA) in 2017 to 37,228.61 ha, or (48.54% of UAA) in 2050 (Fig. 5).

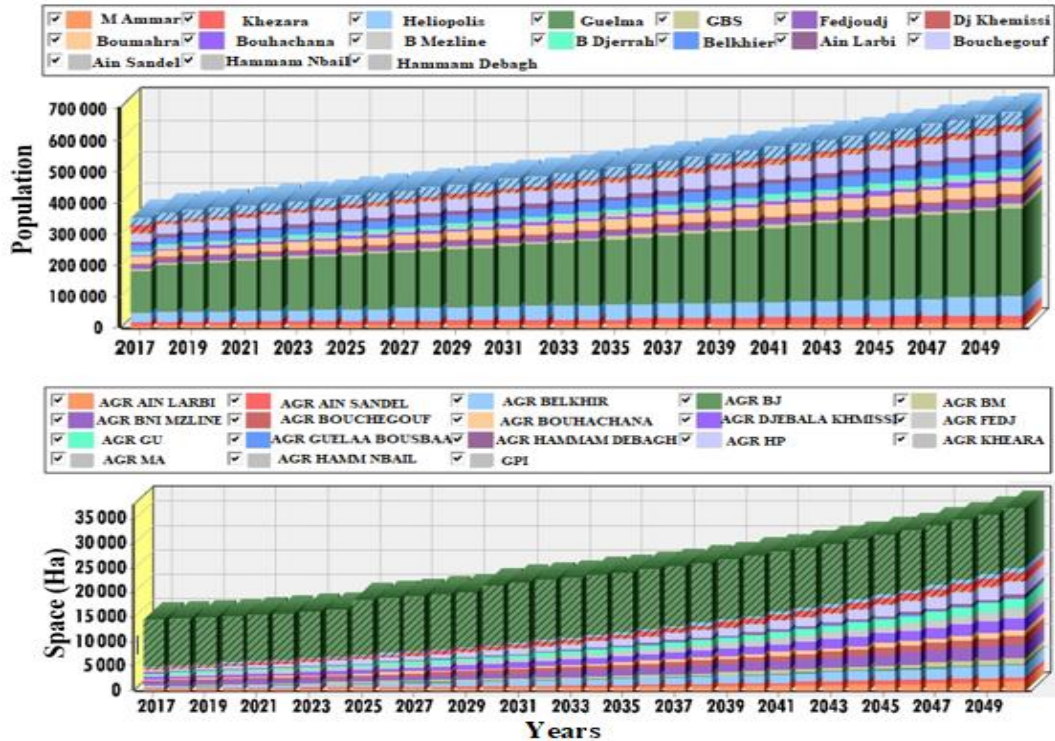


Fig. 5. Evolution of inhabitants and irrigated areas by scenarios.

For water needs, we notice a clear increase from a volume of 80.92 hm<sup>3</sup> to more than 194.83 hm<sup>3</sup> in all the scenarios adopted, mainly linked to the extension of the irrigated land areas. For the reference scenario, a slight increase in water needs is recorded, varying from 80.92 hm<sup>3</sup> in 2017 to 91.10 hm<sup>3</sup> in 2050, following a moderate increase in the population (Fig.6).

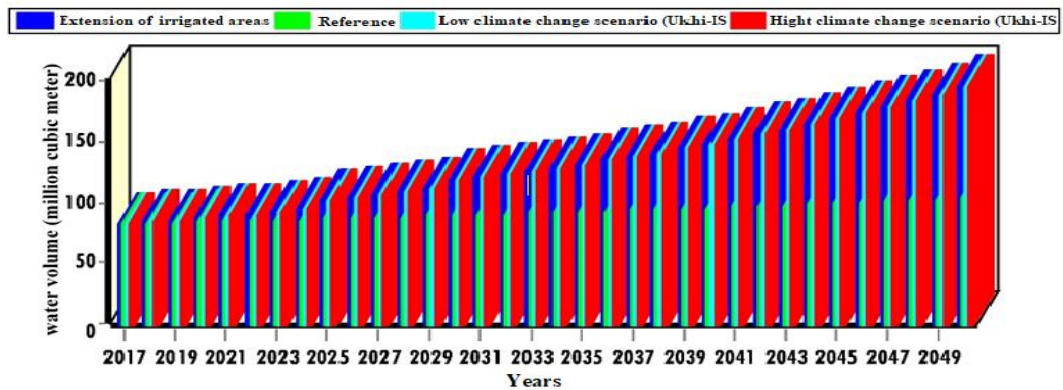


Fig.6. Water demand by scenario (2017-2050).

The total water demand (including losses) in the study area is marked by a considerable increase in all the scenarios adopted (SCC and SETI), going from a volume of 105.23 hm<sup>3</sup> in 2017 to 226.95 hm<sup>3</sup> in 2050 for the reference scenario (RS), the increase in demand is low during the simulation period, ranging from 105.23 hm<sup>3</sup> in 2017 to 114.36 hm<sup>3</sup> in 2050 (Fig.7).

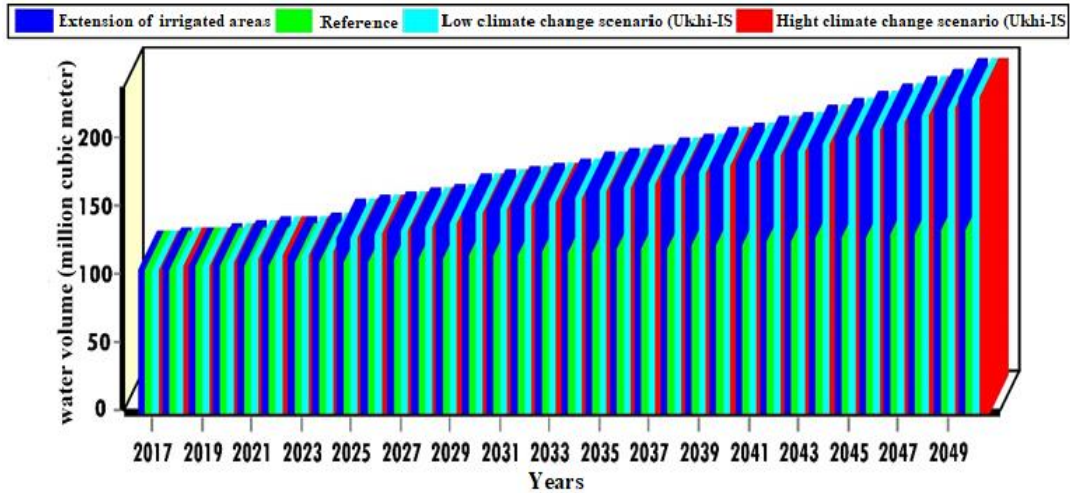


Fig.7. Water total demand by scenario (2017-2050).

For distributed water during 2017 and for all the scenarios adopted, the volume of water distributed is around 45.75 hm<sup>3</sup>. This volume increases to 89.08 hm<sup>3</sup> in 2025, which can be explained by the forecast to achieve an irrigation perimeter of 1700 ha in the Khezaras municipality and the construction of another irrigation perimeter of 1000 Ha at Bouchegouf by 2030. In the year 2050 this same volume increases to reach 123.39 hm<sup>3</sup> (Fig.8).

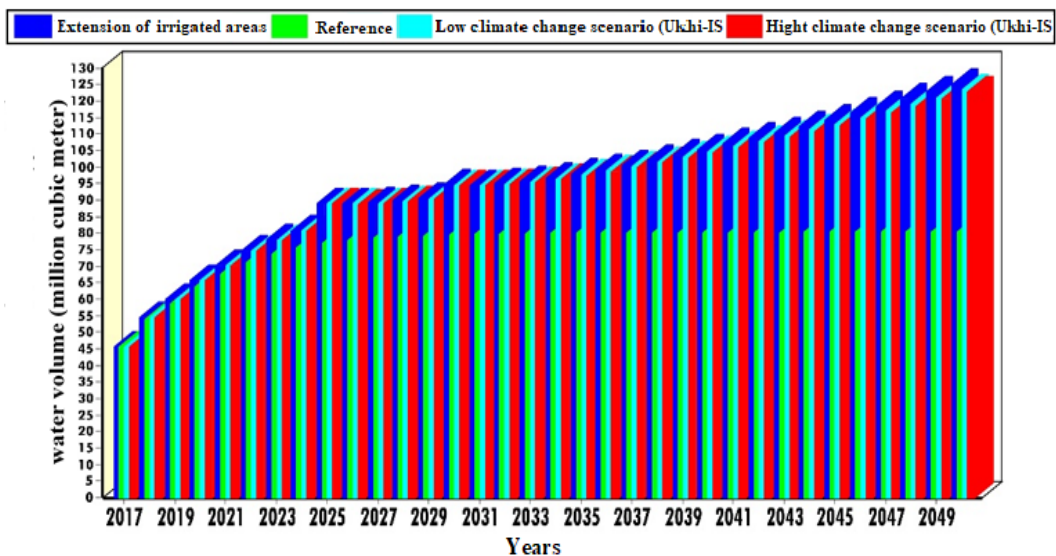
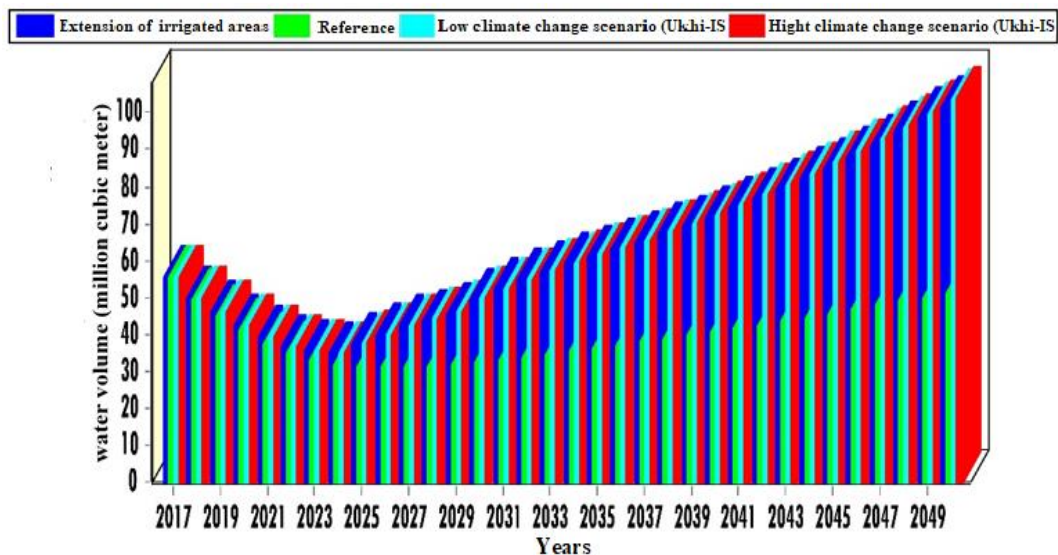


Fig. 8. Water distributed by scenario (2017-2050).

According to the **Fig. 9**, we see an unmet need for water estimated at a volume of  $55.5 \text{ hm}^3$  during the reference year 2017. This deficit distributed between irrigation water (around  $45 \text{ hm}^3 / \text{year}$ ) and drawdown slicks are mainly due to the lack of precipitation during this year. From the year 2025 begins a change resulting in an increase in the deficit interpreted by a lack of  $104.20 \text{ hm}^3$  at the end of the simulation period (2050).



**Fig. 9.** Unmet water demands by scenario (2017-2050).

#### 4. CONCLUSION

In this study we chose the WEAP software which gave us the opportunity to use our data on water resources to simulate their evolution and their users by 2050. The results obtained showed that the middle Seybouse basin is already under water stress, it suffers from water scarcity and is sensitive to drought conditions. The number of inhabitants increases from 346,342 in 2017 to 688,091 inhabitants in 2050, and the surface area of irrigated land jumps from 14,302.5 ha in 2017 to 37,228.61 ha in 2050. The amount of unmet demand for water is greater than the water supplied; available resources such as mean rainfall and outgoing water collection and storage infrastructure, including natural groundwater reservoirs, have failed to meet current and future needs in the middle Seybouse watershed. The scenarios of climate change and extension of irrigated land chosen for this study, show a water deficit from the reference year 2017 with a shortage of  $50.5 \text{ hm}^3$  which will be increasing to  $104.20 \text{ hm}^3$  in 2050. The catchment area of the middle Seybouse presents a glaring shortage at the end of the scenarios.

#### 5. RECOMMANDATIONS

It is urgent that those responsible for water participate seriously in solving this problem by using other resources, namely unconventional water, desalination and exploitation of surface water through the study and realization of dams.

#### Acknowledgements

The data presented in this article are the results of investigations which we carried out with the assistance of the services of hydraulics, agriculture, industry and municipalities. We are very grateful to them.

## REFERENCES

- Abdelguerfi, A. (2003). *Needs assessment in terms of capacity building necessary for the assessment and reduction of risks threatening the elements of biological diversity in Algeria Report number: Synthesis Report* (Volume 5) Affiliation: Consultation Report within the framework of the UNDP Project-FEM-MATE, ALG97 / G31 " Action Plan and National Strategy on Biodiversity.
- Agarwal, S., Patil, J.P., Goyal, V.C. et al. (2019). *Assessment of Water Supply–Demand Using Water Evaluation and Planning (WEAP) Model for Ur River Watershed, Madhya Pradesh, India*. J. Inst. Eng. India Ser. A 100, 21–32, <https://doi.org/10.1007/s40030-018-0329-0>.
- Al-Shutayri, A.S., Al-Juaidi, A.E.M. (2019). *Assessment of future urban water resources supply and demand for Jeddah City based on the WEAP model*. Arab J Geosci 12, 431, <https://doi.org/10.1007/s12517-019-4594-7>.
- Alemu, Z.A., Dioha, M.O. (2018). *Modelling scenarios for sustainable water supply and demand in Addis Ababa city, Ethiopia*. Environ Syst Res 9, 7 (2020). <https://doi.org/10.1186/s40068-020-00168-3>.
- Algerian national statistics office (2018) Unpublished report.
- Fard, M., D., Sarjoughian, H., S. (2021). *A restful framework design for componentizing the water evaluation and planning (WEAP) system*, Simulation Modelling Practice and Theory, **106**, 102199, ISSN 1569-190X, <https://doi.org/10.1016/j.simpat.2020.102199>.
- Gaud, F (1974). Hydrogeological study of the alluvial aquifer of Guelma. Unpublished report.
- Górska, M. (2020). *Optimizing the water allocation system in the Dutch region by adopting the WEAP model*.
- Husain S.A., Rhyme N.H.M. (2021). *Decision Support Method for Agricultural Irrigation Scenarios Performance Using WEAP Model*. In: Abdul Karim S.A. (eds) Theoretical, Modelling and Numerical Simulations Toward Industry 4.0. Studies in Systems, Decision and Control, **319**. Springer, Singapore. [https://doi.org/10.1007/978-981-15-8987-4\\_](https://doi.org/10.1007/978-981-15-8987-4_).
- Höllermann, B., Giertz, S. & Diekkrüger, B. Benin (2010). *2025—Balancing Future Water Availability and Demand Using the WEAP ‘Water Evaluation and Planning’ System*. Water Resources Management, **24**, 3591–3613 <https://doi.org/10.1007/s11269-010-9622-z>.
- Hamlat, A., Errih, M. & Guidoum, A. (2013). *Simulation of water resources management scenarios in western Algeria watersheds using WEAP model*. Arab J Geosci 6, 2225–2236, <https://doi.org/10.1007/s12517-012-0539->.
- Kiniouar, H., Hani, A., Kapelan, Z. (2017). *Water Demand Assessment of the Upper Semi-arid Sub-catchment of a Mediterranean Basin*. Energy Procedia, **119**, 870-882, ISSN 1876-6102, <https://doi.org/10.1016/j.egypro.2017.07.140>.
- Kahlerras, M., Meddi, M., Benabdeltmalek, M. et al. (2018). *Modeling water supply and demand for effective water management allocation in Mazafran basin (north of Algeria)*. Arab J Geosci 11, (547), <https://doi.org/10.1007/s12517-018-3869-8>
- Klose S., Reichert B., Lahmouri A. (2008). *Management Options for a Sustainable Groundwater Use in the Middle Drâa Oases under the Pressure of Climatic Changes*. In: Zereini F., Hötzl H. (eds) Climatic Changes and Water Resources in the Middle East and NorthAfrica. Environmental Science and Engineering. Springer, Berlin, Heidelberg. [https://doi.org/10.1007/978-3-540-85047-2\\_14](https://doi.org/10.1007/978-3-540-85047-2_14).
- Lévite, H., Sally, H., Cour, J. (2003). *Testing water demand management scenarios in a water-stressed basin in South Africa: application of the WEAP model*. Physics and Chemistry of the Earth, Parts A/B/C, **28**, (20–27), 779-786, ISSN 1474-7065, <https://doi.org/10.1016/j.pce.2003.08.025>.
- Omar, M., Moussa, M.A., (2016). *Water management in Egypt for facing the future challenges*. Journal of Advanced Research, **7** (3), 403-412, ISSN 2090-1232, <https://doi.org/10.1016/j.jare.2016.02.005>.
- Saadoun, A., Ali, M.F., Abd Rahman, N.F., Khalid, K. (2014) *An Assessment of Water Demand in Malaysia Using Water Evaluation and Planning System*. In: Hassan R., Yusoff M., Ismail Z., Amin N., Fadzil M. (eds) In CIEC 2013. Springer, Singapore. [https://doi.org/10.1007/978-981-4585-02-6\\_64](https://doi.org/10.1007/978-981-4585-02-6_64).
- SEI (2008) WEAP (Water Evaluation and Planning): User Guide for WEAP-21. Stockholm Environment Institute, Boston. Soc. Civ. Eng. **81**, 695–721.
- Seiber, J., Swartz, C., & Huber-Lee, A. (2005). *User guide for WEAP21*, Stockholm Environment Institute, Tellus Institute, 176 pp.



- Semenov, M. A. Brooks R. J. Barrow E. M. Richardson C. W. (1998). *Comparison of the WGEN and LARS-WG stochastic weather generators for diverse climates*. Climate Research **10** (2): 95–107. <https://doi.org/10.3354/cr010095>.
- Shahraki, et al. (2016). *An application of WEAP model in water resources management considering the environmental scenarios and economic assessment case study: Hirmand Catchment*. Modern Applied Science **10** (5): 49-56.
- Shiklomanov, I. A., Rodda J. C. (2003). *World water resources at the beginning of the twenty-first century*. Cambridge, UK, Cambridge University Press.
- Singh, A. (2014). *Conjunctive use of water resources for sustainable irrigated agriculture*. Journal of Hydrology, **519**, 1688–1697.
- Sulis, A., Sechi, G. M. (2013). *Comparison of generic simulation models for water resource systems*. Environmental Modelling and Software, 40, 214–225.
- Teutschbein, C, Seibert, J. (2012). *Bias correction of regional climate model simulations for hydrological climate-change impact studies: review and evaluation of different methods*. J. Hydrol. **456–457**:12–29. <https://doi.org/10.1016/j.jhydrol.2012.05.052>.
- UKHI (United Kingdom Meteorological Office High Resolution) The Met Office is the UK's national weather service. We provide essential weather services and leading climate science around the world. <https://www.metoffice.gov.uk/research/climate/maps-and-data/regional-climates/index>.
- Vila, J. M. (1980). *The Alpine chain of eastern Algeria and the Algerian-Tunisian borders*, 3 rd cycle thesis, 663 pp, Univ.Paris VI, Orsay.
- Water resources department (2018) data on the quantities of water distributed.
- WEAP 21: (<http://www.weap21.org/>).
- Xue Li, Yue Zhao, Chunli Shi, JianSha, Zhong-Liang Wang, Yuqiu Wang (2015) *Application of Water Evaluation and Planning (WEAP) model for water resources management strategy estimation in coastal Binhai New Area, China*. Ocean & Coastal Management, **106**, 97-109, ISSN 0964-5691, <https://doi.org/10.1016/j.ocecoaman.2015.01.016>.
- Yates, D., Purkey, J., Seiber, A., Huber-Lee, A., Galbraith, H., West, J., Herrod-Julius, S. (2005) *A physically-based, water resource planning model of the Sacramento Basin, California USA*. Am. Soc. Civ. Eng. **81**, 695–721.
- Yazdanpanah, T., Khodashenas, S. R., Davari, K., Ghahraman, B. (2008). *Water resources management in a Watershed with WEAP model (A case study of Azghad watershed)*. Journal of Agriculture Science and Technology, **22** (1), 213–221.
- Zerkaoui, L., Benslimane, M., Hamimed, A. (2018). *Planning and systematic management of water resources by the WEAP model, case of the Mabtouh watershed (northwestern Algeria)*. Arabian Journal of Geosciences **11** (24): 1-17.

## APPLICATION OF GIS IN THE ASSESSMENT OF FLOOD RISK IN THE REGION ZENICA - DOBOJ CANTON

Aida KORJENIĆ<sup>1</sup> , Edin HRELJA<sup>1</sup>, Amina SIVAC<sup>1</sup>, Amra BANDA<sup>1</sup> 

DOI : 10.21163/GT\_2021.162.07

### ABSTRACT:

Flood represents a temporary cover of water that submerges land, usually not covered by water, which is caused by water overflowing the watercourses. The floods that occur in the area of Zenica-Doboj Canton in Bosnia and Herzegovina cause massive damage to agriculture, housing, equipment and civil engineering facilities and can be characterized as hazards. The hydrographic backbone of this Canton is the river Bosna, and the subject of research in this paper is the flood vulnerability in Zenica-Doboj Canton. The result of the work is the production of flood hazard and risk maps using GIS. Geographic Information System (GIS)-based spatial analysis and visual elements have been used frequently in recent years for detection of flood hazard areas and preparation of maps. GIS applications are based on a database and analysis tools which have logical and mathematical relationships between the layers. When creating the flood hazard map, in addition to GIS tools, Hec-RAS was also used as a program intended for the analysis of hydraulic calculations. The results of this paper are of great importance for spatial planning and environmental protection, starting with local communities, municipalities and the entire Canton.

**Key-words:** *Spatial analysis, the Bosnia River, Flood risk, GIS, Physical geography*

### 1. INTRODUCTION

GIS is a data management system that shows different data sets on the same map, such as land use, construction, environmental, groundwater and topography (Ozkan, Tarhan, 2015). GIS and hydraulic models have been recommended for studying flood analysis and flood prediction (Gyóri et al., 2016, Haidu et al., 2017). Geographic Information System (GIS) mapping applications vary to flood hazard mapping, flood hazard management, hydrological data storing and management. Especially, a combination of GIS (Geographic Information System) and HEC-RAS (Hydrologic Engineering Center-River Analysis System) has a great capability in the simulation of flood hazard maps (Kim et al., 2020). Out of all-natural hazards in the world, flood is the most common one. River flood results from the water level overtop, both natural and artificial, of the riverbank, which disturbs human life and properties (Koem, Tantane, 2021). Flood hazard in rivers can be characterized by the probability and intensity of high river flows and their consequent inundations, and it depends on the atmospheric and catchment processes preceding river flood generation (Merz et al., 2010).

Urban floods are one of the most devastating natural disasters globally, and improved flood prediction is essential for better flood management. Today, high-resolution real-time datasets for flood-related variables are widely available (Khan, He, Valeo, 2018). Urbanization and industrialization have led to changes in land tenure over time. Urbanization has caused the increase in impermeable surfaces that contribute significantly to surface runoff, with the most important role going to Effective Impermeable Surfaces (Haidu, Ivan, 2016). Among natural disasters, floods have been the most common in terms of frequency, threat level and caused damage (Gavrilović et al., 2012; Petrović et al., 2015) and this problem has become relevant after several major floods in various parts of Europe and the world in the last decade of the twentieth century, followed by high damage and loss of life. In recent decades, almost a third of all human victims of natural disasters in the world are flood victims, and material damage is estimated at tens of billions of dollars (Jovanović, et al., 2009).

---

<sup>1</sup> University of Sarajevo, Faculty of Science, Department of Geography, 71000 Sarajevo, Bosnia and Herzegovina, [aida.k@pmf.unsa.ba](mailto:aida.k@pmf.unsa.ba), [edinhrelja@pmf.unsa.ba](mailto:edinhrelja@pmf.unsa.ba), [amina.sivac@pmf.unsa.ba](mailto:amina.sivac@pmf.unsa.ba), [amra.banda@pmf.unsa.ba](mailto:amra.banda@pmf.unsa.ba)

Trend analyses show that major flood disasters as well as damages and losses generated by them have increased drastically in recent years (Berz, 2000; Barredo, 2007). Because of the accelerated pace of anthropogenic activity, hazard frequency and intensity is exacerbated, requiring immediate delivery of science-based solutions for mitigation, resilience, and adaptation that can be quickly deployed in any hazard-prone area (Allen-Dumas, Xu, Kurte, Rastogi, 2021). Mitigating these urban water hazards is challenging for watershed management and the urban planning community (Eriksson et al., 2015). Speaking of the causes of floods in recent times, we must point to climate change, because the strongest floods are caused by climatic phenomena such as heavy rainfall, melting snow or their combination (Školjić, Hodžić, 2018). The amount of precipitation, their spatial distribution, intensity and duration are the basic climatological causes of floods. In addition to these causes, the occurrence of floods is also contributed by the capacity of watercourses or watercourse networks to receive and further transmit water runoff, before the onset of precipitation, soil cover and topography (Imamović, 2015). According to the causes, floods can also occur due to the accumulation of ice in streams, landslides or earthquakes, demolition of dams or other anthropogenic effects (Mandych, 2010). Bonacci (2003) states that the natural cause of floods can also be the leakage of water at the mouths of rivers due to waves. Depending on the time of the formation of a water wave, the floods can be calm, torrential and accidental. Calm floods are those of large rivers where it takes ten or more hours to form a water wave. There are torrential floods on mountain watercourses where the water wave is formed in less than ten hours, while accidental floods occur mainly with the demolition of water management or hydropower facilities, and are characterized by the current formation of a large water wave.

Flood risk is a combination of the probability of a flood event and the possible harmful consequences of a flood event for human health, the environment, cultural heritage and economic activity (Jabučar, Lukovac, 2015). It is a measure of the potential damage that could occur when and if flooding occurs and is determined by the "overlap" of spatial data on the elements of hazard on the one hand and the locations of potentially endangered categories on the other.

### 1.1. Floods in Zenica-Doboj Canton

Analysis of the average water level for a multi - year period shows that the river Bosna and its tributaries in the area of Zenica - Doboj Canton have the annual distribution of average water levels, which corresponds to the distribution of precipitation during the year. This can also be seen in the example of the Maglaj area (**Table 1**), (Hydrometeorological Institute of Federation of B&H).

**Table 1.**

**Values of average monthly precipitation (mm) and water level (cm)  
for period 1961 - 1990 (MS Maglaj).**

	<i>I</i>	<i>II</i>	<i>III</i>	<i>IV</i>	<i>V</i>	<i>VI</i>	<i>VII</i>	<i>VIII</i>	<i>IX</i>	<i>X</i>	<i>XI</i>	<i>XII</i>
P (mm)	51.5	47.5	54.3	62.6	76.1	84.5	63.5	69.1	64.9	66.7	74.5	67.4
H (cm)	151.1	143.4	188.7	187.3	149.8	131.9	97.15	78.3	87.7	103.5	121.3	152.7

Source: Hydrometeorological Institute of Federation of Bosnia and Herzegovina (HMIFB&H)

The rise in water levels is influenced by precipitation and melting snow that occurs in the spring. In contrast, during the summer months, the water levels reach minimum values due to less precipitation, as well as high temperatures and increased evaporation. This annual distribution of water levels for a multi-year period corresponds to the pluvial-nival regime, in which two maxima and two minima stand out. The first maximum is related to the spring period (March-April) and the second to the month of December, while the minimums correspond to the winter (February) and summer seasons (August). Extremely high water levels can occur due to short-term but heavy rains, then as a result of melting snow or high groundwater levels, which can contribute to the likelihood of flooding. The average annual values of flows on the river Bosna in this Canton are 58.6 m<sup>3</sup>/s, while the maximum values recorded during May 2014 were 867 m<sup>3</sup>/s, resulting severe flooding (**Fig. 1**).



**Fig. 1.** Flooded area in May 2014, Municipality of Doboj-Jug.

(Source: <http://www.dobojjug.ba/contents/893>).

It is known that the floods during the mentioned year occurred after continuous precipitation of 5 days, and in some parts of the basin, it was determined that the return period occurred once in 500 years. Maximum flows in May 2014 for the hydrological stations listed in the **Table 2**, show their relationship to high waters of return periods from 10 to 500 years, **Table 3**.

**Table 2.**

**High waters ( $m^3/s$ ) on river Bosna for the hydrological stations Doboj, Maglaj, Zavidovići, Raspotočje and Dobrinje**

<i>HS</i>	$Q_{max}$	$min Q_{max}$	$av Q_{max}$	$max Q_{max}$
	2014			
Doboj	4831	556	1441	2533
Maglaj	3579	571	1032	2177
Zavidovići	2552	399	802	1571
Raspotočje	1630	257	608	1326
Dobrinje	1328	238	652	1027

Source: *Hydrological yearbook 2014. Hydrometeorological Institute of Republica Srpska (HMIRS) and Hydrometeorological Institute of Federation of Bosnia and Herzegovina (HMIFB&H).*

**Table 3.**

**Probability of occurrence of high waters of return periods from 10 to 500 years.**

<i>Return period</i>	<i>Doboj</i>	<i>Maglaj</i>	<i>Zavidovići</i>	<i>Raspotočje</i>	<i>Dobrinje</i>
	$m^3/s$				
10	2091	1508	1164	904	600
20	2420	1764	1320	1039	717
50	2795	2120	1520	1220	880
100	3087	2479	1673	1360	1058
500	3936	3272	2091	1700	1375

Source: *Hydrological study for B&H, Hydrometeorological Institute of Republica Srpska (HMIRS) and Hydrometeorological Institute of Federation of Bosnia and Herzegovina (HMIFB&H).*

In the area of Zenica-Doboj Canton, floods have so far occurred on the rivers Bosna, Usora, Krivaja, Gostović, Zgošća, Stavnja, Tešanjka, Bistrička, Liješnica and Papratnica. The hydrographic and hydrological diversity of Zenica-Doboj Canton is the result of a very complex impact of various

components of the natural environment, such as the geological, geomorphological, climatic, pedological and biogeographical characteristics of this area. In the period 1999-2005, the average damage of floods in Zenica-Doboj Canton was huge to the population. In 2001 alone, floods affected 8 municipalities. The consequence of these floods was enormous material damage caused to road infrastructure, housing and economy facilities, agricultural and other lands, water supply facilities, electricity network, grid network, etc., which was estimated at around 9,500,000.00 EUR<sup>2</sup>. During June 2010, rivers Bosnia and Usora with their tributaries, overflowed and flooded both residential and commercial buildings, causing the most damage in municipalities of Kakanj, Maglaj, Doboj-south and Usora.

During the floods in May 2014, Zenica-Doboj Canton experienced major floods (**Fig.1**). At that time, heavy rains lasted almost continuously for five days, submerging the soil, which had previously been saturated with water, with extremely high specific flows and runoff coefficients. The floods reached the largest extent on May 15th, 2014, when the flood area between Zavidovići and Modriča was 99 km<sup>2</sup>, and the volume of floodwater was 401 million m<sup>3</sup>. Analyzes conducted with international expert support in the countries of the Sava River Basin confirmed that the floods in May 2014 were the largest in the last 120 years (ARSO, 2014). Over 3,000 landslides were triggered, and over 43,000 houses were damaged or destroyed. Based on the report of the Cantonal Commission for Damage Assessment (2015), damage of EUR 190,000,000.00 was caused by this natural disaster in the area of Zenica-Doboj Canton<sup>3</sup>. The floods occurred during February and May 2019, and they were reminiscent of the floods in 2014 but there were no fatalities. However, these floods left a significant mark on agricultural land where farmers were most affected, and 13 landslides were triggered. The occurrence of floods (especially with reference to 2014) was influenced by natural and antropogenic factors, including heavy rainfall (level of 500 annual rainfall), a disorder of watercourses, unplanned antropogenic construction of facilities, bridges, retaining walls, the problem of division of responsibilities for coastal maintenance fortifications, outdated approach in watercourse maintenance, lack of flood protection embankments<sup>4</sup>. In the Zenica-Doboj Canton, continuous water monitoring is performed today, including meteorological, hydrological as well as water quality monitoring. This has created the preconditions for the functioning of prognostic meteorological and hydrological-hydraulic models within which flood events can be predicted in real-time and timely notification and alerting related to a possible event can be made.

## 2. STUDY AREA

Zenica-Doboj Canton is located in Bosnia and Herzegovina, with an area of 3,328 km<sup>2</sup>, between 17°44'38" and 18°50'11" E, and 43°54'13" and 44°43'41" N (author's calculation based on GIS data) (**Fig. 2**). Zenica-Doboj Canton consists of ten municipalities in which, according to the last 2013 Census, lives a total of 364,433 inhabitants. The most populated part is along the river Bosna with an average population density of 109.5 inhabitants/km<sup>2</sup> (author's calculation based on GIS and Census data).

---

<sup>2</sup> Assessment of the endangerment of the territory of Zenica-Doboj Canton from natural and other disasters (Procjena ugroženosti teritorije Zeničko-Dobojskog Kantona od prirodnih i drugih nesreća), Zenica. [http://www.zdk.ba/sjednicevlade/sjednice2016/63sjednica/63-16\\_21-07-2016.pdf](http://www.zdk.ba/sjednicevlade/sjednice2016/63sjednica/63-16_21-07-2016.pdf) (Accessed March 28 2021)

<sup>3</sup> The Report of the Cantonal Commission for Damage Assessment from Natural and other Damage on Damage assessment in the area of Zenica-Doboj Canton (Izveštaj Komisije za procjenu šteta od prirodnih i drugih nesreća o procjeni šteta na području Zeničko-dobojskog kantona) [http://zdk.ba/sjednicevlade/sjednice2015/18sjednica/18-04\\_20-07-2015.pdf](http://zdk.ba/sjednicevlade/sjednice2015/18sjednica/18-04_20-07-2015.pdf) (Accessed March 28 2021)

<sup>4</sup> Assessment of the endangerment of the territory of Zenica-Doboj Canton from natural and other disasters (Procjena ugroženosti teritorije Zeničko-Dobojskog Kantona od prirodnih i drugih nesreća), Zenica. [http://www.zdk.ba/sjednicevlade/sjednice2016/63sjednica/63-16\\_21-07-2016.pdf](http://www.zdk.ba/sjednicevlade/sjednice2016/63sjednica/63-16_21-07-2016.pdf) (Accessed March 28 2021)

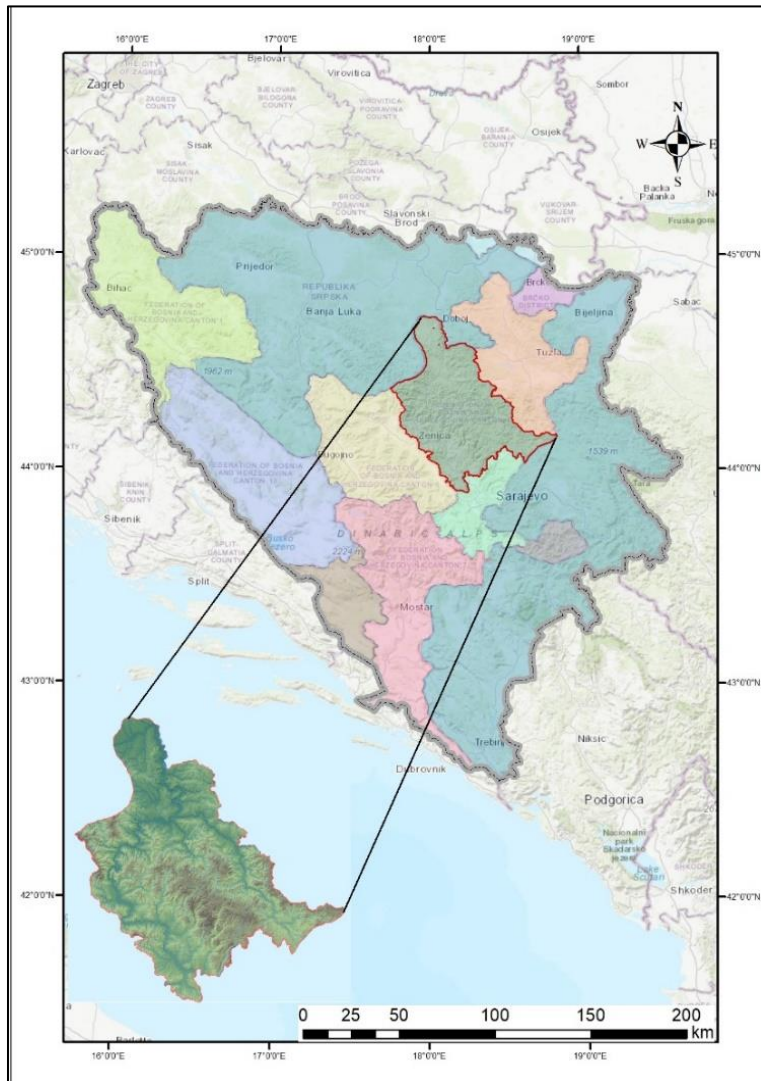


**Fig. 2.** Geographical position of Zenica – Doboš Canton on the map of Bosnia and Herzegovina.

It belongs to the belt of the inner Dinarides, and the landscape of the Canton is characterized by three hypsometrically specific areas: lowland-hilly in the north in the valley of the river Usora (130 – 200 m asl), hilly-mountainous in the central part (201 – 500 m asl) and hilly in the southern part of the Canton (501 – 1473 m asl). The largest spatial coverage is occupied by the category of inclination from  $12^{\circ}$  to  $32^{\circ}$ , namely 56.04%, followed by the category of inclination from  $5^{\circ}$  to  $12^{\circ}$ , occupying 23.23% of the total area of the Canton. The category of inclination from  $2^{\circ}$  to  $5^{\circ}$  or 7.5% of the total area is followed by the slope category between  $32^{\circ}$  and  $55^{\circ}$  which occupies 7.2% of total spatial coverage. The smallest share has the slope category from  $0^{\circ}$  to  $2^{\circ}$  which covers 5.98% of total area of the Canton (Author's calculation based on GIS digital elevation model data). It is noticeable that larger categories of slopes occur mainly in the central part of the Canton, which is primarily due to the mountainous terrain characteristics. As a result of gravity, torrents are formed on such terrains, which flow towards the watercourses of the second, and then towards the watercourses of the first category.

The area of Zenica-Doboš Canton has a mostly temperate continental climate, and in the higher areas mountain climate. Precipitation is evenly distributed throughout the year (**Table 4**), with an



average annual rainfall of 780 mm in the lowlands to 1000 mm in the mountainous areas (Author's calculation based on GIS digital elevation model and vertical pluviometric gradient data).

**Table 4.**

**Average monthly precipitation for a period 2004-2014.**

Month	I	II	III	IV	V	VI	VII	VIII	IX	X	XI	XII
mm	57.06	60.42	51.38	82.61	76.04	73.37	72.76	62.07	89.77	99.81	77.08	81.53

Source: Meteorological yearbooks 2004-2014, Hydrometeorological Institute of Federation of Bosnia and Herzegovina (HMIFB&H)

The river Bosna, in the area of the Canton, has larger tributaries, such as: Stavnja, Fojnička river, Trstionica, Zgošća, Ribnica, Lašva, Babina rijeka, Kočeva, Bistričak, followed by Liješnica, Gostović, Krivaja and Usora. In addition to these tributaries, there are several smaller permanent and occasional watercourses flowing into Bosna (Fig. 3).

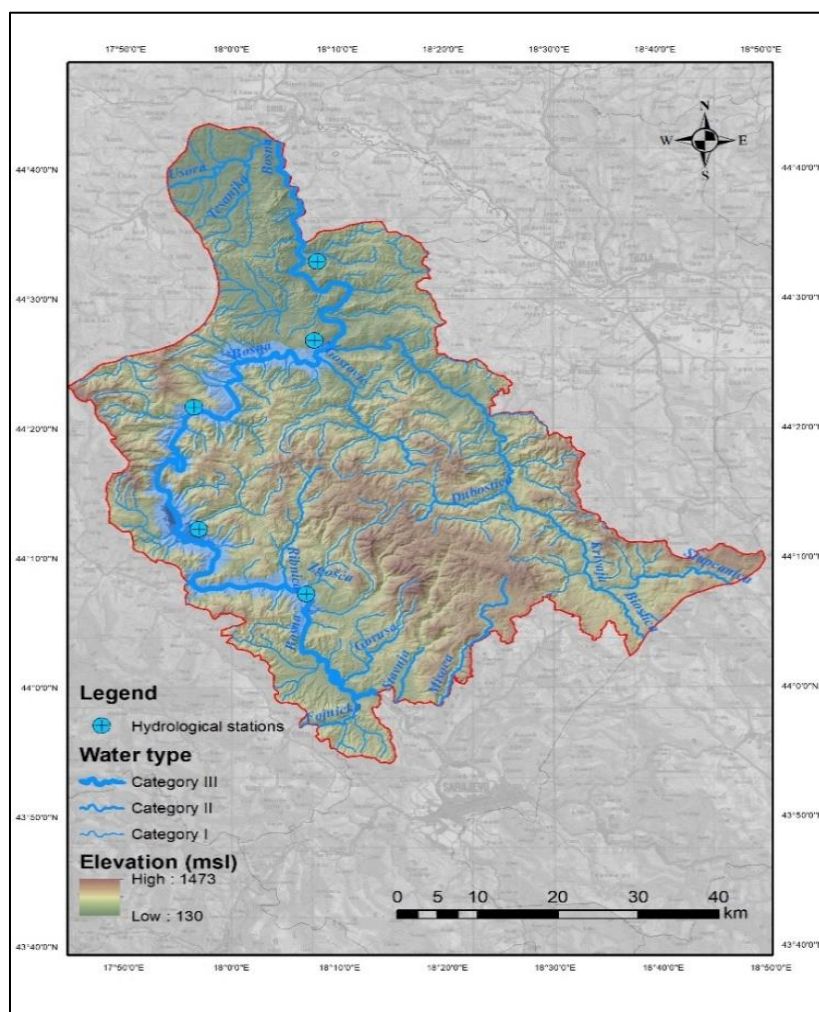


**Fig. 3.** River Bosna with its tributaries and hydrological stations that were analyzed in Zenica – Doboj Canton.

### 3. DATA AND METHODS

#### 3.1. Climate and hydrological data

Database of meteorological parameters, primarily precipitation and hydrological data on water level and flow, was used in this paper. Meteorological monitoring is the responsibility of the Federal Hydrometeorological Institute in Sarajevo (HMIFB&H), while the Agency for the Sava River Basin Sarajevo is responsible for hydrological monitoring of surface waters. The data analyzed in this paper are available for the period from 1961 to 1990, after which the measurements were interrupted due to the war in Bosnia and Herzegovina during the 1990s. The second, comparative period of the analyzed data referred to the period from 2004 to 2019.

#### 3.2. Creating a flood hazard map

The flood hazard map of Zenica-Doboj Canton contains data on the boundaries of the flood area for floods of different return periods, depth or water level, and it was made in several phases. Flood area covers the surface of 233.74 km<sup>2</sup> or 6.95% of total area of Zenica – Doboj Canton. In the first phase, data on more endangered areas were collected, so the river Bosna and the localities that represent the greatest hazard in the Zenica-Doboj Canton in terms of floods were selected. The final results gave a more accurate location of the flood lines, then the water depth on the profiles. In addition, it is possible to perceive the hazard of floods in planning procedures, as well as the analysis of the load (and stability) of facilities in flood areas.

The HEC-GeoRas extension in ArcMap was used to create the map. First of all, it was necessary to obtain a network of Triangular Irregular Networks (TIN) by converting the DEM terrain model. After that, the main river, Bosna, was digitized, and the river Zgošća was selected as a category I watercourse. The length of the main river that has been cultivated is 85.51 km, i.e. the length of flow from the settlement of Papratnica in the municipality of Kakanj all the way to the municipality of Zavidovići. According to our research, the area upstream from the mouth of the Krivaja river into the Bosna river is the most susceptible area to flooding. In addition to rivers, banks and profiles have been digitized at intervals of 800 meters and a width of 900 meters. The connection of the HEC-RAS program with the ArcMap tools was made through the HEC-GeoRas extension, which provides an efficient exchange of input data and results with the ArcGIS software package. The accuracy of determining the width of flooding of watercourses depends on the quality of the DEM terrain model, which is very important, especially for the mountain-valley area such as in the Zenica-Doboj Canton. The Manning coefficient of resistance was used for the paper, combined with the purpose of the land (Corina Land Cover was used in the paper). Manning's equation and other empirical open-channel flow equations are convenient and commonly-used tools for hydrologists and engineers who seek to solve practical problems of channel design, flood wave modelling, and fluvial sediment transport (Dingman, 2009). In research settings, applications of these equations include assessing flow in drainage canals and indirectly estimating peak flood discharges (Lumbroso and Gaume, 2012).

Manning's roughness coefficient (or Gauckler-Manning coefficient) is one of the energy loss coefficients, i.e. it describes the energy loss due to friction of water and open watercourse beds (Lozzi-Kožar and Kožar, 2009). According to these authors, this coefficient varies considerably and depends on a large number of factors, such as surface roughness, vegetation and overgrowth of the riverbed, canal irregularities, branching or joining of watercourses, obstacles, size and shape of canals, canal slope, water height and flow, seasonal changes, temperature, erosion, suspended material. Selecting the appropriate value of Manning's coefficient is very important for the accuracy of the flow calculation in an open watercourse (Hydrological study of the Bosnia River Basin, 2012). After the coefficient was assigned to each land use category, it was used as input data in the HEC-GeoRas extension. Manning's coefficient is of great importance in determining the risk of floods depending on the purpose of the land in the floodplain. Manning's „n“ values should be calibrated whenever observed water surface elevation information is available. When gaged data are not available, values of „n“ computed for similar stream conditions or values obtained from experimental data should be used as guides in selecting „n“ values. There are several references a user can access that show



Manning's „n“ values for typical channels (Brunner, 2016). The highest coefficient is assigned to forest areas (0.40), and the lowest to urban areas, landfills and sports and recreational facilities (0.02), where it is concluded that forest areas and vegetation have a much greater impact on water energy loss, which is not the case with urban areas. The maximum flow rate used,  $Q = 1673.00 \text{ m}^3/\text{s}$ , was also used for the hydraulic calculation, and a 100-year flood was taken into account.

### 3.2. Creating a flood risk map

The flood risk is the probability of damage in the endangered area. The components of risk are the probability of occurrence (as an indicator of cause) and material damage (as an indicator of consequence) (Jovanović, Todorović, Rodić, 2009).

To produce flood risk maps, it was previously necessary to analyze risk indicators. According Jovanović et al. (2009) there are two parameters to express flood damage: maximum damage ( $S_{\text{max}}$ ) - the maximum estimated the value of the property for a given area. This is the upper limit of damage ("total damage"), which cannot be achieved even in the event of major floods, the damage factor ( $\alpha$ ) - an indicator of possible damage, expressed as percentage relative to maximum damage  $S_{\text{max}}$ . Variability of this parameter is defined by the "damage function" - the relationship between the depth of flooding and damage to a particular type purpose area. The monetary amount of potential damage, according to the definition of the above parameters, is defined as:  $S = \alpha \cdot S_{\text{max}}$ . Risk indicators are performed with regard to the following categories: population, economy, protected areas, cultural and historical monuments and IPPC facilities. Based on analysis of weight factors in available methodologies of some EU countries, weight factors were adopted. In each category, weighting factors were assigned, namely: population = 0.4; economy = 0.3; cultural-historical heritage = 0.1; protected areas = 0.1; IPPC plants - out of category (if they are endangered, the risk is 100%) (Jabučar, Lukovac, 2015). The formula used in this analysis is:

$$FR = Sn \times TF \times O \quad (1)$$

where:

$FR$  – risk factor;  $Sn$  – number of dots,  $\text{km}^2$ ;  $TF$  – weighting factor;  $O$  – flood hazard (see Eq. 2).

It should be noted that the flood hazard was obtained with the assumption that the flood depth is 1 m, the flow rate is 1 m/s. The adopted value of flood hazard ( $O$ ) depending on the velocity and depth of the flow is:

$$O = h \times (v + 0.5) \quad (2)$$

where:

$O$  – flood hazard;  $h$  – flood depth (m);  $v$  – flow velocity (m/s); 0.5 – corrective constant (this includes the case of flooding with stagnant water of great depth for which there is an obvious hazard) (Jabučar, Lukovac, 2015).

The risk factor was determined (Table 5), after which each of the listed land uses received its own class based on the risk factor, and then the risk category. Based on the table of risk categories (Table 6,7,8,9,10,11), a summary map of flood risk was made (Fig. 5). The risk factor by categories was determined using the Arc GIS and HEC-RAS programs, as well as on the basis of research by Jovanović et al. (2009).

**Table 5.**

**Tabular presentation of flood risk analysis.**

Land use	$S_n$ ( $\text{km}^2$ )	TF	O	FR
Economy	111.42	0.3	1.5	4011.177
Population	19.42	0.4	1.5	932.1919
Cultural-historical heritage	0.32	0.1	1.5	3.799128
Protected areas	98.49	0.15	1.5	1772.731
IPPC	4.10	1	1.5	491.6624

Table 6.

**Risk factor by population category.**

Risk factor	Class	Risk category
0-49	0	Negligible risk
50-499	$0 < R < 0.25$	Low risk
500-999	$0.26 < R < 0.50$	Moderate risk
1,000-1,499	$0.51 < R < 0.75$	High risk
>1,500	$0.76 < R < 1.0$	Extreme risk

Table 7.

**Risk factor by economy category.**

Risk factor	Class	Risk category
0-49	0	Negligible risk
50-249	$0 < R < 0.33$	Low risk
250-499	$0.34 < R < 0.67$	High risk
>500	$0.68 < R < 1.0$	Extreme risk

Table 8.

**Risk factor according to the category of cultural and historical heritage.**

Risk factor	Class	Risk category
0-499	0	Negligible risk
500-3,499	$0 < R < 0.25$	Low risk
3,500-6,999	$0.26 < R < 0.50$	Moderate risk
7,000-9,999	$0.51 < R < 0.75$	High risk
>10,000	$0.76 < R < 1.0$	Extreme risk

Table 9.

**Risk factor according to the category of protected areas.**

Risk factor	Class	Risk category
0-499	0	Negligible risk
500-1,499	$0 < R < 0.33$	Low risk
1,500-2,499	$0.34 < R < 0.67$	High risk
>1,500	$0.68 < R < 1.0$	Extreme risk

Table 10.

**Risk factor by category of IPPC plants.**

Risk factor	Class	Risk category
0-199	0	Negligible risk
150-299	$0 < R < 0.50$	High risk
>300	$0.51 < R < 1.0$	Extreme risk

Table 11.

**Risk categories for making a summary flood risk map.**

Class (RF)	Risk category
0	Negligible risk
$0 < R < 0.25$	Low risk
$0.26 < R < 0.50$	Moderate risk
$0.51 < R < 0.75$	High risk
$0.76 < R < 1.0$	Extreme risk

#### 4. RESULTS AND DISCUSSIONS

As a result of the calculation and analysis of the used data, a flood hazard map of Zenica – Doboj Canton (**Fig. 4**), was made, which contains floods of medium value ( $T_p \geq 100$  years), flood extent, and water depth (darker color represents depth). The flood risk map (**Fig. 4**) shows that the areas most exposed to flood hazards are precisely those that have been flooded in the recent past.

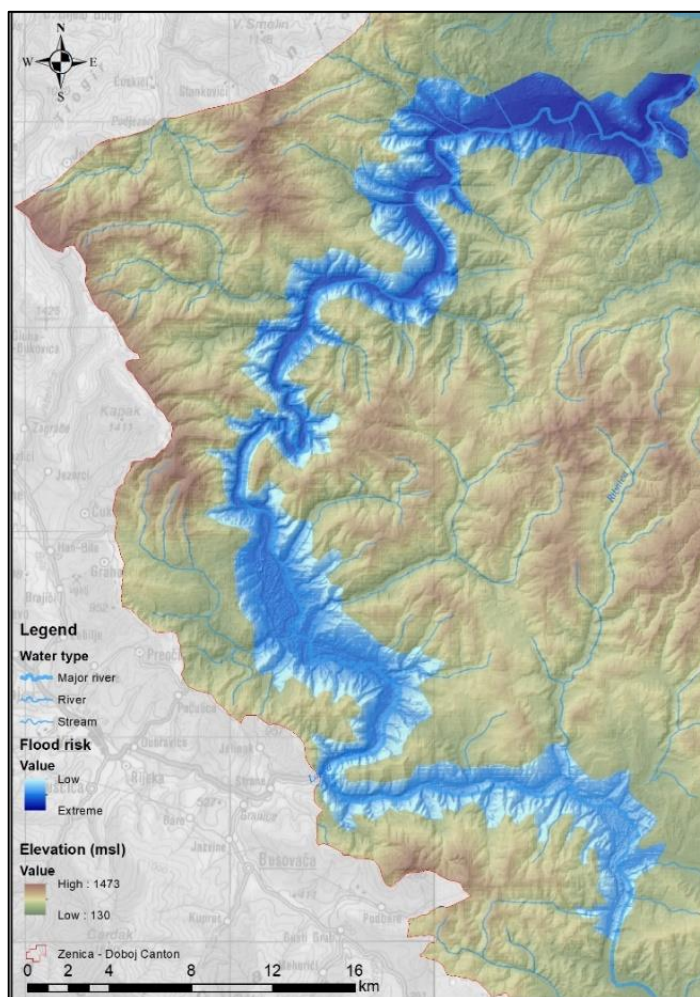


**Fig. 4.** Flood hazard in the area of Zenica - Doboj Canton.

Further analysis found that extreme flood risk occurs in places that are both the most populated and industrially most important, at least when it comes to this floodplain. The number of the potentially affected population is certainly large if we consider the fact that the highest population density is right next to the river Bosna. In the potentially affected area, there are also various economic activities, but also facilities that could cause sudden environmental pollution in case of floods, especially in the area of the City of Zenica where extreme risk occurs.

A large number of settlements are located within the floodplain (**Fig. 5**). Some of them are directly in the category of extreme risk, which means that, due to floods, the population of this area is extremely vulnerable, and the situation is further exacerbated by the proximity of IPPC facilities which would not only endanger the environment but also have a direct impact on population health. The high-risk category mainly includes urban areas with a large population. Smaller, rural-type settlements are at moderate risk. If we analyze the number of inhabitants, according to the 2013 Census, which exists in 62 settlements in this flood coverage, we get the number of 114,005 inhabitants who may be endangered by floods.

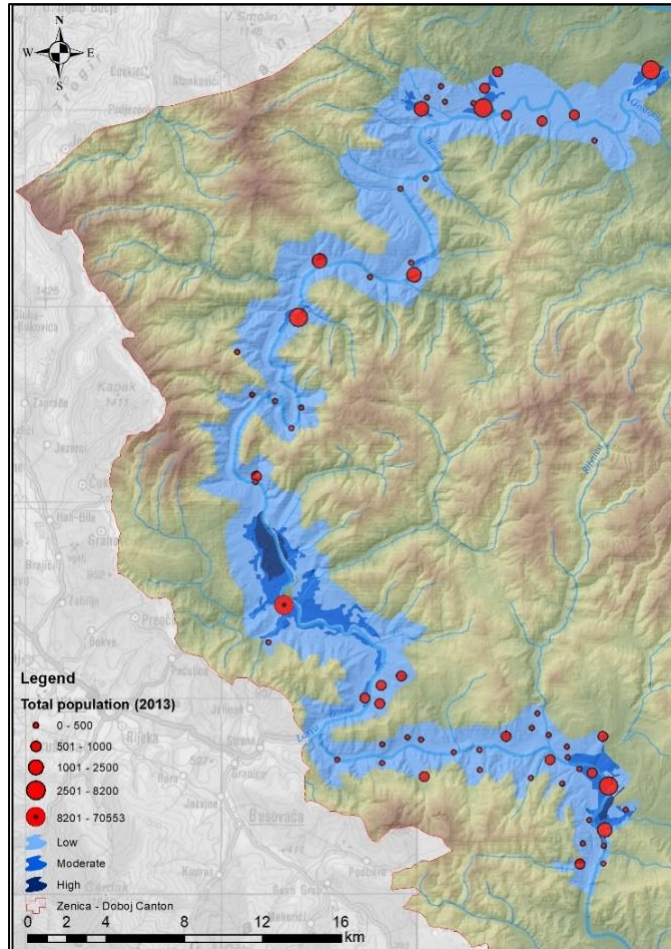


**Fig. 5.** Distribution of settlements in relation to the risk category of Zenica - Doboj Canton.

Given the purpose of the land represented in the flood zone (**Fig. 6**), it can be seen that the largest area is occupied by the economy (47.67%), protected areas (42.13%), followed by the population (8.31%), IPPC facilities (1.75%) and cultural-historical monuments (0.14%). Total flood prone area covers the surface of 233.74 km<sup>2</sup>. The analyzed area is, among other things, the most economically important, most populated, with a developed industry and road and railway infrastructure, so floods leave a great impact on this area.

During the work on this paper, the analysis of the spatial coverage of individual land use categories according to the risk category was performed (**Fig. 7**). Cultural and historical buildings are exposed to negligible risk, with a surface distribution of 0.32 km<sup>2</sup>. No category of land use belongs to the category of low risk, while a part of the economy and the population are exposed to moderate risk, with a spread of 0.45 km<sup>2</sup> and 19.42 km<sup>2</sup>. Protected areas of 98.49 km<sup>2</sup> are exposed to high risk, while the rest of the economy, with a distribution of 110.97 km<sup>2</sup>, and IPPC plants of 4.1 km<sup>2</sup> are exposed to extreme risk.

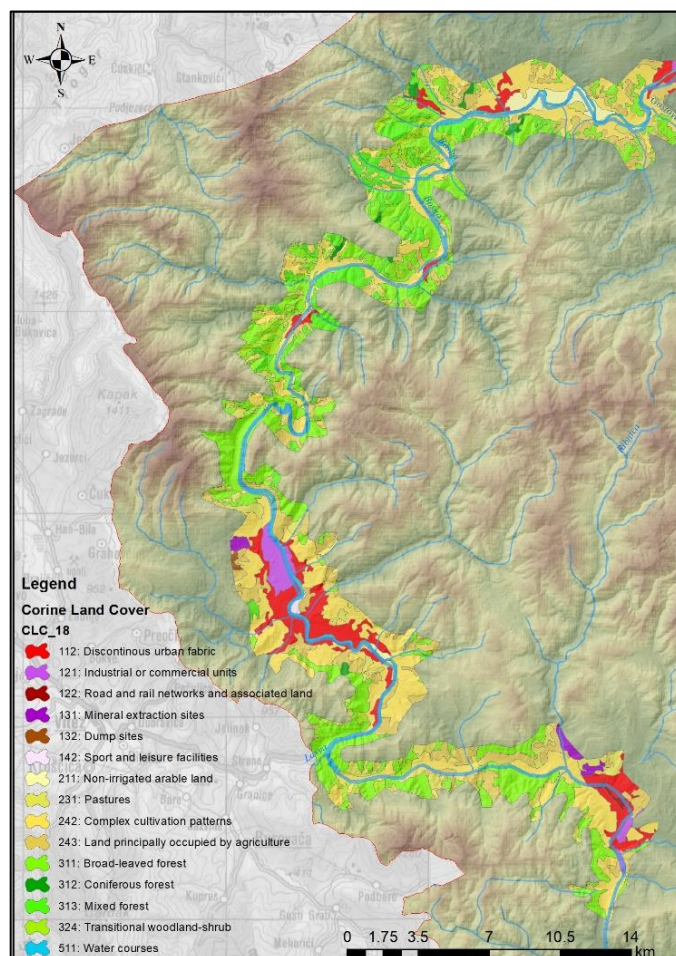


**Fig. 6.** Categories of land use in the flood zone.

In addition to floods, landslides and escarpments are a significant phenomena, especially in the municipalities of Breza, Kakanj, Vareš and Zenica, where there is intensive ore exploitation. The data show that the areas of the municipalities of Maglaj and Žepče are also exposed to landslides as a result of the removal of vegetation<sup>5</sup>. Very little is being done on afforestation, and often just cleared areas

<sup>5</sup> Assessment of the endangerment of the territory of Zenica-Doboj Canton from natural and other disasters, Zenica. [http://www.zdk.ba/sjednicevlade/sjednice2016/63sjednica/63-16\\_21-07-2016.pdf](http://www.zdk.ba/sjednicevlade/sjednice2016/63sjednica/63-16_21-07-2016.pdf) (Accessed March 28 2021)



have been used for agricultural purposes. Due to intensive urbanization and expansion of settlements, construction is becoming more frequent in protected areas than in floodplains, torrents and exploitation areas, and even in landslide areas.

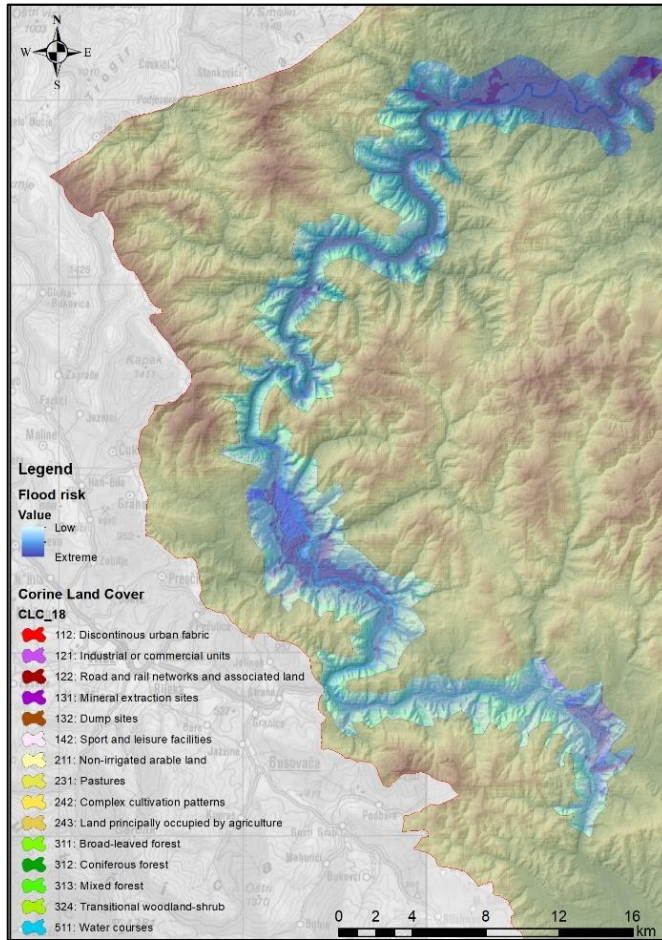


Fig. 7. Synthesis map of land use and flood risk in Zenica-Doboj Canton.

## 5. CONCLUSIONS

Climatic, geological and geomorphological features and landscape are the most important factors for the occurrence of floods in the area of Zenica-Doboj Canton. However, the anthropogenic impact on the environment is even greater than assumed. In support of this thesis we will list only a few anthropogenic factors with exceptional impact on the environment, such as: uncontrolled deforestation, exploitation of minerals, illegal construction, unprofessional irrigation of agricultural land, which directly affected changes in water and soil regime. In the analyzed area, floodplains of tributaries of the river Bosna and tributaries of lower order often coincide. Smaller watercourses are torrential in nature, which is often the catalyst for their higher flow. Particularly critical are the basins of mountain streams from the lower mountains that delimit the valley of the river Bosna. Factors that can affect the reduction of floods or even prevent their occurrence include: regular cleaning and maintenance of watercourses, preparation of studies and other documentation on the state of

watercourses, installation of flood protection embankments, construction of transverse (stone or concrete) barriers in torrents, afforestation, cultivation of vegetation and prevention of uncontrolled logging, removal of unplanned buildings in a narrow flood zone, construction of protective facilities and others. In order to reduce risks and damage, it is crucial to reduce the identified anthropogenic causes of floods in the Bosna River Basin, but also to replace poor agricultural practices with better ones that will adapt to the circumstances, stop unplanned construction in flood risk zones and stop deforestation. To conclude, it is necessary to emphasize the importance of appropriate afforestation measures, which would return the forest to its significant place in the hydrological cycle.

## REFERENCES

- Allen-Dumas, M. R., Xu H., Kurte, K. R., Rastogi, D. (2021) Toward Urban Water Security: Broadening the Use of Machine Learning Methods for Mitigating Urban Water Hazards, *Frontiers in Water*, 2 <https://doi.org/10.3389/frwa.2020.562304>
- ARSO (2014) Environmental Agency of the Republic of Slovenia 2014, Analysis of the flood event in May 2014 in Bosnia and Herzegovina for the Bosnia River Basin within the additional assistance of the Republic of Slovenia - Report, Ljubljana, 2014.
- Assessment of the endangerment of the territory of Zenica-Doboj Canton from natural and other disasters (Procjena ugroženosti teritorije Zeničko-Dobojskog Kantona od prirodnih i drugih nesreća), Zenica. [http://www.zdk.ba/sjednicevlade/sjednice2016/63sjednica/63-16\\_21-07-2016.pdf](http://www.zdk.ba/sjednicevlade/sjednice2016/63sjednica/63-16_21-07-2016.pdf) (Accessed March 28 2021)
- Barredo, J. I. (2007) Major flood disasters in Europe: 1950–2005. *Natural Hazards* 42, 125–148. <https://doi.org/10.1007/s11069-006-9065-2>
- Berz, G. (2000) Flood disasters: lessons from the past—worries for the future, *Proceedings of the Institution of Civil Engineers – Water and Maritime Engineering* 142 (1), 3–8. <https://doi.org/10.1680/wame.2000.142.1>.
- Bonacci, O. (2003) *Ecology of water resources and open watercourses*, (*Ekohidrologija vodnih resursa i otvorenih vodotoka*), Faculty of Civil Engineering and Architecture, University of Split and IGH d.d. Zagreb.
- Brunner, W.G. (2016) *HEC-RAS, River Analysis System Hydraulic Reference Manual*, U.S. Army Corps of Engineers, Institute for Water Resources, Davis.
- Dingman S.L. (2009) *Fluvial Hydraulics*, Oxford University Press Inc, Oxford p. 570
- Eriksson, M., Nutter, J., Day, S., Guttman, H., James, R., and Quibell, G. (2015) Challenges and commonalities in basin-wide water management. *Aquatic Procedia* 5, 44–57. <https://doi.org/10.1016/j.aqpro.2015.10.007>
- Final results of the Census 2013 (Konačni rezultati Popisa 2013) <http://fzs.ba/index.php/popis-stanovnistva/popis-stanovnistva-2013/konacni-rezultati-popisa-2013/> (Accessed March 25 2021)
- Gavrilović, Lj., Milanović Pešić, A. & Urošev, M. (2012). A Hydrological Analysis of the Greatest Floods in Serbia in the 1960-2010 Period. *Carpathian Journal of Earth and Environmental Sciences*, 7 (4), 107–116.
- Györi, M. M., Haidu, I., Humbert, J. (2016) Deriving the floodplain in rural areas for high exceedance Probability Having limited data source. *Environmental Engineering and Management Journal*, 15, 1879-1887. <https://doi.org/10.30638/EEMJ.2016.201>
- Haidu, I., Batelaan, O., Crăciun, A.I., & Domnița, M. (2017) GIS module for the estimation of the hillslope torrential peak flow, *Environmental Engineering and Management Journal*, 16 (5), 1137-1144.
- Haidu, I., Ivan, K. (2016). Évolution du ruissellement et du volume d'eau ruisselé en surface urbaine. Étude de cas: Bordeaux 1984-2014, France. *La Houille Blanche*. <https://doi.org/10.1051/lhb/2016050>
- Hydrological study of surface waters of Bosnia and Herzegovina, Bosnia River Basin. Main document, 2012. Water Management Institute d.d. Sarajevo, Federal Hydrometeorological Institute (Hidrološka studija površinskih voda Bosne i Hercegovine, Sliv rijeke Bosne, Glavna knjiga, „Zavod za vodoprivredu“ d.d. Sarajevo, Federalni hidrometeorološki zavod), Sarajevo.



- Hydrological yearbook 2014., Hydrometeorological Institute of Republica Srpska (HMIRS) and Hydrometeorological Institute of Federation of Bosnia and Herzegovina (HMIFB&H), <http://www.fhmzbih.gov.ba/podaci/hidro/godisnjak/2014%20godina.pdf>
- Imamović, A. (2015) Causes of floods in the Bosna River Basin with reference to the floods in May 2014, *Flood risk management and mitigation of their harmful consequences* (Uzroci poplava u slivu rijeke Bosne s osvrtom na poplave u maju 2014. godine), ANUBiH. <https://doi.org/10.5644/PI2015-161-11>
- Jabučar, D., Lukovac, N. (2015) Implementation of the EU Floods Directive in BiH, *Flood risk management and mitigation* (Implementacija EU Direktive o poplavama u BiH, *Upravljanje rizicima od poplava i ublažavanje njihovih štetnih posljedica*), p. 256-266, <https://doi.org/10.5644/PI2015-161-24>
- Jovanović, M., Prodanović D., Plavšić, J., Rosić N., Srna P., Radovanović M. (2014) Problems in making flood risk maps, *Water Management* 46 (Problemi pri izradi karata ugroženosti od poplava) 267-272.
- Jovanović, M., Todorović, A. & Rodić, M. (2009) Flood risk mapping. *Water management* Vol 41., No. 1-3 (Kartiranje rizika od poplava).
- Khan, U.T., He J., Valeo C. (2018) River flood prediction using fuzzy neural networks: an investigation on automated network architecture, *Water Science & Technology*, 2017, 1, 238–247. <https://doi.org/10.2166/wst.2018.107>
- Kim, V., Tantanee, S., Suparta, W. (2020) Gis-Based Flood Hazard Mapping Using Hec-Ras Model: A Case Study of Lower Mekong River, Cambodia, *Geographia Technica*, Vol 15, Issue no.1/2020, pp. 16-26, [https://doi.org/10.21163/GT\\_2020.151.02](https://doi.org/10.21163/GT_2020.151.02)
- Koem, Ch., Tantanee, S. (2021) Flood Disaster Studies: A Review of Remote Sensing Perspective in Cambodia, *Geographia Technica*, Vol 16, Issue 1, 2021, pp. 13-24, [https://doi.org/10.21163/GT\\_2021.161.02](https://doi.org/10.21163/GT_2021.161.02)
- Lozzi-Kožar, D., Kožar, I. (2009) Determination of flow resistance coefficient, *Građevinar* 61 (2009) 6, pp. 547-556
- Lumbroso, D., Gaume, E. (2012) Reducing the uncertainty in indirect estimates of extreme flash flood discharges, *J. Hydrol.*, 414–415, pp. 16-30, <https://doi.org/10.1016/j.jhydrol.2011.08.048>
- Mandych, A. F. (2010). Classification of Floods (Chapter), Encyclopedia of Life Support. Natural Disasters Vol. II, ed. W.M. Kotlyakov, UNESCO, Eolss Pbl. Co., 63-88.
- Merz, B., Hall, J., Disse, M., and Schumann, A. (2010) Fluvial flood risk management in a changing world. *Natural Hazards and Earth System Sciences* 10, 509–527, <https://doi.org/10.5194/nhess-10-509-2010>
- Ozkan, S. P., Tarhan, C. (2016) Detection of Flood Hazard in Urban Areas Using GIS: Izmir Case, *Procedia Technology* 22, 373 – 381., <https://doi.org/10.1016/j.protecy.2016.01.026>
- Photo: Flooded area in May 2014, Municipality of Doboj-Jug, <http://www.doboijug.ba/contents/893> (Accessed 3rd April 2021)
- Petrović, A. M., Dragičević, S. S., Radić, B. P., Milanović Pešić, A. (2015). Historical torrential flood events in the Kolubara river basin. *Natural Hazards* 79, 537–547. <https://doi.org/10.1007/s11069-015-1860-111>
- Školjić, R., Hodžić, N. (2018) Implementation of projects in the Zenica-Doboj Canton, *Water and me*, No. 97 (Realizacija projekata u Zeničko-dobojskom kantonu)
- The Report of the Cantonal Commission for Damage Assessment from Natural and other Damage on Damage assessment in the area of Zenica-Doboj Canton (Izveštaj Komisije za procjenu šteta od prirodnih i drugih neseca o procjeni šteta na području Zeničko - dobojskog kantona) [http://zdk.ba/sjednicevlade/sjednice2015/18sjednica/18-04\\_20-07-2015.pdf](http://zdk.ba/sjednicevlade/sjednice2015/18sjednica/18-04_20-07-2015.pdf) (Accessed March 28 2021)

## SENTINEL 2 IMAGERY AND BURN RATIOS FOR ASSESSING THE JULY 5, 2021 WILDFIRES SEVERITY IN THE REGION OF KHENCHELA (NORTHEAST ALGERIA)

Nouar BOULGHOBRA<sup>1</sup>

DOI : 10.21163/GT\_2021.162.08

### ABSTRACT:

Wildfire events are majeure natural risks occurring in multiple ecosystems worldwide, and lead to significant damages on their human, ecological and socioeconomic components. This research interested on evaluating and mapping the recent and exceptional wildfires occurred in the Aures Mounts System near Ain Mimoun in July 5, 2021. Multidates Sentinel 2 images, the differenced Normalized Burn Ratio dNBR and its Relativized dNBR (RdNBR) have been used for extract and evaluate the recently burned areas. Results reveal that he July 5 wildfires lead to the loss of 6,607 ha (9 %) of Aleppo pine forest cover and municipalities of Tamza and Chelia were more damaged, with respectively 4,143 and 2,166 ha of burned superficies. In addition to the high-vulnerability to fire risk occurrence, essentially due to topographic and morphological features, the study area exhibited also favoring climatic features before and during the fire event occurrence, high daily temperatures and high variable wind directions were prominent factors in accelerating the fire spreading and increasing the fire extent. This study concludes that Sentinel 2, dNBR and especially RdNBR are effective geoinformatic data and indices for assessing, classifying and mapping burn severity extent due to wildfire events. To attenuate damages, it is necessary to adopt risk mitigation plans based on efficient measures to be applied before, during and after the fire events occurrence.

*Key-words: Wildfire, July 5, Khenchela, Sentinel 2, Relativized Burn Ratio*

### 1. INTRODUCTION

Forest fires occur in multiple regions worldwide and have been subject of many researches, interested essentially on assessment, mapping, and risk evaluation using often geomatic-based approaches (Rogan & Franklin, 2001; Roy et al., 2006; Furtună & Holobacă, 2013; Parks et al., 2014; Arellano et al., 2017; Parajuli et al., 2020), and often by adopting field measurement-based methodologies (Cocke et al., 2005; Cai & Wang, 2020).

In addition to the man-made activities, northern Mediterranean ecosystems are characterized by highly favoring climatic and physical circumstances for the forest fire occurrence, leading to multiple and repetitive wildfires events in France, Italy, Spain and Greece, especially during the last two decades, leading to significant damages (San-Miguel-Ayanz et al., 2017). In the southern Mediterranean, Algeria is facing important and recurrent forest fire risk events. According to Madoui (2002), 118,624 ha of forest areas were loosed due to fires from 1979 to 1995. Causes of forest fires in Algeria are multiples; according to Benkheira (2018), 75 % are of unknown causes, 23 % are due to premeditated human activity and 2 % are related to agricultural activities.

Northeast Algeria, the Aures Mountains belong to the Saharan Atlas System; this region is characterized by high altitudes (up to 2,328m), that this is the main reason for receiving more than 1,000mm of annual precipitation (Meharzi, 1994), leading to the growth of important forest cover. The Aures region is suffering a critical occurrence of forest fires events; according to the forest conservatory of Khenchela, more than 40 wildfires took place in the Aures from 2016 to 2018. Nevertheless, few researches interested in studying, assessing and mapping this major hazard: Rahmani and Benmassoud (2019) used remotely sensed data and GIS for modeling and mapping the

---

<sup>1</sup> Scientific and Technical Research Centre on the Arid Regions CRSTRA, University campus Mohamed Keider, BP 1682 RP, Biskra 07000, Algeria, [boulghobra.n@gmail.com](mailto:boulghobra.n@gmail.com)

Forest fire hazard in the region of Khenchela, by applying the Analytical Hierarchy Process AHP method considering related factors, namely vegetation types, topography and the anthropogenic activities. They reported that the Aures Mountain forests are considered as highly vulnerable to the wildfire hazard. The United Nations Satellite Centre and United Nations Institute for Training and Research (UNOSAT/UNITAR, 2012) used fine resolution RapidEye satellite imagery satellite for assessing and mapping the August 18, 2012 wildfires in the Aures Mountains (Regions of Biskra, Batna and Khenchela), they reported that wildfire damaged about 295 Km<sup>2</sup> (29,500 ha) of pine and oak forests. The year 2021 presented extreme meteorological conditions across entire Algeria, exceptional temperatures and heat waves exceeding 45 °C (113 °F) during late June, led to a multiplicity of wildfires in multiples regions such as Tebessa (Mountains of El-Atef) and Tikjda (Tell Atlas in Bouira governorate). In the region of Aures System west of the city of Khenchela, a wide wildfire took place in July 5 near the Ain Mimoun. During 5 days (July 5 to 10), the fires spreads in different directions and damaged significant forest superficies through Tamza, Chelia, Bouhmama and Ain Ouanjal municipalities, official preliminary reports declare the wildfires as man-made caused and estimate the forest loss to be 8,245 ha.

This research aims to assess and mapping the July 5, 2021 wildfires extents in the region of Khenchela, using time-series of Sentinel 2 images, and the relativized burn radio index RdNBR for extracting burnt superficies through the damaged municipalities. The study also interested on analyzing and understanding the climatic and topo-morphological circumstances of this wildfire genesis and propagation.

## 2. STUDY AREA

The study area is located west of the city of Khenchela (400,000 habitants), it extends over a superficies of 921 Km<sup>2</sup> (921,000 ha) and encloses 10 municipalities. Topographic pattern highlights the predominance of highly elevated landscape (**Fig. 1**) composed of prominent mountains (Djebel in Ar.) and hells (Kef, Rass in Ar.): Dj. Djahfa in the south (1,571m), the west-east chain alignment of Dj. Chelia (2,328m), Dj. Faraoun (2,071m), Kef Tifekrissa (1,900m) and Rass Serdoune (1,671m), in addition to the northern parallel chain mainly composed of Dj. Aures (1,571m), Dj. Tizi Ala (1,271m).

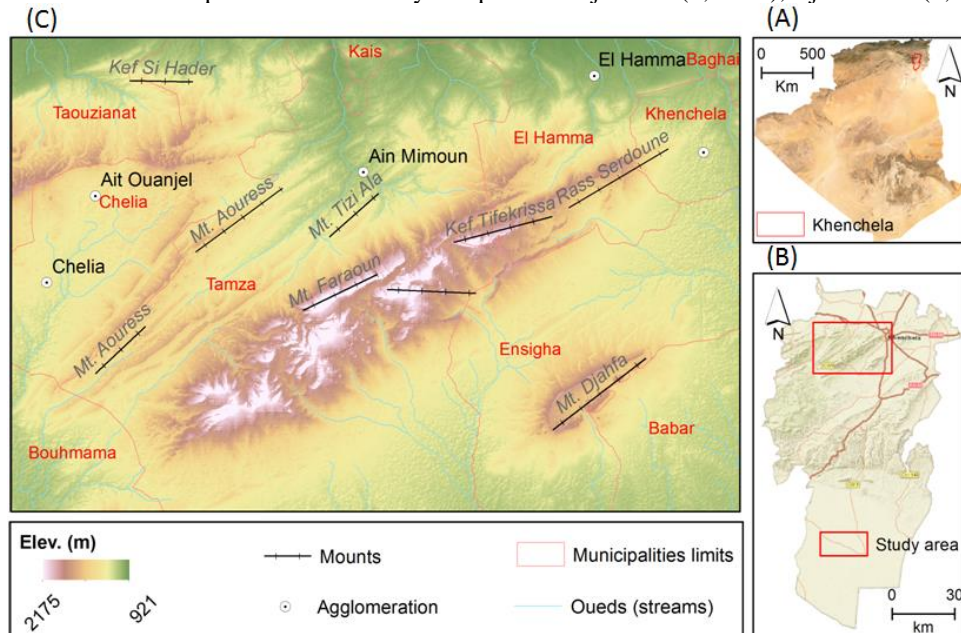


**Fig. 1.** (A) Localization of Khenchela governorate in northeast Algeria. (B) Localization of the study area in north of Khenchela. (C) Digital Elevation Model DEM by the Shuttle Radar Topography Mission SRTM of 40X40m resolution ([www.usgs.gov](http://www.usgs.gov)), showing the major hypsometric patterns of the study area

Regarding the geological map by Kazi Tani and Oussedik (1977), the high-lands lithology is mainly composed of lower cretaceous (Aptian limestone), Albian marls, sandstones and dolomite in the middle areas; northern parts are composed of Tortonian Miocene sandstones, whereas low-lands parts correspond to quaternary plains. The region of Khenchela is characterized by Mediterranean climate, mean temperatures range from 1.8 °C in January to 27 °C in July; maximum temperatures could reach 40 °C. Mean annual precipitation is about 400mm in the meteorological station of El Hamma (987m ASL). However, rainfalls can reach 1,200mm depending on altitudes and exposure (Meharzi, 1994); these conditions contrast leads to the growth of important forest cover essentially composed of Aleppo pine (*Pinus halepensi*), Altas cedar (*Cedrus atlantica*), Holm oak (*Quercus ilex*) and Juniper (*Juniperus*), often protected as biosphere reserves and national parks.

### 3. DATA AND METHODS

#### 3.1. Satellite imagery

For geospatially assessing and mapping of the July 5, 2021 wildfires extent in the region of Khenchela, it had been necessary to use multi dates satellite images corresponding to the pre, during and post fire phases. In addition to the required analysis scale and the study purpose, availability was a determinant criterion for choosing the data type. Time-series of high-resolution optical imagery were used, namely the Sentinel 2 (Copernicus Program) images dated May 21, July 5 and July 10, corresponding respectively to the pre, during and post fires phases. In total, 6 images were used since it was necessary to constitute image mosaic for each date, by assembling tiles couple having the scene centers (path/row) 193/035 and 193/036. Images are open source available, they present minimum cloud cover (less than 1 %); they are of Level-2A quality, i.e. are atmospherically corrected and are orthorectified and projected according to the Universal Transverse Mercator system zone 32.

Each satellite image provides multi spectral bands in both visible and infrared domains, wavelengths are ranging from the blue (0.458–0.522 µm) to the short wave infra red SWIR 2 (2.100–2.280 µm). After converting the bands on Geotiff format, and being of 20m of spatial resolution, the Short Wave Infra-Red 1 (SWIR 1) and Short Wave Infra-Red 2 (SWIR 2) bands were resampled to 10m to be spatially homogenized with the visible domain bands resolution. Besides, images were calibrated from radiance to surface reflectance to allow calculating the required spectral indices.

#### 3.2. Differenced Normalized and Relativized Burn Ratios for extracting burned areas

Extraction of the damaged superficies due to wildfires in the study area was performed using the Normalized Burn Ratio NBR (ranging from -1 to 1); this derived index is based on the Near Infrared (NIR) and the Shortwave Infrared 2 (SWIR2) bands of the Sentinel 2 images, it is based on peak reflectance of both vegetation and mineral soil to provide an index of the amount of vegetation present on the landscape before and after the fire event, and this according to the formulae:

$$NBR = \frac{NIR - SWIR2}{NIR + SWIR2} \quad (1)$$

where:

*NBR* - Normalized Burn Ratio  
*NIR* - Near Infrared  
*SWIR2* - Shortwave Infrared 2

Spectrally, the NBR is the opposite of the Normalized Difference Vegetation Index NDVI developed by Rouse et al. (1974), which refers to the NIR and Red spectral bands, and often used to discriminate vegetative cover abundance. Burned areas correspond to low reflectance pixels in the Near Infrared and high reflectance in the Short Wave Infra-Red 2 band; consequently, high NBR values indicate abundant vegetation, whereas very low values (close to -1) indicate recently burnt areas. For both pre fire (May 21) and post fire (July 10) images, NBR was calculated under Geographic Information System software; thereafter, recently burned areas due to the July 5 wildfire could be than calculated using the bi-dates difference according to the formulae:

$$dNBR = NBR_{pre-fire} - NBR_{post-fire} \quad (2)$$

where:

$dNBR$  – bi-dates difference

$NBR_{pre-fire}$  –  $NBR$  of pre fire images

$NBR_{post-fire}$  –  $NBR$  of post fire images

However,  $dNBR$  values could be influenced by the atmospheric conditions during image acquisition, this contributes on confusing recently burned areas and originally unvegetated superficies during the pre fire phase (Roy et al., 2006; Rose et al., 2016). Parks et al. (2014) suggest using the Relativized Burn Ratio  $RdNBR$ , for being more accurate and reliable in measuring and classifying burn severity.  $RdNBR$  severity maps could provide an adequate assessment of the degree of damages (Mallinis et al., 2018; Konkathi & Shetty, 2021); it can be calculated according to the following equation:

$$RdNBR = \frac{dNBR}{NBR_{pre-fire} + 1.001} \quad (3)$$

where:

$RdNBR$  - Relativized Burn Ratio

Both  $dNBR$  and  $RdNBR$  produced maps were classified into different fire severity levels, based on the scale developed by the *U.S. Geological Survey Earth Resources Observation and Science Center* (Table 1). Spatial distribution of different burn severity percentages was carried out, mapped and discussed.

**Table 1.**

**Fire severity levels assigned to  $dNBR$  classes.**

Severity No.	Severity Level	$dNBR$ range
1	Enhanced Regrowth, High	$\leq -0.251$
2	Enhanced Regrowth, Low	-0.250 to -0.101
3	Unburnt	-0.100 to 0.099
4	Low Severity	0.100 to 0.269
5	Moderate-Low Severity	0.270 to 0.439
6	Moderate-High Severity	0.440 to 0.659
7	High Severity	$\geq 0.660$

## 4. RESULTS AND DISCUSSION

### 4.1. Wildfire vulnerability and pre fire circumstances

The ignition and combustion initiation require the presence of external heat source, combustible materials (as vegetation) and oxygen; afterward, the wildfire intensity and propagation depend on multiple factors such as climatic conditions (wind velocity/direction, temperature, humidity...), physical context of the ecosystem (slopes, aspect, morphology ...) and the vegetation types and composition (Merdas, 2007). The combination of these factors increases forest ecosystem vulnerability to fire occurrence. According to Rahmani and Benmassoud (2019), the Aures Mounts forests are high-risk regions, presenting highly favorable conditions to fire propagation, and this is due to multiple factors: 1) Predominance of high relief associated with steep slopes exceeding 45 %; 2) Predominance of medium to high piedmonts and mountains landscapes and; 3) the land cover is mainly constituted of high-combustibility species as Holm oak and Aleppo pine. Besides, the year 2021 is characterized with exceptional heat waves occurrences through entire Algeria reaching 49 °C in Saharan regions; the region of Khenchela as well was marked by extremes daily records, the July 5 wildfire was preceded by long period of ascending temperatures. From June 24 to July 5, daily maximum temperatures exhibit a continuous increasing from 39 to 44 °C; in associated with high



evapotranspiration and pluviometric drought, this could contribute on considerably favoring the fire occurrence aptitude, which was initiated July 5 near Ain Mimoun agglomeration.

#### 4.2. Wildfire initiation and propagation

First fire events initiated July 5, 2021 near the village of Ain Mimoun. Investigation of the during-fire Sentinel 2 image which was taken at 10:21 AM, allows to visualize a series of 20km length and oriented southwest-northeast, composed of multiples and scattered ongoing fires exceeding 20 sites (Fig. 2B), signifying that fires were simultaneously initiated (at least timely close), and that they rapidly spread during short time.

Regarding the elevation map, it can be noticed that all of the fires occurred in the Mounts: Dj. Aouress (northwest), Dj. Tizi Ala (north) and Dj. Faraoun (south) on high altitudes, and along steep slopes, this can a favoring factor in fires spreading. Besides, wind direction was also a determinant agent since it was highly variable. In July 5, wind direction was 125° azimuth and oriented south east (Fig. 2A); July 6, air temperature increased to be 45°, daily-wind as well changed direction to be 70° and oriented north-east east, July 7 it changed to 258° according to the west-south west trend, this could be recognized and confirmed by visualizing the wildfire smoke trend (Fig. 2C). Later, wind directions were as well changed to 200° and 245° during July 8 and July 9 respectively (Fig. 2D). Therefore, highly-changing wind directional variability could be a major factor in rapid propagation of the fires, especially in presence of highly-combustible forest specie as Aleppo pine (Mitsopoulos & Dimitrakopoulos, 2007).

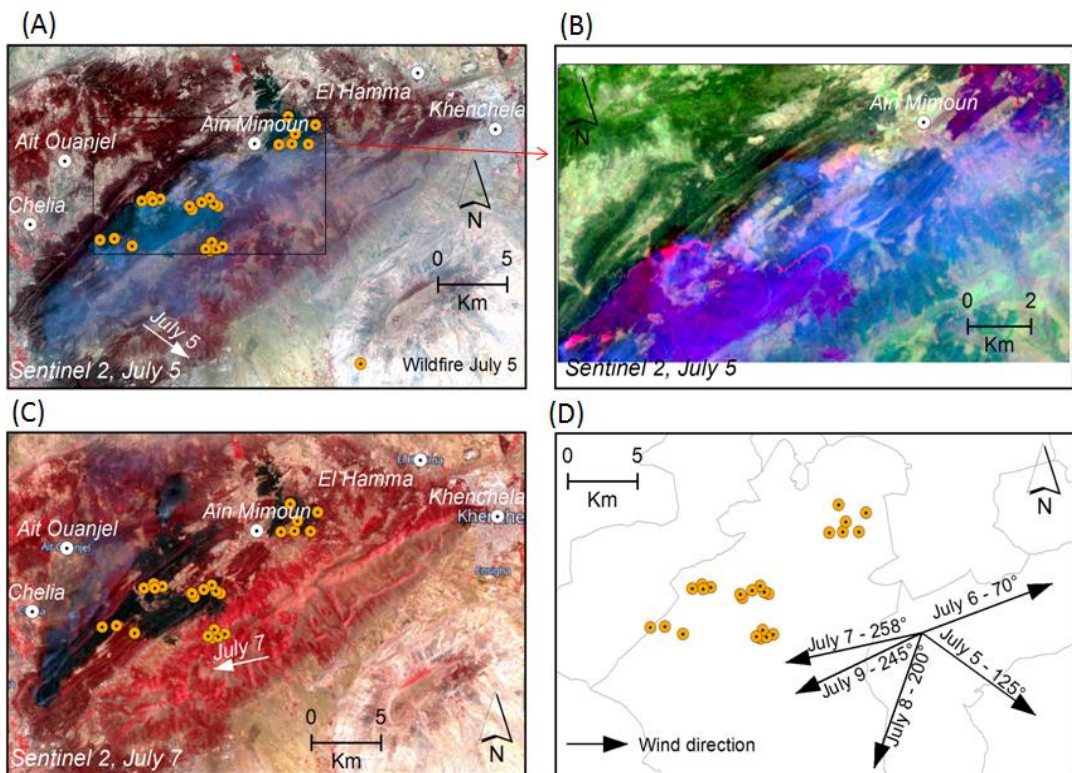


**Fig. 2.** (A) False color composite B8-B4-B3 of the Sentinel 2 image dated July 5 (during fire), with superimposed ongoing wildfire sites, note that the smoke direction is corresponding to the wind direction. (B) Excerpt of the July 5 image showing ongoing-fires in orange color. (C) False color composite B8-B4-B3 of the Sentinel 2 image dated July 7 (during fire); note that the smoke direction changed trending as response to the daily-wind direction. (D) Wind-rose showing directional variability from July 5 (fire starting) to July 9; note that the fire spreading was accelerated due to the high wind variability

### 4.3. Post fires and burned areas distribution

After 5 days of activity, the fire events were completely ended July 10; consequently, daily temperatures decrease gradually from 43°C in July 10 to 33°C in July 17.

The pre fire NBR map was ranged from -0.88 (no vegetation/bare soil) to 0.93 corresponding to healthy vegetation cover (variable-density Aleppo pine), the post fire NBR map presents a significant changing in pixel values that ranged from -0.97 to 0.98, where very low values correspond spatially to moderate and dense forest during the pre fire period.

**Table 2** and **table 3** summarize rates and distribution of burn severity levels, respectively based on the reclassification of dNBR (**Fig. 3A**) and RdNBR maps (**Fig. 3B**); burnt areas are also evaluated and delimited (**Fig. 3C**, **Fig. 3D**).

**Table 2.**

**Distribution of burnt areas based on differenced normalized burn ratio dNBR.**

Fire Severity classes	Municipalities				Total (ha)	Total (%)
	Bouhmama	Tamza	Chelia	Kais		
Enhanced Regrowth, High	0	0	2	0	3	0
Enhanced Regrowth, Low	0	44	9	0	53	0
Unburnt	2,971	31,454	19,219	1,731	55,375	73
Low Severity	348	5,078	3,038	464	8,929	12
Moderate-Low Severity	88	2,099	1,206	14	3,407	4
Moderate-High Severity	185	1,653	861	16	2,715	4
High Severity	150	3,461	1,838	11	5,459	7
Total	3,742	43,789	26,173	2,237	75,941	100
Subtotal High Severity (burnt)	335	5,114	2,698	27	8,175	11

**Table 3.**

**Distribution of burnt areas based on relativized burn ratio RdNBR.**

Fire Severity classes	Municipalities				Total (ha)	Total (%)
	Bouhmama	Tamza	Chelia	Kais		
Enhanced Regrowth, High	0	1	4	0	5	0
Enhanced Regrowth, Low	0	14	7	0	21	0
Unburnt	3,061	32,341	19,617	1,770	56,789	75
Low Severity	267	5,365	3,377	433	9,442	12
Moderate-Low Severity	135	1,925	1,002	15	3,077	4
Moderate-High Severity	224	2,343	1,367	19	3,953	5
High Severity	55	1,800	799	1	2,654	3
Total	3,742	43,789	26,173	2,237	75,941	100
Subtotal High Severity (burnt)	279	4,143	2,166	19	6,607	9

Based on both dNBR and RdNBR maps, no significant high and low enhanced regrowth occurs, unburnt area classes predominates with respectively 73 and 75 %, only 12 % of the forest cover is of low severity and 4 % is of moderate-low severity. In addition to the localization of ongoing fire sites on the during-fire image dated July 5 (**Fig. 2A**), the visualization and interpretation of the post fire image confirm that these classes correspond to unburnt areas. In the opposite, high and moderate-high severity classes (dNBR or RdNBR  $\geq 0.440$ ) correspond to the effective total of burnt areas. By considering dNBR, total burnt area is about 8,175 ha (11 %) with more damages in Tamza (5,114 ha) and Chelia (2,698 ha). Differently, the total of effective burnt areas based on RdNBR is about 6,607 ha (9 %), distributed on 4 main municipalities: Tamza (4,143 ha), Chelia (2,166 ha), Bouhmama (279 ha) and kais (19 ha).

The accuracy of both dNBR and RdNBR in assessing burn severity is carried out; dNBR index is often overestimating damaged areas by presenting bias due to considering unburnt areas (**Fig. 3E**), RdNBR is more accurate since it delimitates high severity class in well accordance with effective burnt areas (**Fig. 3F**), this conclusion is in coherence with many similar studies (Arellano et al., 2017;



Quintano et al., 2018; Konkathi & Shetty, 2021) confirming that relativized dNBR is more appropriate and accurate in assessing high severity due to wildfires using Sentinel 2 and Landsat images.

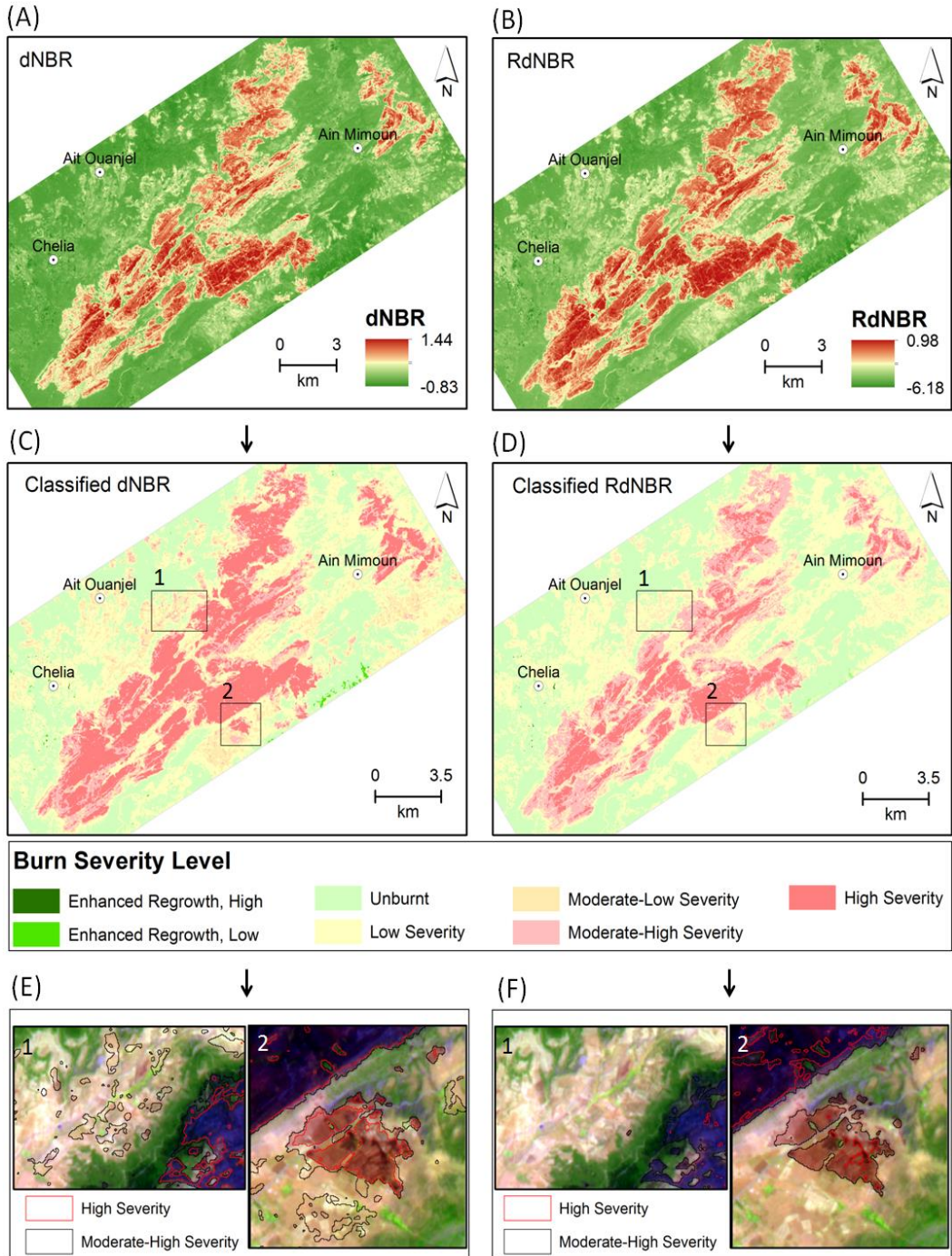


**Fig. 3.** (A) dNBR map showing delta NBR of pre and post fire. (B) RdNBR map. (C) Classified dNBR map showing severity level classes. (D) Classified RdNBR map showing severity level classes. (E) Zoom-in excerpts showing high fire severity precision based on dNBR classification. (F) Zoom-in excerpts showing high fire severity precision based on RdNBR classification

Most of the fires occurred in the northern mounts series, Tamza situated in the south-facing versant and Chelia located in the north-facing versant, they were the most damaged municipalities with 100 % of the total burned superficies. South, the higher mounts of Dj. Faraoun is separated from the northern mounts series by a relatively flat piedmont of low slopes (less than 15 %); this natural character could be the limiting factor of fires spreading toward more southern areas. In addition to the topo-morphological consideration, the 0.5mm precipitation occurred in July 7 could be a contributing factor in decreasing the combustibility aptitudes, and consequently limiting fire-propagation speed. 6,607 ha as total burned areas represent about 0.9 % from the east-Algerian forest superficies (800,239 ha), and 5 % from the total forest cover of Khenchela governorate estimated at 131,069 ha; the July 5, 2021 fire event is the second most degrading wildfires occurring in Khenchela after the August 18, 2012 which led to the loss of 15,000 ha and the emission of 1,000 Gg of CO<sub>2</sub> equivalent (Benkheira, 2018).



**Fig. 4.** (A) Ongoing wildfire dated July 5, 2021. (B) Juxtaposed moderate and high burn severity areas, note that high severity areas manifest damages in all stratum, whereas moderate severity areas is marked by unburnt tree stratum. (C) Juxtaposed low, moderate and high burn severity areas, note that highly burnt areas correspond to the cliff steep slopes that is a favoring factor is fire propagation. Photos courtesy by the forest directorate of Khenchela, cell of communication (2021)

## 5. CONCLUSION

This research is a case study conducted in the Aures Mounts System east of Khenchela, Algeria. It was interested on assessing the fire severity levels, and delimitating recent burnt areas due to the wildfires occurred near Ain Mimoun in July 5, 2021, using multitudes Sentinel 2 satellite imagery and burn ratios.

Results revealed that the July 5 fire event was due to favoring climatic, natural and topomorphological factors to the forest fire initiation and propagation, and this during pre and post fire phases. The domination of highly-elevated landscape characterized by steep slopes piedmonts, the dominance of highly-combustible trees species as Aleppo pine, are main factors in classifying the entire Aures Mounts among the high fire risk regions. The wildfire day was preceded by a long period of high and continuous daily temperature, this was a prominent factor on increasing the fire occurrence, the post fire period also was marked by highly-variable wind direction and, this pattern may be a determinant factor in the wildfire propagation during 5 days.

Based on differenced normalized burn ratio dNBR, highly-burnt area was assessed to be 8,175 ha. Differently, relativized dNBR allowed to accurately evaluating highly-damaged areas to be 6,607 ha of forest cover fully composed of Aleppo pine, with exceptional damage rates in municipalities of Tamza and Chelia, and this is due to their geo-situation in the south-facing and north-facing versants of the Dj. Aouress mounts, where the topography was an important factor in accelerating the fire spreading over the mounts system.

This study shows that Sentinel 2, dNBR and especially RdNBR are effective data and indices for assessing, classifying and mapping burn severity extent due to wildfire events. Nevertheless, it is important that future researches should be complemented with field assessment, soil analysis and floristic surveys for a better evaluation and more reliable interpretation, related to other ecological factors such as forest stratum (using Composite Burn Index CBI), density, trees species, biomass consumption etc.

Visualizing satellite images shows that the Aures Mounts forests are well equipped with firebreaks system; this could be an effective measure in attenuating the wildfire severity and propagation in such highly-vulnerable areas. Nevertheless, it is also important to adopt appropriate strategies and integrated risk mitigation plans, before, during and after the fire events occurrence.

## REFERENCES

- Arellano, S., Vega, J.A., Rodríguez Y Silva, F., Fernández, C., Vega-Nieva, D., Álvarez-González, J.G., Ruiz-González, A.D. (2017) Validation of the remote sensing indices dNBR and RdNBR to assess fire severity in the Oia-O Rosal (Pontevedra) wildfire in 2013. *Revista de Teledetección*, 49, 49-61.
- Benkheira, A. 2018. Forest fires in Algeria: analysis and perspectives. General Directorate of Forests. Ministry of the Interior and Local Authorities (DZ). Last access on July 2021, <https://www.interieur.gov.dz/images/LES-FEUX-DE-FORTS-EN-ALGRIE--ANALYSE-ET-PERSPECTIVES--Pr-Benkheira.pdf>, (Original title in French).
- Cai, L. & Wang, M. (2020): Is the RdNBR a better estimator of wildfire burn severity than the dNBR? A discussion and case study in southeast China. *Geocarto International*, DOI: 10.1080/10106049.2020.1737973
- Cocke, A.E., Fulé, P.Z., Crouse, J.E. (2005) Comparison of burn severity assessments using Differenced Normalized Burn Ratio and ground data. *International Journal of Wildland Fire*, 14, 189-198
- Furtună, P. & Holobacă, I.H. (2013) Forest fires study using remote sensing and meteorological indicators. Study Case. *Geographia Technica*, 8(2), 23-37.
- Kazi Tani, M.N. & Oussedik, M.M. (1977) Geological Map of Algeria, Sheet of Khenchela, Ministry of Industry and Energy, Algeria, (Original Title in French).
- Konkathi, P. & Shetty, A. (2021) Inter comparison of post-fire burn severity indices of Landsat-8 and Sentinel-2 imagery using Google Earth Engine. *Earth Sci Inform*, 14, 645-653.
- Madoui, A. (2002) Forest fires in Algeria: history, report and analysis. *Forêt Méditerranéenne*, tome XXIII (1), 23-30, (Original title in French).

- Mallinis, G., Mitsopoulos, I., Chrysafi, I. (2018) Evaluating and comparing Sentinel 2A and Landsat-8 Operational Land Imager (OLI) spectral indices for estimating fire severity in a Mediterranean pine ecosystem of Greece. *GIScience & Remote Sensing*, 55(1), 1-18.
- Meharzi, M.K. (1994) The role of orography in the spatial distribution of precipitation in the Aures Massif. *Méditerranée*, tome 80, 73-78, (Original title in French).
- Merdas, S. (2007) Report of forest fires in some Algerian governorates, cases of east Algeria: Bejaia, Jijel, Setif and Bordj Bou-Arredj, University Mentouri of Constantine, Algeria, (Original title in French).
- Mitsopoulos, I.D. & Dimitrakopoulos, A.P. (2007) Canopy fuel characteristics and potential crown fire behavior in Aleppo pine (*Pinus halepensis* Mill.) forests. *Ann. For. Sci.*, 64, 287-299.
- Parajuli, A., Gautam, A.P., Sharma, S.P., Krishna, K.B., Sharma, G., Thapa, P.B., Bist, B.S., & Poudel, S. (2020) Forest fire risk mapping using GIS and remote sensing in two major landscapes of Nepal. *Geomatics, Natural Hazards and Risk*, 11(1), 2569-2586.
- Parks, S.A., Dillon, G.K., Miller, C. (2014) A New Metric for Quantifying Burn Severity: The Relativized Burn Ratio. *Remote Sens.*, 6, 1827-1844.
- Quintano, C., Fernández-Manso, A., Fernández-Manso, O. (2018) Combination of Landsat and Sentinel-2 MSI data for initial assessing of burn severity. *Int J Appl Earth Obs Geoinf*, 64, 221-225.
- Rahmani, S. & Benmassoud, H. (2019) Modeling of forest fire risk spatial distribution in the region of Aures, Algeria. *Geoadria*, 24(2), 79-91.
- Rogan, J. & Franklin, J. (2001) Mapping wildfire burn severity in southern California forests and shrublands using enhanced thematic mapper imagery. *Geocarto Int.*, 16(4), 91-106.
- Rouse, J.W., Haas, R.W., Schell, J.A., Deering, D.W., Harlan, J.C. (1974) Monitoring the vernal advancement and retrogradation (Greenwave effect) of natural vegetation. NASA/GSFCT Type III Final report, Greenbelt, MD, USA.
- Roy, D.P., Boschetti, L., Trigg, S.N. (2006) Remote Sensing of Fire Severity: Assessing the Performance of the Normalized Burn Ratio. *IEEE Geoscience and remote sensing letters*, 3(1), 112-116.
- San-Miguel-Ayanz, J., Oom, D., Artes, T., Viegas, D.X., Fernandes, P., Faivre, N., Freire, S., Moore, P., Rego, F., & Castellnou, M. (2020) Forest fires in Portugal in 2017. In: Casajus Valles, A., Ferrer, M., Poljanšek, K. & Clark, I. (eds.) Science for Disaster Risk Management 2020: acting today, protecting tomorrow, EUR 30183 EN, Publications Office of the European Union, Luxembourg.
- UNOSAT/UNITAR, 2012. Wildfires in northern Algeria 18 august 2012. Palais des Nations, Geneva, Switzerland. Last access on July 2021, <https://reliefweb.int/map/algeria/wildfires-northern-algeria-18-august-2012>.



## FLASH FLOOD HAZARD MAPPING USING SATELLITE IMAGES AND GIS INTEGRATION METHOD: A CASE STUDY OF LAI CHAU PROVINCE, VIETNAM

Quoc Lap KIEU<sup>1</sup> 

DOI : 10.21163/GT\_2021.162.09

### ABSTRACT:

Lai Chau is a typical mountainous province of Vietnam, with a natural area of 9068.78 km<sup>2</sup>, this is a province that frequently occurs flash floods. This paper presents the results of the application of Satellite images, combining the GIS - AHP - MCA integration method to create a zoning map and warn of flash floods in Lai Chau province. The results of this study indicate the analyses and appraisals over 6 primary factors that incite flash flood, including the characteristics of geomorphology, the properties of soils, the types of forests and fractional vegetation cover, the slope of local drainage basins, average annual rainfall and the river/stream density of the region. The zoning map showing flash flood potentials has determined that 33.55% (3042.5 km<sup>2</sup>) of the area had an extremely high risk of flash flood occurrences, 44.42% of the area had a medium risk and 22.03% had a risk of flash flood at the low or very low level. Zoning map and flash flood warnings have great significance in preventing flash floods and minimizing damage in the study area.

*Key-words: Spatial analysis, Satellite images, GIS, flash flood, Vietnam*

### 1. INTRODUCTION

Flash flood calculation is an essential component of flash flood hazard mapping. However, the formation of flash floods is complicated. Flash floods also often occur in ungauged catchments, posing an even greater challenge to flash flood simulations. Many scholars have conducted studies on flash flood simulations. For example, developed a spatially distributed hydrological model on the basis of physical process representation (Roux et al., 2011); Proposed the physically based, space-time distributed hydrological model MARINE (model of anticipation of runoff and inundations for extreme events) and the geomorphological instantaneous unit hydrograph (GIUH) has been derived from the geomorphological characteristics of a catchment and used in simulation of the surface runoff hydrographs for ten rainfall events in the Ajay Catchment in eastern India (Estupina-Borrell et al., 2006; Kumar et al., 2007). Growing knowledge of flash flood mechanisms shows that the morphometric variables of a catchment control its hydrological response (Moussa, 2003; Angillieri, 2008). Based on this understanding, the geomorphological unit hydrograph (GUH) has become one of the most popular methods for estimating hydrological processes when data are inadequate (Du et al., 2009; Diakakis, 2011). Several studies concerning the risk of flash floods have described the initial versions and the evolution of a hydrological model adapted for very small watersheds (Domnița, 2012, Haidu et al., 2019). The model is based on the SCS-CN method for the rainfall excess (Haidu et al., 2017).

Nowadays, application of GIS in research and flash flood warning is a fairly popular and highly effective method. Studies regarding based on remote sensing and GIS mainly use the FFPI model to create flash flood warning maps (Gregory, 2010; Zogg, 2016; Ballesteros et al., 2017; Costache et al, 2019). Studies used the data of slopes, soil types, soil utilization types and vegetation cover to build a potential map, which provided excellent support for flash flood forecasting activities (Bajabaa, 2014; Roxana, 2018). There were also studies on the index of flash flood occurrences, serving flash flood warnings based on indexes of the relationship between vegetation and ridge slopes as well as indexes of flash flood occurrences through remote sensing data and GIS (Elkhrachy et al., 2015; Tehrany et al., 2015; Park et al., 2018; Khosravi et al., 2019). Studies regarding flash floods

<sup>1</sup>Thai Nguyen University of Sciences, Thai Nguyen City, Vietnam, lapkq@tms.edu.vn

susceptibility mapping by integrating frequency ratio and index of entropy with multilayer perceptron and classification and regression tree (Cao, 2016; Popa, 2019; Yi, 2021).

In Vietnam, studies regarding forecasting and warning flash floods are much limited. Nevertheless, some recently have been implemented with the primary focus on the construction of zoning maps for flash flood warnings. Remarkably, there are the study building a zoning map of flash flood risks, serving disaster control activities in Yen Bai province (La et al., 2009); the study building a map for early flash flood warnings in Thuan Chau district, Son La province (Lai et al., 2018); studying status and building flash flood zoning maps for some mountainous regions in Vietnam (Nong et al., 2020). That most of the studies employed the approach of hydrology – hydraulics, applying the FFPI, HEC-RAS, SWAT, and other models to construct flash flood warning maps. Besides, some warning maps were built based on approaching flash floods at mountain ridges, which results in zoned areas according to only the ridges. Consequently, this approach lacks calculations in detail and limited applicability. Moreover, the aforementioned studies often focused on only statistical data, ultimately leading to a lack of online warning abilities. Flash floods in mountainous regions often occur suddenly without any fixed rules, intensity and damage. Flash flood in Lai Chau province of Vietnam occurs rapidly, generally within a few hours of rainfall and sometimes accompanied by landslides, mudflows, bridge collapse, damage to buildings and fatalities (Duong et al., 2020). Lai Chau province is the primary neighborhoods of populations from minor ethnic groups. As a result, the capability of coping with flash floods is limited. There has been no scientific study serving weather forecasts, warnings, techniques against natural disasters and flash floods. Therefore, studying the application of satellite images and GIS integrated models to create a map of flash flood hazard in Lai Chau province has scientific and practical significance. The research results will contribute to warning and mitigating damage caused by flash floods.

## 2. STUDY AREA

Lai Chau is a province in the Northwest Vietnam, located about 400 km far from Ha Noi to the southeast, between  $21^{\circ}51' - 22^{\circ}49'$  North latitude and  $102^{\circ}19' - 103^{\circ}59'$  East longitude (**Fig. 1**). Lai Chau terrain is formed by mountain ranges running Northwest - Southeast direction, with many high peaks as Pu Ta Leng - 3096 m high. The province owns high and steep mountains, alternated with deep and narrow valleys. Hoang Lien Son Mountain range in the east, Song Ma Mountain in the west. Between two mountains above is the lowland belonging to Da river area with many limestone plateaus running from Phong Tho (Lai Chau province) to Quan Son (Thanh Hoa province). With 265.095km of border line sharing with China, the province has an important position in geography and national security. Lai Chau features the sub-tropical climate. The average temperature is about  $21^{\circ}\text{C} - 23^{\circ}\text{C}$  divided into 2 seasons following the humidity, rainy season and dry season.

Lai Chau province has 9068.78 square kilometers, 8 administrative units including Lai Chau City and 8 districts of Muong Te, Sin Ho, Nam Nhun, Tam Duong, Phong Tho, Tan Uyen,

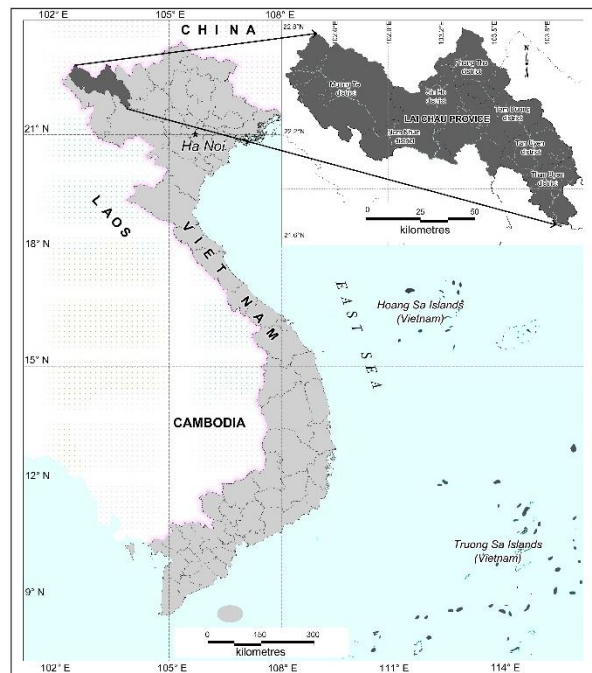


**Fig. 1.** Location of the Lai Chau province on a map of Vietnam.

and Than Uyen. The province has more than 400 thousand of people of 20 ethnic groups living together, in which Thai ethnic people cover the majority of population in Lai Chau with 131.822 people, accounting for 34% of the total population. The other ethnic groups consist of H'Mong people 86.467 people (22.30%), Kinh ethnic group 54.027 people (13.94%), Dao ethnic people 51.995 people (13.41%), Ha Nhi ethnic people 14.658 people (3.78%) and other ethnic minorities (Statistical Office of Lai Chau Province, 2020). Local people mainly plant corn, cassava, upland rice, herbs, and etc on hills and wetland rice in valleys, while they also do exploitations in forests. These forms of agricultural cultivation are completely free and much dependent on natural conditions, leading to an incline in terms of flash flood potential and subsequently increasing damage. According to statistical data obtained in 20 years (from 2000 to 2020) in Lai Chau province there have been 42 flash floods, leading to the deaths of 68 people, 112 injured, 1479 houses devastated and total economic damage that is estimated up to 35 million USD (Vietnam Disaster Prevention and Control Office, 2020). Through investigations and surveys, flash flood forming factors in the research location are relatively typical with the characteristics of basins, partitioned terrains, high slopes, and flows that tend to aggregate. Moreover, in recent times the forest vegetation cover of Lai Chau tends to decrease; combined with the unsustainable form of agricultural cultivation of the people, the impact of climate change, erratic heavy rain, increases the intensity and impact of flash floods.

### **3. DATA AND METHODS**

#### **3.1. Study data**

Flash flood hazard map in Lai Chau province employed the data from various sources, including field surveys and investigations data, statistical data, observative data, satellite images, paper maps, and data from relevant publications. The data of terrains were inherited, cited from terrain maps of Lai Chau province with a map scale of 1:500,000. Data regarding slopes were built on Digital Elevation Models (Data center, Vietnamese Ministry of Natural Resources and Environment, 2021). Geomorphologic maps were constructed based on original morphology, combined with GIS analyses from terrain maps, geologic maps, satellite images, and field data. Pedologic data, the characteristics of samples, types of soils, soil horizons, and mechanical composition were from surveys, and the inheritance of analyses over 50 soil horizons, which represent 10 types of soils covering the research location (Soils and Fertilizers Research Institute, 2020). Data regarding forests and vegetation cover were obtained from Sentinel 2 satellite images with a resolution of 10×10m, includes four satellite imagery, was downloaded free from the U.S Geological Survey website (<https://earthexplorer.usgs.gov/>), date January 18, 2021. Rainfalls were collected from the rainfall database of the Institute of Hydrology and Meteorology Science and Climate Change covering a range of 60 years (1960 – 2020), combined with observative data regarding rainfalls from 9 IMETOS weather stations located in the research area. Finally, data relating to flash flood status (location, intensity, effect range, time) in 20 years (2000 – 2020) were achieved from statistic documents in combination with field investigations and interviews with local people in the research area.

#### **3.2. Study methods**

This study used the method of processing remote sensing images, with the Envi software, images with a resolution of 10x10m from Sentinel 2 satellites were processed to form maps of forests and vegetation cover in the research location. More specifically, there were 2 options to process the images, including the NDVI differencing method and the Post Classification method, in which the radiation of vegetation cover in the research location was calculated through the formula of  $\varepsilon = 1.0094 + 0.047 \ln(\text{NDVI})$  (Pu et al., 2008). Additionally, the method of processing remote sensing images also provided data and supplemented the updates of terrain maps and geomorphologic maps for the research area (Asadzadeh, 2016). GIS was the primary technique used in analyses and the formation of a zoning map that evaluated the risks of flash floods. There were 2 algorithms in GIS spatial analysis, including the spatial stacking algorithm and the categorization algorithm (Goodchild, 2003;



Jia, 2017; Shirowzhan, 2019). Spatial data were processed with the ArcGIS software, subsequently forming maps with the QGIS software. In addition, this study also utilized the Digital Elevation Models (DEM) in the analysis of factors including terrain and geomorphology (Wessel et al., 2018). The spatial interpolation algorithm of GIS was also used to analyze and forecast rainfalls (Comber et al., 2019).

In this study, GIS is integrated with Analytic Hierarchy Process (AHP) and Multi-Criteria Analysis (MCA) to determine the weights and evaluate the factors that generate flash floods in Lai Chau province. The AHP method was used to confirm the reliability of a matrix determined from the Consistency Ratio (CR) among flash flood forming factors. The Consistency Ratio is calculated through the Consistency Index (CI) and the Random Consistency Index (RI). The formula of calculation is as follows:

$$CR=CI/RI. \quad (1)$$

In the equation:  $CI = \lambda_{max} - n / n - 1$ ;  $\lambda_{max}$  is the average value of the consistency vector;  $n$  is the number of criteria;  $RI$  is random.

Therefore, it depends on the number criteria brought in comparisons; in this case,  $n = 6$ . From the appendix of AHP,  $RI = 1,25$ . If the value of  $CR$  is less than or equal to 0.1, the consistency among factors in the matrix is assured. (Saaty, 1987).

MCA method combining hydrologic models and local geomorphology with the support of GIS (Triantaphyllou, 2000; Thoma, 2008). Employing this technique, this study focused on the determination of factors that formed flash floods in the research area and simultaneously combined the goal with statistical data for comparisons, ultimately leading to the hierarchy of the capability to cause flash floods of information layers. With the application of GIS in determining weights, the spatial integration of factors and weights in order to build a map of flash flood potentials at the research area was executed in accordance with the following function:

$$F(m) = \sum_{i=1}^n W_i \cdot X_i \quad (2)$$

In the equation:  $F(m)$  is the map of flash flood potentials,  $W_i$  is the weight of factor ( $i$ ),  $X_i$  is factor ( $i$ ), and  $n$  represents the number of flash flood forming factors (this study,  $n = 6$ ).

Moreover, during the execution of this study, many field surveys were conducted to comprehensively evaluate the research area, collect relevant documents and data, and verify the study results. More remarkably, the data of flash floods occurring throughout history and the locations of occurrences in 20 years (2000 – 2020) were investigated and confirmed by interviewing local people. The study also combined the collection of statistical data regarding natural conditions, social and economic status, and the status of flash floods in the research area. The system of those aforementioned methods was employed to construct flash flood hazard mapping in Lai Chau province (Fig. 2).

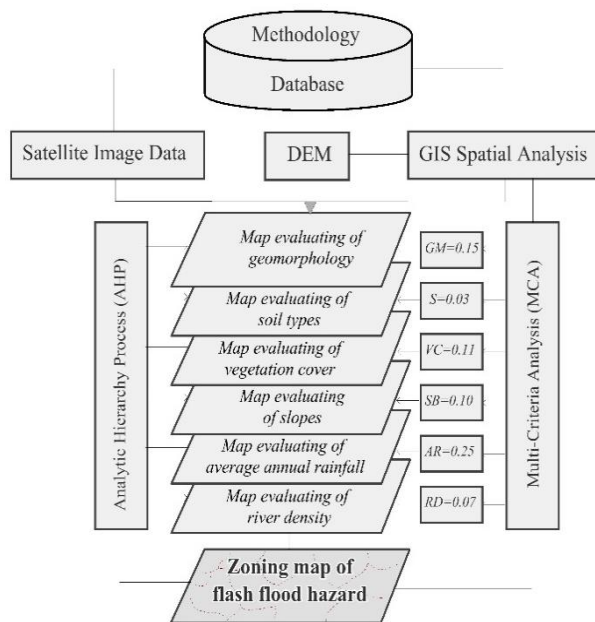


**Fig. 2.** Model of applying Satellite images and GIS integration method in flash flood warnings in Lai Chau province, Vietnam

## 4. RESULTS AND DISCUSSIONS

### 4.1. Evaluation of factors forming flash floods in Lai Chau province

The study at Lai Chau province shows that the occurrence of flash floods primarily involves local drainage basins. According to statistical data, the slope of basins is great at the locations of flash flood occurrences, coming with thin vegetation cover of below 10%, maximum rainfalls over 150 mm/day, soil types with medium/low permeability, and geomorphology that is V-shaped or resembles water-aggregating valleys. Many publications regarding flash floods in Vietnam have identified 6 fundamental factors that potentially form flash floods in mountainous regions, including: the characteristics of geomorphology, the properties of soil, vegetation cover, the slopes of drainage basins, average annual rainfall, and river density (Lai et al., 2018; Nong et al., 2020). Simultaneously, most of those studies have agreed on categorizing the potential of flash flood forming into 5 levels of intensity: "very low" risk of flash floods, "low" risk of flash floods, "medium" risk of flash floods, "high" risk of flash floods, and "very high" risk of flash floods. Referencing relevant studies in combination with statistical data, factors that potentially formed flash floods at Lai Chau province and the levels of intensity were determined and shown in **Table 1**.

**Table 1.**

**Criteria of assessing flash flood risks at Lai Chau Province.**

Level	Characteristics of geomorphology	Soil properties	Vegetation cover (%)	Slopes (degree)	Average annual rainfall (mm)	River density (km/km <sup>2</sup> )
<b>Very low</b>	Flat surfaces, arches with low slopes, no water aggregating, top surfaces higher than 1000 m, wave-like, weak erosions acting	Alisol or limestone mountains	>55	<10	<1000	<0.5
<b>Low</b>	Abrasively erosive ridges, intermediately slippery ridges, sunken and severely weathered	Dark soil or mountainous humus	40-55	10-20	1000-1500	0.5-1.5
<b>Medium</b>	Slippery ridges, sunken and winding, erosive ridges on different stones	Oxisols on sandstone, ferralsols on limestone	25-40	20-30	1500-2000	1.5-2.5
<b>High</b>	Erosive drains erosive ditches capable of aggregating water while raining, aggregated and abrasive surfaces	Oxisols degraded due to rice cultivation, oxisols and humus	10-25	30-40	2000-2500	2.5-3.5
<b>Very high</b>	Cavitated troughs, V-shaped water aggregating troughs, cavitated and water aggregating grounds	Strongly erosive soils, tones, aggregating sloped soils	<10%	>40	>2500	>3.5

Based on the table of criteria that assessed flash flood forming factors at Lai Chau province, the employment of collected data and analytical functions of GIS resulted in a map that assessed flash flood forming factors on the surfaces of buffer zones in drainage basins. There were 6 information layers, including the characteristics of geomorphology (GM), soil types (S), vegetation cover (VC), slopes of drainage basins (SB), average annual rainfall (AR), and the river/stream density (RD). The map system that assessed the intensity of those layers was divided into 5 levels, corresponding to the risks of flash floods ranging in very low, low, medium, high and very high. The results of assessing information layers are demonstrated in **Fig. 3** and **Table 2**.

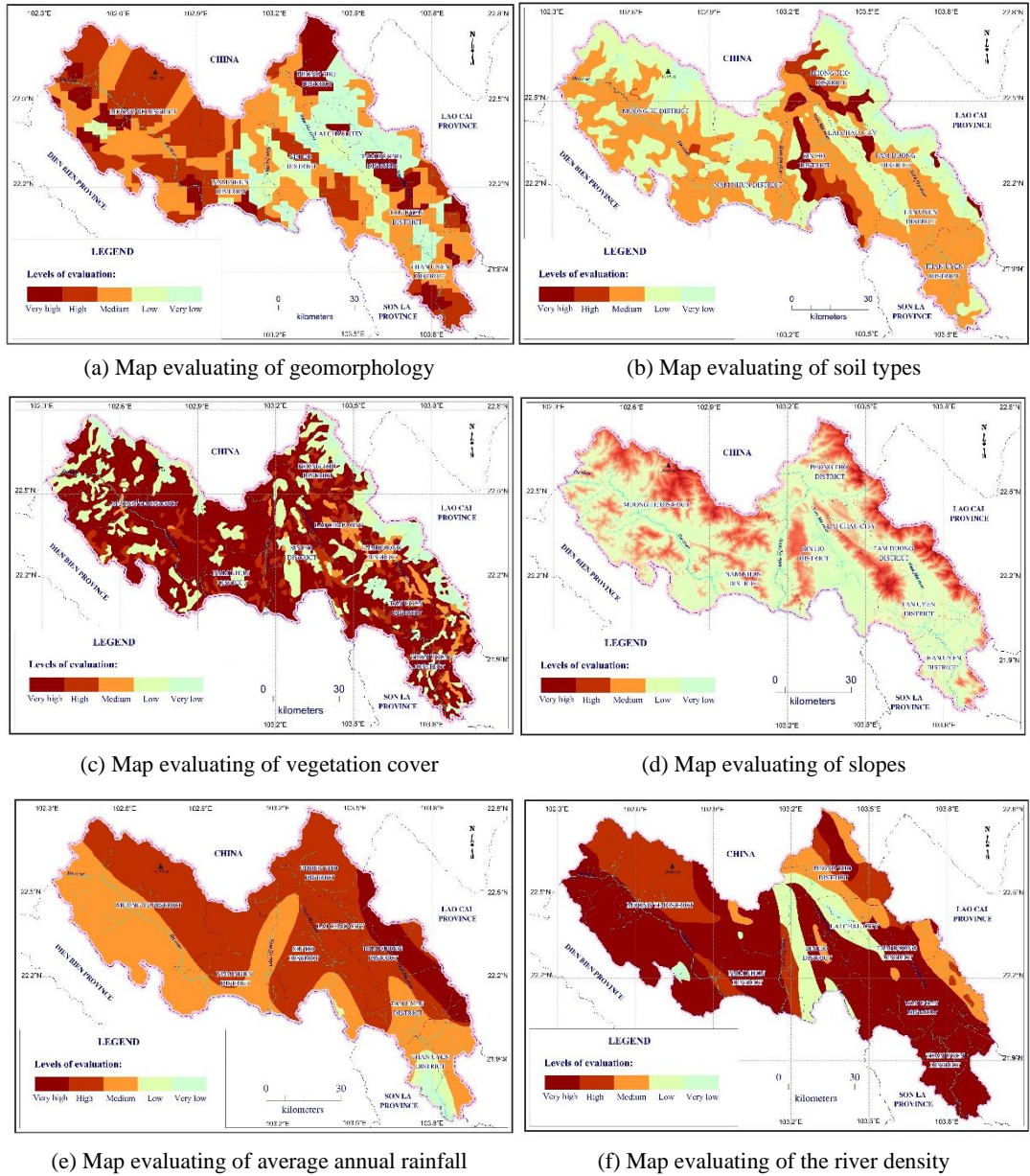


**Fig. 3.** Maps system evaluating the risk of factors that cause flash floods in Lai Chau province.

**Table 2.**

**Results of assessment of factors causing flash floods in Lai Chau province (km<sup>2</sup>).**

Level	GM	S	VC	AR	SB	RD
Very low	737.09	1207.05	798.85	1320.41	107.32	220.72
Low	1292.94	2603.65	1542.01	2263.57	162.00	677.35
Medium	3164.00	3577.63	1017.54	3097.90	3654.04	1643.25
High	2710.41	808.94	1634.14	1633.29	4195.72	1608.83
Very high	1164.35	871.51	4076.24	753.62	949.71	4918.63

### 4.2. Mapping of flash flood hazard in Lai Chau province

The AHP was utilized in calculating the weights of information layers that evaluate flash flood risks at Lai Chau Province. Results are shown in **Table 3**. Specifically, the results include: A Consistency Index CI of 0.069; A Random Consistency Index determined according to 6 factors forming flash flood RI of 1.25; and A Consistency Ratio  $CR = CI/RI = 0.069/1.25 = 0.055$ . Therefore, as the CR index is less than 0.1, the reliability of this study is assured.

**Table 3.**

**Matrix of weights for information layers that evaluate flash flood risks in Lai Chau province.**

Information layer	GM	S	VC	SB	AR	RD	Total	Weight
<b>GM</b>	0.14	0.12	0.16	0.17	0.18	0.11	0.88	<b>0.15</b>
<b>S</b>	0.02	0.03	0.02	0.04	0.04	0.02	0.17	<b>0.03</b>
<b>VC</b>	0.08	0.13	0.08	0.18	0.08	0.13	0.68	<b>0.11</b>
<b>SB</b>	0.06	0.15	0.09	0.12	0.08	0.12	0.62	<b>0.10</b>
<b>AR</b>	0.36	0.18	0.19	0.26	0.28	0.25	1.52	<b>0.25</b>
<b>RD</b>	0.06	0.13	0.04	0.05	0.07	0.04	0.39	<b>0.07</b>

With the weights shown in **Table 3**, the F(m) function was clarified with the application of Formula 2 as follows:

$$F(m) = 0.15 * GM + 0.03 * S + 0.11 * VC + 0.10 * SB + 0.25 * AM + 0.07 * RD \tag{3}$$

Employing the analysis spatial model GIS, the stack of information layers regarding factors that formed flash floods resulted in a zoning map identifying the areas with potential risks of flash floods in Lai Chau province (**Fig. 4**). Areas of flash flood risk levels by district administrative unit of Lai Chau province are shown in **Table 4**.

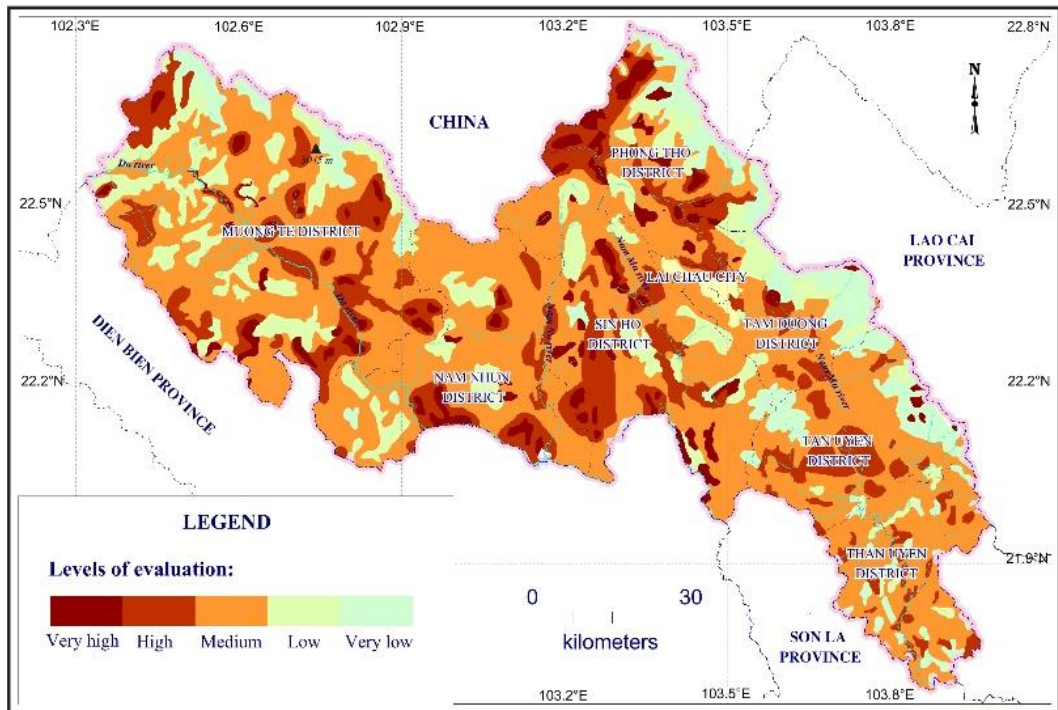


**Fig. 4.** Mapping of flash flood hazard in Lai Chau province.

Table 4.

Area of flash flood risk levels by administrative unit of Lai Chau province (km<sup>2</sup>).

No	District/city	Very low	Low	Medium	High	Very high
1	Lai Chau city	1.38	15.90	6.98	5.11	0.00
2	Tam Duong district	122.64	191.78	303.09	45.41	20.68
3	Tan Uyen district	98.20	154.21	551.20	105.66	85.38
4	Than Uyen district	61.44	94.11	565.85	75.46	20.08
5	Phong Tho district	188.32	282.70	384.56	200.04	108.52
6	Sin Ho district	200.46	246.44	789.00	312.07	127.71
7	Nam Nhun district	120.40	179.42	837.51	261.09	130.47
8	Muong Te district	494.18	657.75	1025.45	490.98	225.48
	<b>Total</b>	<b>1103.60</b>	<b>1938.90</b>	<b>4028.66</b>	<b>1469.11</b>	<b>528.51</b>

### 4.3. Discussion

The analysis results show that the area with a high and very high potential for flash floods accounts for 33.55% of the province's natural area, mainly concentrated in areas with steep slopes, the terrain tends to accumulate water, vegetation is mainly shrub or bare ground, typical sloping soil. The largest area belongs to Phong Tho and Sin Ho districts. This result completely coincides with the statistical documents on the locations of flash floods in the past in Lai Chau province from 2000 to the present (Statistical Office of Lai Chau Province, 2020). Especially in the area of Tua Sin Chai commune, Can Co commune of Sin Ho district; Mu Sang commune, Dao San commune, Vang Ma Chai commune in Phong Tho district. Statistics show that in the past 20 years, there have been 1-2 flash floods per year. Some small areas have a high level of potential risk assessment for flash floods, but in fact no flash floods have been recorded. These areas are often due to the hydrological network that does not tend to converge, the geomorphology is quite stable, and the terrain types are difficult to generate floods.

The study also shows that the factors that cause flash floods in Lai Chau province, including topography, geomorphology, slope, soil type, vegetation, and hydrological characteristics, are all less volatile. They can be analyzed and evaluated accurately. The factor of annual average rainfall has great variation, is the main factor causing flash floods. However, the average value of rainfall in the year doesn't accurately reflect the cause of flash floods. The factor of daily rainfall is the decisive factor for the formation of flash floods in the basin.

Studies on flash floods in mountainous areas of Vietnam also show that in areas with high risk of flash floods, as long as the amount of rain per day reaches above 200 mm, it is almost certain that flash floods will occur (La, 2009; Nong et al., 2020, Kieu et al., 2021). The factor of maximum rainfall during the day must be selected as the main factor for forecasting and early warning of flash floods. The biggest difficulty in the mountainous areas of Vietnam is the very sparse rainfall monitoring system, the lack of daily rainfall forecast data. Therefore, the study proposes to strengthen the system of automatic rainfall monitoring stations in the warning area with high risk of flash floods. Rainfall monitoring stations need to improve their accuracy, it must be able to connect to the national weather forecasting system. The reality shows that flash floods in Lai Chau province are very complicated. In many cases, flash floods occurred due to sudden causes such as landslides, flow blockage causing sudden accumulation of water in the basin (Duong et al., 2020). In this case, a satellite image system, online radar connected to the flash flood warning system is required.

The novelty of this study is flash floods were approached through drainage basins, which is considered a relatively closed system including small tributaries. Furthermore, when there is rain, the indexes of buffer surfaces would be used to determine the mode of transportation and aggregation of flows within the area of drainage basins (Oliveira et al., 2019). Lai Chau province possess high slopes, when rain exceeds limits, the flows aggregate to form a flash flood. Additionally, each drainage basin has a particular mechanism of flash flood occurrences.

The map of zoning and flash flood warning in Lai Chau province is built based on remote sensing and GIS integrated model. Remote sensing technology provided satellite image for the analyses of factors that formed flash floods, such as terrains, geomorphology, pedologic factors, flows, vegetation, etc. The GIS integrated model was responsible for processing spaces, forming maps of forecasts, and flash flood warnings. The results have been applied in Lai Chau province, initially offering great effectiveness in flash flood forecasting and warning. The model from this study is applicable in flash flood drainage areas at localities in mountainous regions of Vietnam.

## 5. CONCLUSIONS

Flash floods are extremely dangerous and unpredictable natural disasters. Flash flood hazard mapping using satellite images and GIS integration method is of great significance in early warning of flash floods, contributing to mitigating damage caused by flash floods. Research in Lai Chau province has analyzed the factors that cause flash floods and established a map of flash flood risk zoning.

Research results have identified 6 main factors that cause flash floods including geomorphological characteristics, soil properties, forest types and vegetation cover, basin slope, average annual rainfall, and the river density. The flash flood risk zoning map has identified 33.55% of Lai Chau province's area at high and very high risk of flash floods, 44.42% of the area at medium level, 22.03% of the area at low risk. low and very low. Thus, Lai Chau province is assessed as one of the provinces with the highest risk of flash floods in Vietnam.

## ACKNOWLEDGEMENTS

The author gratefully acknowledges Ministry of Natural Resources and Environment in Vietnam, the People's Committee of Lai Chau Province, Thai Nguyen University of Science provided data and other necessary facilities for this study.

## REFERENCES

- Angillieri, M.Y.E., 2008. Morphometric analysis of Colanguil River Basin and flash flood hazard, San Juan, Argentina. *Environ. Geol.* 55(1), 107-111.
- Asadzadeh S., Souza C.R., 2016. A review on spectral processing methods for remote sensing. *International Journal of Applied Earth Observation and Geoinformation.* 47, 69-90.
- Bajabaa, S., Masoud, M., Ai-Amri, N., 2014. Flash flood hazard mapping based on quantitative hydrology, geomorphology and GIS techniques (case study of Wadi Al Lith, Saudi Arabia). *Arabian J. Geosci.* 7(6), 2469-2481. Doi: 10.1007/s12517-013-0941-2
- Ballesteros, C., Jiménez, J. A., Viavattene, C., 2017. A multi-component flood risk assessment in the Maresme coast (NW Mediterranean). *Natural Hazards*, 90(1), 265–292.
- Cao, C., Xu, P., Wang, Y., Chen, J., Zheng, L., Niu, C., 2016. Flash Flood Hazard Susceptibility Mapping Using Frequency Ratio and Statistical Index Methods in Coalmine Subsidence Areas. *Sustainability*, 8, 948-961. Doi.org/10.3390/su8090948
- Comber A., Zeng W., 2019. Spatial interpolation using areal features: A review of methods and opportunities using new forms of data with coded illustrations. *Geography Compass.* Doi.org/10.1111/gec3.12465
- Costache, R., Pham, Q. B., Sharifi, E., Linh, N. T. T., Abba, S. I., Vojtek, M., Khoi, D. N., 2019. Flash-Flood Susceptibility Assessment Using Multi-Criteria Decision Making and Machine Learning Supported by Remote Sensing and GIS Techniques. *Remote Sensing.* 12(1), 106-120.
- Diakakis, M., 2011. A method for flood hazard mapping based on basin morphometry: Application in two catchments in Greece. *Nat. Hazards* 56(3), 803-814.



- Du, J.K., Xi, H., Hu, Y.J., Xu, Y.P., Xu, C.Y., 2009. Development and testing of a new storm runoff routing approach based on time variant spatially distributed travel time method. *J. Hydrol.* 369(1-2), 44-54.
- Duong, T.L., Do, V.T., Le, V.H., 2020. Detection of flash-flood potential areas using watershed characteristics: Application of Cau river watershed in Vietnam. *J. Earth Sys. Sci.* 129, 1–16.
- Domnița, M., 2012. Runoff modeling using GIS. Application in torrential basins in the Apuseni Mountains. Ph.D Thesis, Cluj Napoca, 271 pp.
- Elkhrachy, I., 2015. Flash flood hazard mapping using satellite images and GIS tools: A case study of Najran City, Kingdom of Saudi Arabia (KSA). *Egypt. J. Remote Sens. Space Sci.* 18, 261-278.
- Estupina-Borrell, V., Dartus, D., Ababou, R., 2006. Flash flood modeling with the MARINE hydrological distributed model. *Hydrology Earth Syst. Sci. Discuss.* 3(6), 3397-3438.
- Goodchild M.F., Haining R.P., 2003. GIS and spatial data analysis: Converging perspectives. *Papers in Regional Science.* 83(1), 363-385.
- Haidu I., Crăciun A.I. & Marian R.A., 2019. Risk scenarios for flash-floods in the rural area generated by combined hazard, technologic and natural, *Carpathian Journal of Earth and Environmental Sciences*, 14, 1, 181-190. Doi :10.26471/cjees/2019/014/070
- Haidu, I., Batelaan, O., Crăciun, A.I., & Domnița, M., 2017. GIS module for the estimation of the hillslope torrential peak flow. *Environmental Engineering and Management Journal*, 16, 5, 1137-1144.
- Jia P, Cheng X, Xue H, Wang Y., 2017. Applications of geographic information systems (GIS) data and methods in obesity-related research. *Obesity Reviews.* 18(4), 400-411.
- Kieu, Q.L., Tran, D.V., 2021. Application of geospatial technologies in constructing a flash flood warning model in northern mountainous regions of Vietnam: a case study at Trinh Tuong commune, Bat Xat district, Lao Cai province. *Bulletin of Geography. Physical Geography Series*, 20 (2021), 31–43.
- Kumar, R., Chatterjee, C., Singh, R.D., Lohani, A.K., Kumar, S., 2007. Runoff estimation for an ungauged catchment using geomorphological instantaneous unit hydrograph (GIUH) models. *Hydrol. Process.* 21(14), 1829-1840.
- La, T.H., 2009. Research and develop flash flood risk zoning maps to serve the prevention of flash floods for Yen Bai province. *Journal of Meteorology and Hydrology.* 211 (2), 11-15.
- Lai, T.A., Nguyen, N.T., Pham, X.C., Le, N.N., 2018. Building an early warning system for flash floods in mountainous areas, testing it in Thuan Chau district, Son La province. *Journal of Science and Technology of Vietnam.* 60 (8), 28-35.
- Nong, T.H., Tran, V.K., 2020. Study flash floods and landslides in the middle mountains areas of northern Vietnam in 2018 and 2019. *Journal of Science and Technology of Thai Nguyen University.* 225 (07), 168-175.
- Moussa, R., 2003. On morphometric properties of basins, scale effects and hydrological response. *Hydrol. Process.* 17(1), 33-58.
- Oliveira, E. A., Pires, R. S., Oliveira, R. S., Furtado, V., Herrmann, H. J., Andrade, J. S., 2019. A universal approach for drainage basins. *Scientific Reports.* 9(1). Doi: 10.1038/s41598-019-46165-0
- Park, S.J., Lee, C.W., Lee, S., Lee, M.J., 2018. Landslide susceptibility mapping and comparison using decision tree models: A Case Study of Jumunjin Area, Korea. *Remote Sens*, 10, 1545-1560.
- Popa, M. C., Diaconu, D. C., 2019. Flood and Flash Flood Hazard Mapping Using the Frequency Ratio, Multilayer Perceptron and Their Hybrid Ensemble. *Proceedings.* 48(1), 6-21.
- Pu, R., Gong, P., Tian, Y., Miao, X., Carruthers, R. I., Anderson, G. L., 2008. Using classification and NDVI differencing methods for monitoring sparse vegetation coverage: a case study of saltcedar in Nevada, USA. *International Journal of Remote Sensing.* 29(14), 3987–4011.
- Roux, H., Labat, D., Garambois, P.A., Maubourguet, M.M., Chorda, J., Dartus, D., 2011. A physically-based parsimonious hydrological model for flash floods in Mediterranean catchments. *Nat. Hazards Earth Syst. Sci.* 11(9), 2567-2582.
- Shirowzhan S., Sepasgozar S., 2019. Spatial Analysis Using Temporal Point Clouds in Advanced GIS: Methods for Ground Elevation Extraction in Slant Areas and Building Classifications. *ISPRS International Journal of Geo-Information.* 8(3), 110-120.
- Saaty, T.L., 1987. The analytic hierarchy process - What it is and how it is used. *Mathl Modelling.* (3), 161-176.

- Statistical Office of Lai Chau Province, 2020. Statistics of natural disasters for the period 2000 - 2020. Statistical Publishing House, 255-287.
- Tehrany, M.S., Pradhan, B., Jebur, M.N., 2015. Flood susceptibility analysis and its verification using a novel ensemble support vector machine and frequency ratio method. *Stoch. Environ. Res. Risk Assess*, 29, 1149-1165.
- Thomas L, Saaty, 2008. Decision making with the analytic hierarchy process. *Int. J. Services Sciences*, 1(1), 167-175.
- Triantaphyllou, E., 2000. Multi-Criteria Decision-Making Methods: A Comparative Study; Kluwer Academic Publishers: Dordrecht, The Netherlands.
- Vietnam Disaster Prevention and Control Office, 2020. Report on flash floods and landslides in mountainous areas in the period 2000-2020.
- Vietnam of Soils and Fertilizers Research Institute, 2020. Research on land characteristics of Lai Chau province for the development of key agricultural crops. Provincial key scientific projects. Lai Chau, December, 2020.
- Wessel B., Huber M., Wohlfart C., Marschalk U., Kosmann D., 2018. Accuracy assessment of the global TanDEM-X Digital Elevation Model with GPS data. *ISPRS Journal of Photogrammetry and Remote Sensing*. 139, 171-182.
- World Meteorological Organization, 2019. Flash Flood Guidance System with Global Coverage.
- Yi W., Yang, M., 2021. Flood susceptibility mapping by integrating frequency ratio and index of entropy with multilayer perceptron and classification and regression tree. *Journal of Environmental Management*. 289 (1), 235-251. Doi: 10.1111/jfr3.12683
- Zogg, J., Deitsch, K., 2013. The Flash Flood Potential Index at WFO Des Moines, IA. NWS Technical Report, National Weather Service. Doi: 10.1515/geo-2018-0047

## **GEOGRAPHIC INFORMATION SYSTEM FOR FLOOD MANAGEMENT BY CASCADE MODEL PREDICTIVE CONTROL (MPC)**

**Kajwis KLAHAN<sup>1</sup> , Suwatana CHITTALADAKORN<sup>1</sup>, Sitang PILAILAR<sup>1</sup>**

DOI : 10.21163/GT\_2021.162.10

### **ABSTRACT:**

The number of river floods has increased worldwide, as well as in Nakorn Ratchasima Province in Thailand. To prevent disasters, the **Royal Irrigation Department (RID)** constructed thirteen regulating structures to control discharges. Currently, the local controllers spatially control these structures to minimize the subsystem's damage, regardless of the effects on the overall system performance. In this study, the concept of combining real-time flood management tools and the cascade **Model Predictive Control (MPC)** as well as application of GIS has been proposed and verified with the 2013 flood event. The distributed control of the existing hydraulic structures on the large scale of the Lamtakong River made optimal use of the retention basin storage capacity with the considerations of both local performance and global system interactions. The model proposes an optimal gate opening of each cascade at the specified time, from the beginning until the end of flood hydrographs. The results of the controlled water level indicate the efficiency of the CMPC, which is more satisfied satisfactory than the PID and practice technique of RID, as evidenced by the water level of 0.5 m that is lower than the level of the riverbank at Nakhon Ratchasima City. A comparison of flood areas between the historical flood in year 2013 and Management by CASCADE MPC shows by GIS flood map that in the case of Management by CASCADE MPC, it can reduce the flood area in Nakhorn Ratchasima city by almost 60%.

**Key-words:** *Model Predictive Control; Cascade MPC; Flood management; Flood Map; GIS*

## **1. INTRODUCTION**

River floods are a natural hazard that causes loss of life, devastating damage to properties, and adverse economic and environmental impacts (Vermuyten 2018). They typically occur when rivers exceed their embankments due to long periods of rainfall. As a result, the number of river floods has increased worldwide during the last decade, as well as in Thailand. **Fig.1** shows the historical flood of 2010 (RID 2020) in Nakorn Ratchasima Province in the northeastern part of Thailand that caused suffering to more than one million people (**Fig. 1**), and four deaths. The damages covered the municipality area, the paddy fields, and farms. It seems that the flood warning system and situation management did not efficiently operate. Although the actual situation at the advent of upstream events was reported to the central operation center, the flood forecast, and scenario analysis seem not to have been appropriately performed due to the complication of the river network and existing management scheme. The problem caused difficulty for the local water administration of the Royal Irrigation Department (RID), who spatially controls the thirteen regulating structures along the Lamtakong River.

---

<sup>1</sup> *Department of Water Resources Engineering, Kasetsart University, Bangkok, Thailand; kajwis.k@ku.th, fengswc@ku.ac.th, fengstpl@ku.ac.th*

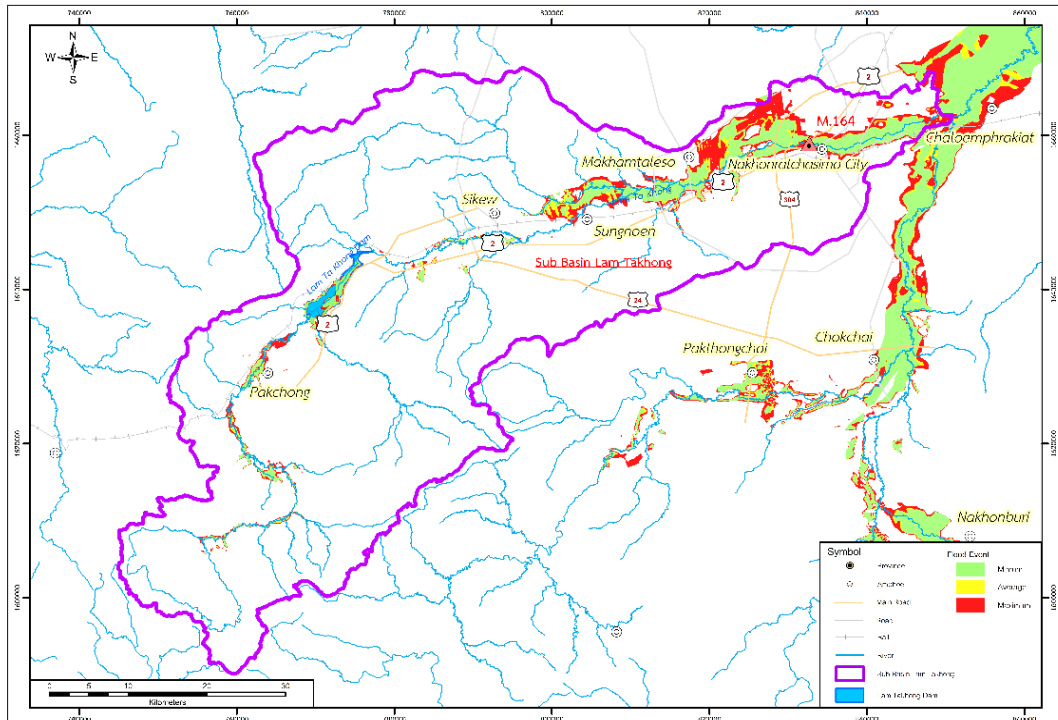


Fig. 1. Historical flood map of Lamtakong River, year 2013.

## 2. STUDY AREA

The Lamtakong River is the most important tributary of the Mun River in northeastern Thailand, and its upstream section is between Khao Faa, Pak Chong District, Nakhon Ratchasima Province, and Khao Falami, Muang Nakhon Nayok District. It flows through communities in Pak Chong District, Sikhio District, Sung Noen District, and Nakhon Ratchasima City Municipality until it drains into the Mun River at Chakkarat District, with a total length of about 220 km. **Fig. 2** illustrates the flow schematic of the Lamtakong River, with several branches, and the Lamtakong Dam at Sikhio District upstream. The most important one is the Lamboriboon River, which has a total length of 35 km. It flows almost parallel to the Lamtakong through Muang Nakhon Ratchasima District and converges with the original Lamtakong at Chaloem Phrakiat District before flowing into the Mun River.

In normal condition, the water is conserved mainly for irrigation purposes under the allocation of the RID staff, who are responsible for controlling the hydraulic structures with movable gates, as depicted in **Fig. 2**. Thus, the flow is controlled reach to reach. However, under the condition that the flow at the M.164 water metering station exceeds 65 cum/s, the situation is then shifted to flood surveillance. Eleven gates are promptly raised to 50%; the opening and closing of the gates are then manually controlled based on the local staff's expertise with the consideration of flow time lag from reach to reach. It means that objective functions and constraints are changed as conditions dictate.

According to the floods and damages to the communities and economic areas in Nakhon Ratchasima in the past, centralized control seems impossible due to the large-scale river systems. Likewise, the local water administration of RID appears incapable of spatially handling the hydraulic structures well. Therefore, this study proposes the concept of combining flood management with the cascade Model Predictive Control, taking the most advantage of the existing complex thirteen regulating structures to control the flow, and present the results of the analysis for flood areas that can be alleviated by a GIS system.

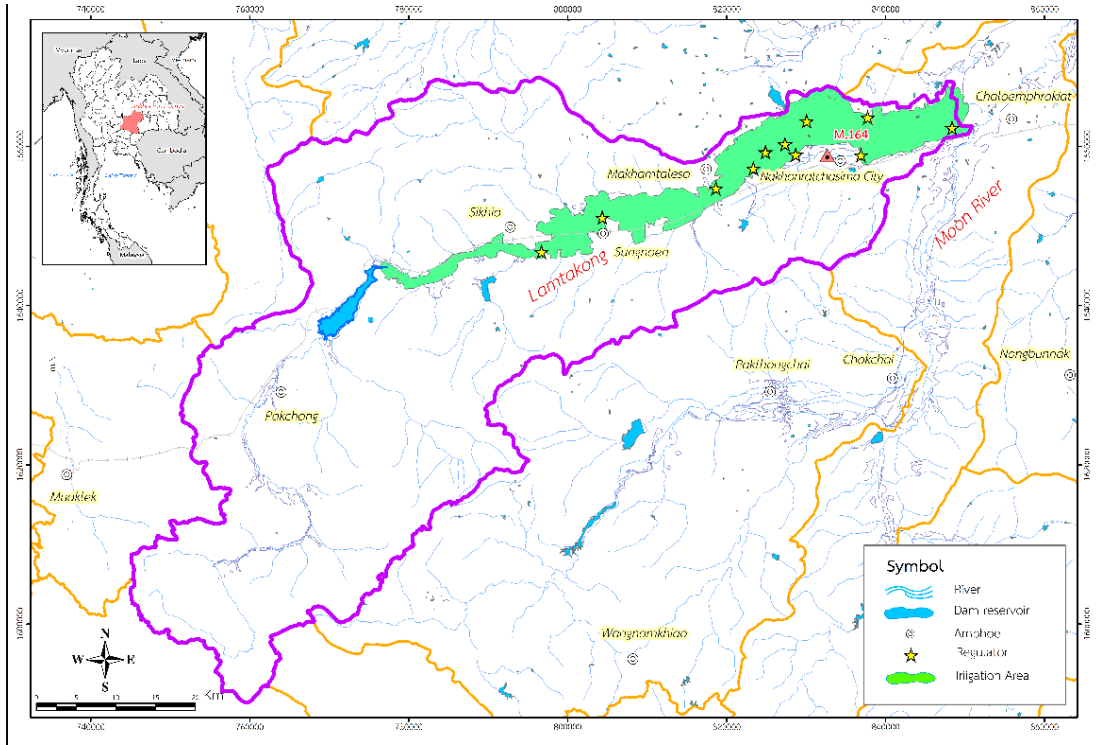


Fig. 2. Study area and river network.

### 3. DATA AND METHODS

#### 3.1. Flood Management Model

Real-time water control models for flood forecasting and reservoir operations have been developed for several decades. The United States Army Corps of Engineers has developed water control systems that consist of data acquisition and processing, precipitation analysis, flow forecasting, reservoir system analysis, including data and simulation result graphical display since 1982 (Leon et al., 2014). During the same period, another flood management type model was developed by the Savannah District of the United States Army Corps of Engineers (USACE - Environmental Laboratory 1987). It consists of the rainfall-runoff model, hydrologic (lumped) routing computations for reservoirs, and hydraulic (distributed) unsteady flow routing based upon the numerical solution of Saint Venant equations. Later, Unver et al., 1987 (USACE - Environmental Laboratory 1987) developed a real-time management model by combining techniques for one-dimensional unsteady flow routing, rainfall-runoff modeling, graphical display, and interactive software capability. However, each model's accuracy depends on catchment characteristics and catchment response to rainfall, types of flood forecasting models, and various uncertainties, significantly influencing the decision-making process. Therefore, it is necessary to consider uncertainties in the real-time control process and real-time flood forecasts.

Model Predictive Control (MPC) has been found to eliminate model deviations and limit performance loss due to uncertainties. It is also known for its proactive control strategy, which is an advantage for future flood events. Breckpot et al. (2013) reported that MPC was successfully used for flood control and set-point control of the Demer river in Belgium, consisting of multiple reaches, gates, junctions, and reservoirs. Besides, the study of Falk et al. (2016) also indicated that MPC could solve the optimization problem of gates and dams in a large-scale river network in Australia.

### 3.2. Model Predictive Control

Model Predictive Control (MPC) originates from the chemical process industry, but it has great value in various applications ranging from food processing to automotive and aerospace applications (Breckpot, 2013).

Since it formulates the control problem as an optimization problem, it has been used for river control during different operating conditions (Barjas Blanco et al., 2008; Evans et al., 2011; Wahlin and Zimbelman, 2018; López Rodríguez et al., 2017; Nguyen et al., 2017; Wang et al., 2017; and Tian et al., 2017). Furthermore, the predictive control strategies are widely accepted due to the intuitiveness and explicit constraint handling.

MPC is a control strategy that uses the system's model to make future predictions to minimize the objective function. Blanco (2008) mentioned that the three primary components of MPC are as follows:

- a process model is used to determine the future outputs within a time window with length  $N$ , the prediction horizon. These future outputs are determined by future control actions and the current state of the system.

- an objective function is minimized. The objective function is typically a quadratic function that tries to minimize the water level errors and the gate movement by adjusting the unknown control inputs. Typically, the objective function is also subject to constraints.

- once the sequence of future control actions that minimize the desired objective function is determined, only the first set of control actions is implemented in the system. The system is then updated by measuring the target level.

In this study, the process model is nonlinear, as various process conditions and disturbances demand suitable process identification. All model predictive control algorithms minimize the following optimization algorithm by minimizing the cost function  $J$ .

A generic MPC framework is described as:

$$\text{Current state: } x_o = x \quad (1)$$

$$\text{System model: } x_{k+1} = f(x_k, u_k) \quad (2)$$

$$\text{Cost function: } J(x_o) = \min \sum_{k=0}^{N-1} l_k(x_k - u_k) \quad (3)$$

where:

$N$  is the prediction horizon,  $X_K$  (e.g., measured water level) and  $U_K$  (e.g., target water level) are two constraints given for the states  $X_K$  and the inputs  $U_K$  at a time step  $k$ , respectively.

The reasonable values are predicted by the system model, thus reaching an expected control performance. For the MPC design, the cost function and constraints are the main two sections. Here, the current state,  $X_o$ , is used as the initial state for control predictions. The prediction process is continually repeated further to calculate the control signals in every time step. The basic idea of MPC (Song et al., 2020) is using a process model that predicts the system's behavior over a specified (finite) prediction horizon, as shown in **Fig. 3**.



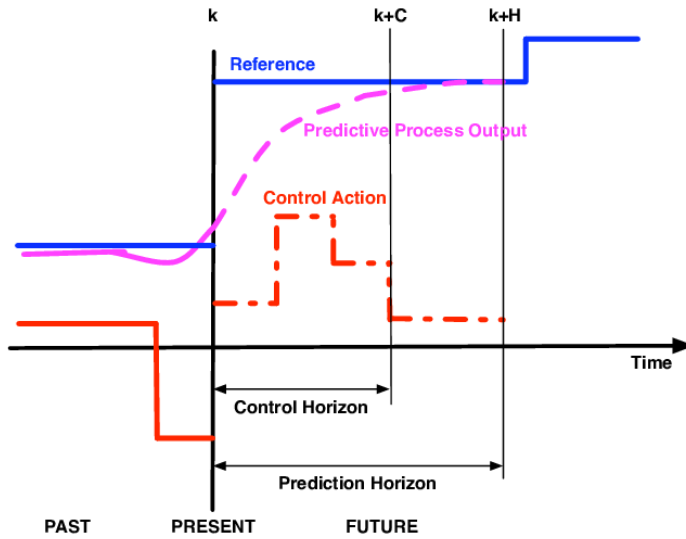


Fig. 3. Model Predictive Control Basis.

3.3. Cascade Concept

The original hydrodynamic analysis is considered holistic with related variables from upstream to downstream, i.e., inflow, cross-section, dimensions of key regulators with its water level upstream-downstream, gate operation information, and downstream boundary. It centrally considers all the regulators in the system by opening and closing gate various discharges. The analysis needs to consider many variables and intricate patterns; then there could be a considerable number of alternatives. Such a centralized controlling system from a big picture perspective would make spatial decisions errors. Besides, in the case of more than ten thousand possible alternatives (Fig. 4), it would give rise to extensive use of computational resources and cause delays in assessing a situation and making decisions to manage a flooding situation that arises. Thus, the decentralized approach will scale better for a large and complex system. Each controller's objective is to locally determine the actions appropriate to a situation and optimize the system's behavior.

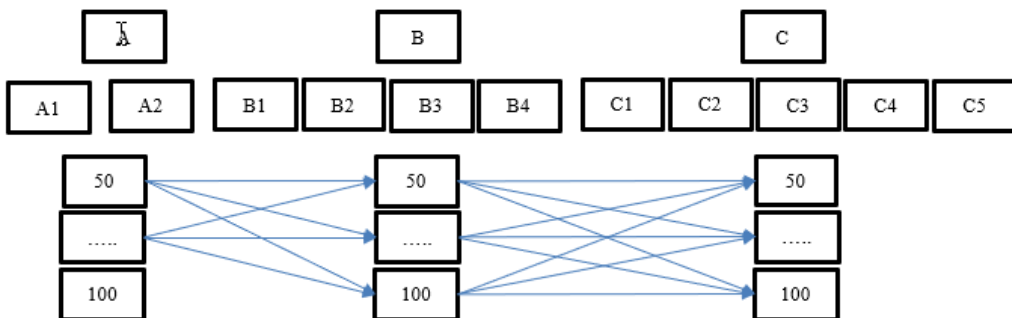
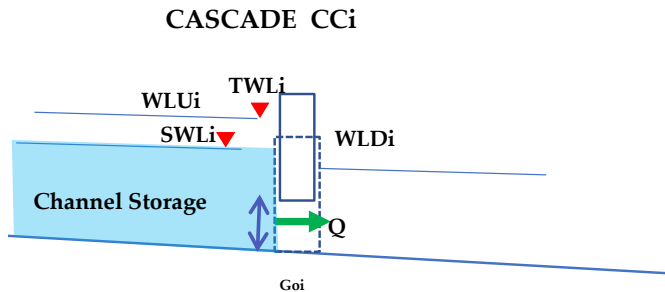


Fig. 4. Case of the Considered Integral System.

Combining the optimized decentralized control in terms of the big picture of the system would lead to better results; thus, the cascade management concept is considered. The complex river system is divided into reaches according to the sets of regulators. The physical constraints of each reach are concerns; thus, the local target water level is set, as the cascade's concept is shown in **Fig. 5**. The proper gate opening and closing will be rapidly defined to optimize the flow with less downstream effect. Since the proper spatial alternatives are evaluated, the global effect will then be assessed from the downstream control strategy. Once the final system measures are set up, the system's new state is further updated.



**Fig. 5.** Concept of Cascade's Control Water Level.

The concept of Cascade's Control Water Level is shown in **Fig. 5**, where  $TWLi$  is Target Water level upstream at cascade  $i$ ,  $WLUi$  is Calculate Water level upstream at cascade  $i$ ,  $SWLi$  is Storage Water upstream at cascade  $i$ , and  $WLDi$  is Calculate Water level downstream at cascade  $i$ .

### 3.4. Methodology

The methodology for making the decision is shown in **Fig. 6**. It is started by collecting data such as topography, cross section, land use, digital terrain model, hydrology, and regulator dimension. Next step is to set cascade network and to input the collected data to the geodatabase in the HEC-RAS. The water profile in the cascade will then be calculated by the HEC-RAS hydrodynamic model, and the CASCADE MPC is applied to find the optimum gate opening for each time step. The target water level will then be checked and measured. If it is close to a target value, it will transmit the parameters to perform a calculation in the subsequent cascade. The system will continue calculating until all cascades are completed and gotten the optimum result of gate operation setting. Finally, the result water level data will be exported in ARC-GIS to create a GIS flood map area for making a decision.

This study presents the concept of combining real-time flood management tools and the cascade MPC, so it is tested under a hypothetical condition that there are adequate onsite CCTVs to report real-time water levels and situations with sufficient computer resources. First, the flood situation is of primary concern, in which the condition of local flood management limits with its reach's embankment elevation is monitored. Then the global image is re-calculated under the condition of water level monitoring at the M.164 station. However, the lateral flow is excluded; just the channel flow from downstream of the Lamtakong Dam. Thus, the 2013 flood conditions, where the maximum flow was 90 cum/s, which was lower than the maximum capacity of the Lamtakong River, are applied in this test.

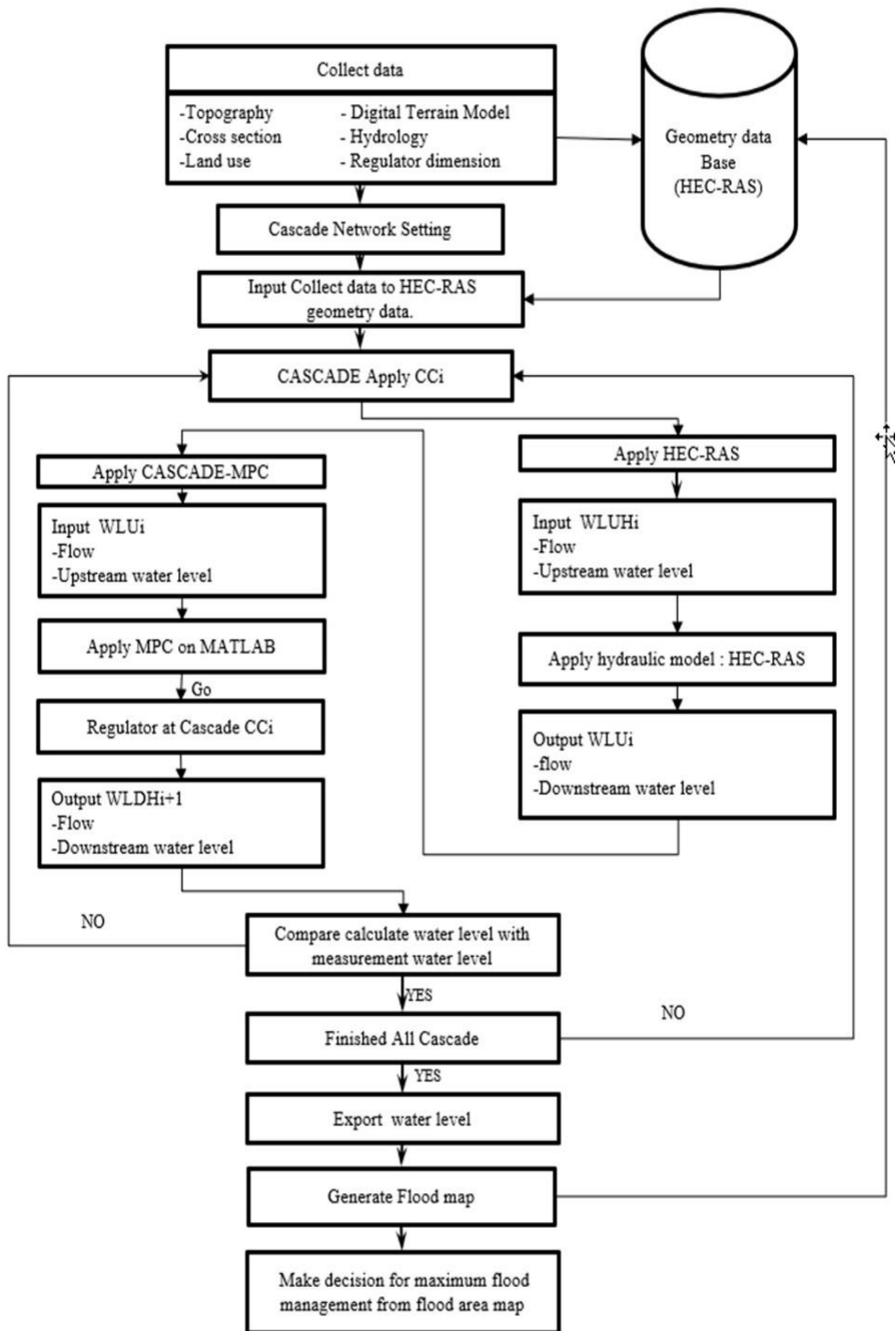
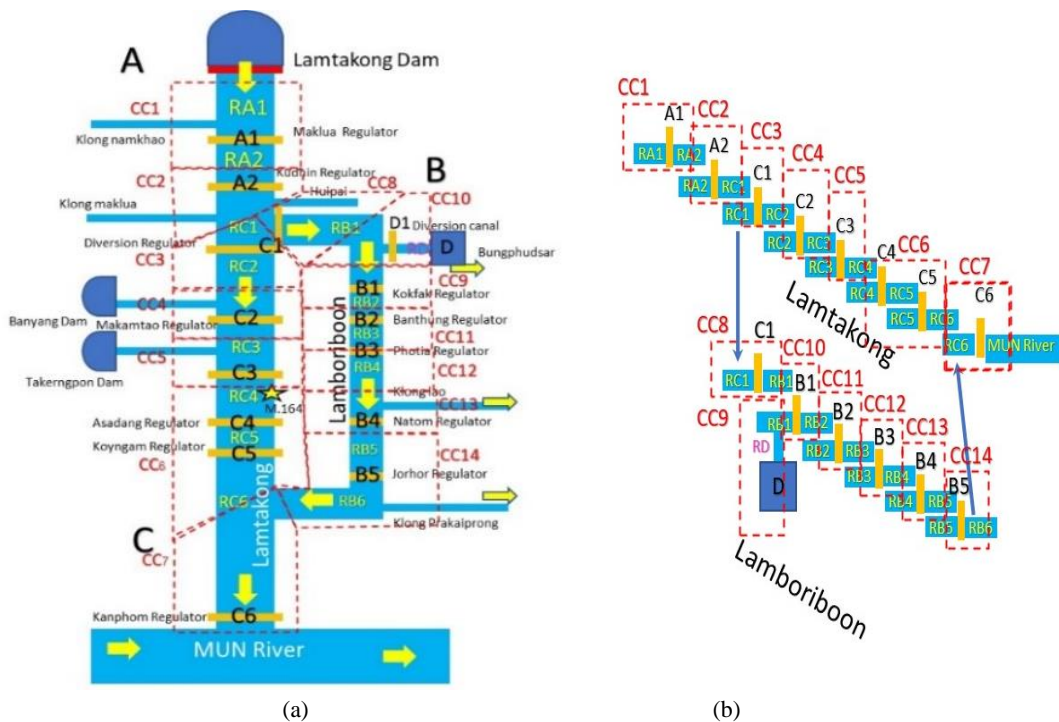


Fig. 6. Summarized procedure of study.

### 3.4.1. Cascade Network Setting

According to the existing hydraulic structures, the 220 km of the concerned Lamtakong River is divided into seven cascades, CC1 to CC7, as shown in Fig. 7. The capacity of each reach is 0.65, 0.24, 0.19, 0.24, 0.28, 0.24, and 0.32 MCM, respectively. The study also includes the 35 km of the Lamboriboon River that flows parallel to the Lamtakong and converges with the original Lamtakong at Chaloe Phrakiat District. It is divided into seven cascades as well where each reach's capacity is 0.95, 0.033, 0.16, 0.23, 0.068, 0.068, and 0.12 MCM, respectively.

Once the flow from upstream enters CC1, all gate setting heights are precalculated, and then the water level of each reach is analyzed. The water level at M.164 is rechecked since it is the surveillance point to protect the Nakorn Ratchasima City Municipality. If there is a possibility of a flood, the excess water will be diverted towards the Lamboriboon River, with some water diverted through the diversion canal to Bungphudsar Reservoir in CC10. Again, the gate opening height of all regulators downstream of CC3 will be re-calculated. The global image of the basin will then be re-looped. The optimized gate settings will finally be proposed to the local controllers within a few minutes of the completion of the computer simulation.



**Fig. 7.** Lamtakong and Lamboriboon Systems Cascade.

(a) Schematic of system cascade. (b) Profile of system cascade.

Fig. 8 illustrates the cascade concept where each reach's optimization is for adjusting the manipulated variable based on the MPC control to minimize the target's water level error.  $WLU_i$  is the water height at the upstream section,  $WLD_i$  is the water height at the downstream stretch,  $Q$  is the flow through each regulator,  $G_{oi}$  is the Gate opening for regulator  $i$ ,  $s_i$  is the slope of each cascade,  $CC_i$  is Cascade number  $i$  where  $i$  is from 1 to 14 and  $L_i$  is the length from reach  $CC_i$ . Since each reach of Lamtakong and Lamboriboon has different characteristics, it results in differences in target water level, as shown in Table 1.

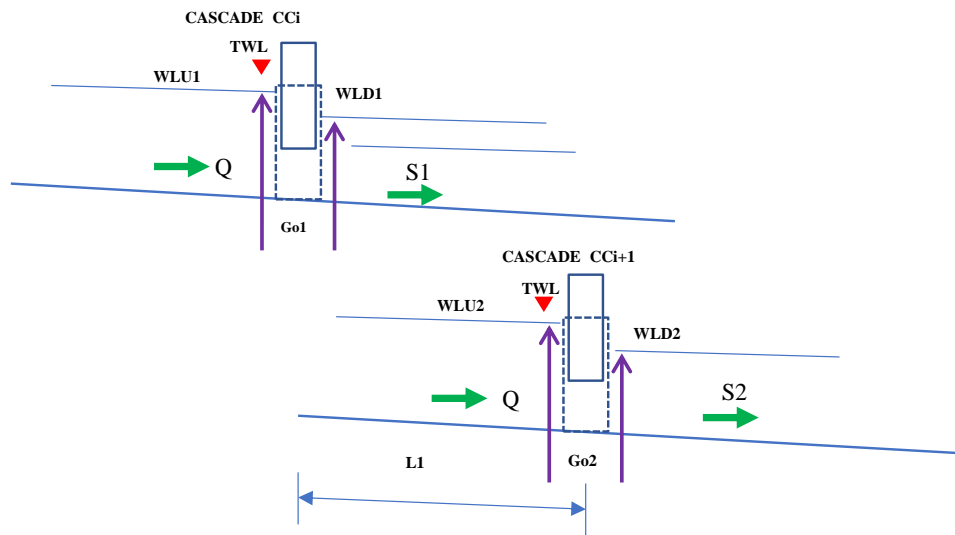


**Fig. 8.** Cascade Analysis Concepts.

**Table 1.**

**Physical Characteristics of Cascades of Lamtakong and Lamboriboon.**

Dimension	Lamtakong						
	CC1	CC2	CC3	CC4	CC5	CC6	CC7
Length of cascade (L,m.)	33,000	12,000	19,250	9,100	8,150	11,500	12,770
Target water level, TWL	219	209	194	188	183	175	167
gate width	4.5	4.5	6.0	4.5	4.5	3.5	2.5
gate height	1.8	1.8	3.3	3.0	5.2	4.0	4.0
n of gate	5	5	1	4	3	3	5
Gate coefficient	0.6	0.6	0.6	0.6	0.6	0.6	0.6
Bed slope (S)	0.00046	0.00030	0.00125	0.00031	0.00055	0.00098	0.00070
Manning n.	0.00032	0.00032	0.00032	0.00032	0.00032	0.00032	0.00032
Dimension	Lamboriboon						
	CC8	CC9	CC10	CC11	CC12	CC13	CC14
Length of cascade (L,m.)	19,250	1,870	1,890	8,600	3,750	6,380	11,520
Target water level, TWL	194	192	191	185	183	179	174
gate width	6.0	4.2	3.0	4.0	4.0	4.0	4.0
gate height	3.3	4.3	3.0	4.5	3.0	1.8	1.8
n of gate	5	2	2	3	3	3	3
Gate coefficient	0.6	0.6	0.6	0.6	0.6	0.6	0.6
Bed slope (S)	0.0008	0.00010	0.00053	0.00317	0.00023	0.00107	0.00078
Manning n.	0.00032	0.00032	0.00032	0.00032	0.00032	0.00032	0.00032

The collected geometry data of river system and topography data are imported into the geodatabase for use in HECRAS (see **Fig. 9**).

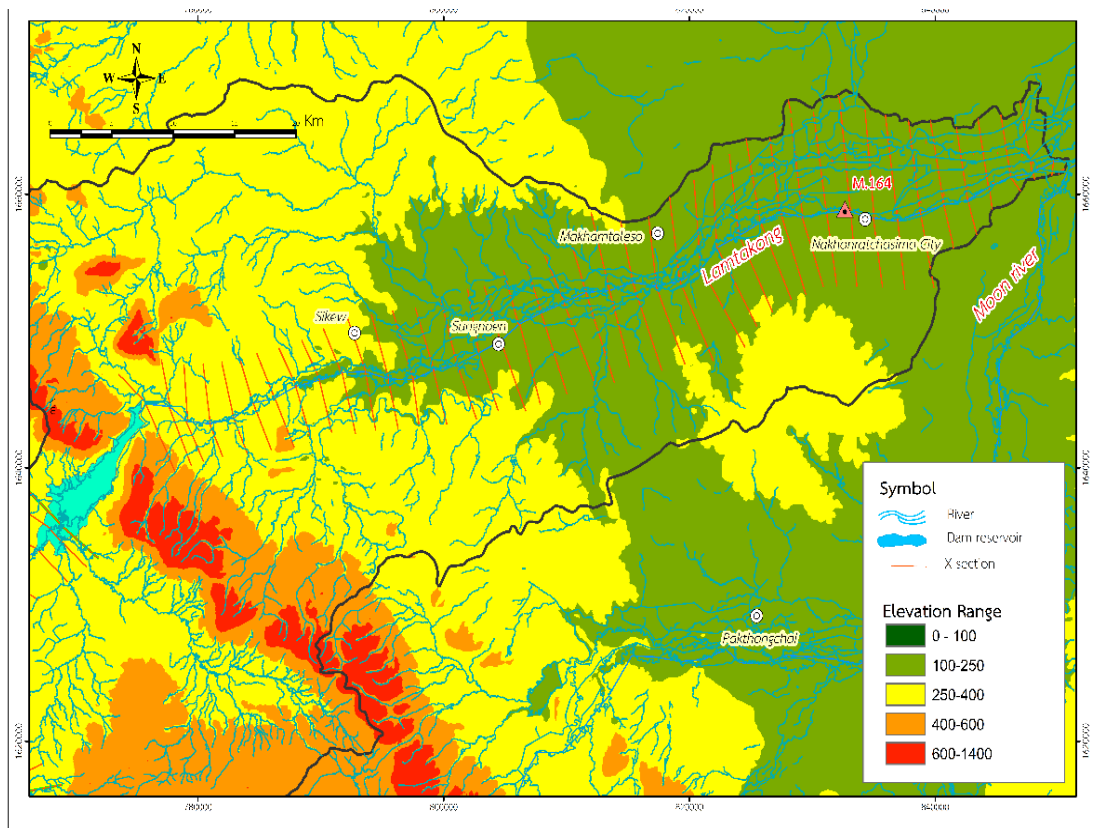


Fig. 9. Geometry data.

### 3.4.2. Cascade MPC development

#### (1) HECRAS and MPC links

This study attempts to manage flows both on local and global scales. For the single cascade calculation, the profile of the water level from the upstream cascade to the downstream cascade is calculated by HEC-RAS which is a widely used software application that can perform one and two-dimensional hydraulic calculations for a full network of Lamtakong Basin.

The combination HEC-RAS and cascade model established in this study will involve applying MATLAB scripts to write input files, reading output files, making plots, executing parallel computations, and performing fully-automated functions of HEC-RAS through a HEC-RAS CONTROLLER (Modelling and Leon 2018). Water level Upstream ( $H_u$ ) from HEC-RAS will be sent to MPC (Fig. 10).

The discharge of each cascade's sliding gate depends on the difference between the water heights of upstream  $H_u$  and downstream  $H_d$  around the hydraulic gates. Therefore, it can be calculated as equations (4) and (5):



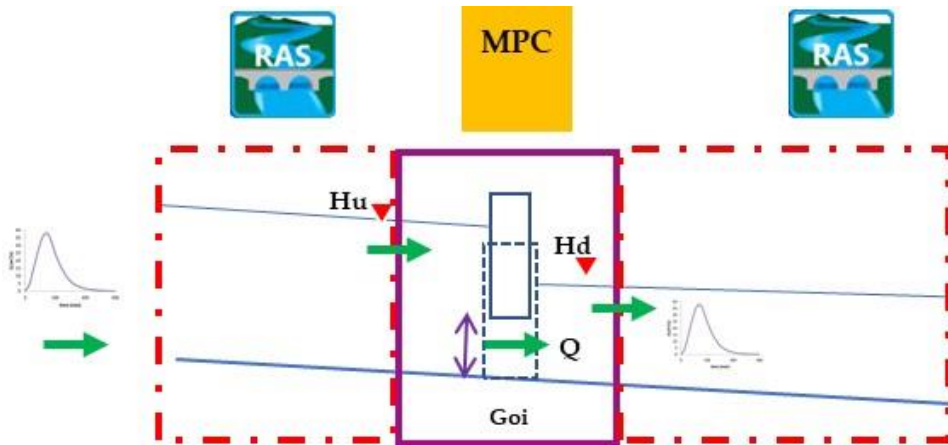


**Fig. 10.** Cascade Model link concept.

$$Q=C.Go.L\sqrt{2g(H_U-H_d)} \quad (4)$$

$$H_u=H_d+\frac{\left(\frac{Q}{C.G.L}\right)^2}{2g} \quad (5)$$

where:

$L$  is the width of the structure (m),  $H_u$  and  $H_d$  are the water levels upstream and downstream,  $C$  is the discharge coefficients (0.6-0.7), and  $Go$  is the gate's opening.

From equation (9), a prediction model calculates the upstream water level at the regulator in each cascade to use with the MPC in the next step. Equation (5) can be converted to a prediction model in MATLAB Simulink.

## (2) Cost Function for Optimization

The regulatory control for each regulator in the cascade expects an automatic adjustment of the controlled structures with reliability and durability. For instance, a gate is moved up and down to regulate the flow rate at the end of a reach close to the reference value (set-point). The control input  $u$ , i.e., the acceleration command, is calculated by solving the constrained optimization problem below during each sampling period; the cost function of each controller is as shown in equation (6):

$$\min_U J = \sum_{i=1}^N (TWL_i - CWL)^2 Wx_i + \sum_{i=1}^N \Delta u_i^2 Wu_i \quad (6)$$

where:

$CWL$  (Control Water Level) is the controlled variable over the prediction horizon  $p$ ,  $TWL$  (Target water level) is the target reference water level value,  $u$  is manipulated input (gate opening) over prediction horizon  $p$ , and  $Wx_i$  and  $Wu_i$  are the weighting matrices of appropriate dimensions.

### (3) MPC Parameter

MATLAB®, Simulink®, and Model Predictive Control Toolbox™ were used to simulate cascade networks. The optimization problem is solved by a QP solver, based on the KWIK algorithm, in the Model Predictive Control Toolbox. The "MPC Controller" block is used to model the controller and run the closed-loop simulation with the plant model in Simulink. C-code can be generated from the MPC block for the implementation to an embedded microprocessor. The simulation applied the cascade dimension from **Table 1** and the simulation parameters from **Table 2**.

Table 2.

Simulation Parameters.	
Parameter	Value
Prediction horizon (p)	60
Control horizon (Np)	2
Simulation time (T)	60 min.
Time step (T)	5min
Weight.MV	0
Weight.OV	1

#### 3.4.3. HECRAS Configuration

Cascade MPC examined flow profile in river with HECRAS model, calibrate model using the measured values of the M.164 station. The results are shown in **Fig.11**, with a confidence value of  $r^2$  of approximately 0.9928.

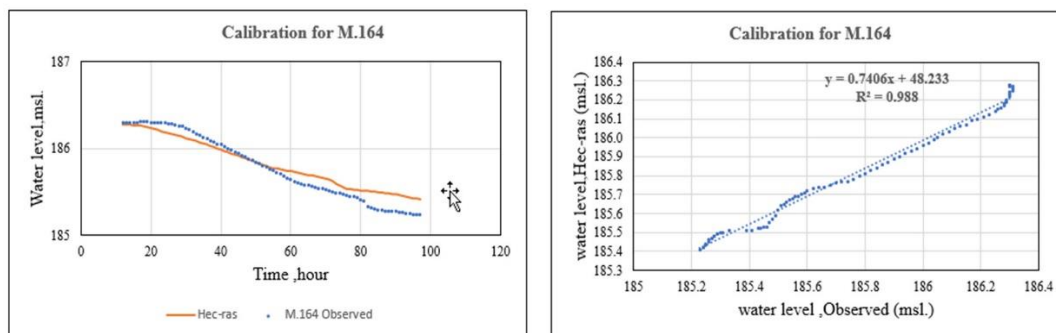


Fig. 11. Calibration for M.164 at Nakhorn Ratchasrima City.

## 4. RESULTS AND DISCUSSIONS

### 4.1. Cascade Network Test Run

According to the existing hydraulic structures in the Lamtakong River, the cascades were considerably divided into three groups, A, B, and C, which are the upper stream reaches before reaching the junction of the Lamboriboon River, the Lamboriboon River, and the Lamtakong River, respectively, from the boundary of Group A to the lower stream where the Lanboriboon converges back with the main Lamtakong, as shown in **Fig. 7**. The cascade test run was conducted using the October 2013 flood event where the maximum flow through the city was 25 cms. **Fig. 12** shows the examples of water levels along the C group cascade, which consist of CC3, CC4, CC5, CC6, and CC7, compared with the target water level of the reach. The proper gate opening of each regulator in the cascades from 19:00 October 23, 2013, to 13:00 October 24, 2013, is summarized in **Table 3**.

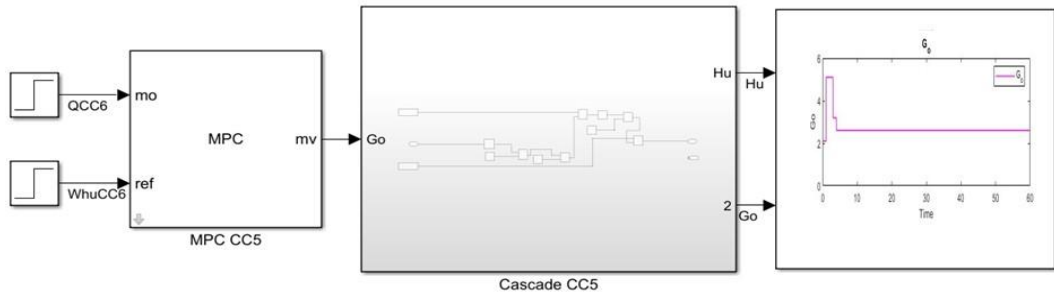


Fig. 12. Control diagram and recommend gate opening for CASCADE CC5.

Table 3.

**Proper Lifting Height of each Gate in the Cascade, Recommended by MPC.**

Cascade	Gate Lifting Height (M.)	Time	
		From	To
CC3	2.5 to 1.5	10/23/2013 19.00	10/23/2013 20.00
CC4	3.0 to 1.8	10/23/2013 21.30	10/23/2013 22.30
CC5	4.5 to 2.2	10/24/2013 00.30	10/24/2013 01.30
CC6	4.0 to 2.0	10/24/2013 4.00	10/24/2013 05.00
CC7	4.0 to 2.0	10/24/2013 12.00	10/24/2013 13.00

**4.2. Flood Management Comparison**

This study has applied the cascade MPC control to manage a flood by utilizing a stream's maximum capacity, using existing regulators in rivers. First, the target water level of each reach is designated under local constraints; then the best-case water level condition is calculated using looping procedures in spatial and global scales, in order of steps. Finally, the suggested water level for the flood period operation is further implemented and controlled by the gate opening set.

Fig 13 illustrates water levels at Nakhon Ratchasima city, both the actual situation and the circumstance under the pro-posed gate management strategy. The 0.5 m water level which was lower than the riverbank indicates the advantage of applying the cascade MPC during the peak flow period.

Fig. 14 illustrates the comparison of the GIS flood map in year 2013 and the flood map that was controlled by Cascade MPC. The figure shows that Cascade MPC can reduce the areas of a flood map in the city from 15,939 Rai to 5,944 Rai (more than 60%.)

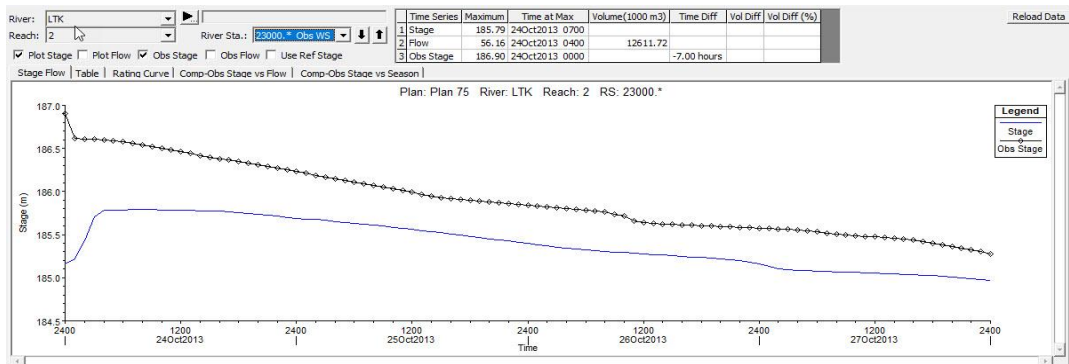
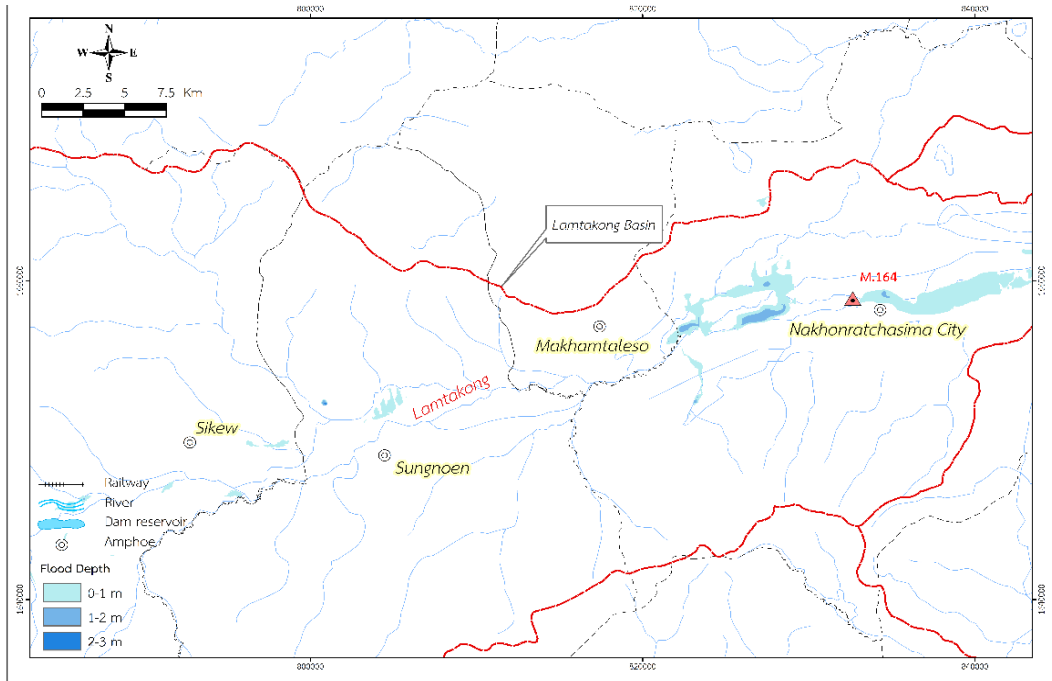
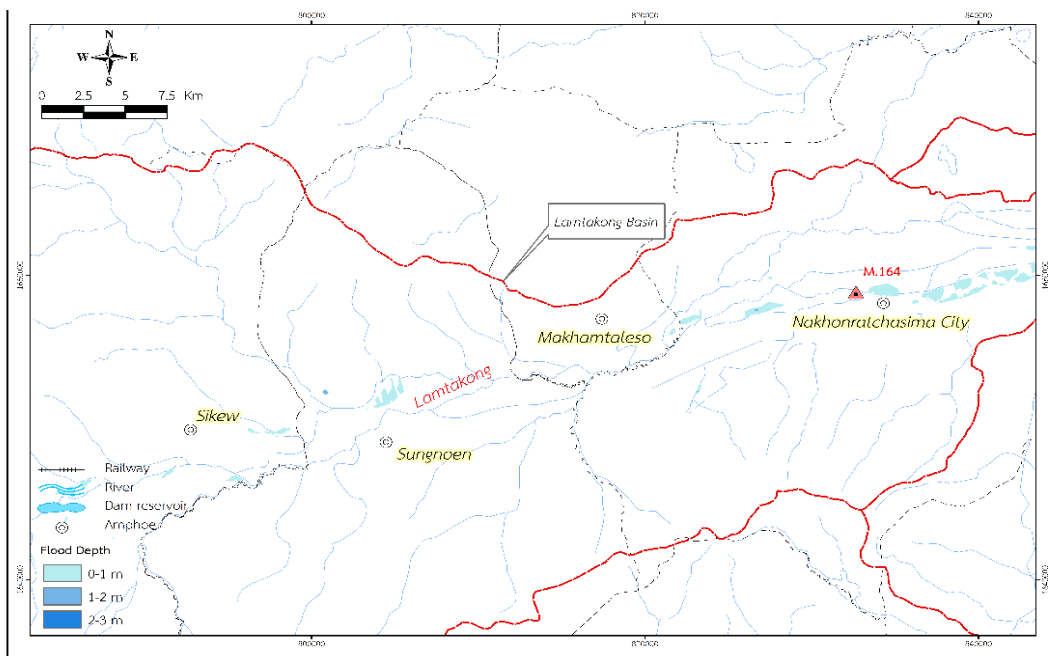


Fig. 13. Comparison of water level at Nakhon Ratchasima City between actual conditions and the result from Cascade MPC.



a) Existing condition in year 2013.



b) Flood management by Cascade MPC.

**Fig. 14.** Comparison of existing flood map in year 2013 and flood map by Cascade MPC.

## 5. CONCLUSIONS

The Lamtakong River in Nakorn Ratchasima Province is a large-scale river with several branches that flows through communities to eventually converge with the Mun River downstream. Generally, the water is conserved for irrigation purposes; thus, the local RID staff manually regulates the hydraulic structures based on their experience with water levels. However, during a flood period, the regulator's function is shifted to prevent and mitigate disaster along flood-affected communities and economic areas. Although any flood situation is reported from the upstream reaches to the command center from time to time, operating the movable gates in the river is a local decision that depends on operators' experiences. Regardless of the effects on the overall system performance or a future situation, it could cause an unpredictable impact on other areas.

This study proposes the concept of combining real-time flood management with the cascade Model Predictive Control, taking the most advantage of the pre-existing thirteen regulating structures and controlling the flow cascade to cascade. The 2013 flood event, where the maximum flow was 90 cum/s, is applied to the Lamtakong River and the Lamboriboon branch to verify the proposed concept. First, the flood situation is of primary concern, in which the condition of local flood management limits with its reach embankment elevation. Once the flow upstream enters the system, all gate setting heights are precalculated, and the water level at the monitoring station, M.164, is rechecked. The real-time gate opening data is updated. The gate opening height of all regulators downstream are recalculated and compared with the target water level. The global image of the basin will then be re-looped. The objective functions and constraints are changed. The model then goes through the optimization process using the trial gate opening step, Go, until it meets the minimum error point. Under the global flood prevention conditions, the optimized gate settings are finally proposed to the local controllers within a few minutes of computer analyses.

The comparison of the flood map between the historical flood in year 2013 and flood management with the cascade Model Predictive Control shows that the cascade MPC model can alleviate flooding in the city by almost 100%. Notably, there are still flood areas on both sides of Lamtakong in the paddy field areas, in an acceptable situation. In addition, comparing with the actual situation in 2013, according to the gates operating under the MPC recommendation, the water level at Nakhon Ratchasima City was 0.5 m lower than the riverbank and can alleviate the GIS flood area by more than 60 percent. This indicates the advantage of applying the proposed concept of combining real-time flood management with the cascade MPC during the peak flow period.

## REFERENCES

- Barjas Blanco, Toni, Patrick Willems, Bart De Moor, and Jean Berlamont. 2008. 41 IFAC Proceedings Volumes *Flooding Prevention of the Demer River Using Model Predictive Control*. IFAC. <http://dx.doi.org/10.3182/20080706-5-KR-1001.00613>.
- Breckpot, Maarten et al. 2013. "Flood Control of the Demer by Using Model Predictive Control." *Control Engineering Practice* 21(12): 1776–87. <http://dx.doi.org/10.1016/j.conengprac.2013.08.008>.
- Department(RID)Thailand., Royal Irrigation. 2020. "Hydrology Data." <http://hydro-4.rid.go.th/>.
- Evans, R. et al. 2011. "Real-Time Optimal Control of River Basin Networks." *IFAC Proceedings Volumes (IFAC-PapersOnline)* 44(1 PART 1): 11459–64.
- Falk, Anne Katrine Vinther, Craig MacKay, Henrik Madsen, and Peter Nygaard Godiksen. 2016. "Model Predictive Control of a Large-Scale River Network." *Procedia Engineering* 154: 80–87. <http://dx.doi.org/10.1016/j.proeng.2016.07.422>.

- Leon, Arturo S., Elizabeth A. Kanashiro, Rachele Valverde, and Venkataramana Sridhar. 2014. "Dynamic Framework for Intelligent Control of River Flooding: Case Study." *Journal of Water Resources Planning and Management* 140(2): 258–68.
- López Rodríguez, F., K. Horváth, J. García Martín, and J. M. Maestre. 2017. "Mobile Model Predictive Control for the Évora Irrigation Test Canal." *IFAC-PapersOnLine* 50(1): 6570–75.
- Modelling, Environmental, and Arturo Segundo Leon. 2018. "Controlling HEC-RAS Using MATLAB Controlling HEC-RAS Using MATLAB." (October 2016): 1–13.
- Nguyen, Le Duy Lai, Ionela Prodan, Laurent Lefevre, and Denis Genon-Catalot. 2017. "Distributed Model Predictive Control of Irrigation Systems Using Cooperative Controllers." *IFAC-PapersOnLine* 50(1): 6564–69. <https://doi.org/10.1016/j.ifacol.2017.08.612>.
- Song, Mengjie, Ning Mao, Haoran Zhang, and Cheng Fan. 2020. Advanced Analytic and Control Techniques for Thermal Systems with Heat Exchangers *Model Predictive Control Applied toward the Building Indoor Climate*. Elsevier Inc. <http://dx.doi.org/10.1016/B978-0-12-819422-5.00021-9>.
- Tian, Xin et al. 2017. "Efficient Multi-Scenario Model Predictive Control for Water Resources Management with Ensemble Streamflow Forecasts." *Advances in Water Resources* 109: 58–68.
- USACE - Environmental Laboratory. 1987. "Wetlands Delineation Manual -Final Report." 1(January): 143. [http://www.lrh.usace.army.mil/Portals/38/docs/USACE 87 Wetland Delineation Manual.pdf](http://www.lrh.usace.army.mil/Portals/38/docs/USACE%2087%20Wetland%20Delineation%20Manual.pdf).
- Vermuyten, Evert. 2018. "Real-Time Flood Control by Means of Model Predictive Control and a Reduced Genetic Algorithm." (July).
- Wahlin, Brian, and Darell Zimbelman. 2018. "Canal Automation for Irrigation Systems: American Society of Civil Engineers Manual of Practice Number 131." *Irrigation and Drainage* 67(1): 22–28.
- Wang, Y. et al. 2017. "Optimal Management of Barcelona Water Distribution Network Using Non-Linear Model Predictive Control." *IFAC-PapersOnLine* 50(1): 5380–85. <https://doi.org/10.1016/j.ifacol.2017.08.1070>.



## APPLICABILITY OF TOOLS FOR BROWNFIELD REGENERATION IN THE CZECH REPUBLIC: A REGIONAL PERSPECTIVE

Jaroslav ŠKRABAL<sup>1</sup> , Petra CHMIELOVÁ<sup>1</sup> , Kamila TUREČKOVÁ<sup>1</sup> , Jan NEVIMA<sup>1</sup> 

DOI: 10.21163/GT\_2021.162.11

### ABSTRACT:

In the current period marked by the need to address a number of economic and social challenges in the context of the sustainable development of towns and municipalities, the issue of the regeneration and reuse of brownfields is a topic that can help find an effective solution on the local, national and international level. The aim of this article is to assess the use of tools in the process of the regeneration of brownfields on the territory of municipalities with extended competence in the Czech Republic. The information contained in this paper was compiled on the basis of a primary survey. It was found that the highest number of abandoned buildings and premises are located in regions which were focused on industrial and mining activities in the past. Furthermore, the authors found that brownfield sites have been regenerated and reused successfully in the territory of the Czech Republic. Based on the relevant survey, the most frequently used financial tools employed by municipalities with extended competence (MEC) for the regeneration of brownfield sites in the last 10 years included municipality budgets, European subsidy programmes and national subsidy programmes. According to the survey, non-financial tools used for the successful regeneration of brownfields included own activities and support from the CzechInvest agency. The motives of municipalities and towns located in the territory of individual MECs in the relevant country included mainly a new use of buildings (the rescue of historical buildings/premises and unused industrial parts of a village/town) in the territory of the MEC. The results of the article also highlights the regional differences of the studied area in the case of the existence and use of various financial and non-financial instruments in the process of brownfield regeneration in individual MECs in the Czech Republic.

**Key-words:** *municipality with extended powers, tools, brownfields, regeneration, spatial analysis, Czech Republic*

## 1. INTRODUCTION

Re-using and regenerating derelict and abandoned areas constitutes an important element in sustainable land use policy and planning (Klusacek, et al. 2021). According to Tureckova et al. (2018), soil degradation is one of the most important environmental challenges facing our society in recent times. In Eastern and Central Europe, these changes are significantly modified by the processes of privatisation and the profound changes in grant policies (Krejci et al., 2019). Abandoned buildings and sites are an integral part of cities in Central Europe (Tureckova et al., 2017). Brownfields that are in the inner city, near the inner city or near other municipal subcentres are generally well-connected with the current technical and social infrastructures (Koch et al. 2018. Skrabal, 2020). The proximity to an upper-level regional center is of crucial importance for decisions with respect to how (and if) brownfields will be reused (Navratil et al., 2019). Brownfield prioritization tools help identify the most useful investments in the possibility of regenerating abandoned buildings and sites for efficient land recycling. Some of the benefits they can bring include economic, environmental, but also social ones, for example reducing crime. The prioritization tools developed so far are targeted at decision-makers (urban planners, regional development agencies, national and regional authorities, grant agencies, etc.) who are responsible for broad territories (cities, regions or states) (Chrysochou et al., 2012, Pizzol et al., 2016). In the past, several tools were developed to help support brownfield regeneration. The most important tools that have been developed will be listed here. Pizzol and

---

<sup>1</sup> School of Business Administration in Karvina, Silesian University in Opava, 733 40 Karviná, Czech Republic, skrabal@opf.slu.cz; chmielova@opf.slu.cz; tureckova@opf.slu.cz; nevima@opf.slu.cz.

colleagues developed two decision-support systems called SYRIADE (Pizzol et al., 2011, Zabeo et al., 2011, Agostini et al., 2012) and the Timbre Brownfield Prioritization Tool (TBPT) (Pizzol et al., 2016, Bartke et al., 2016, Frantal et al., 2015, Alexandrescu et al., 2017). SYRIADE has been developed to support regional authorities in the ranking of potentially contaminated sites and brownfields for the priority of investigation, when information on site-specific investigation and risk is not available. SYRIADE considers environmental impacts, economic aspects, and shareholders' perspectives (Limasset et al., 2018). Another tool to strengthen brownfield regeneration which has been developed is the Timbre (Tailored Improvement of Brownfield Regeneration in Europe) Brownfield Prioritization Tool (TBPT), developed as a web-based solution to assist stakeholders with identifying which brownfield sites should preferably be considered for redevelopment or further investigation, taking into account a set of success factors properly identified through a systematic stakeholder engagement procedure (Pizzol et al., 2016). Among the factors that determine the successful regeneration of brownfields (so-called success factors) in different geographical and political contexts (i.e. in different European countries) is key to supporting investors and decision-makers in reducing uncertainties and thus increasing the likelihood of success of the regeneration process (Meyer and Lyons, 2000, Thornton et al., 2007, Frantal et al., 2013).

Within the TBPT, these success factors are integrated by means of a Multi Criteria Decision Analysis (MCDA) methodology which includes stakeholders' requalification objectives and perspectives related to the brownfield regeneration process and takes into account the three pillars of sustainability (i.e., economic, social and environmental dimensions). The tool will help to allocate available and limited resources, time and energy to those areas that are assessed as being the most critical, urgent or profitable to be regenerated. The targeted users of the tool are represented by state, regional and local authorities and other representatives of public administration, urban planners, regional development agencies, grant agencies, site owners (individuals or consortia of owners), investors, developers, consultants, and researchers. The Timbre Brownfield Prioritization Tool (TBPT) has been developed to assist stakeholders in ranking brownfield sites according to their redevelopment potential (Pizzol et al., 2016).

The development of the Timbre Brownfield Prioritization Tool took place between June 2011 and May 2014 as part of the EU-funded Timbre project. The TBPT was developed within the "prioritization" work package, headed by one member of the Timbre consortium (the Institute of Geonics, Czech Republic). Seven other partners, including two research institutes, two universities, one national environmental authority, one small enterprise and one brownfield portfolio holder were formally involved in this work package. This means that they took part in formal and informal meetings to discuss what worked (and what did not) in two respects: (1) developing the tool, that is, obtaining a final output to show to the project's funders and (2) tailoring the tool to its would-be users. These two goals overlapped but pursuing them both proved challenging while constructing the network (Alexandrescu et al., 2017).

Subsequently, we can mention another project to support the regeneration of brownfields such as the project RESCUE (Regeneration of European Sites in Cities and Urban Environments) studied several revitalization methods practised to encourage the sustainable use of brownfields and identified best practices for taking local sustainability into account in future revitalization projects (Bartke and Schwarze, 2015). There are many other tools that have been developed and contributed to enhancing brownfield regeneration. Within the general instruments, which will be analysed in this article, it is mainly the use of financial instruments in the form of grant programs, various budget support, etc. For non-financial instruments, support forms of various agencies such as the CzechInvest agency or other forms of support in the form of communication of other agencies and, last but not least, own activities in the process of brownfield regeneration are taken into account.

The aim of this article is to assess the use of tools in the process of the regeneration of brownfields on the territory of municipalities with extended competence in the Czech Republic. The article is designed as follows, where the Introduction is followed by a second chapter focused on the data and methodology of the paper. The third chapter contains the results based on the stated aim of the paper. This chapter is divided into individual subsections, which present individual results based on

geographical aspects. The next chapter (Chapter 4) pays attention to the discussion. At the end, a Conclusion is drafted, which summarizes the essential results that the authors of the paper have reached.

## **2. DATA AND METHODOLOGY**

The given issue of the studied area mainly concerns the situation regarding brownfields in the regions of municipalities with extended powers (hereinafter referred to as "MECs") in the territory of the Czech Republic. The existence of abandoned buildings and areas is very evident in the Czech Republic, especially in various regions, such as structurally disadvantaged regions. The reason for the existence of these buildings and areas is mainly the transformation of the economy after 1989. Another reason for the occurrence of brownfields is the return of property to the original owners after 1989 and last but not least, the situation is affected by growing competition within the market economy in individual regions, with both capital and human resources moving to stronger regions with large agglomerations. There are many factors that are behind the emergence of abandoned buildings and areas. It is clear, however, that the occurrence of brownfields is more than obvious in a given republic. Among the ways to eliminate the occurrence of abandoned buildings and areas is to find and use individual tools that can help solve the problem, especially finding a new use for existing brownfields. The regeneration and reuse of abandoned buildings and areas is important especially for the development of individual regions. Based on these circumstances, the authors of the paper decided to address this issue, especially the usability of tools (financial/non-financial) in the process of the regeneration of brownfields in the MECs in the Czech Republic.

There are 205 municipalities with extended powers (MEC) in the territory of the given state. These are so-called municipalities of the 3rd degree and are an intermediate element of the transferred competence of self-government between regional authorities and other authorities (below that are authorized municipal authorities and the lowest is all other municipal authorities). Compared to other municipal authorities, municipal authorities of municipalities with extended powers thus have some additional areas of competence, not only for their own, basic administrative district, but usually also for other municipalities in the vicinity.

Based on the studied area and the selection of MEC regions within this area of the topic, the authors of the paper chose the method of questioning for their primary research. In terms of the choice of contacting the addressees, the method of questioning was chosen for Internet (electronic) questioning. It is a quick form of data collection and then examining and comparing the individual results between regions in the case of a given contribution between MEC regions.

As mentioned above, the authors of this paper focus mainly on the usability of tools (financial/non-financial) in the process of the regeneration of brownfields in the MEC in the Czech Republic. During the creation of the research, a questionnaire (electronic questionnaire) was created, which contained a total of 11 questions. Based on the creation of individual questions, the authors of the paper focused primarily on the situation regarding the existence of brownfields in the MECs. Furthermore, the questions focused on successfully regenerated abandoned buildings and areas in the regions. The third part of the questionnaire survey was focused on the use of financial and non-financial instruments in the process of brownfield regeneration. The last part of the research paid attention to the reasons that forced the MEC regions to regenerate abandoned buildings and grounds. The questions in the given research were closed, where the respondents had to choose the individual options offered and open, where the participants of the given research had the opportunity to comment on the given question without restriction.

The questions of the given research were processed and discussed between the individual authors of the paper on the basis of the detailed study area. In addition, the research questions were created in the electronic tool Google Forms, which helps to create, submit and process various research items. After the creation of the questionnaire survey, a cover letter was created, which contained basic information about the research. An essential part of the original letter was a link that directed the respondents to the research. The cover letter was then sent electronically to all MECs via data boxes.

Data boxes in the Czech Republic are a state-guaranteed electronic communication tool that replaces paper letters. It serves mainly for communication with public authorities.

Individual MECs or, as mentioned above, the so-called municipalities of the 3rd degree are mostly cities and their municipal authorities are therefore mostly municipal authorities. A cover letter referring to the research was sent to the authorities concerned. The given MECs then form smaller regions, which are shown in the figure below (**Fig. 1**). The description of individual MECs in a given figure is the designation of individual cities with municipal authorities under which the MEC regions fall.



**Fig. 1.** Geographical representation of MECs within the territory of the Czech Republic.  
(Source: CSO, 2021).

The primary research based on the chosen method of questioning, when the electronic questionnaire was created, took place from 11 January and the end of data collection was 16 May 2021. The authors of the research addressed the given respondents or the given MEC only once in one wave. It was stated above that 205 MECs of the research return were addressed at a relative frequency of 47.3%, with 97 MECs participating in the research in absolute terms. **Fig. 2** shows the designation of the MECs that participated in the research. It can be said that all regions at the NUTS 3 level, to which individual MECs belong, are thus represented. For better clarity, how many MECs participated in the research in each NUTS 3 region is shown in the table below (**Table 1**).

**Table 1.**

**Regional comparison of return on primary research.**

NUTS 3	Number of MECs [number]	Number of answers in absolute terms [number]	The total return in relative terms [%]
Central Bohemian Region	26	14	53.9
South Bohemian Region	17	10	58.8
Plzeň Region	15	10	66.7
Karlovy Vary Region	7	2	28.6
Ústí nad Labem Region	16	5	31.3
Liberec Region	10	1	10.0
Hradec Králové Region	15	7	46.7
Pardubice Region	15	6	40.0
Vysočina Region	15	6	40.0
South Moravian Region	21	10	47.6
Olomouc Region	13	5	38.5
Zlín Region	13	7	53.9
Moravian – Silesian Region	22	14	63.6
<b>Total</b>	<b>205</b>	<b>97</b>	<b>47.3</b>

Source: based on own survey, 2021.



**Fig. 2.** Highlighted MECs that participated in the research.  
(Source: based on own survey, 2021).

MECs are categorised in individual regions of the Czech Republic (NUTS 3), as can be seen in the figure. The authors then focused on the response rate of the survey at the regional level of NUTS 3. The information about the response rate in individual regions of NUTS 3 is recorded in the table below (**Table 1**). The table shows the name of NUTS 3 regions with the number of MECs in the relevant regions. The third column focuses on the absolute expression of the response rate of the addressed MECs. The last column of the table pays attention to the relative response rate of addressed respondents (MECs).

On the basis of the findings, it can be said that the overall response rate of the primary survey was 47.3%. Within the regional comparison, we can see in the table above that the highest response rate was in the Plzeň Region and the lowest response rate was in the Liberec Region in relation to the number of MEC regions in individual NUTS 3 regions in the Czech Republic.

Based on the research, the results of the questionnaire survey were examined in more depth on the basis of an overall comparison and subsequently according to individual geographical conditions. Among the geographical conditions, MECs within the border area were examined. This is an area located along or closer to state borders. Border regions often suffer from the historical consequences of their peripheral location, a lack of integration into predominant structures and the resulting isolation. The number of MECs located in the border area is 61 in absolute terms. 28 MECs located in a given geographical area participated in the survey in absolute terms. If we look at the relative frequency of respondents who participated in the research in the case of the border, then the value reaches 45.9%. **Fig. 3**, which is shown below, shows the regions that occur at the border.

Data on MEC regions in the border area were further examined by the authors from a geographical point of view of the northern and southern part within the country. The regions in the north are characterized by industrial activity and the southern part of the border is considered mainly as regions that are not so burdened by industrial activity. In the northern part of the country, there are three structurally affected regions, where the most abandoned buildings and areas within the country occur. The regions that can be classified as structured regions include: Karlovy Vary, Ústí nad Labem and Moravian-Silesian regions. For this consequence, the given comparisons between the northern and southern regions of the MEC were also documented. There were 14 MEC regions in both the northern and southern parts. The given distribution of regions is shown in the figure below (**Fig. 4**).



**Fig. 3.** MEC regions in the border area following participation in research.  
(Source: based on own survey, 2021).



**Fig. 4.** Northern and southern regions of MECs on the border following the participation in research.  
(Source: based on own survey, 2021).

Other comparisons of MEC regions on the basis of research were compared on the periphery. These are regions that are located in the interior of the country or on the border. For these regions, it was found that 17 MEC regions participated in the survey. The given regions are highlighted in the figure below (Fig. 5).





**Fig. 5.** MEC regions occurring in peripheral areas following primary research.  
 (Source: based on own survey, 2021).

The last regions examined are the regions that are located in the middle position (inner position of the grouped regions). These are regions that do not occur on the border or in the periphery of geographical areas. Furthermore, there are larger agglomerations in these regions, with a higher density of both inhabitants, etc. Based on the research, it was found that the research was attended in absolute terms by 52 MEC regions, which are, as mentioned above, concentrated in the internal position of the geographical group. **Fig. 6** shows the regions (MECs) that participated in the research in highlighted colour.

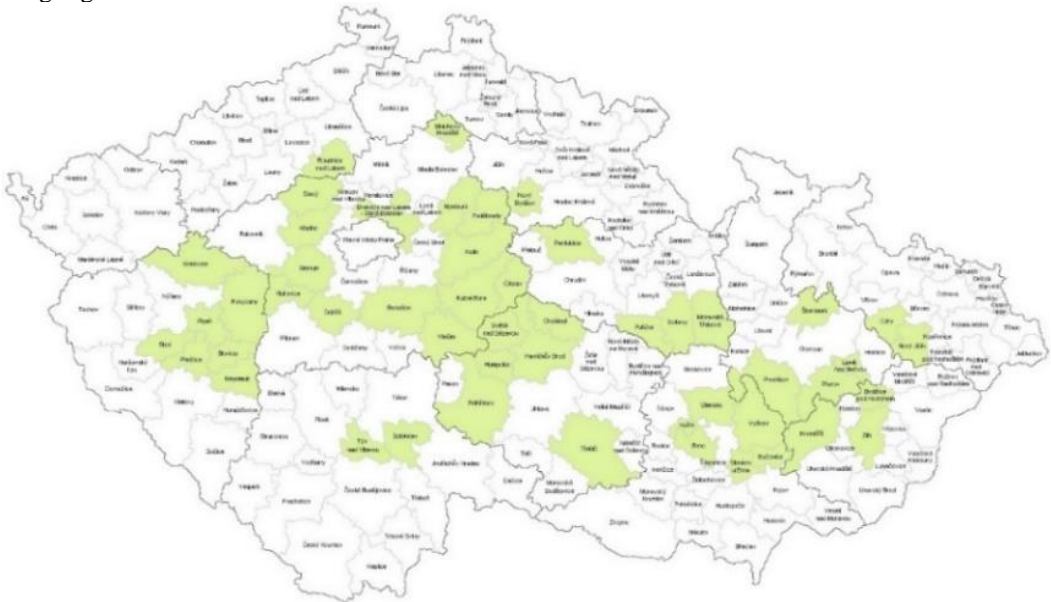


**Fig. 6.** MEC regions in an internal position following participation in the primary research.  
 (Source: based on own survey, 2021).

### 3. RESULTS

The third chapter is designed to interpret the results that the authors of the article arrived at on the basis of the selected primary research (questionnaire survey) and the method of selecting the method of comparing the results between the various regions of the MEC. When interpreting the results, the most significant results from the questionnaire survey based on all MEC regions will be presented first. The next part of this chapter will be used to compare individual MECs according to the information given in the previous chapter.

#### 3.1. Results of the Questionnaire Survey in Relation to all MEC Regions

The mentioned subchapter will focus on the results of the questionnaire survey within all MECs. As mentioned above, 97 respondents (MEC) participated in the absolute frequency and the relative expression was 47.3%. The most important results of the questionnaire survey will now be presented.

It was stated above that the first part of the primary research focused on the existence of brownfields from the perspective of MEC. The addressed respondents were asked to choose if there are any abandoned buildings or premises, so-called brownfield sites, in their territory (MEC). On the basis of the primary survey results, it can be said that, in relative terms, 85.6% (83 responses) of the addressed respondents chose "Yes", and the remaining 14.4% (14 responses) stated there were no brownfields in their territory.

Then, in the structured questionnaire survey, the authors asked whether any brownfields had been regenerated successfully in their territory (MEC) in the last 10 years. In relative terms, the authors of the primary survey recorded 61.9% (60 responses) of "Yes" answers, where the respondents answered that brownfield sites had been regenerated successfully on their territory in the last 10 years. The "No" option was selected by 37.1% (36 responses) of the survey respondents. One respondent did not comment on the question, while in relative frequency it was 1.0%.

The next question paid attention to whether the addressed MEC participated actively in the regeneration. Here, the addressed respondents could choose from two options, the first one being "Yes" and the other option was "No, the regeneration of brownfields was arranged by the private sector". In total, the question was answered by 88.7% of respondents (86 responses), where 37.1% (36 answers) selected the option that their MEC actively participated in the regeneration of brownfields. The remaining 51.6% (50 answers) of the addressed respondents stated that the regeneration of abandoned building or premises was arranged by the private sector. The last group consisted of respondents who did not participate in the survey, i.e. in the relative frequency of 11.3% (11 responses).

The essence of the whole survey is constituted by the following two questions, which focused on the use of financial and non-financial tools in the process of the regeneration of brownfields in the last 10 years in the territory of the MEC. First of all, the results focusing on financial tools will be commented on, where the relevant question was answered by 79.4% of respondents (77 responses); the remaining 20.6% (20 responses) of the addressed representatives of the MECs did not respond to the question. It is important to note that the respondents could choose from multiple options. The respondents who answered the question most frequently responded that no financial tools had been used. The second most frequent response was municipality budgets and then European subsidy programmes. The results are shown in the figure below (**Fig. 7**). The applicability of European subsidy programmes in the case of the regeneration of brownfields in the territory of the Czech Republic was studied by Tvrdon and Chmielova (2020), who proved that there is a certain time delay in the regeneration of abandoned buildings and premises in the Czech Republic compared to Western European countries. Other results of the study indicate that there are considerable differences between NUTS 3 and NUTS 2 regions within the country in the case of the number of existing brownfields, as well as their possible regeneration and reuse.

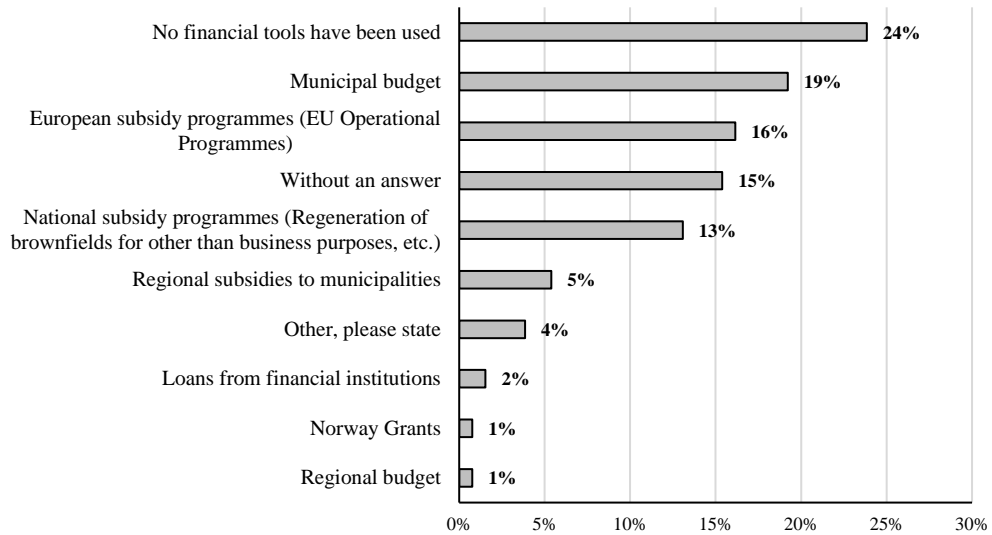


**Fig. 7.** Use of financial instruments in the process of brownfield regeneration in the last 10 years. (Source: based on own survey, 2021).

The following question asked the addressed respondents to choose non-financial tools used in the last 10 years in the brownfield regeneration process. As stated above, the addressed respondents of the MECs could choose from multiple options. The question was answered by 82.5% of the addressed respondents (80 answers); the remaining 17.5% of the interviewed MEC representatives did not respond to the question. The figure below (Fig. 8) shows the responses to the question. From the given research it was found that the MECs most often stated that they use their own activities, with a relative frequency of 23%. It was further stated that no financial instrument was used. Last but not least, the non-financial tools used by the MECs to regenerate brownfields on the basis of research included the placement of information on brownfields in the state/regional database of brownfields and the subsequent support of the CzechInvest agency. The agency manages and coordinates the activities connected, among other things, with the administration of the database of brownfields at the state and regional level (NUTS 3), where it has its regional branches.

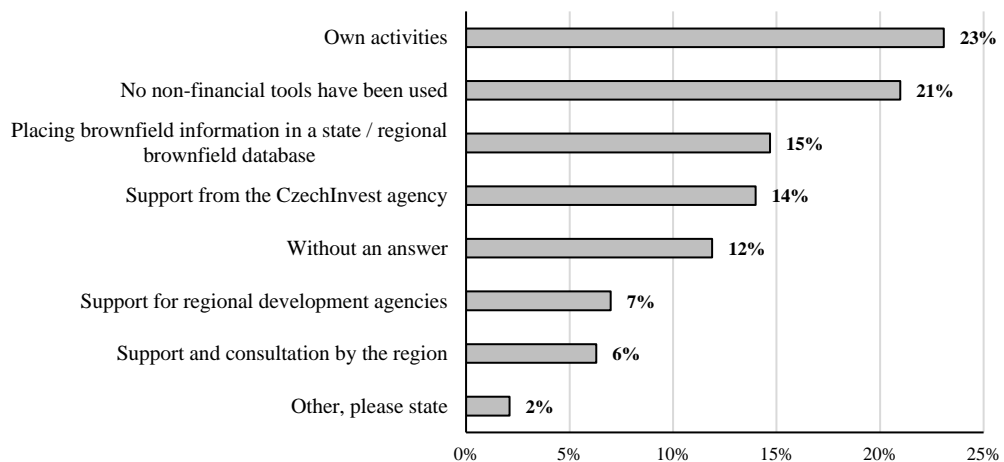


**Fig. 8.** Use of non-financial instruments in the process of brownfield regeneration in the last 10 years. (Source: based on own survey, 2021).

The next question asked the addressed respondents to state the tool (financial/non-financial) that helped them most and/or which they consider to be most efficient/most suitable. Within this question, the respondents did not choose from options, but were asked to write their answer down. This question was answered by 49.48% of the respondents; the most frequent tools they stated included subsidy programmes (EU funds, national financial means intended for the regeneration of brownfields), the active cooperation of interested parties (owners, investors, agencies) and consultations with the CzechInvest agency on possible ways of obtaining funds and other supporting information. Within this question, 50.52% respondents (49 responses) did not answer.

The last question of the survey focused primarily on the identification of reasons that had made the MEC representative regenerate brownfield sites on their territory. The character of the question was intended to make the respondents write down a text answer, not to choose from options. The question was answered by 58.76% of respondents (57 responses); the most frequent reasons predominantly included: the new use of a building (premises), rescue of a historical building/premises, the non-used industrial part of a municipality/town in the territory of the MEC, and the problematic situation with the structural stability of a building in the relevant cadastral territory.

### **3. 2. Results of MEC Regions Occurring in Border Areas**

The next subchapter will focus on the results of a questionnaire survey within the MEC regions located at the border. Part of this subchapter will be the publication of the results of the MEC regions that participated in the research located on the border within the northern and southern part of the country. The number of respondents from the border area that participated in the questionnaire survey in absolute terms was 28, where in relative frequency it is 28.9% of all MECs that participated in the primary survey. Based on the results below, which will be based on the border regions, the number of MEC regions in absolute terms will be 28 registered in both parts of 14 MEC regions.

The first part of the questions, as mentioned above, focused on the existence of brownfields in the given MEC regions. Based on the results of the research, it was found that the existence of brownfields in the borderland in relative frequency is evident in 78.6% of MECs. The stated value is obtained on the basis of data where MEC regions from the border area stated that abandoned buildings and areas occur in their regions. In the northern part of the country, in the case of the MEC regions, it was found that the occurrence of abandoned buildings and areas in this area is higher than in the southern part. From the results, which compared the northern and southern regions on the basis of the border, the authors found that the occurrence of brownfields is evident in absolute frequency in 12 MEC regions in the northern border and in 10 MEC regions in the southern border.

Another question that will be examined in this paper on the basis of border data is whether the regeneration of brownfields in the given regions has taken place in the last 10 years. Based on the results obtained from the primary research, it can be said that 68% of respondents in relative frequency stated that brownfields were regenerated in the given regions. In absolute frequency, there are 19 MEC regions out of 28 (the number of MEC regions that participated in the research). In the case of a comparison between MEC regions in the northern and southern parts of the border, the research showed that in the northern regions, 9 MEC regions answered in absolute frequency, that they had regenerated brownfields in the last 12 years and, in absolute terms, 7 MEC regions have chosen this option. The remaining regions either stated that there was no regeneration of abandoned buildings and areas in the given MECs or did not comment on the issue.

Another question was whether the specific MEC was actively involved in the regeneration of brownfields. The results of the research within the border regions of the MEC showed the possibility "Yes" was stated by 13 regions of the MEC (in relative frequency 46%). The remaining regions mentioned the option "No, the regeneration of brownfields was provided by the private sector itself" in the case of absolute frequency, there are 12 regions (43%) and the remaining three MEC regions did not comment on the issue (11%). In the northern part of the regions, 9 MEC regions stated in absolute terms that they were actively involved in regeneration. In the regions in the southern part of

the border, 4 MEC regions expressed their opinion in absolute terms (29%). The remaining regions stated that they did not take an active part in the regeneration or did not answer the question.

An important question of the research was the indication of which financial and non-financial instrument has helped residents the most (MEC) in the case of brownfield regeneration in the last 10 years. As mentioned above in the comparison of all MEC regions for these questions, respondents (MEC) had the opportunity to choose more options. For financial instruments at the border, within the relative frequency of 24%, municipal budgets and subsequently European subsidy programs dominated (20%) and the possibility where the respondents stated that no financial instruments were used. The fourth option that the respondents chose were national subsidy programs, where in relative frequency it is 17% of responses from the research. Other options will not be commented on here due to the small relative values. If we look at the comparison of the results between the northern regions of the MEC and the southern ones, the results are approximately identical in both cases. The given regions are dominated by financial resources from national and European funds for the regeneration of brownfields. Furthermore, the authors of the paper were interested in what non-financial instruments they have used in the last 10 years in the process of brownfield regeneration. In the given regions, the option "Own activities" dominated, while in relative frequency it is 22%. Other options were the same, at 16%, where it was the support of the CzechInvest agency, the support of regional and development agencies and the placement of information on brownfields in the state/regional database of brownfields. A necessary research issue was the reason that led the MEC regions to regenerate brownfields. At the border, it is mainly a question of answering the question, especially the new use of buildings and premises and the removal of unsightly buildings, which can pose a threat to the health of the population. As mentioned above, this was a textual answer to the question.

### **3. 3. Results of MEC Regions Occurring in Peripheral Areas**

The next part of the mentioned chapter will focus on the interpretation of results within the MEC regions located in the periphery. The number of MEC regions that participated in the given border research was 17 MEC regions within the relative frequency. This is a relative value of 17.5% of all returned questionnaires.

In the case of the analysis of the questions, it was found that 15 regions of the MEC in absolute terms stated that there are abandoned buildings or areas in its territory. Furthermore, in the case of another question, it was found that in the regions that occur on the periphery, there were 12 regions in absolute terms, where the regeneration of brownfields has taken place in the last 10 years. An essential part of the survey was the question of whether the MEC specifically participated actively in the regeneration of brownfields. Here, it was found that in 8 cases of MEC regions, the respondents answered that they were actively involved in the given regeneration. The "No" option was chosen in absolute terms by 6 respondents and the three survey participants did not comment on the question. In the case of financial instruments in the given regions, most research participants addressed stated that they had used national funds for the regeneration of brownfields in the last 10 years, with a relative frequency of 30%. Furthermore, the same 15% of respondents chose options such as the use of European funds for the regeneration of brownfields and subsequently that the funds were not used for the regeneration of abandoned buildings and areas. Other options will not be commented on here due to the small relative values of the given options. In the case of non-financial instruments, the consultations and support of the CzechInvest agency dominated in the given regions. In relative frequency it is 25% and subsequently the option "Own activities" was on the same relative values. The third option mentioned by the respondents was to place the information in the state/regional brownfields database. This response option had a relative frequency of 22% in the study. Another question was directed to the respondents to indicate which tool helped the most in the case of the regeneration of an abandoned building or area. From the given analysed answers, it was found that most respondents wrote that it was funds in the form of subsidies. The last question of the research focused on the situation, which was to state the reasons that the respondents or MEC caused the

regeneration of brownfields. Of the MEC regions located on the periphery, the most frequent answer was that it was a new use of buildings, premises and the removal of unsightly buildings.

### 3. 4. Results of MEC Regions Occurring in the Middle Position Areas

The last area analysed will be the regions that occur in the internal position. It was found that these are 52 MEC regions, which are located in this part of the geographical area. If we look at the relative frequency in the case of participation of MEC regions in research, which are located in the above-mentioned area, it is 53.6%. The issues in the given MEC regions will now be analysed.

The number of respondents who stated that brownfields occur in their territory (MEC) was answered in absolute frequency by 46 respondents. In relative frequency, this is 88.5% of the surveyed participants based on answers solely from regions that are in an internal position. The remaining regions replied that there were no abandoned buildings or areas in its territory. Another question was focused on whether the MEC territory had successfully regenerated brownfields in the last 10 years. Here, 29 out of 52 respondents expressed an absolute frequency that there was a successful regeneration in its territory. In relative frequency, this is 71%. The remaining regions, or 23 MEC regions, replied that brownfields had not been regenerated in its territory. Following the question, the authors of the paper further addressed whether the MEC was actively involved in brownfield regeneration. It was found that only 15 MEC regions answered 'Yes' while the other 32 regions replied that regeneration was carried out by the private sector itself. In relative frequency, this is 62%.

The main research issues included questions focused on the financial and non-financial brownfield regeneration instruments that the MEC has used over the last 10 years. Among the financial instruments of the regions in the internal position, most respondents reported that they used municipal budgets at a relative frequency of 17%. Respondents reported in the greatest relative frequency the possibility that no funds were used at a relative frequency of 31%. Subsequently, 18% of respondents did not comment on the issue; the fourth option in relative frequency was that the MEC representatives contacted used European brownfield regeneration programmes. In the case of non-phony instruments for MEC regions located in the internal position, the most respondents in relative frequency were found to be 31% who reported that no non-financial instruments had been used. Another possibility from the surveyed participants was that they used their own activities, at a relative frequency of 23%. Subsequently, 16% of respondents did not comment on the question. The fourth option, at a relative frequency of 11%, was to state that the survey participants used the placement of information on brownfields in the state/regional database of brownfields. Other response options will not be commented on due to the low relative frequency.

The following question was aimed at respondents to indicate which tool helped the most in the case of brownfield regeneration. Most respondents stated that the most suitable tool for brownfield regeneration was the use of subsidy funds. Another option was to negotiate with the owners in the case of brownfield regeneration. The reasons that led the participants to address the regeneration of brownfields were mainly the new use of buildings and premises and the threat of the building collapsing. Another possibility that the respondents mentioned was the threat of environmental burdens associated with brownfields.

### 3. 5. Evaluation of Tools Between Individual Analysed MEC Regions

**Fig. 9** below shows the complete results in relative terms for the use of financial instruments in the brownfield regeneration process between the individual MEC regions analysed, which were examined above. If we look at the more detailed results of the picture, we can observe that, in the case of MECs which are located on the border, the budgets of municipalities, European and national programs for the regeneration of brownfields are more preferred. MEC regions located in peripheral areas mainly use national budgets for brownfield regeneration. MEC regions in the internal position make the most of the possibilities offered, especially municipal budgets and European operational programs.

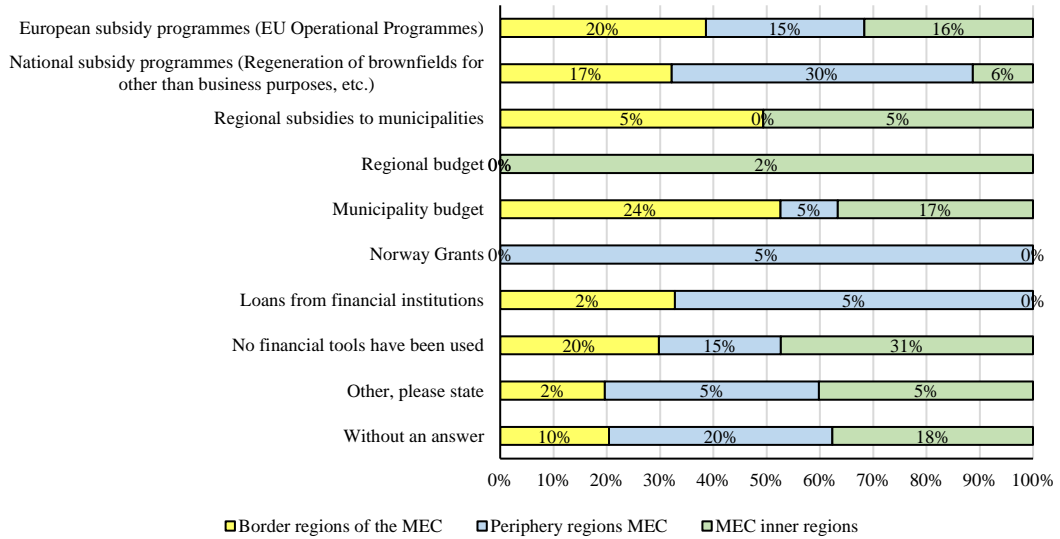


**Fig. 9.** Comparison of the use of financial instruments between MEC regions.  
 (Source: based on own survey, 2021).

The next figure (**Fig. 10**) focuses on the usability of non-financial instruments in the process of brownfield regeneration between individual MEC regions. If we analyse the table below, we can say that the MEC regions on the border mostly use their own activities, the support of the CzechInvest agency and the support of regional development agencies or other abominable institutions. In the last 10 years, the MEC regions in the area of peripheries have mostly used non-financial instruments such as their own activities, support from the CzechInvest agency and the placement of information on brownfields in the state/regional database of brownfields. Other regions examined were MEC regions in the internal position. If we do not analyse the results that the respondents did not use any non-financial instruments or did not answer the question, then the most used tool in this area is the use of their own activities and placing information about brownfields in the state/regional database of brownfields.

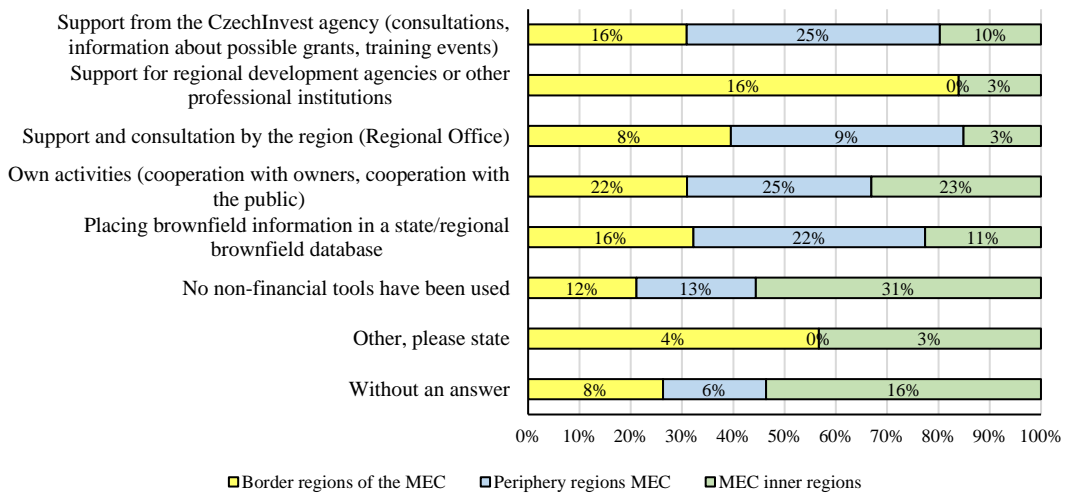


**Fig. 10.** Comparison of the use of non-financial instruments between MEC regions  
 (Source: based on own survey, 2021).



#### **4. DISCUSSION**

The research focused on brownfield regeneration tools in individual MEC regions in the Czech Republic. From the given results it is evident that individual MEC regions are aware of this problem with the existence of abandoned buildings and areas, which is mainly influenced by various policies both in the past and in the present (Krejci et al., 2021). This fact was also reflected in the results of the research, where 86% of the respondents stated that there are abandoned buildings and areas in its territory. Furthermore, in the presence of brownfields, it is important to take into account the geographical structure of regions (Frantal et al., 2013), whereas mentioned in the paper in the northern regions, especially in the border there is a greater proportion of abandoned buildings and areas than in the southern regions of the country (Martinat et al., 2016). Furthermore, it was found that most of the addressed MECs, which participated in the questionnaire survey in the last 10 years, performed the regeneration of brownfields. Here again we can compare the fact between the regions in the northern border and southern from the above results and it is clear that the regions that occur in the northern border, to a greater extent indicated that the regeneration of brownfields took place on its territory. This fact was also found in the comparison of MEC regions in the inner territory. Here, the respondents stated to a large extent that the given regeneration took place on its territory. The most significant problem that appears in the regeneration of brownfields is primarily the property rights that are associated with the buildings and areas. Most of the existing brownfields in the country are privately owned and this problem seems to be justified, as the given owners may not have any interest or sufficient funds for possible regeneration (Tureckova et al., 2018).

Based on the research, it was found that the regeneration of abandoned buildings and areas in the given MECs, which participated in the research, was provided by the private sector itself. In the case of a comparison between the individual analyzed regions, we can notice that the border regions primarily stated that the regeneration of abandoned buildings and areas was mainly provided by the public sector in the case of analysing results in internal regions.

It is also clear that the regions of the MEC are trying to use a variety of financial and non-financial instruments that are designed to support the regeneration of brownfields, which were identified from the research. As part of the analysis of all MEC regions that participated in the research, municipal budgets dominated among financial instruments, and non-financial instruments mostly reported their own activities. In the case of comparisons between regions on the basis of geographical point of view, border regions most often stated that they used municipal budgets in the case of financial instruments, national subsidies dominated in peripheral regions and subsequently most often mentioned municipal budgets as the most used financial instrument. In the case of the use of non-financial instruments, it can be noted that on the basis of the analysis of all regions, own activities were most often mentioned. In the comparison between regions in the case of geographical point of view, it can be said that own activities dominated in the border area. This fact was also found in the regions in the periphery and in the middle position. It was stated in the periphery that the regions used consultations with the CzechInvest agency in case of the possibility of brownfield regeneration.

Respondents also stated in the given analyzed regions that one of the most used tools that helped them was financial support in the form of subsidy titles for the regeneration of brownfields. The reason that mainly influenced them to the process of restoration and use of abandoned buildings and areas was mainly the new use of the buildings and facilities or the problematic situation with the statics of buildings.

The above results of the research helped us to look at the fact about the regeneration of brownfields between individual MEC regions in the Czech Republic and in relation to regional differences within the geographical location of the regions, which are, as mentioned above, very evident. The obtained results, which were presented in this paper, can contribute to new possibilities how to effectively adapt the regeneration of brownfields based on regions occurring in different geographical locations in the Czech Republic.

## 5. CONCLUSIONS

The paper focused on the application of tools in the process of the regeneration of brownfields in the territory of a municipality with extended competence (MEC) in the Czech Republic. In the paper, the authors analysed the primary survey which was conducted from 11 January to 16 May 2021. On the basis of the information contained in the paper, it can be said that 47.3% of the addressed respondents participated in the survey. It was found out that the highest number of abandoned buildings and premises can be found predominantly in regions with a problematic situation in the area of industrial and mining activities (Ústí nad Labem and Moravian-Silesian regions). Furthermore, the authors focused on the number of successfully regenerated brownfields in the last 10 years in the territory of the MEC; it was found here that the highest number of successfully regenerated abandoned buildings and premises was located in the South Moravian, Moravian-Silesian and South Bohemian regions. According to Tonin and Bonifaci (2020), the reconstruction of brownfields is decisive for the urban revitalisation of each town or village due to the fact that the soil is a valuable and non-renewable source and an important production factor for the whole economic system of each cadastral territory. Nowadays it is important to pay attention to the regeneration of brownfields in urban environments importance to the utilization of smart technology in the Czech Republic. Research according to Klusacek et al. 2020 identified that there are different factors which determine the successful implementation of smart city concept during the process of brownfields regeneration in the conditions of the post-socialistic urban environment. The concept of smart cities is strongly tied to technologies, and the project creating smart neighbourhoods requires substantial financial investments. The most essential issues of the whole survey included issues focusing on the application of financial and non-financial tools in the brownfield regeneration process. The most frequently used financial tools identified within the survey included primarily municipality budgets, European subsidy programmes and national subsidy programmes. The most frequent nonfinancial tools included own activities of MEC, support from the CzechInvest agency (the agency dealing with the support of business activities in the Czech Republic and managing the National Brownfield Database in the relevant country) and the placement of information about brownfields in the state/regional database of brownfields.

The research also focused on regional comparisons of MECs based on geographical location, where the authors examined the MEC regions in the border area, where the results were further analyzed in more detail based on MEC regions in the northern and southern parts of the country. The research was carried out on the basis of the fact that the northern part of the country has been heavily industrialized in the past and it is clear that there are a large number of abandoned buildings and grounds in these areas. Subsequently, the authors performed an analysis of MECs located in peripheral areas. These are MEC regions that do not occur in the border and internal position of the state. The last regions analyzed were MEC regions, which occur in the middle position of the above state. The results showed that there are some differences between the analyzed regions. In the northern regions of the MEC, abandoned buildings and areas were found to be more common than in the southern regions of the MEC. This fact is obvious, as mentioned above from the predominant industrialization of the regions concerned. Subsequently, the results pointed to the fact that the regions in the northern areas had a greater regeneration of brownfields in the past than the MEC regions in the southern areas. Furthermore, there are regional differences in the case of regeneration of abandoned areas provided by the public or private sector. There are differences mainly in the border regions and the middle regions. The MEC regions in the border area most often stated that the regeneration of brownfields was ensured by the public sector, and in the MEC regions in the internal position it was found that the reuse of abandoned buildings and areas was mostly provided by the private sector itself. An interesting finding was the comparison of results in the case of the use of financial and non-financial instruments within the regions examined. In the case of border regions and regions in the middle position, the budgets of municipalities dominated within the financial instruments for the reuse of brownfields. For the regions in the periphery, it was stated that national subsidy programs were most often used. If we look at the results in the case of non-financial instruments in the process of brownfield regeneration, we can notice that most regions, based on geographical scope, stated that they were most often used in the process of their own activities. The MEC regions, which are located

on the periphery, further stated that the consultations of the CzechInvest agency were used. Examining the results of the given primary research as a whole is not very effective, because the given results can distort the unexplored regional differences that obviously exist. It is necessary to examine the results also on the basis of the geographical scope of the regions, which can help us to obtain more information about the results and comparisons between regions.

It is important to point out that the research had some limitations when the number of respondents in the case of a regional comparison was not the same. Another limitation is the fact that when filling in the results, respondents stated in certain cases that they do not have information on brownfields in the MEC territory, because in case of using information on brownfields they use the National Brownfields Database managed by CzechInvest or regional databases of abandoned facilities and sites which are mostly analysed at the NUTS 3 level. The fact that the questionnaire survey was established as pilot research also seems important. It is obvious that when researching the issue focused on MEC regions in the field of brownfields and the use of tools for their regeneration, it is important in the future to use other procedures, methods and data that can contribute to new findings and interesting results in the case. On the basis of the findings, it is important to prioritise the use of existing abandoned buildings to building on the agricultural land. According to Squires and Hutchison (2021) the development of brownfield sites includes both private and public costs resulting from the soil contamination. In addition, brownfields create negative externalities concerning the viability of real estate, and are considered to be hazardous for their development. The application of tools (financial, non-financial) is a basic prerequisite for the successful regeneration and reuse of an abandoned building or premises, which could serve for new purposes in the following years, and contribute to the development of the area or territory.

## ACKNOWLEDGMENT

This paper was supported by the project SGF/7/2020 „The measures of the public sector for the strengthening of the regeneration potential of brownfields in the area of the Czech Republic. “



This paper was supported by the Ministry of Education, Youth and Sports Czech Republic within the Institutional Support for Long-term Development of a Research Organization in 2021.

## REFERENCES

- Agostini, P., Pizzol, L., Critto, A., D'Alessandro, M., Zabeo, A. & Marcomini, A. (2012) Regional risk assessment for contaminated sites Part 3: Spatial decision support system. *Environment International*, 48, 121 – 132.
- Alexandrescu, F., Klusacek, P., Bartke, S., Osman, R., Frantal, B., Martinat, S., Kunc, J., Pizzol L., Zabeo, A., Giubilato, E., Critto & Bleicher, A. (2017) Actor networks and the construction of applicable knowledge: the case of the Timbre Brownfield Prioritization Tool. *Clean Technologies and Environmental Policy*, 19, 1323 – 1334.
- Bartke, S., Martinat, S., Klusacek, P., Pizzol, L., Alexandrescu, F., Frantal, B., Critto, A. & Zabeo, A. (2016) Targeted selection of brownfields from portfolios for sustainable regeneration: User experiences from five cases testing the Timbre Brownfield Prioritization Tool. *Journal of Environmental Management*, 184, 94 – 107.
- Bartke, S. & Schwarze, R. (2015) No perfect tools: Trade-offs of sustainability principles and user requirements in designing support tools for land-use decisions between greenfields and brownfields. *Journal of Environmental Management*, 153, 11–24.
- CSO (2021). Czech Statistical Office. Available from: <http://www.un.org/sustainabledevelopment/> [Accessed May 2021].
- Frantal, B., Kunc, J., Klusacek, P. & Martinat, S. (2015) Assessing success factors of brownfields regeneration: international and inter-stakeholder perspective. *Transylvanian Review of Administrative Sciences*, 44, 91 – 107.
- Frantal, B., Kunc, J., Novakova, E., Klusacek, P., Martinat, S. & Osman, R. (2013) Location Matters! Exploring Brownfields Regeneration in a Spatial Context (A Case Study of the South Moravian Region, Czech Republic). *Moravian Geographical Reports*, 21 (2), 5-19.

- Frantal, B. & Martinat, S. (2013) Brownfields: A geographical perspective. *Moravian Geographical Reports*, 21 (2), 2-4.
- Chrysochou, M., Brown, K., Dahal, G., Grada-Carvajal, C., Segerson, K., Garrick, N & Batgtoglou, A. (2012) A GIS and indexing scheme to screen brownfields for area-wide redevelopment planning. *Landscape and Urban Planning*, 105 (3), pp. 187-198.
- Klusacek, P., Konecny, O., Zgodova, A. & Navratil, J. (2020) Application of the Smart City Concept in Process of Urban Recycling - Case Study of Špitálka in Brno, Czech Republic. *DEUROPE (The Central European Journal of Regional Development and Tourism)*, 12 (1), pp. 22-40.
- Klusacek, P., Navratil, J., Martinat, S., Krejci, T., Golubchikov, O., Picha, K., Skrabal, J. & Osman, R. (2021) Planning for the future of derelict farm premises: From abandonment to regeneration? *Land Use Policy*, 102, 105248.
- Koch, F., Bilke, L., Helbig, C. & Schlink, U. (2018) Compact or cool? The impact of brownfield redevelopment on inner-city micro climate. *Sustainable Cities and Society*, 38, 31–41.
- Krejci, T., Navratil, J., Martinat, S., Frazier, J. R., Klusacek, P., Picha, K., Skrabal, J. & Osman R. (2021) Spatial Unevenness of Formation, Remediation nad Persistence of Post-Agricultural Bornwfields. *Land*, 10 (3), 325.
- Krejci, T., Navratil, J., Martinat, S., Picha, K., Klusacek, P., Osman, R. & Skrabal, J. (2019) Current use of former communist agricultural properties in South Bohemia. In: *XXII. International Colloquium on Regional Sciences*. Brno: MU ESF Brno, 665-671.
- Limasset, E., Pizzol L., Merly, C., Gatchett, M. A., Le Guern, C., Martinat, S., Klusacek, P. & Bartke, S. (2018) Points of attention in designing tools for regional brownfield prioritization. *Science of The Total Environment*, 622 – 623, 997 – 1008. "
- Martinat, S., Dvorak P., Frantal B., Klusacek, P., Kunc J., Navratil J., Osman R., Tureckova K. & Matthew, R. (2016) Sustainable urban development in a city affected by heavy industry and mining? Case study of brownfields in Karvina, Czech Republic. *Journal of Cleaner Production*, 118, pp. 78-87.
- Meyer, P. B. & Lyons, T. S. (2000) Lessons from private sector Brownfield redevelopers -planning public support for urban regeneration. *Journal of the American Planning Association*, 66 (1), 46–57.
- Navratil, J., Martinat, S., Krejci, T., Picha, K., Klusacek, P., Skrabal, J. & Osman, R. (2020) The fate of socialist agricultural premises: To agricultural 'brownfields' and back again? *Moravian Geographical Reports*, 27 (4), 207 – 216.
- Pizzol, L., Critto, A., Agostini, P. & Marcomini, A. (2011) Regional risk assessment for contaminated sites Part 2: Ranking of potentially contaminated sites. *Environment International*, 37 (8), 1307-1320.
- Pizzol, L., Zabeo, A., Klusacek, P. Giubilato, E., Critto, A., Frantal, B., Martinat, S., Kunc, J., Osman, R. & Bartke, S. (2016) Timbre Brownfield Prioritization Tool to support effective brownfield regeneration. *Journal of Environmental Management*, 166, 178-192.
- Skrabal, J. (2020) What Can we Learn from Brownfield Databases? Exploring Specifics of The Location of Brownfields in The Czech Republic. *Geographia Technica*, 15 (2), 191-201.
- Squires, G. & Hutchison, N. (2021) Barriers to affordable housing on brownfield sites. *Land Use Policy*, 102, 105276.
- Tonin, S. & Bonifaci, P. (2020) Assessment of brownfield redevelopment opportunities using a multi-tiered approach: A case in Italy. *Socio-Economic Planning Sciences*, 71, 100812.
- Thornton, G., Franz, M., Edwards, D., Pahlen, G. & Nathanail, P. (2007) The challenge of sustainability: incentives for brownfield regeneration in Europe. *Environmental Science & Policy*, 10 (2), 116–134.
- Tureckova, K., Martinat, S., Skrabal, J., Chmielova, P. & Nevima, J. (2017) How local population perceive impact of brownfields on the residential property values: some remarks from postindustrial areas in the Czech Republic. *Geographia Technica*, 12 (2), 150–164.
- Tureckova, K., Nevima, J., Skrabal, J. & Martinat, S. (2018) Uncovering patterns of location of brownfields to facilitate their regeneration: Some remarks from the Czech Republic. *Sustainability*, 10 (6), 224–234.
- Tvrdoň, M. & Chmielova, P. (2020) Interlinkages Between Strategic, Financial and Regional Frameworks of Brownfield Regenerations: the Case of The Czech Republic. *Geographia Tehcnica*, 16 (1), 113-127.
- Zabeo, A., Pizzol, L., Agostini, P., Critto, A., Giove, S. & Marcomini, A. (2011) Regional risk assessment for contaminated sites Part 1: Vulnerability assessment by multicriteria decision analysis. *Environment International*, 37 (8), 1295 – 1306.

# ARTIFICIAL NEURAL NETWORKS FOR THE CLASSIFICATION OF SHRIMP FARM FROM SATELLITE IMAGERY

Ilada AROONSRI<sup>1</sup>, Satith SANGPRADID<sup>2</sup>

DOI: 10.21163/GT\_2021.162.12

## ABSTRACT:

Shrimp production was the high demand for the popular in the global market in Thailand. The change of land use is important for the management and monitoring of land use changed. The objectives of this paper to (1) classification of shrimp farm using artificial neural networks (ANN) technique from the Sentinel-2 imagery. (2) change detection of land use changes map among 2015, 2018, and 2020. The land use classification based on ANN technique and the accuracy assessment by used the confusion matrices and kappa coefficient. The classify of land use classes divide into built-up, forest, water bodies, paddy field, shrimp farm, and field crop. The change detection methods used was the image differencing technique was performed to the land use changes map. The result of land use classification show that the field crop area was 80% cover the most area. The result of land use changed show that built-up, paddy field, and shrimp farm increased throughout between year 2015 to 2020. The shrimp farm between year 2015 to 2020 to increasing trend of related with the shrimp production was the high demand for the popular in the global market.

**Key-words:** *Sentinel-2 imagery, Supervise classification, Land use change detection, artificial neural networks (ANN).*

## 1. INTRODUCTION

Nowadays, shrimp farming in Thailand has been cultivating shrimp for domestic consumption and exports for a long time over the past 20 years. In the year 2020, the exports of production from shrimp farming are expected to increase to 350,000 tonnes (Thai Shrimp Association, 2019). Shrimp production was the high demand for the popular in the global market in Thailand. According to the shrimp is the most popular food consumed due to the reasons the farmers changed an agricultural area into the shrimp farming. The rapid change from agriculture to shrimp farming should be an issue associated with land degradation and water pollution. Therefore, it is necessary to plan and manage environmental impacts and social conflicts that have occurred in the area. The shrimp farming mapping is important for monitoring the land use changed in these areas.

The study of land utilization is very importance for managing dynamics for land use and demand of the population (Yaday et al., 2010). Planning and managing the change of land use in the area is the first priority for future land use planning to resource and sustainable development process.

---

<sup>1</sup> Department of Business Digital, Faculty of Management Sceinces, Valaya Alongkorn Rajabhat University Under the Royal Patronage, 1, Moo 10, Klong 1, Klong Luang, Pathum Thani 13180, Thailand; E-mail: ilada@vru.ac.th

<sup>2</sup> Research unit of Geo-informatics for Local Development and Department of Geoinformatics, Faculty of Informatics, Mahasarakham University, Kantarawichai District, Maha Sarakham 44150, Thailand; E-mail: satith.s@msu.ac.th

Currently, the geo-informatics technology has been applied for the land use changed by used the processed from the satellite images. It has been very useful to classified the land use mapping for the monitor and analyze of land use in the area (Jomsrekrayom et al., 2021; Pradabmook & Laosuwan, 2021). Satellite Imagery an important in the sustainable development of shrimp aquaculture by providing information about land use/land cover, water quality, and coastal infrastructure (Rajitha et al., 2007). Satellite imagery has been used to monitoring areas of shrimp aquaculture, as well as to classify of land use change related aquaculture or specifically of land use in an area. Satellite imagery can support both of small and large-scale mapping of aquaculture for a better understanding and management and improve the quantifying of fish and shrimp ponds and associated production volumes to ensure comparable statistics between countries and regions (Ottinger et al, 2017; Stiller et al., 2019).

There several techniques for land use classification from satellite imagery based on supervised classification method such as parallelepiped, minimum distance, maximum likelihood, and mahalanobis distance. The maximum likelihood technique is the most popular for classify the land cover in coastal landscapes and classify of shrimp aquaculture (Alonso-Perez et al., 2003). However, the classifier method based rely upon field severing to collect the data or visual interpretation to identify shrimp pond shape samples as inputs of models (Dorber et al., 2020). The maximum likelihood technique assigned a class of land used based on the probability that a pixel belonging to a particular class that a normally distributed dataset exists, and that the statistical parameters. The classification accuracy of the maximum likelihood technique depending on the training samples are then used to train the classifier to classify the spectral data into a thematic map (Du & Wang, 2007). Machine learning is an emerging advanced classification methodology with supervised classification methods, such as random forest (RF), support vector machine (SVM), and artificial neural networks (ANN), there are can perform better than traditional classification method (Erbek et al., 2004; Maung & Sasaki, 2021).

Recently, machine learning methods have been used widely in satellite imagery to classify land use classification, monitoring, land use change detection, and prediction of land use change. The supervised machine learning classifier such as RF, SVM, and decision tree (DT) (Toosi et al., 2019; Ahmad, 2013; Ge et al., 2020). Currently, the application of Sentinel-2 has used widely in generally for land use monitoring (Urban et al., 2021; Migas-Mazur et al., 2021; Punalekar et al., 2021), precision agriculture (Santaga et al., 2021), fire monitoring (Kovacs, 2019; Vanderhoof et al., 2021), drought assessment (Varghese et al., 2021) and maritime monitoring (Costantino et al., 2020). In addition, Sentinel-2 has been spatial resolution varies from 10 m to 60 m and temporal resolution are only available every 5 days. In this paper, focused on ANN technique was used widely to classify the satellite image data to accuracies higher than of the tradition classification techniques (Foody et al., 1995; Toshniwal, 2005; Mahmon & Yaacob, 2014). The objective of this paper to (1) classification of shrimp farm using ANN technique from the Sentinel-2 imagery. (2) change detection of land use changes map among 2015, 2018, and 2020.

## 2. MATERIALS AND METHODS

### 2.1. Study area and data collection

This study was conducted at Yang Talad district, Kalasin province, Thailand (**Fig. 1**). The study area has tropical monsoon weather and the average temperature ranges from 26.9 - 28.2 degrees Celsius. The study are lies between 16.28° to 16.60° N Latitude and 103.15° to 103.50° E Longitude.

Sentinel-2 Imagery is a European wide-swath, high-resolution, multi-spectral imaging mission. The spectral resolution of Sentinel-2 imagery shown in **Table. 1** (USGS EROS Center,2015).

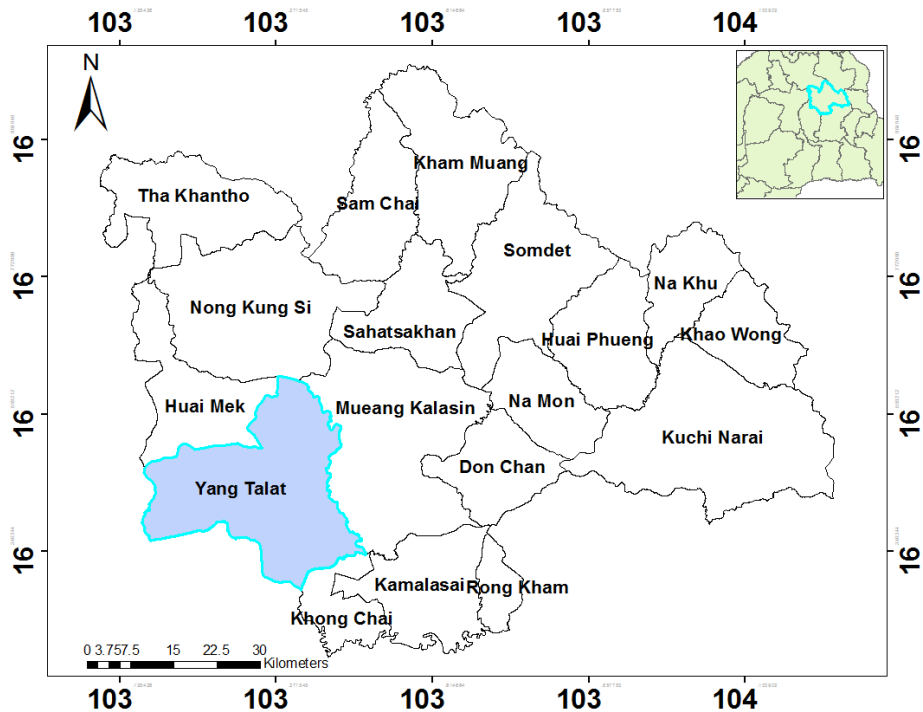


Fig. 1. Study area.

Table. 1

Characteristics of the Sentinel-2 Imagery.

Spatial resolution (m)	Band Number	S2A		S2B	
		Central Wavelength (nm)	Bandwidth (nm)	Central Wavelength (nm)	Bandwidth (nm)
10	2	492.4	66	492.1	66
	3	559.8	36	559	36
	4	664.6	31	664.9	31
	8	832.8	106	832.9	106
20	5	704.1	15	703.8	16
	6	740.5	15	739.1	15
	7	782.8	20	779.7	20
	8a	864.7	21	864	22
	11	1613.7	91	1610.4	94
	12	2202.4	175	2185.7	185
60	1	442.7	21	442.2	21
	9	945.1	20	943.2	21
	10	1373.5	31	1376.9	30



The Sentinel-2 imagery was acquired on dates 22 October 2015, 26 October 2018, and 23 October 2020 in order to classify the land use classification historical and current of shrimp farm cover. The spatial resolution of Sentinel-2 imagery is  $10 \times 10$  m was used for colour composites of Bands 8,4, and 3 to select the training area and classification of land use. Band combination is created by band combining of spectral data to improve a particular land use. A significant advantage of multispectral images is important to detected the difference surface of the area by the spectral of band combination. Band 8 (Near InfraRed) is very important in terms of ecological monitoring, since the Near InfraRed is the spectrum reflected by the water present in plants. False colour composite of Bands (RGB 8,4,3) was used for classified the vegetation appear red color and water bodies or shrimp farm with appear navy or black color.

## 2.2. Image classification from Sentinel-2 imagery

To survey the land use classes of shrimp farm in the Yang Talad study area, a field survey for collection of training samples and validation were primarily collected from field observations. Data collection by record the land use types including: built-up (Bu), forest (F), water bodies (W), paddy field (Pf), shrimp farm (Sf), and field crop (Fc), respectively.

### 2.2.1 Image classification using artificial neural networks (ANN)

An ANN is a computing system designed based on the structure of the biological neural network of the human nervous system and processes information. The systems of ANN have many layers is also call a multi-layer perceptron with the input layer, a hidden layer, an output layer, each of these layers has a specific purpose. These layers consist of nodes for takes input from the previous layer according to the requirements and transfers them to the next layer show in **Fig. 2**.

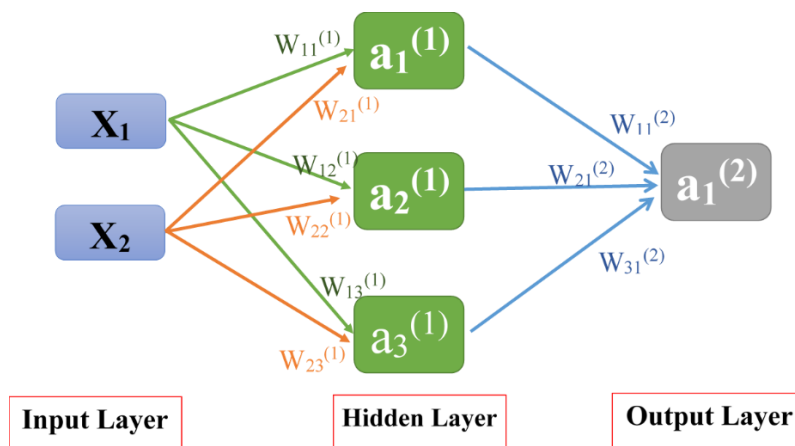


**Fig. 2.** Structure of a neural network.

The input nodes receive data in a format that can be expressed as numbers. The data is presented as the activation value, where each node receives a number. This data is passed to the network, depending on the strength of the connection (weight). These weights to calculate the weighted sum of inputs and applying an activation function (sigmoid, unit step, linear, etc.) in hidden layer to generate data their output layer. The several ANN models have been applied in land use classification such as Hopfield network, self-organizing competition, radial basis function, multilayer perception,

and multilayer perception with back propagation (Mas & Flore, 2008; Xiong et al., 2008; Shrestha et al., 2012). This paper used standard backpropagation for the classifier of land use classes. The error backpropagation was used for back propagated through the network and weight adjustment using a recursive method.

### 2.2.2 Land use Classification Types

Land use classes of the paper were categorized into six land types: built-up (Bu), forest (F), water bodies (W), paddy field (Pf), shrimp farm (Sf), and field crop (Fc) using the ANN classifiers with the regions of interest (ROI) for the training samples of land use classes. The training polygons or ROI was selected as represented of each class in the satellite imagery by digitized on the image based on the prior knowledge of the field surveyed and visual interpretation. The accuracy assessment of this paper using confusion matrices base on binomial probability theory with the desired level of confidence of 85 percent. The 300 samples of the reference point evaluate the classification procedure by using overall accuracy and the kappa coefficient.

### 2.2.3 Land use change detection

The percentage of land use change from the classification map from the map 2015, 2018, and 2020 in the study area. The process to identify the difference of classification map between map 2015 – 2018, and 2018 – 2020 was used the change detection technique. The various technique of change detection techniques has been applied to the monitoring of land use change including image differencing (Lu et al., 2004; Panuju et al.,2020), principal component analysis (Lu et al., 2004; Panuju et al.,2020), and change vector analysis (Lu et al., 2004; Panuju et al.,2020; Sangpradid, 2018). This paper used the image differencing technique was performed to classification the map by subtracts the first date image from a second date image on the digital image value between pixel by pixel.

## 3. RESULTS

### 3.1. The result of land use classification

The results of land use classification map for the years 2015, 2018, and 2020 as shown in **Fig. 3, 4, and 5**, respectively. The area of the land use classifications from the ANN technique shown the percentage values of an area shown in **Table. 2**. The land use classes for the year 2015 in this table show that the area cover by built-up was 2.16%, forest was 12.64%, water bodies was 1.93%, paddy field was 1.71%, field crop was 79.88%, and shrimp farm was 1.67%.

**Table 2.**

**The areas and percentage values of LU classes for the years 2015, 2018, and 2020.**

Classes	2015		2018		2020	
	sq.km	%	sq.km	%	sq.km	%
built-up	15.00	2.16	15.71	2.26	20.99	3.03
forest	87.69	12.64	65.35	9.42	59.88	8.63
water bodies	13.42	1.93	12.88	1.86	12.93	1.86
paddy field	11.85	1.71	5.76	0.83	13.70	1.98
field crop	554.03	79.88	579.85	83.61	567.59	81.84
shrimp farm	11.55	1.67	14.01	2.02	18.45	2.66

The land use classes for the year 2018 show that the area cover by built-up was 2.26%, forest was 9.42%, water bodies was 1.86%, paddy field was 0.83%, field crop was 83.61%, and shrimp farm was 2.02%. The land use classes for the year 2020 show that the area cover by built-up was 3.03%, forest was 8.63%, water bodies was 1.86%, paddy field was 1.98%, field crop was 81.84%, and shrimp farm was 2.66%. The accuracy assessment of land use classified technique using the confusion matrices and kappa coefficient were used the 300 points of randomly by the stratified sampling methods. The overall accuracy and the kappa coefficient as shown in **Table 3,4, and 5**.

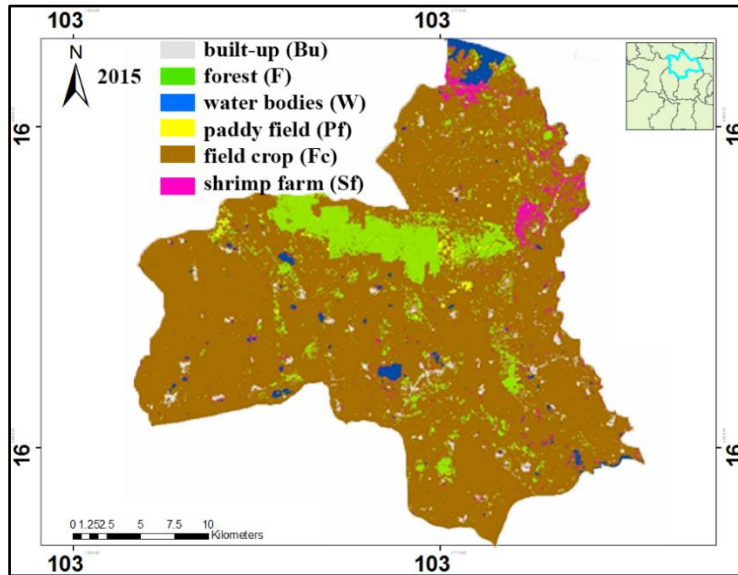


**Fig. 3.** The land use classes map for the years 2015 of the Yang Talad, Kalasin province, Thailand.

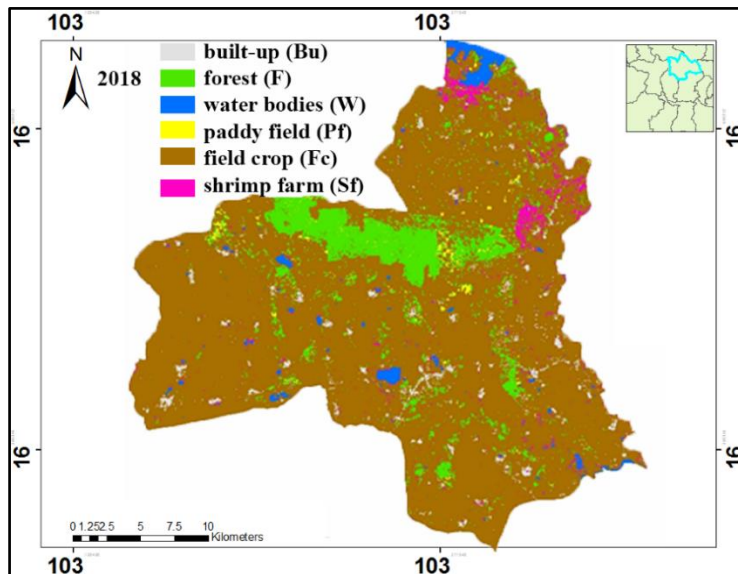


**Fig. 4.** The land use classes map for the years 2018 of the Yang Talad, Kalasin province, Thailand.

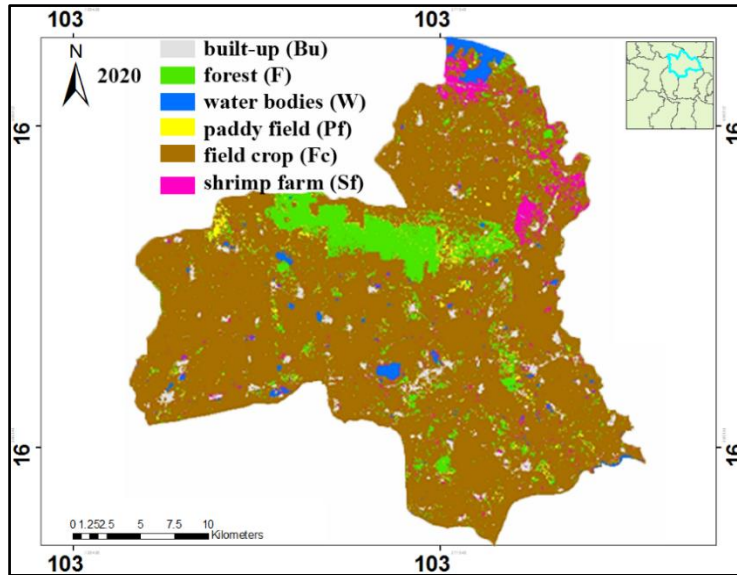


Fig. 5. The land use classes map for the years 2020 of the Yang Talad, Kalasin province, Thailand.

Table 3.

Confusion matrices and kappa coefficient of land use classified for the years 2015.

Classes	Reference data						total
	Bu	F	Wb	Pf	Fc	Sf	
Bu	47	0	0	0	2	0	49
F	0	46	0	2	0	1	49
Wb	0	0	47	0	0	0	47
Pf	0	4	0	46	0	1	51
Fc	3	0	0	2	47	2	54
Sf	0	0	3	0	1	46	50
total	50	50	50	50	50	50	300

Table 4.

Confusion matrices and kappa coefficient of land use classified for the years 2018.

Classes	Reference data						total
	Bu	F	Wb	Pf	Fc	Sf	
Bu	47	0	1	0	0	0	48
F	0	46	0	3	0	1	50
Wb	1	0	46	0	2	0	49
Pf	0	4	0	45	0	1	50
Fc	2	0	1	2	47	2	54
Sf	0	0	2	0	1	46	49
total	50	50	50	50	50	50	300

The accuracy assessment of land use classification using the confusion matrices for year 2015 show that the overall accuracy was 93 % and the kappa coefficient was 0.916 as shown in **Table 3**. The accuracy assessment of land use classification using the confusion matrices for year 2018 show that the overall accuracy was 92.33 % and the kappa coefficient was 0.910 as shown in **Table 4**. The accuracy assessment of land use classification using the confusion matrices for year 2020 show that the overall accuracy was 91.66 % and the kappa coefficient was 0.90 as shown in **Table 5**.

**Table 5.****Confusion matrices and kappa coefficient of land use classified for the years 2020.**

Classes	Reference data						total
	Bu	F	Wb	Pf	Fc	Sf	
Bu	45	0	0	0	1	1	47
F	0	47	0	1	0	0	48
Wb	0	1	46	1	0	2	50
Pf	2	1	0	46	2	0	51
Fc	3	1	1	1	46	2	54
Sf	0	0	3	1	1	45	50
total	50	50	50	50	50	50	300

**3.2. The result of Land use change detection**

The results of the land use change detection were performed by image differencing method show that in **Table 6**. The area of land use change between year 2015 and 2018 show that built-up area increased was 4.67%, forest area decreased was 25.48%, water bodies decreased was 3.99%, paddy field decreased was 51.44%, field crop increased was 4.66%, and shrimp farm increased was 21.28%. The area of land use change between year 2018 and 2020 show that built-up area increased was 33.66%, forest area decreased was 8.37%, water bodies increased was 0.36%, paddy field increased was 138.05%, field crop decreased was 2.11%, and shrimp farm increased was 31.74%. The area of land use change between year 2015 and 2020 show that built-up area increased was 28.52%, forest area decreased was 46.44%, water bodies decreased was 3.79%, paddy field increased was 13.50%, field crop increased was 2.39%, and shrimp farm increased was 37.41%.

**Table 6.****The area of land use change detection on years 2015, 2018, and 2020.**

Classes	Chang detection (2015-2018)		Chang detection (2018-2020)		Chang detection (2015-2020)	
	sq.km	%	sq.km	%	sq.km	%
built-up	0.70	4.67	5.29	33.66	5.99	28.52
forest	-22.34	-25.48	-5.47	-8.37	-27.81	-46.44
water bodies	-0.54	-3.99	0.05	0.36	-0.49	-3.79
paddy field	-6.10	-51.44	7.95	138.05	1.85	13.50
field crop	25.81	4.66	-12.26	-2.11	13.56	2.39
shrimp farm	2.46	21.28	4.45	31.74	6.90	37.41

#### 4. DISCUSSION AND CONCLUSIONS

As the result of the land use classification for the year 2015, 2018, and 2020 found that the area of Yang Talad district about 80 % cover by field crop area. Meanwhile, the shrimp farm area covers about 2.66 %. The classification accuracy of the ANN technique shows that the overall accuracy and kappa coefficient higher than 91.66 % and 0.90, respectively. The results accuracy assessment by the producer's accuracy of the ANN technique for the year 2015 show that built-up was 94%, forest was 92%, water bodies was 94%, paddy field was 92%, field crop was 94%, and shrimp farm was 92%. The producer's accuracy of the ANN technique for the year 2018 show that built-up was 94%, forest was 92%, water bodies was 92%, paddy field was 90%, field crop was 94%, and shrimp farm was 92%. The producer's accuracy of the ANN technique for the year 2020 show that built-up was 90%, forest was 94%, water bodies was 92%, paddy field was 92%, field crop was 92%, and shrimp farm was 90%. The results of land use classes map of the year 2015, 2018, and 2020 show that the pink color of land use maps show the area of shrimp farm compared with the surveyed and visual interpretation was the accurate with the shrimp farm area existing.

In addition, the comparison of the results of the land use classify show with similar research such as Dorber et al. (2020) presented the remote sensing can be use to provide spatially explicit land-use change information of shrimp aquaculture. The results of accuracy assessment show that the accuracy of the spatial resolution of Sentinel-2 similar with Costantino et al. (2020). The land use change detection show that forest area decreased throughout between year 2015 to 2020 was 46.44%. The land use of built-up, paddy field, and shrimp farm increased throughout between year 2015 to 2020. The shrimp farm between year 2015 to 2020 to increasing trend of related with the shrimp production was the high demand for the popular in the global market in Thailand (Thai Shrimp Association. (2019). The shrimp farm area increased was 37.41%. Furthermore, the results of land use change of shrimp farm can be used for predicting the future land use by using the prediction model such as land change modeler or Ca-Markov model.

#### ACKNOWLEDGMENT

This paper was supported by Faculty of Informatics, Maharakham University and Research unit of Geo-informatics for Local Development, and Faculty of Management Sciences, Valaya Alongkorn Rajabhat University Under the Royal Patronage.

#### REFERENCES

- Ahmad, A. (2013). Comparative analysis of supervised and unsupervised classification on multispectral data. *Applied Mathematical Sciences*, 7(74), 3681 – 3694.
- Alonso-Pereza, F., Ruiz-Lunab, A., Turnerc, J., Berlanga-Roblesb, C.A., & Mitchenson-Jacobc, G. (2003). Land cover changes and impact of shrimp aquaculture on the landscape in the Ceuta coastal lagoon system, Sinaloa, Mexico. *Ocean & Coastal Management*, 46,583–600.
- Costanino, D., Pepe, M., Dardanelli, G., Baiocchi, V. (2020). Using optical satellite and aerial imagery for automatic coastline mapping. *Geographia Technica*, 15(2), 171-190.
- Dorber, M., Verones, F., Nakaoka, M., Sudo, K. (2020). Can we locate shrimp aquaculture areas from space? – A case study for Thailand. *Remote Sensing Applications: Society and Environment*, 20, 1-9.
- Erbek, F. S., Özkan, C., & Taberner, M. (2004). Comparison of maximum likelihood classification method with supervised artificial neural network algorithms for land use activities. *International Journal of Remote Sensing*, 25(9), 1733-1748.
- Foody, G.M., McCulloch, M.B., & Yates, W.B. (1995). Classification of remote sensed data by artificial neural networks: Issues Related to training Data Characteristics. *Photogrammetric Engineering & Remote Sensing*, 61(4), 391-401.

- Ge, G., Shi, Z., Yang, X., Hao, Y. (2020). Land use/cover classification in an arid desert-oasis mosaic landscape of China using remote sensed imagery: Performance assessment of four machine learning algorithms. *Global Ecology and Conservation*, 22, 1-9.
- Jomsrekrayom, N., Meena, P., Laosuwan, T. (2021). Spatiotemporal Analysis of Vegetation Drought Variability in the Middle of the Northeast Region of Thailand Using TERRA/MODIS Satellite Data. *Geographia Technica*, 16 (Special Issue), 70-81.
- Kovacs, K.D. (2019). Evaluation of burned areas with Sentinel-2 using snap: the case of Kineta and Mati, Greece, July 2018. *Geographia Technica*, 14(2), 20-38.
- Lu, D., Mausel, P., Brondizio, E., & Moran, E. (2004). Change detection techniques. *International Journal of Remote Sensing*, 25(12), 2365-2407.
- Lu, D., & Weng, Q. (2007). A survey of image classification methods and techniques for improving classification performance. *International Journal of Remote Sensing*, 28, 823–870.
- Mahmon, N.A., & Ya'acob, N. (2014). A review on classification of satellite image using artificial neural network (ANN). *IEEE 5th Control and System Graduate Research Colloquium, Aug. 11 - 12, UiTM, Shah Alam, Malaysia*.
- Mas, J.F., & Flores, J.J. (2008). The application of artificial neural networks to the analysis of remotely sensed data. *International Journal of Remote Sensing*, 29(3), 617-663.
- Maung, W.S., & Sasaki, J. (2021). Assessing the natural recovery of mangroves after human disturbance using neural network classification and Sentinel-2i in Wunbaik Mangrove Forest, Myanmar. *Remote Sensing*, 13, 52.
- Migas-Mazur, R., Kycko, M., Zwijsacz-Kozica, T., Zagajewski, B. (2021). Assessment of Sentinel-2 images, support vector machines and change detection algorithms for bark beetle outbreaks mapping in the Tatra mountains. *Remote sensing*, 12, 3314.
- Ottinger, M., Clauss, K., & Kuenxer, C. (2017). Large-scale assessment of coastal aquaculture ponds with Sentinel-1 time series data. *Remote Sensing*, 9, 440;
- Panalekar, S.M., Thomson, A., Verhoef, A., Humphries, D.J., Reynolds, C.K. (2021). Assessing suitability of Sentinel-2 bands for monitoring of nutrient concentration of pastures with a range of species compositions. *Agronomy*, 11, 1661.
- Panuju, D.R., Paull, D.J., Griffin, A.L. (2018). Change detection techniques based on multispectral images for investigating land cover dynamics. *Remote Sensing*. 2020, 12, 1781.
- Pradabmook, P., Laosuwan, T. (2021). The integration of geo-informatics technology with Universal Soil Loss Equation to analyze areas prone to soil erosion in Nan Province. *ARPN Journal of Engineering and Applied Science*, 18(8), 823-830.
- Rajitha, K., Mukherjee, C.K., & Chandran R.V. (2007). Applications of remote sensing and GIS for sustainable management of shrimp culture in India. *Aquacultural Engineering*, 36, 1–17.
- Santaga, F.S., Agnelli, A., Leccese, A., Vizzari, M. (2021). Using Sentinel-2 for simplifying soil sampling and mapping: two case studies in Umbria, Italy. *Remote sensing*, 13, 3379.
- Sangpradid, S. (2018). Change vector analysis using integrated vegetation indices for land cover change detection. *International Journal of Geoinformatics*, 14 (4), 71-77.
- Shrestha, S., Bochenek, Z., & Smith, C. (2012). A comparison of supervised classification techniques for land cover classification for the Warsaw Region using SPOT 4 imagery. *First Sentinel-2 Preparatory Symposium, Frascati, Italy*, 23–27 April 2012, ESA SP-707, July 2012.
- Stiller, D., Ottinger, M., & Leinenkugel, P. (2019). Spatio-temporal patterns of coastal aquaculture derived from Sentinel-1 time series data and the full Landsat archive. *Remote sensing*, 11, 1707.
- Thai Shrimp Association. (2019). Shrimp situation in the Thailand of 2020. <http://inlandfisheries.go.th/images/pdf/sT1.pdf> (in Thai).
- Toosi, N.B., Soffianian, A.R., Fakheran, S., Pourmanafi, S., Ginzler, C., & Waser, L.T. (2019). Comparing different classification algorithms for monitoring mangrove cover changes in southern Iran. *Global Ecology and Conservation*, 19, 1-16.
- Toshniwal, M. (2005). Satellite image classification using neural networks. *3rd International Conference: Sciences of Electronic, Technologies of Information and Telecommunications*, March 27-31, TUNISIA.
- Urban, M., Schellenberg, K., Morhenthal, T., Dubois, C., Hirner, A., Gessner, U., Mogonong, B., Zhang, Z, Baade, J., Collett, A., Schmulius, C. (2021). Using Sentinel-1 and Sentinel-2 time series for slangebos mapping in the Free State Province, South Africa. *Remote sensing*, 13, 3342.



- USGS EROS Center.2015. *USGS EROS Archive - Sentinel-2*. [https://www.usgs.gov/centers/eros/science/usgs-eros-archive-sentinel-2?qt-science\\_center\\_objects=0#qt-science\\_center\\_objects](https://www.usgs.gov/centers/eros/science/usgs-eros-archive-sentinel-2?qt-science_center_objects=0#qt-science_center_objects).
- Varghese, D., Radulovic, M., Stojkovic, S., Crnojevic, V. (2021). Reviewing the potential of Sentinel-2 in assessing the drought. *Remote sensing*, 13, 3355.
- Vanderhoof, M.K., Hawbaker, T.J., Teske, C, Ku, A., Noble, J. (2021). Mapping wetland burned area from Sentinel-2 across the southeastern United State and its contributions relative to Landsat-8 (2016-2019). *Fire*, 4, 52.
- Xiong, Y., Zhang, Z. & Chen, F. (2010). Comparison of artificial neural network and support vector machine methods for urban land use/cover classifications from remote sensing images. *International Conference on Computer Application and System Modeling (ICASM 2010)* ,52-56.
- Yaday, P., Kapoor, M. & Sarma, K. (2010). Land use land cover mapping, change detection and conflict analysis of Nagzira – Navegaonc, central India using geospatial technology. *International Journal of Remote Sensing and GIS*, 1(2), 90-98.

## FUNCTIONAL LAND AND EMOTIONAL LANDSCAPE. DRY STONE CONSTRUCTIONS IN LA GARRIGA D'EMPORDÀ IN THE 19TH CENTURY

Ramon RIPOLL <sup>1</sup>, Jordi GOMIS <sup>2\*</sup>, Carlos TURÓN <sup>3</sup>, Gabi BARBETA <sup>4</sup>,  
Miquel-Àngel CHAMORRO <sup>5</sup>

DOI: 10.21163/GT\_2021.162.13

### ABSTRACT:

The relationship between traditional farmers with the physical characteristics of the site (material function) has long been analysed, but rarely has farmers' cultural relationship with their geographical environment (emotional function) been upheld. To demonstrate this duality implies finding farmland created both due to material profitability or family subsistence and due to psychological necessity or personal self-realization. For example, the transformation in the nineteenth century of desolate, stony unproductive landscapes in la Garriga d'Empordà -Catalonia- (of some 8 km<sup>2</sup>) into farmland, for poorer peasant families meant not only a minuscule means of material progress but above all a major means of social hope and human dignity. To confirm this duality is to corroborate that many functional territories are also emotional landscapes for those who farm them, mainly during the period of major agricultural expansion in Europe due to the growth in population at the onset of the modern era.

*Key-words:* Regional poverty, Usable land, Variable plots, Dry stone, Landscape.

### 1. INTRODUCTION

The following analysis of la Garriga d'Empordà defines a local situation that is also a reflection of global concepts. It seeks to demonstrate the relationship between natural geography and agricultural geography especially in highly unfavourable situations (regional poverty), the legal uniqueness, of medieval origin, of access to land (beneficial ownership/usufruct), the parallels between social regeneration and the democratization of private property (variable geometry), the construction work done by the agricultural workers themselves (dry stone), obtaining supplementary agricultural income by the most neglected rural families and, finally, to underline the hypothesis of personal self-realization developed in parallel. So, the purpose of this article is to enrich the general concepts based on an example of agricultural transformation (la Garriga d'Empordà).

The interest in this subject lies in delving into the geographical, historical and agricultural reasons justifying first its emergence and then its abandonment. Hence, the paper begins with the introduction that relates population growth to employment in agriculture, continuing with the relationship between the legal systems governing access to property and social emancipation, the organic organization of the territory and the variable geometry of its ownership and, finally, territorial transformation and building technology.

---

<sup>1, 4, 5</sup> *Universitat de Girona, C/Maria Aurèlia Capmany 61, 17003-Girona, Spain, ramon.ripoll@udg.edu, gabriel.barbeta@udg.edu, mangel.chamorro@udg.edu*

<sup>2, 3</sup> *Universitat Rovira i Virgili, Av. Països Catalans 26, 43007-Tarragona, Spain, \* jordi.gomis@urv.cat, carlos.turon@urv.cat*

The methodology used is based on surveying plans of the most representative elements, studying the territory from the existing cartography, research at the notarial archives of lease contracts, and lastly, the theoretical analysis of the concepts raised. Regarding the latter, it is worth mentioning the spatial concepts of the humanization of space such as organic form, variable geometry, etc. (Aalto, 1977); the survival of the characteristics of one era over another through rupture, transition, cohabitation, etc; and on the democratization of agriculture, preindustrial farming, etc. (Terrades, 1984).

## 2. REGIONAL POVERTY

First, let us recall the great population growth during the nineteenth century which explains the increase in farmed land and, therefore, the widespread use of land for agricultural purposes. Improvements in hygiene, diet and medicine during this period led the population to double in few years. Specifically, in the Alt Empordà region in Catalonia, where the study area, la Garriga, is located, the population almost doubled in less than a century. It went from 41,280 inhabitants in 1787 to 73,867 in 1857 (i.e., an increase of 79% in seventy years). It should be mentioned that this calculation does not include the first migratory movements from rural parts of the Empordà to the city. This means that the population of Alt Empordà increased 6% less than the growth rate of Catalonia during these 70 years (899,531 to 1,661,291 inhabitants). This increase in population is related to the expansion of vineyards and olive groves to poorer, inland mountainous areas. All of this would suggest that the land area devoted to farming reached its peak in Catalonia in the mid-nineteenth century (Congost, 1999).

Such demographic expansion allowed the entire population to grow, and especially agricultural workers, salaried farmers and labourers, who earned a living by doing temporary work (quarries, forests and crops). These workers either owned nothing (had no land) or they had very small properties (small plots), and were forced to perform temporary, precarious, irregular work. This socioeconomic situation underlies the agricultural transformation of the area of la Garriga d'Empordà formed by several municipalities (Avinyonet de Puigventós, Vilanant, Llers...), characterized by being relatively flat (between 125 and 218 m above sea level), classified as dry and low rainfall (between 400 and 1,000 l/m<sup>2</sup> per year), mostly covered in stone (limestone), located near the sea (20 km) and exposed to the north wind (that can reach speeds of 130 km/h).

It should be noted that this agricultural transformation (mass planting of vineyards and olive groves) took place through interventions in small-scale farms. Each such property was transformed and farmed by a labourer who either owned or leased the land. Such agricultural organization lasted until the late nineteenth century, which is when olive trees completely replaced vineyards as a result of the arrival of the phylloxera plague (in 1879). The predominant olive cultivation continued until the mid-twentieth century when these microcrops started to be abandoned, again for socioeconomic reasons.

The consequences of this agricultural intervention at la Garriga d'Empordà (**Fig. 1**), in the nineteenth and in the first half of the twentieth centuries, was the creation of surprising historical heritage made of retaining walls and dry-stone walls as well as vineyard huts and access roads made implementing the dry-stone construction technique. Undoubtedly, upholding the dual, material and mental function of this surprising agricultural transformation (both due to its extent and speed of execution) especially requires answering the questions: What was the influence between legislation and the democratization of property? What is the significance of the variable geometry of the space - territory-? How does the dry-stone construction technique revalorize the territory? What psychological ties between the person who transforms and the landscape transformed last in time?

It should be noted that this agricultural transformation (mass planting of vineyards and olive groves) took place through interventions in small-scale farms. Each such property was transformed and farmed by a labourer who either owned or leased the land. Such agricultural organization lasted until the late nineteenth century, which is when olive trees completely replaced vineyards as a result of the arrival of the phylloxera plague (in 1879).



**Fig. 1.** Situation and location of la Garriga d'Empordà (drawing R. Ripoll, private archive, 2020).

The predominant olive cultivation continued until the mid-twentieth century when these microcrops started to be abandoned, again for socioeconomic reasons. The consequences of this agricultural intervention at la Garriga d'Empordà, in the nineteenth and in the first half of the twentieth centuries, was the creation of surprising historical heritage made of retaining walls and dry-stone walls as well as vineyard huts and access roads made implementing the dry-stone construction technique. Undoubtedly, upholding the dual, material and mental function of this surprising agricultural transformation (both due to its extent and speed of execution) especially requires answering the questions:

What was the influence between legislation and the democratization of property?

What is the significance of the variable geometry of the space -territory-?

How does the dry-stone construction technique revalorize the territory?

What psychological ties between the person who transforms and the landscape transformed last in time?

In terms of practical research, a large number of general, simply descriptive studies have been performed in most countries including Italy, France, Germany, Ireland, Croatia, Cyprus, Greece, Malta, Catalonia, etc. (Miralles et al, 2002), with very partial, always fragmented contributions. Moreover, in terms of historical investigation, fewer studies have been conducted, though they go into greater depth. In the case of Catalonia concrete studies on land and areas of dry stone in the pre-industrial period are important and explain the circumstances behind the fortune amassed by farmers, the desire of temporary rural workers to have land, etc. (Congost & To, 1999). Meanwhile, there is a lack of studies that relate dry stone with the transformation of the landscape in the nineteenth century and the new cultural and personal relations with the region, barring highly isolated cases (McHarg, 2000). This situation amply justifies this research and its goal of relating practical, historical and cultural analysis with dry stone constructions at the same time. Thus, the aim is to provide new data on the dynamics of rural Catalonia in the nineteenth century and redefine social models (Congost, 2008). Also, based on unpublished sources, it seeks to look in greater depth into the importance of personal self-realization and psychological well-being of rural workers which, according to some authors, led to a new way of existence in the world (Aguiló, 1999). Thus arises the cultural concept of the place, according to Aristotelian thought of location mixed between private and common space (Artigas & Sanguinetti, 1993), both the result of territorial transformation and personal self-realization. This duality is advocated generally by some authors (Berque, 2009) or is intentional, according to other scholars (Ballart, 2018). Novel research, in view of the work conducted to date, anticipating such highly topical statements as equality between fieldwork and natural laws (Boada & Zahonero, 1999), the landscape as a system of organized, interacting elements (De Bolós, 1992), multi-sensory presence in territorial transformations at the beginning of the modern era (De Castro, 1997), and even the superimposition of various levels in regional life: natural, agricultural, social and personal (Berque, 2009). Specifically, the 316 plots of our selected sample have been studied, and their perimeter geometrical characteristics have been studied (shape, surface area and elevations), as well as the constructive characteristics of their dry stone walls (shape, length and thickness). These data describe the types of plots and their location. This work method has been based on the consultation of sources such as: cadastral plans, graphic documentation of the Cartographic Institute of Catalonia, aerial photographs from different years, as well as direct surveys of multiple dry stone constructions. The plans presented were made specifically by the team that drafted this article without resorting to any external references. On a theoretical level, the entire Comptadoria d' Hipoteques property register of the Girona Archive has been trawled to obtain plot lease contracts in the nineteenth century in La Garriga d'Emporda (tenant name, place of origin, cost, years of lease, leased surface area, etc.).

### **3. DEMOCRATIZATION OF PROPERTY (BENEFICIAL OWNERSHIP AND LEASE)**

Catalan law dating back to the early medieval period extends up to the nineteenth century. This is first through emphyteusis (Congost, 2010), or the purchase of a small rural property, and second through contracts for the lease of a piece of land. Thus, the first legal means available to the farm labourer or small farmer to access land (from the late medieval to well into the contemporary era) is certainly the purchase of the beneficial ownership of a small agricultural property. In this case the landlord, who owns a large expanse of land (legal title), grants unlimitedly, perpetually or over a very long time, a piece of land to the buyer worker or farmer to work, farm and use it (beneficial ownership) in exchange for an annual payment or emphyteutic lease (according to the Arbitral Decision of Guadalupe of 1486 that allows unlimited beneficial ownership).

Thus, the two types of owners (title and beneficiary) do not cancel each other out but rather complement each other. The complexity of this system, the lack of the landlord's control over the

farmers, as well as political, social and economic changes over the centuries all favoured farmers enjoying beneficial ownership and harming the interests of the legal title-holding landlords. And it is precisely in this general decline of legal title to property that most mass sales took place (medium- and small-sized parcels of land) with beneficial ownership rights to farm workers and small farmers of small pieces of land in la Garriga d'Empordà. Specifically, the cadastral register of 1736 declares 7,350 m<sup>2</sup> (3.5 vessanes) of olive trees and 39,900 m<sup>2</sup> (19 vessanes) of vineyards, and similar amounts are declared in 1808. However, by 1826 12 times more was declared (567,000 m<sup>2</sup>, or 280 vessanes) between vineyards and olive trees in the area of la Garriga d'Empordà. (Fèlix, 2012). The second legal means of access is through the traditional lease of a piece of land. In this case it is usually rented from the farmer of the beneficial ownership that has excess farmland or waste land and forests. In the case of la Garriga d'Empordà, leases of medium- and small-sized plots of land were practised (Congost, 2010). Among the most important properties in the area, we must mention Comella farm, in Vilanant, as an example of the management and sale of the beneficial ownership of plots in la Garriga d'Empordà. The management of land lease is also very significant of Mas Molar farm, in Llers, from the mid-nineteenth century, and is still clearly visible today. In this case, 28 rectangular parcels can be identified with a width: depth ratio of 1:2.5 to 1:3.5 (1:3 on average) and surface areas ranging from 5,634 m<sup>2</sup> to 9,368 m<sup>2</sup> (averaging 7,754 m<sup>2</sup>). Specifically, it is documented that in the mid-nineteenth century (26-10-1851) the owner of Mas Molar (Antoni Molar) leased eight parcels for a short time (five years) to different villagers (**Fig. 2**). The description of the rental sets out that seven of them have a surface area of three vessanes and one has four (always with the wording "more or less") (AHG, 1841-1862).

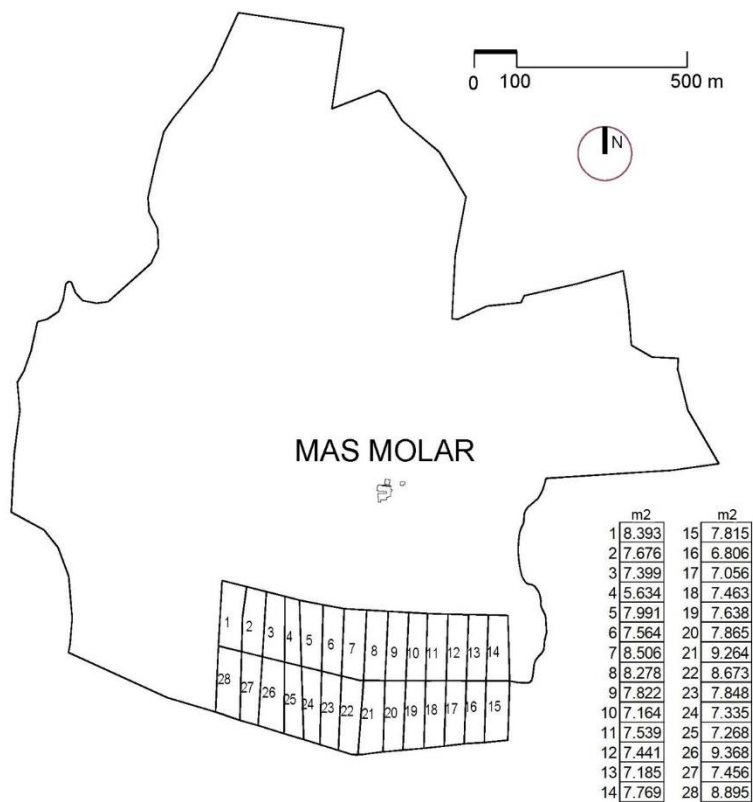


**Fig. 2.** Plot plan of Mas Molar in the mid nineteenth century (drawing R. Ripoll, private archive, 2020).

#### 4. VARIABLE GEOMETRIZATION (TRADITIONAL LANDSCAPE)

The facilities for buying or renting rural farmland in the nineteenth century in la Garriga d'Empordà are what led to the unique organization of this landscape (variable geometry). It was the result of a new type of landscape that developed between tradition and modernity, and is characterized by being dynamic (Bolòs, 2004), influenced by the organic evolution of social, economic, political and legal aspects and allowing continuous self-management; complex (Chouquer, 2000), defined due to reasons of geography, orientation and history that provide a wealth of morphology; and especially beneficial (Aston & Philpin, 1988), based on the demand for land by rural workers that benefits variable incomes (beneficial ownership) and harms fixed incomes (legal title ownership).

Geometric freedom and territorial fragmentation, typical of the traditional world, serving the needs of each user in a direct, simple and measured manner. The morphological study area is specifically the central part of la Garriga d'Empordà (6,338,138 m<sup>2</sup> or 633 hectares). This area includes 316 properties (according to the current cadastre of 2020). The surface area of each farming unit is the result of the balance between supply and demand as well as productivity and financial cost of buying or renting. The harmonization of these four variants is what mainly defines their size. Thus, the most common plots are small (149 plots) of a surface area ranging from 2,100 to 10,500 m<sup>2</sup> (1 to 5 vessanes), followed by medium-sized plots (90 plots) whose surface area ranges from 10,500 to 21,000 m<sup>2</sup> (5 to 10 vessanes). To a lesser extent we find very small parcels (30 plots) of less than 2,100 m<sup>2</sup> (1 vessana) and large plots (47 plots) over 21,000 m<sup>2</sup>. These sizes are intended to cover family consumption with surpluses being sold locally (**Table 1**). Most plot boundaries are marked by dry stone walls between 0.5 to 1 m in height.

**Table 1.**

**Parcel surface characteristics**

PLOTS (2.100 m <sup>2</sup> = 1 "vessana")	MUNICIPALITIES						TOTALS	
	Avinyonet		Llers		Vilanant			
	ut	m <sup>2</sup>	ut	m <sup>2</sup>	ut	m <sup>2</sup>	ut	m <sup>2</sup>
LARGE > 21.000 m <sup>2</sup> ( >10 "vessanes")	11	506.468	20	2.545.890	16	989.010	47	4.041.368
MEDIUM: 10.500 to 21.000 m <sup>2</sup> (5 to 10 "vessanes")	20	307.788	48	699.782	22	297.590	90	1.305.160
SMALL: 10.500 a 2.100 m <sup>2</sup> (1 to 5 "vessanes")	56	332.518	38	278.999	55	340.638	149	952.155
VERY SMALL < 2.100 m <sup>2</sup> ( <1 "vessana")	14	18.303	4	8.172	12	12.980	30	39.455
	101	1.165.077	110	3.532.843	105	1.640.218	<b>316</b>	<b>6.338.138</b>

With regard to topography, there is a direct relationship between the gentle relief of la Garriga d'Empordà and the morphological organization of the plots. These parcels' contours range from 150m to a height of 218m above sea level (**Fig. 3**). Most plots are established in areas of little gradient ranging between 2 and 10% (approximately three-fifths). The remainder are established on land on more pronounced gradients of between 10 and 20% (approximately one-fifth) and the rest on slopes exceeding 20%. In the latter case, the areas of greatest gradient, or areas with torrents, the gradient may range from 45 to 65%, a feature that prevents the construction of terraces. At some points, there is a greater relationship between topography (contour) and plot (property shape). In this regard the relationship should be noted between the highest point in the area (118.2 m) and the 11 plots occupying it (around plots LL-63 and LL-64). Generally, gradients are smoothed by earth-retaining dry-stone walls of 0.5 to 1 m in height.



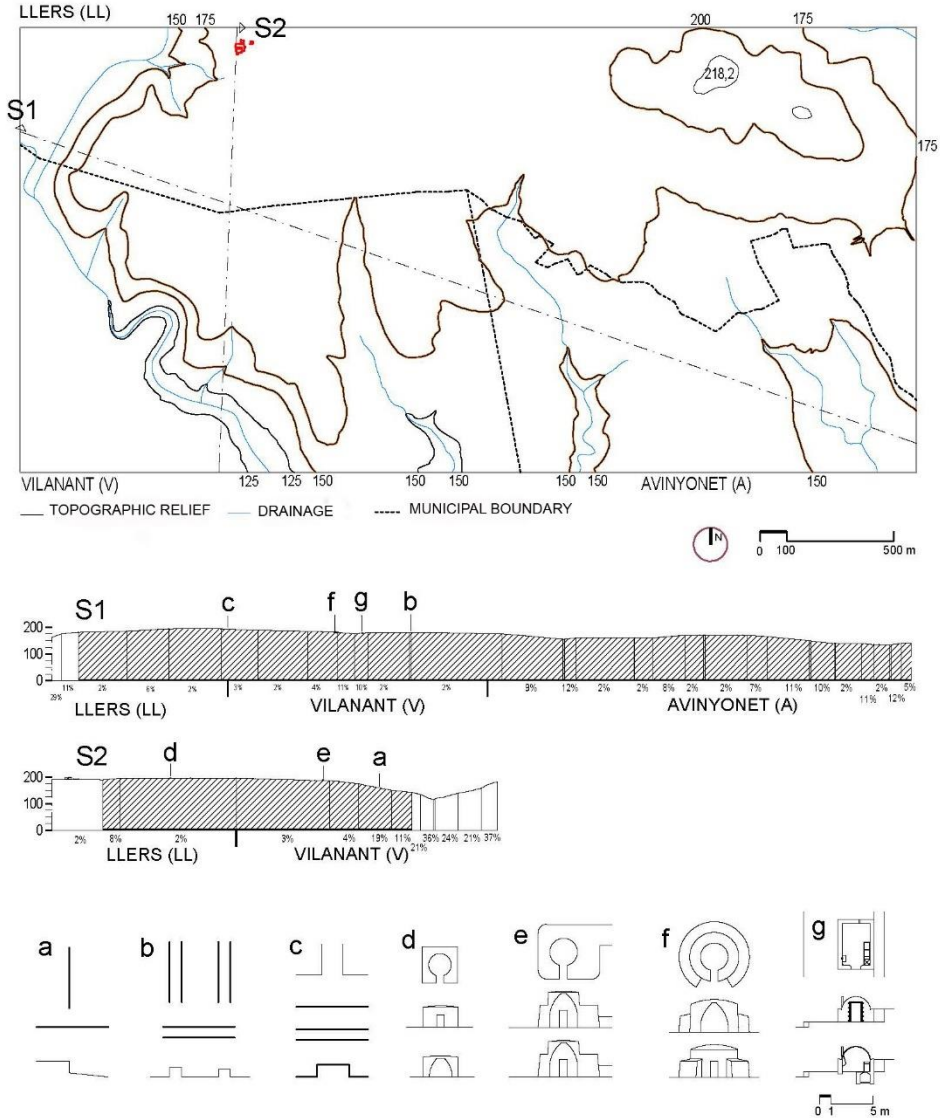


Fig. 3. Topographical study (drawing R. Ripoll, private archive, 2020).

Road access to the different properties is a third important aspect of the definition of variable morphology. We can identify one main road (wider than 3 m) that connects the villages of Llers and Avinyonet de Puigventós (6 km long). Along this length (north to south) 37 plots (12%) are organized and have access, creating an obvious morphological dependence between the shape of the plot and the road. The secondary roads (between 1.5 and 3 m wide) link most plots and are public. Most of these roadways are marked by dry stone walls of between 0.5 and 1 m in height. A third type of tertiary roadways (less than 1.5 m wide) provide access to the most isolated plots and arise from private agreements of passage between owners, or they take advantage of water drainage areas as thoroughfares. Finally, there is clear relationship between the municipal boundary line and the morphology of the plots that align with it. In this sense a total of 85 plots are recorded. So, the alignment of nearly one-third of properties (27%) coincides with the municipal boundary line (Fig.4).

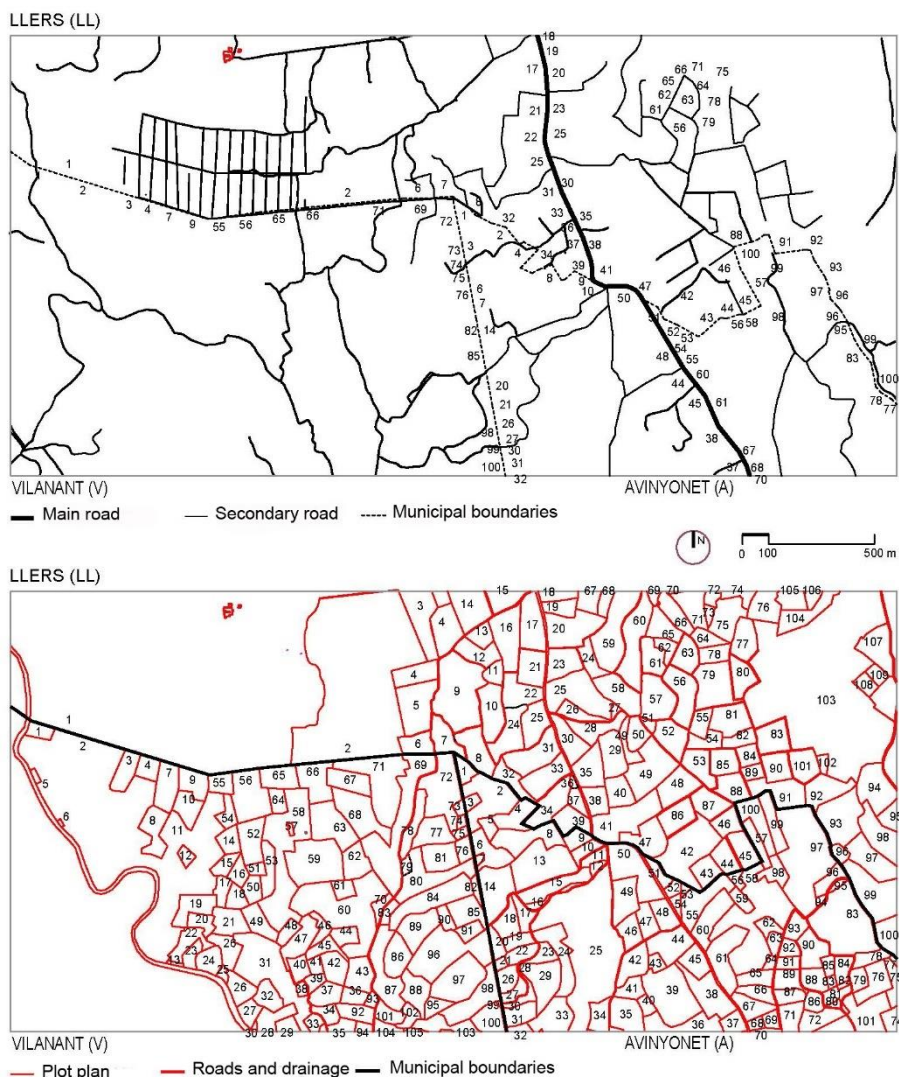


Fig. 4. Study of plots (drawing R. Ripoll, private archive, 2020).

## 5. CONSTRUCTION TECHNIQUE (DRY STONE)

The relationship between construction technique and the spatial organization of each plot is also evident. In this case, it is the owner or lessee of each parcel that examines, decides and carries out such organization. This self-build construction directly fuses agricultural function and construction technique. The technology used for construction creates retaining walls to facilitate the accumulation of earth, boundary walls to facilitate the accumulation of surplus stone, corbel vaults that facilitate the creation of domes with rings of horizontal stones that close successively, and finally vaults formed by an arch of dry-stone forming voussoirs, etc. These vaults allow building shacks for shelter against bad weather, especially for workers who are from neighbouring villages. The most common tools for working with dry stone are the mallet and the iron bar. These constructions were built by the owners and lessors of the piece of land themselves. Thus, the most common system of construction was self-build, and the more experienced labourers even helped build walls and huts for other owners.

The walls are begun directly on the ground, previously removing the surface layer of the terrain. They are erected with a slight slope on one side (earth retaining walls) or on both sides with rubble inside (in separating walls). In either case, the stones are each selected and placed geometrically to achieve maximum contact surface with each other, with the aid of wedges of smaller stones. In la Garriga d'Empordà, walls are not excessively high due to the slight gradients and the characteristics of the geometry of the stone, rendering it hard to position. Both its rounded shape and its high average compressive strength (66 Mpa) mean it is hard to work and hinder its direct use in construction. It should also be stated that there are no special additional elements in the walls as could be stairs, paving, doorways, ramps, etc. The role of the dry wall on each plot is clear (from 2 to 7 linear metres of wall per m<sup>2</sup> of plot) creating different, unique solutions and compositions on each plot (**Table 2**).

**Table 2.****Parcel construction features**

	TOTAL SURFACE AREA		FARMED AREA		FARMLAND DRY STONE WALLS		UPPER FARMED CONTOUR	LOWER FARMED CONTOUR	GRADIENT OF FARMED AREA	GRADIENT OF UNFARMED AREA	
	m <sup>2</sup>	m <sup>2</sup>	%	m	m/m <sup>2</sup>	m	m	%	%		
<b>d</b>	8.278	8.278	100	429	5	192,5	187,5	3	0	LL-1(8)	
<b>e</b>	266.907	182.481	100	3.344	2	193,0	176,0	4	51	V-11	
<b>f</b>	51.013	51.013	100	2.160	4	186,5	180,5	1	0	V-58	
<b>g</b>	21.554	21.554	100	1.501	7	184,5	170,5	6	0	V-68	

Most huts are built using a corbel vault. This is due to technical ease, the simplification of complementary means and speed of execution. Moreover, huts with vousoirs are located around quarry areas due to the availability of more skilled labour. Most of the huts have a circular interior floor plan (between 2 and 3 m in diameter) and are square as well as circular outside with thick walls (between 1 and 1.5 m). To improve the stability of the huts, buttress walls are built around them (between 0.8 and 1.5 m wide) and crowns that reduce the weight of the dome forming rings, etc. (**Fig. 5 & Fig. 6**).

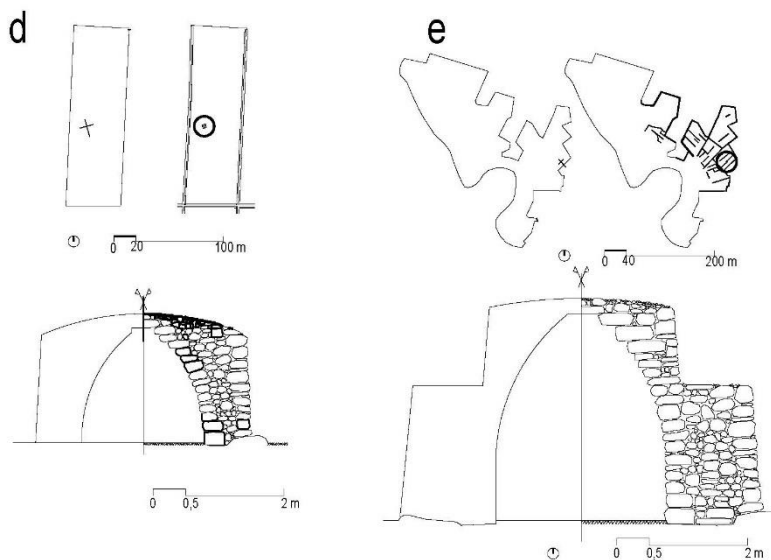


**Fig. 5.** Examples of constructions on plots d (LL-1(8)) and e (V-11)  
(Drawing: R. Ripoll, p. archive, 2020).

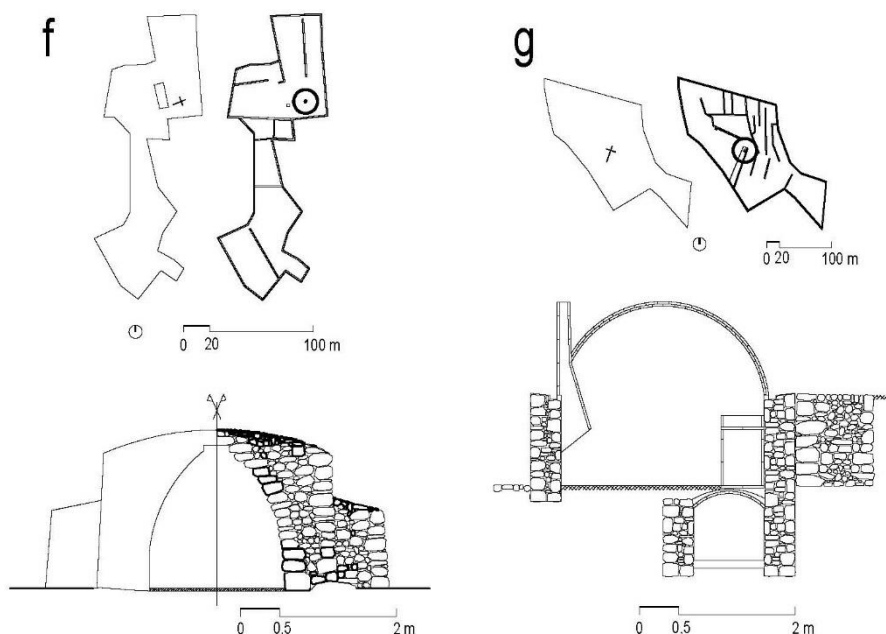


**Fig. 6.** Examples of constructions on plots f (V-58) and g (V-68)  
(Drawing: R. Ripoll, p. archive, 2020).

## 6. CONCLUSION

The relationship between traditional farmers and the physical characteristics of the site is clear and the building work carried out by farmers on the territory is demonstrated in this investigation. There is a direct relationship between the geographical environment, agricultural needs, local materials and technical means. This explains the coherent, cohesive, free and genuine morphology. Such a course of action involves some modification of the landscape and of the territory, like many places in the Mediterranean that have been developed in parallel and in similar fashion. The first conclusion is the importance of being familiar with, interpreting and using local stone which reduces transport costs (locally-sourced materials), production costs (the materials are used in their natural form), and the management and implementation time (self-building).

It can also be deduced that behind locally-sourced materials, natural forms and self-building, there is not just a material functional motivation (physical function) but also a personal motivation for self-realization (emotional function). We agree with authors that emphasize the self-management and self-confidence of traditional farmers (PLA, 1975, 156-7), but we disagree when this is limited to the merely mechanistic and economic aspect of the traditional agricultural landscape (PLA, 1968, 427). We can conclude that the harmonious, free transformation of landscape in la Garriga d'Empordà would not have been possible without deep (physical and mental) identification with the land. Then we can begin to say that the aesthetic of the enjoyment of the present landscape is rooted in the pre-industrial traditional world.

According to the results, it can be stated that in the nineteenth century many transformations of the territory imply clearly present-day landscape values: well-managed and ordered, organic and dynamic, heterogeneous and diverse, harmonious and free, singular and unique, or productive and aesthetic. Other values can also be found: deep-rooted and dynamic, calm and free, respectful and enigmatic, and above all, that contribute to individual and social well-being. Management of the territory based on self-building with concepts typical of construction, architecture and the contemporary landscape such as the expressive force of the gravity or heaviness of forms (Campo, 2010,) and the biodiversity generated by dry stone constructions (Llagostera, 2014).

These conclusions reaffirm that the transformation of la Garriga d'Empordà in the nineteenth century for poorer peasant families meant not only a minuscule means of material progress but above all a major means of social hope and human dignity.

## REFERENCES

- AHG, Comptadoria d'Hipoteques de Figueres (1841-1862). Girona: Arxiu històric de Girona.
- Aalto, A. (1977). La humanización de la arquitectura. Barcelona: Tusquets editores.
- Aguiló, M. (1999). El paisaje construido. Una aproximación a la idea de lugar. Madrid: Colegio de Ingenieros de caminos, canales y puertos.
- Artigas, M, Sanguinetti, J.J. (1993). Filosofía de la naturaleza. Pamplona: Eunsa.
- Aston, T.H., Philpin, C.H.E. (1988). El debate Brenner. Estructura de clase agraria y desarrollo económico de la Europa preindustrial. Barcelona: Novagràfik.
- Ballart, J. (2018). Paisaje y patrimonio. Madrid: Arqueología Editorial.
- Berque, A. (2009). El pensamiento paisajero. Madrid: Editorial Biblioteca Nueva.
- Boada, M., Zahonero, A. (1999). Media ambient. Una crisi civilitzadora. Barcelona: Edicions de la Magrana.
- Bolós, J. (2004). Els orígens medievals del paisatge català. L'arqueologia del paisatge com a font per a conèixer la història de Catalunya. Publicacions de l'Abadia de Montserrat. Barcelona.
- Campo, A. (2010) Pensar con las manos. Buenos Aires: Editorial Nobuko.
- Chouquer, G. (2000). L'étude des Paysages. Essais sur leurs formes et leur histoire. Paris: Edicions Errance.
- Congost, R. (2008). Història agrària dels Països Catalans. Barcelona (III). Edicions de la universitat de Barcelona.
- Congost, R. (2010). La pedra seca. Evolució, arquitectura i restauració. Figueres: Brau edicions.
- Congost, R., To, Lluís (1999). Homes, masos, història. La Catalunya del nord-est (segles X-XX). Barcelona: Publicacions de l'Abadia de Montserrat.
- De Bolós, M. (1992). Manual Ciencia del Paisaje. Teoría, étodos y aplicaciones. Barcelona: Editorial Masson.
- De Castro, C. (1997). Geografía en la vida cotidiana. De los mapas cognitivos al prejuicio regional. Barcelona: Ediciones del Serbal.
- Fèlix, J. (2012). Les barraques de pedra seca de la Garriga d'Empordà. Figueres: Brau edicions.
- Llagostera, S. (2014). VII Trobada d'estudi per a la preservació de la pedra seca als Països Catalans. Olot: Patronat d'Estudis històrics d'Olot i Comarca.
- McHarg, Ian. (2000). Proyectar con la naturaleza. Barcelona: Gustavo Gili
- Miralles, F., Marín, M., Montfort, J. (2002). Els homes i les pedres. La pedra seca a Vilafranca (Castelló): Un paisatge humanitzat. Castelló: Diputació de Castelló.
- Pla, J. (1968). Viatge a la Catalunya Vella. Barcelona: Edicions Destino.
- Pla, J. (1975). Els pagesos. Barcelona: Edicions Destino.
- Terrades, I. (1984). El món històric de les masies. Barcelona: Curial.

## FLOOD RECONSTRUCTION OF 1<sup>st</sup> JANUARY 2020 STORM IN AN URBAN HOUSING AREA OF TANGERANG SELATAN, INDONESIA

Marelianda AL DIANTY<sup>1</sup>, Frederik J. PUTUHENA<sup>2</sup>, Darrien Y.S. MAH<sup>3</sup>,  
Rosmina A. BUSTAMI<sup>3</sup>, Fachrian KANAFANI<sup>4</sup>

DOI: 10.21163/GT\_2021.162.14

### ABSTRACT:

The storm in the early hours on the first day of 2020 had recorded the highest intensity of rainfall since 1996. It deluged Jakarta as the capital city of Indonesia and the surrounding satellite cities which including Tangerang Selatan. An urban housing area in Tangerang Selatan, located adjacent to the Ciputat river is selected as study area. The area was affected by floods since the urban housing was established. The United States Environmental Protection Agency's Storm Water Management Model version 5.1 was used for finding out the hydrological and hydraulic problems. The model indicated that the flows from the sub-catchments did not contribute to cause flood. It was discovered that backwater effects occurred in the Ciputat river was the main cause of flooding. Thus, the existing drainage channels were overwhelmed by additional flow from the river.

*Key-words:* Drainage, Reconstruction, Runoff rainfall, SWMM, Backwater.

### 1. INTRODUCTION

An extraordinary storm on 1<sup>st</sup> January 2020, hitting Jakarta city had smashed the rainfall record in the Indonesian capital city for the last quarter-century. The intensity of rainfall was due to monsoon season and a high amount of water vapour in the air. It was recorded at least dozens had been killed and 60,000 displaced. Flash flood had occurred in several urban areas with flood depths ranged at 30-70 cm. The water level reading of the Ciliwung River that passes through the Jakarta city were reaching up to the level of 860 cm that indicated second-level alert status. About 75 percent of the houses close to the Ciliwung riverbanks, and 25 percent in the basin areas were flooded. The occurrence of the flooding was pointed to two factors, likely narrowing of the river and poor urban drainage. This can be proven from the early warning system in the downstream dam did not enter an alert status when the upstream effected area and its surroundings began to be flooded.

Flash floods are generally caused by excessive rainfall in a short and intensive-phase storm (Tarasova et al., 2019; Zanchetta and Coulibaly., 2019). It is relatively little in terms of the number of human deaths (Bryndal et al., 2017). Diakakis et al. (2019) had reported a flash flood in the urban area in Greece, known as a tragic disaster, had caused the loss of 24 people, making it the deadliest flood in a period of 40 years. Subsequently, Paprotny et al. (2018) reported that high flood losses in 37 European countries had prompted the creation of a new database of damaging floods since 1870. Barichivich et al. (2018) had reported that historical extreme flooding in the Amazon region was a combination of Atlantic warming and Pacific cooling. Akter et al. (2020) had reported that Chittagong city in Bangladesh experienced regularly flooding during monsoon seasons. Prior to this, Borga et al. (2014) presented that flash flood in the Italian Alps region, it was more frequent and destructive due to climate change.

---

<sup>1</sup>Department of Engineering Project, Geohydra Consulting Group, Jakarta, Indonesia, [aldianty@geohydra.com](mailto:aldianty@geohydra.com)

<sup>2</sup>Center Urban Studies, Universitas Pembangunan Jaya, Tangerang Selatan, Indonesia, [fj.putuhena@upj.ac.id](mailto:fj.putuhena@upj.ac.id)

<sup>3</sup>Faculty of Engineering, Universiti Malaysia Sarawak, Kota Samarahan, Malaysia, [ysmah@unimas.my](mailto:ysmah@unimas.my),  
[abrosmina@unimas.my](mailto:abrosmina@unimas.my)

<sup>4</sup>PT. Maju Total Persada, West Jakarta, Indonesia, [fachrikanafani@gmail.com](mailto:fachrikanafani@gmail.com)

Urban drainage is a component in housing planning and one of the basic facilities designed to meet the needs of the community. As mentioned by Burian and Edward (2015), urban drainage is an important aspect that must be built for water and waste runoff media that must be well designed to accommodate rainwater and prevent flooding. As well, Patrick et al. (2019) defined a good drainage system should be able to accommodate as much water discharge as possible. So, if the water discharge exceeds the estimate planned at the initial stage, the drainage will accommodate poorly the function and drain it. It takes a few minutes to several hours for the floodwaters to drain and the rainwater returns to the sewers and the floodwaters are slowly subsided. Although it can be resolved in a short time, it causes inconveniences for instance traffic jams, property damage and some cases human lives (Mah et al., 2020). Besides, the increasing urban population that continues to increase in a relatively short time period, requires good facilities and infrastructure. An increasing population is followed by the amount of waste, both in the forms of garbage and liquid waste (Honihg et al., 2020). If it is not reinforced by an adequate drainage channel thus it will cause water overflowing the channel at times of high flow events. Apart from water conveying, the drainage is also used for bathing, washing, cooking and other human activities (Wu et al., 2020).

Storm Water Management Model (SWMM) is a drainage modelling platform, in which the model could simulate and observe flooding in urban areas (Akter et al., 2020). As identified by Mah et al. (2019), SWMM version 5.0 was used to conduct modelling of a residential-based drainage system that incorporated with a stormwater detention system. Conversely, Al Dianty (2020) used SWMM to find effective drainage using the Bio pore Infiltration Hole (LRB) that was built in an urban area to absorb a flood discharge of about 0.3282 m<sup>3</sup>/s. This model simulated the conditions and natures of the infiltration to calculate the discharge of flood in eight rain events in urban areas, hence, to prevent extreme rainstorms (Bai et al., 2019). As well, Arjenaki et al. (2020) used SWMM to test Low Impact Development (LID) measures subjected to hydrological analyses in return periods of 2, 5, and 10 years

This research is intended to do SWMM simulation and thereafter evaluation of the tremendous flooding of 1<sup>st</sup> January 2020 in an identified effected urban area. Furthermore, the direction of the research is to perform the assessment on the suitability between discharge and volume of drainage channels which is recommendatory for solving the urban drainage problems (Brown and Borst., 2016; Akter et al., 2020; Al Dianty., 2020).

## 2. MATERIALS AND METHODS

### 2.1. Study Area

An urban housing area located in Ciputat District, Tangerang Selatan, Indonesia was identified as study area (**Fig. 1**). Residents of the area have been suffering from repeating flood. The drainage conditions in the area are no longer able to drain runoff effectively into the existing drainage system. The drainage conditions and dimensions of the urban housing drainage channel are depicted in **Table 1** and **Fig. 2**.

The urban housing area has  $\pm$  600 units of houses with an area of  $\pm$  15.44 ha. Flooding in the area was recorded in January 2013, January 2014, and most recently, January 2020. Reconstruction of the January 2020 flood was done during the pandemic Covid-19 period. The data were collected and prepared through direct observation, interviews, field survey on the characteristics of housing area conditions, infrastructure, existing drainage, and road conditions.

The variables used in the study included (1) physical conditions of drainage (drainage plan, channel conditions and network patterns), (2) Non-physical conditions (community behaviours and related governance), (3) Basic physical conditions of the area (slope, length, width, and rainfall data on January 1, 2020).





Fig. 1. Map of study area.



Fig. 2. Drainage condition.

**Table 1.**  
Dimensions of the urban housing drainage channel.

Type	Width (m)	Depth (m)
A	2	1.5
B	0.5	0.7
C	0.3	0.4

## 2.2. Intensity of rainfall

The intensity of rainfall is the input value in the form of time series, in which the Monobe Formula is used to calculate the concentration-time in each existing channel. The relationships between intensity, duration of rain and frequency of rain is usually expressed in terms of the Intensity-Duration-Frequency (IDF) curve as in Equation 1:

$$I = \frac{R_{24}}{24} \left[ \frac{24}{t_c} \right]^{\frac{2}{3}} \quad (1)$$

where

$I$  = intensity of rainfall (mm/hr);

$R_{24}$  = maximum daily rainfall for 24 hours (mm);

$t_c$  = time of concentration (s).

## 2.3. Rainfall Hyetograph

Rainfall hyetograph is a histogram of rainfall with intervals of time as abscissa and rain depth as ordinate. The hyetograph data are inputted into the SWMM model for drainage modelling. While beforehand, the Alternating Block Method (ABM) is a simple way to create a hyetograph plan from the IDF curve (Yen and Chow, 1980). The method is designed for the distribution of average rainfall intensity over time of storm. The hyetograph produced by this method is the rain that occurs in  $n$  series of consecutive time intervals with a duration is 1 hour for time  $T_d = n \times \Delta t$ . Where  $t_c$  is the intensity of rainfall for the 24 hours of the yearly period in Eq.2. Finally, the hyetograph is ordered like a triangular curve.

$$\text{Hyetograph} = t_c \cdot it \quad (2)$$

where

$t_c$  = time of concentration (s).

$it$  = Intensity  $R_{24}$

## 2.4. Drainage Modelling

SWMM drainage modelling was started with sub-catchment analysis. It was carried out by using Google Earth, considering several variables such as area (in hectares), lowest elevation, highest elevation, width, and % slope. The Google application assisted in determining the total area, sub-catchment area, pervious and impervious coverage. Water tightness in each sub-catchment was investigated so that the land use was designated as a settlement and the concrete lining was about 15%. The hyetograph data mentioned above was inserted to the rain gauge interface as a provider of precipitation data for one or more sub-catchments in the study area. The type of rain gauge was specified. Then, junctions were digitized into the modelling platform where these were to display the connections of the channels. It also displayed the meeting of the artificial channel with the natural channels such as a river or stream. Data like the length of the main channel was taken from Google Earth, which was presented in 80 junctions and one outfall. Next, links were digitized to represent conduits for the water flows and the variables such as shape, maximum depth, length, and roughness. The links had different properties, depending on the site conditions. These links were connected by junctions in each existing sub-catchment. We used a value of 0.02 for the conduit's roughness coefficient because generally, most conduits are made of concrete that had rough surfaces on the conduits. The SWMM's hydraulic simulation engine was based on Manning equation (Bellos et al., 2018). It was a function of relationships between discharge ( $Q$ ), cross-sectional area ( $A$ ), circle radius ( $R$ ), and slope ( $S$ ). Furthermore, it could perform checking on drainage capacity. If it predicted a conduit was flooded, it means that the capacity of the conduit was unappropriated. In this regard, the dimensions of the conduit was modified and the simulation was reran until an appropriate dimension was found.

### 3. RESULTS

#### 3.1. Determination of Rainfall Intensity

The calculation was carried out by processing the maximum amount of rainfall intensity on 1<sup>st</sup> January 2020 which was found as 377 mm/hr. It was designed as daily rainfall in **Table 2**. As identified by Al Dianty et al. (2020), the shorter of the rainfall, the higher the intensity of rainfall as well as the greater of return period, the higher the intensity of rainfall.

**Table 2.**

**Intensity of rainfall.**

Time (Hour)	R24	Time (Hour)	R24
	377 mm/hour		377 mm/hour
0.116	431.557	11	26.425
0.231	271.864	12	24.935
0.347	207.471	13	23.640
0.463	171.264	14	22.500
0.578	147.591	15	21.489
1	130.699	16	20.584
2	82.335	17	19.768
3	62.833	18	19.029
4	51.868	19	18.356
5	44.698	20	17.739
6	39.583	21	17.171
7	35.717	22	16.646
8	32.675	23	16.160
9	30.207	24	15.708
10	28.158		

#### 3.2. Determination of Rainfall Hyetograph

Based on ABM mentioned in Section 2.3, the peak hyetograph was found at 71.926 mm, as well presented in **Fig. 3**. It represented the characteristics of an extreme flood. The method that was demonstrated here endorsed a synthetic hyetograph in a dimensionless form in different durations, as reported by Ellouze et al. (2019).

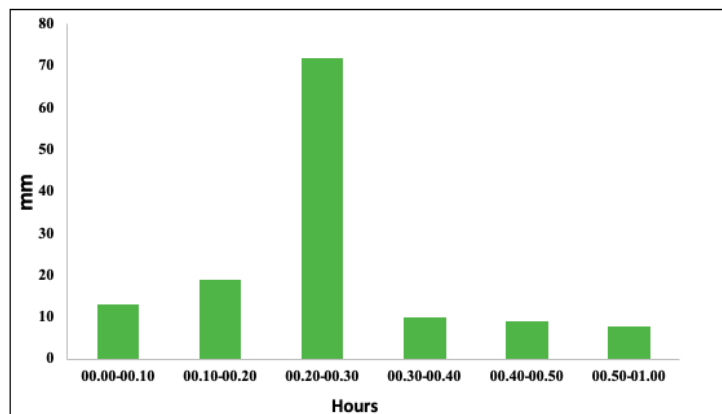


**Fig. 3.** Rainfall Hyetograph.

### 3.3. SWMM Modelling Outcomes

The drainage modelling was carried out after the hydrological analysis and hydraulic process were completed. The study area was divided into 43 sub-catchments, while the drainage system was represented in 80 junctions, 80 conduits and 1 outfall. The big number of the mentioned components was to mimic the actual values in the study area as much as possible. Furthermore, to run the simulation, an error rate should be less than 10%. The developed SWMM model was found with an error value about -0.51% for surface runoff and -0.02% is for flow routing. The results of the simulation indicated that the drainage channels are still capable to accommodate the runoff. It can be observed in **Fig. 4**. On another note, there was high peak runoff from the surface runoff in **Fig. 5**.

The peak runoff that occurred in the 4<sup>th</sup> hour in the sub-catchment 1 until sub-catchment 43 was estimated at 0.09 m<sup>3</sup>/s (**Fig. 5**), while the maximum simulation occurred in the first hour where it is 0.02 m<sup>3</sup>/s.

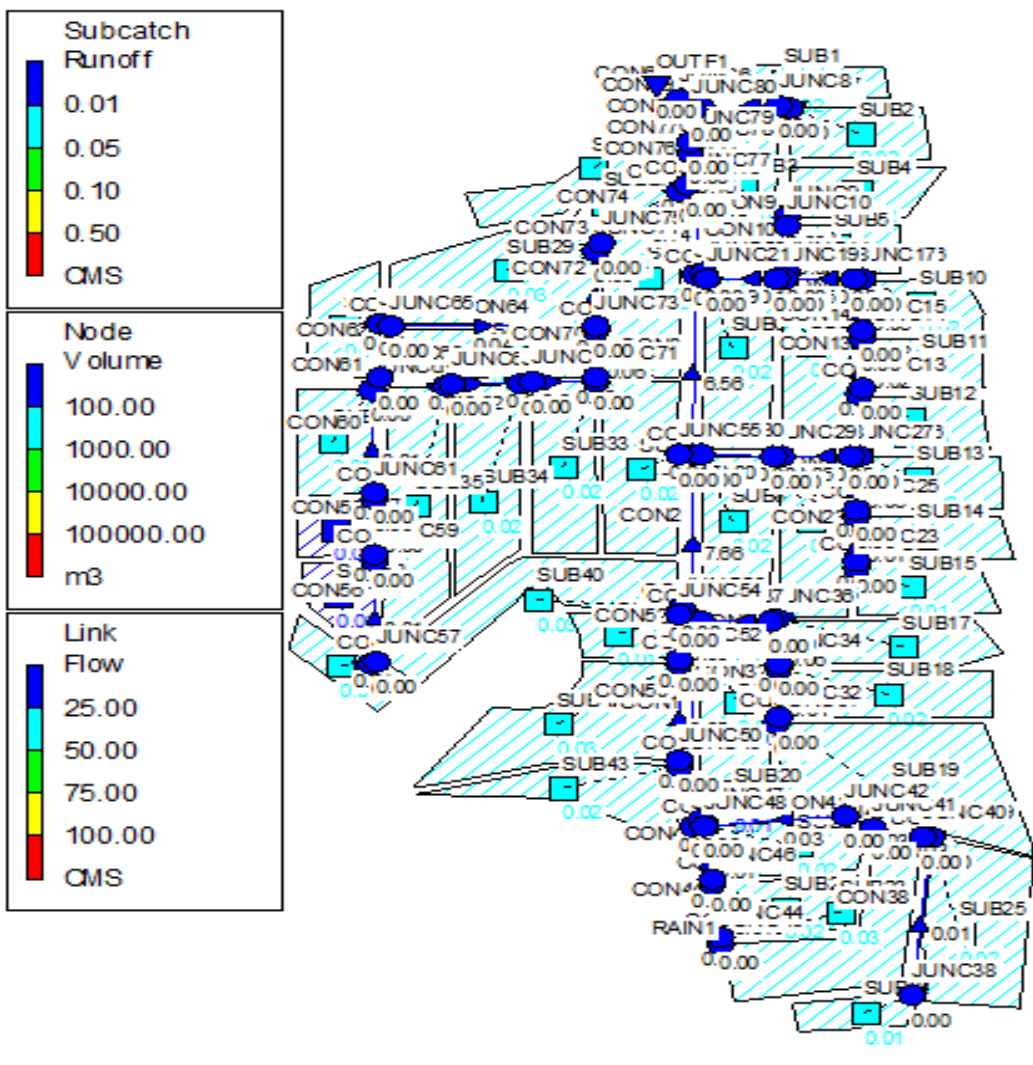


**Fig. 4.** Sub-catchment Simulation Area.

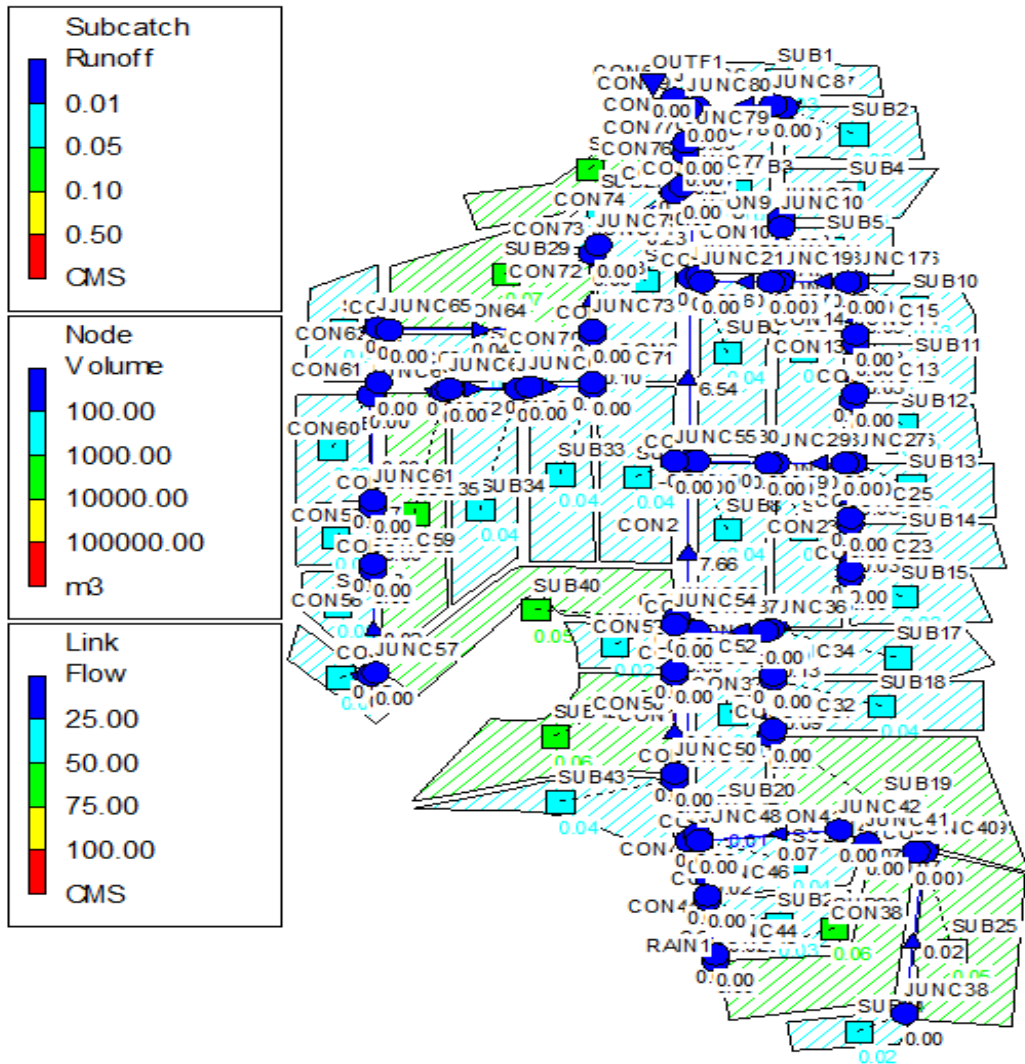


Fig. 5. Runoff Sub catchment.

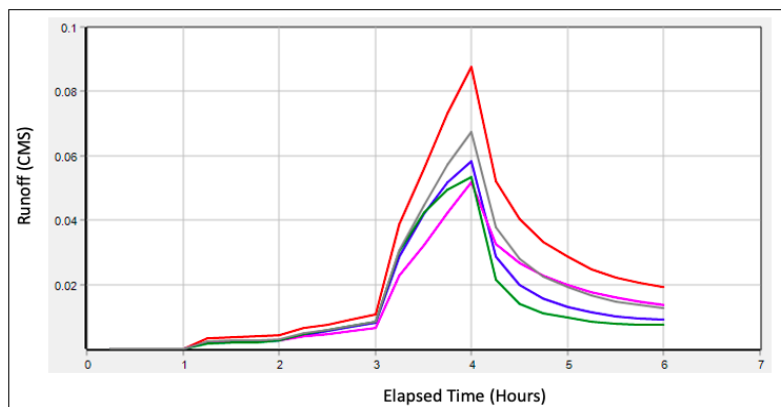
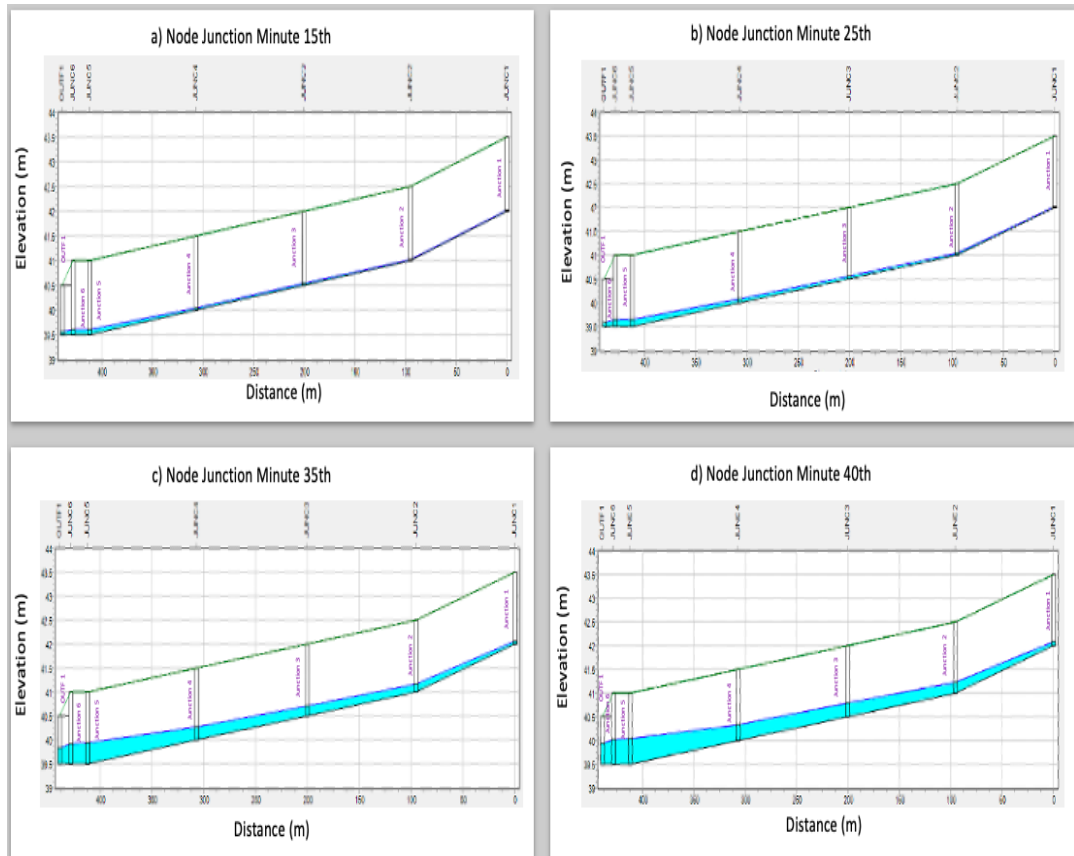


Fig. 5. Runoff Simulation.



The simulation was continued on 15<sup>th</sup> minute – 40<sup>th</sup> minute runoff flow for long node junction namely junction 1, junction 2, junction 3, junction 4, junction 5, junction 6, and outfall 1, it is presented in **Fig. 6**. It was done after obtaining runoff discharge from each existing sub-catchment. The dimensions used in the simulation were about 2-meter width and 1.5-meter depth. The highest water level occurred between 35<sup>th</sup> and 40<sup>th</sup> minutes was about 50 cm. It was found that the runoff flow in the main channel was not fully filled.



**Fig. 6.** Long node junction at minute 15<sup>th</sup> – 40<sup>th</sup>.

### 3.4 Discussion

The condition of the drainage channel greatly affects the smooth flow of water, if there is a blockage in one of the drainage networks, there will be a reduction of water storing capability in the drainage channels. Therefore, the authors focus on the active processes of the urban flash floods through analysis and simulation modelling. The site surveys did not find anything that could disrupt the water flow in the existing drainage channels. However, photographs taken during the 1<sup>st</sup> January 2020 flood event showed there were overflow in main channel junctions 1 and 2 (**Fig. 7**).

As explained by Mahmoodian (2018), urban drainage modelling needed the development of sophisticated simulators due to the various underlying surfaces and drainage processes. Zhou et al. (2016) demonstrated the flood simulation models required a four-step phases, namely (1) selection of roughness zones; (2) generation of synthetic data from water depth, flow, velocity, and roughness height combinations; (3) calculation of shear stresses using a physically based equation; and (4) estimation of the model parameters through regression.

Whilst other key aspects of modelling were discussed by Tarasova et al. (2019) who had justified multicriteria approaches which were needed seasonal classifications between effects and causative mechanisms. Meanwhile, the recent modelling distinguishes Mignot et al. (2020) by laboratory probation in a single street intersection, surface-sewer exchanges, the array of obstacles and quasi-realistic urban districts.



**Fig. 7.** Floodwater Overflow taken on 1<sup>st</sup> January 2020.



**Fig. 8.** Backwater in Ciputat River taken on 1<sup>st</sup> January 2020.



The site surveys also did not find any illegal buildings along the Ciputat river. Therefore, there was no modification to the natural waterways that could invite flooding. Regarding the natural waterway modification, Haidu and Ivan (2016) demonstrated Digital Terrain Model and Digital Surface Model to examine the trend of increasing runoff volume. While Gibson et al. (2016) highlighted Cellular Automata (CA) as a simulation method based on an ordinary square grid, thereby saving set-up time for configuring terrain data into irregular triangular nets for urban surface flooding modelling.

Another discovery was coming from Ciputat river. The reduction of drainage dimensions had contributed to backwater effects in the main channel where it entered junction 1 until junction 6 towards the outfall shown in **Fig.8**. The back water has caused the existing branches and the storage channel could not drain the water because the trunk condition was full. This evidence showed the main channel of drainage was not enough to accommodate runoff from the sub catchment. In this situation, we proposed to perform urban drainage management. Bermudez et al. (2018) challenged the idea by real-time 1D-2D dual drainage model in terms of peak surface flood volume and maximum flood.

## 5. CONCLUSIONS

The flash flood on 1<sup>st</sup> January 2020 was recorded as the worst disaster of an urban housing in Tangerang Selatan, Indonesia since it was established. The maximum intensity of rainfall was about 377 mm/hr. The channel could not hold the backwater therefore no longer adequate to accommodate runoff from the sub-catchments. The result of main drainage connected by junction 1 until junction 6, there was no visible overflow on the channel. Likewise, other junctions that connect the branch and collection of conduits. Nevertheless, the modelling outcome showed the channel will be fully charged in the 35<sup>th</sup> and 40<sup>th</sup> minutes. The founding was based on the condition of the main channel was full; thus, the branches and connecting channels were obstructed to discharge water flow to the main channel. The rainfall-runoff problem can be controlled through a proper and adequate drainage system. Moreover, additional modelling of urban water management recommended to use for simulation comparison. The drainage system should have abilities to keep the areas from backwater, control the runoff, control channel surface wastewater due to the accumulation of rainfall-runoff.

## ACKNOWLEDGMENT

The authors acknowledge the Institute of Research and Community Service (LPPM), Universitas Pembangunan Jaya (UPJ) for the funding through internal grants - Tertiary Research Excellence with the title “Sustainable Drainage Systems” and International Matching Grant Scheme with Universiti Malaysia Sarawak (UNIMAS). We like to thank the Regional Meteorology, Climatology and Geophysics Agency (BMKG) of Tangerang Selatan and Pondok Hijau residents.

## REFERENCES

- Akter, A., Tanim, A.H & Islam, M.K. (2020) Possibilities of urban flood reduction through distributed-scale rainwater harvesting. *Water Science and Engineering*. 13 (2): 95 -105, DOI: <https://doi.org/10.1016/j.wse.2020.06.001>
- Al Dianty, M., Arbaningrum, R and Putuhena, F.J. (2020) The Linked of Effect Climate for Determining Design Flood of Tenggang River. *Geographia Technica*. 15: 3-12, DOI: [http://dx.doi.org/10.21163/GT\\_2020.151.17](http://dx.doi.org/10.21163/GT_2020.151.17)
- Al Dianty, M. 2020. Analysis of Bio pore Drainage System to Control the Floods in the urban cluster. *Technology Reports of Kansai University*. 62 (8): 4599 – 4609.

- Arjenaki, M.O., Sanayei, H.R.Z. Heidarzadeh, H. and Mahabadi, N.A. 2020. Modeling and investigating the effect of the LID methods on collection network of urban runoff using the SWMM model (Case study: Shahrekord City), *Modelling Earth Systems and Environment*. 7: 1-16, DOI: <https://doi.org/10.1007/s40808-020-00870-2>
- Bellos, V., Nalbantis, I., and Tsakiris, G. (2018) Friction Modeling of Flood Flow Simulations. *Journal of Hydraulic Engineering*, 144 (12): 1-10, DOI :[https://doi.org/10.1061/\(ASCE\)HY.1943-7900.0001540](https://doi.org/10.1061/(ASCE)HY.1943-7900.0001540).
- Barichivich, J., Gloor, E., Peylin, P., Brienen, R.J.W., Schöngart, J., Espinoza, J.C and Pattanayak, K.C. (2018) Recent intensification of Amazon flooding extremes driven by strengthened Walker circulation. *Science Advance*. 4(9): 1-7, DOI: <https://10.1126/sciadv.aat8785>.
- Bai, Y., Zhao, N., Zhang, R., and Xiaofan, Z. 2019. Storm Water Management of Low Impact Development in Urban Areas Based on SWMM. *Water*. 11(1): 33-49, DOI: <https://doi.org/10.3390/w11010033>
- Bermudez, M., Ntegeka, V., Wolfs, V and P.Willems. (2018) Development and Comparison of Two Fast Surrogate Models for Urban Pluvial Flood Simulation. *Water Resources Management*. 32: 2801-2815, DOI: <https://doi.org/10.1007/s11269-018-1959-8>
- Borga, M., Boscolo, P., Zanon F and Sangati, M. (2014) Hydrometeorological Analysis of the 29 August 2003 Flash Flood in the Eastern Italian Alps. *Journal of hydrometeorology*. 8 (5): 1049 – 1061, DOI: <https://doi.org/10.1175/JHM593.1>
- Bryndal, T., Franczak, P., Krocak, R., Cabaj, W and Kołodziej, A. (2017) The impact of extreme rainfall and flash floods on the flood risk management process and geomorphological changes in small Carpathian catchments: a case study of the Kasiniczanka river (Outer Carpathians, Poland). *Natural Hazards*. 88: 95–120, DOI: <https://doi.org/10.1007/s11069-017-2858-7>
- Brown, R.A., and Borst, M. (2016) Evaluating the Accuracy of Common Runoff Estimation Methods for New Impervious Hot-Mix Asphalt. *Journal of sustainable water in the built environment*. 2 (2): 1 -19, DOI: <https://doi.org/10.1061/JSWBAY.0000806>
- Burian, S.J., and Edwards, F.G., (2015) Historical perspectives of urban drainage. in *Proc Global Solutions for Urban Drainage, ASCE, US*, 40 (6): 1-16, DOI: <https://ascelibrary.org/doi/10.1061>
- Carbajal, J.P., Leito, J.P., Albert, C., and Riekerman, J. (2017) Appraisal of data-driven and mechanistic emulators of nonlinear simulators: The case of hydrodynamic urban drainage model, Environmental modelling, and software. *Environmental Modeling and Software*, 92: 17-27, DOI: <https://doi.org/10.1016/j.envsoft.2017.02.006>
- Diakakis, M., Andreadakis, E, Nikolopoulos, E.I., Spryrou, N.I., Gogou, M.I., Deligiannakis, G., Katsetsiadou, N.K., Antonidis, Z., Melaki, M., Georgakopoulos, A., Tsaprouni, L., Kalogiros, J., & Lekkas, E. (2019) An integrated approach of ground and aerial observations in flash flood disaster investigations. The case of the 2017 Mandra flash flood in Greece. *International Journal of Disaster Risk Reduction*. 33: 290-309, DOI: <https://doi.org/10.1016/j.ijdrr.2018.10.015>
- Ellouze, M., Abida, H., and Safi R. (2019) A triangular model for the generation of synthetic hyetographs. *Hydrological Sciences*. 54 (2) :287 – 301, DOI : <https://doi.org/10.1623/hysj.54.2.287>
- Gibson, M.J., Savic, D.A., Djordjevi, S., Chen, A.S. Fraser, S., and Watson, T. (2016) Accuracy and computational efficiency of 2D urban surface flood modelling based on cellular automata. *Procedia Engineering*. 154: 801 – 810, DOI: <https://doi.org/10.1016/j.proeng.2016.07.409>
- Haidu, I and Ivan, K. (2016). Évolution du ruissellement et du volume d'eau ruisselé en surface urbaine. Étude de cas : Bordeaux 1984-2014, *France La Houille Blanche*. 5 : 1-6. DOI 10.1051/lhb/201605
- Honingh, D., Emmerik, T.Y., Uijttewaal, W., Kardhana, H., Hoes, O., and Giesen, N.V.D. (2020) Urban River Water Level Increase Through Plastic Waste Accumulation at a Rack Structure. *Frontiers in Earth Science*. 8 (28) 1-8, DOI: <https://doi.org/10.3389/feart.2020.00028>.
- Lyroutia, L.S.V., Chen, A.S., Khoury, M., Gibson, M.J., Kostaridis, A., Stewart, D., Wood, M., Djordjevic, S & Savic, D.A. (2020) Assessing and visualising hazard impacts to enhance the resilience of Critical Infrastructures to urban flooding. *Science of The Total Environment*. 708 :1-14, DOI: <https://doi.org/10.1016/j.scitotenv.2019.136078>
- Mah, D.Y.S., Bustami, R.A., Putuhena, F.J and Al Dianty, M. (2020) Testing the Concept of Mitigating Overflowing Urban Drain with Permeable Road. *International Journal of Advanced Trends in Computer Science and Engineering*. 9(5):7878-7882, DOI : <https://doi.org/10.30534/ijatcse/2020/139952020>
- Mah, D.Y.S., Ngu, J.O.K., Taib, S.N.L. and Mannan, M.A. (2019) Modelling of compartmentalized household stormwater detention system using SWMM5. *International Journal of Emerging Trends in Engineering Research*. 8 (2): 344-349, DOI: <https://doi.org/10.30534/ijeter/2020/17822020>

- Mahmoodian, M. (2018) A Hybrid Surrogate Modelling Strategy for Simplification of Detailed Urban Drainage Simulators. *Water Resources Management*. 32: 5241–5256, DOI : <https://doi.org/10.1007/s11269-018-2157-4>
- Mignot, E., Li, X., and Dewals, B. (2020) Experimental modelling of urban flooding: A review. *Journal of Hydrology*. 568: 334-342, DOI: <https://10.1016/j.jhydrol.2018.11.001>
- O'Shea, T.E and Lewin, J. (2020) Urban flooding in Britain: an approach to comparing ancient and contemporary flood exposure, *Natural Hazards*. 104: 581–591, DOI: <https://doi.org/10.1007/s11069-020-04181-8>.
- Paprotny, D., Sebastian, A., Nápoles, O.M., and Jonkman, S.N. (2018) Trends in flood losses in Europe over the past 150 years. *Nature Communications*. 19 (1985): 1-12, DOI: <https://doi.org/10.1038/s41467-018-04253-1>
- Patrick, M., Mah, D.Y.S., Putuhena, F.J., Wang, Y.C., and Selaman, O. (2019) Constructing depth-area-duration curves using public domain satellite-based precipitation data International. *Journal of Hydrology Science and Technology*. 9 (3): 281-302, DOI: [https:// 10.1504/IJHST.2019.102317](https://10.1504/IJHST.2019.102317)
- Tarasova, L., Blöschl, G., Merz, R., Merz, B., Kiss, A., Basso, A., Guse, B., Anwar, F., Kreibich, H., Pidoto, R., Wietzke, L., Bárdossy, A., Krug, A., Lun, D., Thomy, H.M., Pidoto, R., Primo, C., Seidel, J., Vorogushyn, S., and Wietzke, L. (2019) Causative classification of river flood events,” *WIREs Water*. 6 (4): 1353-1376, DOI: <https://doi.org/10.1002/wat2.1353>.
- Wu, J., Wu, Z.Y., Lin, H.J., Ji, H.P and Liu, M. (2020) Hydrological response to climate change and human activities: A case study of Taihu Basin, China. *Water Science and Engineering*. 13(2): 83-94, DOI: <https://doi.org/10.1016/j.wse.2020.06.006>
- Yen, B.C., and Chow, V.T. (1980) Design hyetographs for small drainage structures. *J. Hydraul. Div. ASCE*. 106 (HY6) : 1055– 1075, <https://cedb.asce.org/CEDBsearch/record.jsp?dockey=0009521>
- Zhou, Q., Yu., W., Chen, A.S., Jiang, C and Fu, G. (2016) Experimental Assessment of Building Blockage Effects in a Simplified Urban District,” *Procedia Engineering*. 154: 844 – 852, DOI: <https://doi:10.1016/j.proeng.2016.07.448>
- Zanchetta, A.D.L., and Coulibaly, P. (2020) Recent Advances in Real-Time Pluvial Flash Flood Forecasting, *Water*. 12: 570-599, DOI : <https://10.3390/w12020570>

## BUILDING AND EXPLORING NETWORK DATA MODEL FOR A SEASON LEVEL CLIMATE CHANGE STUDY FOR FIVE LARGE CITIES IN HUNGARY

Zsolt MAGYARI-SÁSKA<sup>1</sup> 

DOI : 10.21163/GT\_2021.162.15

### ABSTRACT:

Since a few years or decades, climate change has an impact felt in a very visible way in everyday life. People are increasingly confronted with its negative effects. Naturally, scientific research on the subject is multiplying. The present exploratory study attempts to present a network modelling approach on studying climate change. Networks are increasingly present in different areas of life, but have not played a significant role in climate research. This publication attempts to assess climate changes at five municipalities in Hungary by developing and analyzing three network data models. The developed different data models provide an opportunity to approach climate change from different perspectives, as the change itself is multifaceted. Data analyses are based solely on the structural indicators of the constructed networks, the measured weather characteristics only contributing to the construction of the data model. The obtained results for each location and season are complex, but interpreting them together helps to see the variations and their different nature.

**Key-words:** *Graph model, Data mining, Big data, Complex network, Similarity measure, R-CRAN.*

### 1. INTRODUCTION AND AIMS

Climate change is now a phenomenon that has largely convinced even the most skeptical. Today, reporting on extreme natural phenomena is no longer just a sensational news, it has become part of everyday life. Ordinary people are also facing the consequences of climate change, as it affects many aspects of their lives, whether it is related to agriculture, tourism or even their everyday security. This has led the scientific community to intensify its efforts to study climate change. Good research requires good data models and the right methods to go with them.

The idea that other research methods could be used to study the climate has been constantly developing. Since the weather that generates the climate implies a succession of data, and these large or small periods, form a temporal chain, logically raise the question of whether, Moran's First Law (Moran, 1950), issuing the spatial similarity could be applied for time (events closer in time are more similar than events further apart in time). Of course, that is not necessarily true, as aggregated data of weather for a later day, week or month may be more similar to a past period with similar duration than weather of a day, week or month immediately before it.

However, the existence of the link, the connection, the correlation between periods that may be distant in time is a real situation, and the study of it may prove useful as it indicates the dynamics of weather change. The study of it need a proper data model. One of the most high-profile scientific innovations of recent years is the use of networks (Barabási, 2013), which has very diverse application areas such as community detection (Li and Maini, 2005; Magyari-Sáska, 2019), medicine and life sciences (Light et al., 2005; Hopkins, 2007), economy analysis (Borgs et al, 2007; Emmert-Streib et al., 2018), security (Arquilla and Ronfeldt, 2001). Missing from all these broad applications is climate assessment.

---

<sup>1</sup> Babeş-Bolyai University, Faculty of Geography, Gheorgheni University Extension, 535000 Gheorgheni, zsolt.magyar@ubbcluj.ro

The aim of this research is to develop a new network-based data model and research methodology for climate research and to apply it in Hungary. At urban level there are just a few climatic studies for Hungary or for other countries (Probáld, 2014; Stone, 2012), but climate change at city level is an important as they are both generating factors and victims of it (Bulkeley, 2012; Hunt and Watkins, 2011). Since in 2021 daily meteorological data series for the period 1901-2020 for five municipalities of Hungary (Budapest, Debrecen, Pécs, Szeged and Szombathely) are available, which is suitable for the climate studies to be carried out, both in terms of time period and level of detail.

The data aggregation period in this study will be at the level of seasons, as several studies have examined the change and shift of seasons (Thompson, 2009; Magyar-Sáska and Dombay, 2020). A network model will be developed in which nodes represent the seasons, while the links between them will be established according to which new node (period) is (are) most similar to the previous period(s). The proper evaluation of this data model allows the assessment of climate change in terms of weather variability.

## 2. WEATHER DATA AND THE NETWORK MODELS

A set of daily meteorological data between 1901 and 2020 was available from the official site of the National Meteorological Service of Hungary. The dataset includes records on the average, minimum and maximum temperature as well as the precipitation quantity for every day. The original dataset was homogenized as for every meteorological station several relocations and measurement instruments changes has been done over the years. The location of the five cities covers the different regions of Hungary.

The network model used in this study is based on the similarity of the weather parameters between the time periods. In case of this research the nodes in the network are seasons, while the links are placed between them according to the best similarity. To obtain a similarity value based on which the edges of the network can be placed, at first we had to aggregate the weather values. This process has meant an upscale of the original data. The following 32 aggregated values were calculated for every season: average, minimum, maximum, standard deviation, maximum deviation and average of the daily variation of daily mean, minimum and maximum temperatures, maximum of the daily maximum temperature variation, maximum variation over the whole time interval based on daily maximum and minimum, total amount of precipitation, total amount of precipitation from fog, total liquid precipitation, total solid precipitation, number of days without precipitation, number of days with hail, number of days with thunderstorms, number of days with snow showers, number of days with hail and thunderstorms and number of thundery days.

In order to build up network models, a similarity index should be defined to express the combined similarity of different weather characteristics of two aggregation periods. Since the values of each weather characteristic are presented on different scales and orders of magnitude, it was necessary to normalize these values beforehand. A similarity index can be constructed by trying to condense (e.g. using a linear combination) the standardized values of the weather characteristics into a single value and then designating the difference between these values as the similarity index. In this case, the question that rises at what extent the different characteristics are involved in the formation of the weather, what their information content is, whether they need to be weighted and, if so, what these weights should be. Applying this direction would have been very subjective.

The similarity index can be created without combining the weather characteristics into one value. There are several methods to determine the similarity between two vectors, each consisting of several values (in our case weather characteristics). One of the best known is correlation, but there are several others as Jaccard index, multidimensional Euclidean, Minkowski or even Hamming distance, or cosine similarity (Tan et al., 2005). I have used the latter, since this indicator is often used in data mining (Han et al., 2012) and shows how the values of two vectors have the same orientation. By definition, the cosine similarity measure is the cosine of the difference between the outcome vectors defined in a multidimensional (the number of dimensions is equal to the number of features in the vectors) space (eq. 1).

$$\text{sim}(v, w) = \frac{v \cdot w}{\|v\| \times \|w\|} = \frac{\sum_{i=1}^n v_i \times w_i}{\sqrt{\sum_{i=1}^n v_i^2} \times \sqrt{\sum_{i=1}^n w_i^2}} \quad [1]$$

After several attempts three network models were adopted to carry out the data analysis. Even if the construction for all of them is based on the similarity index, each tries to catch the reality from a different point of view. The first network model is based on preferential attachment between nodes considering their show up in time. Every new node will be attached to that one in the existing model to which has a highest similarity value. The result will be a tree. The second model disregards the time in the construction process, as every node will be attached the which has the highest similarity value not considering if that node represents a time period before or after the node on process. The result in this case is a disconnected graph. The third network model starts from the complete network (all nodes are connected to each), but at final will remain just those links which are part of the shortest routes between each node pair. The result will be a connected graph. Each of the selected network model has a different view on similarity between the nodes. By respecting the time flow, the first model is more suitable to catch the changes. The second model concentrates on the highest similarity and by this can emphasized the compactness or spread of the climate. The third model wants adds the possibility for a node to be connected to multiple others in order to get the highest similarity to all other nodes. This model also makes possible to study the compactness of the climate but unlike model two it can take the global similarity between node pairs.

The data aggregation process and the network model construction for each of the five municipalities was carried out based on R functions (Ihaka and Gentlman, 1996) as individual and manual data processing was out of question due to the high amount of data. Beside the base R system the igraph package (Csárdi and Nepus, 2006) was used to perform all the network related operations such as network creation, adding edges, determining shortest paths, weighting the graph etc. For network visualization the Cytoscape software were used (Shannon et al., 2003) having some basic network analysis possibilities as well.

### 3. RESULTS AND DISCUSSION

Using the first data model, which is based on preferential linkage between aggregation periods using highest similarity, all seasons can be identified very clearly for all five municipalities (**Fig. 1**). Using the radial representation in Cytoscape, it is easy to interpret in climate changing terms the longer arms extending outwards or the fan-like shapes spreading out from the center, even if the automatic placement algorithm in some cases does not place them side by side.

The longer the elongations are, the more they represent a new changing direction of the season, while the fan shapes represent a higher stability of the season. On this basis, while Budapest shows a roughly equal variation between seasons, Debrecen shows a pronounced change in the summer compared to the other seasons. As the number of nodes is also significant on the stretching arm, the summer change at Debrecen is a multi-year change, unlike in cases of autumn at Pécs, the spring at Szeged or the winter at Szombathely. In these locations there are some outliers, but they contain contains only a few nodes.

However, some nodes in the network are displaced, being present in the branch of another season category (**Fig. 2**). If we look at these situations summarized in **Table 1**, the cases when a node is not in his seasonal branch, we can find the following highlighted situations:

- winter in spring branch; this situation occurs in all cities except Debrecen and in 44% of the cases in the last 30 years. This type of divergence is particularly marked in the case of Budapest. All these situations indicate mild winters.

- winter in autumn branch; is the case of Budapest alone and occurs only in three cases, in the past, more than 30 years ago, but also indicates mild winters.

- spring in summer branch; we find this situation in case of Budapest and Pécs, indicating warm springs. 71% of these situations have occurred in the last 30 years.

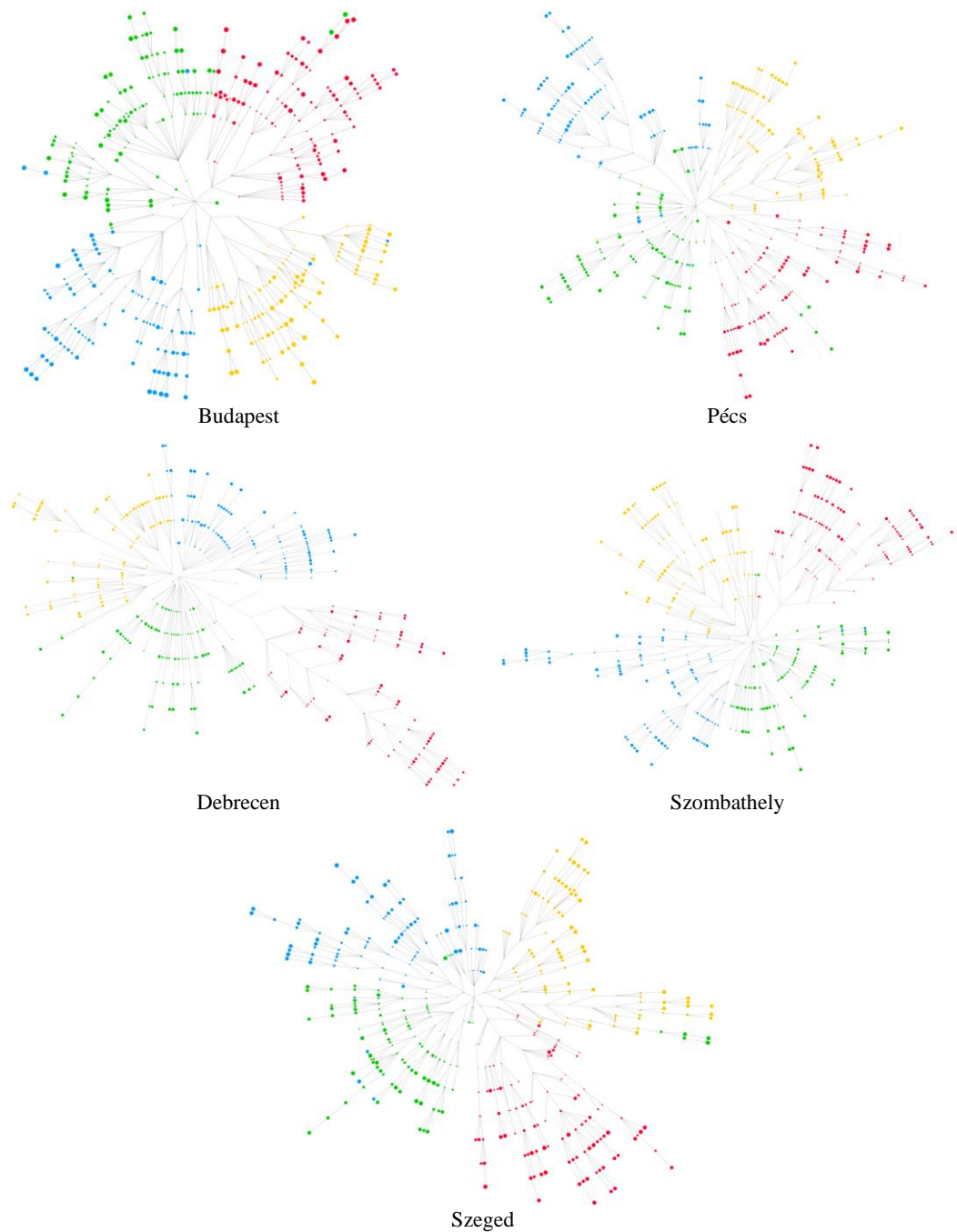


**Fig. 1.** – Network data models based on preferential connectivity with radial representation  
(*colors meaning – winter:blue; spring: green; summer: red; autumn: yellow*)

It is noticeable that winter branches do not contain other seasons, winter does not "attract" other seasons, but rather in some cases dissolves into spring or autumn.



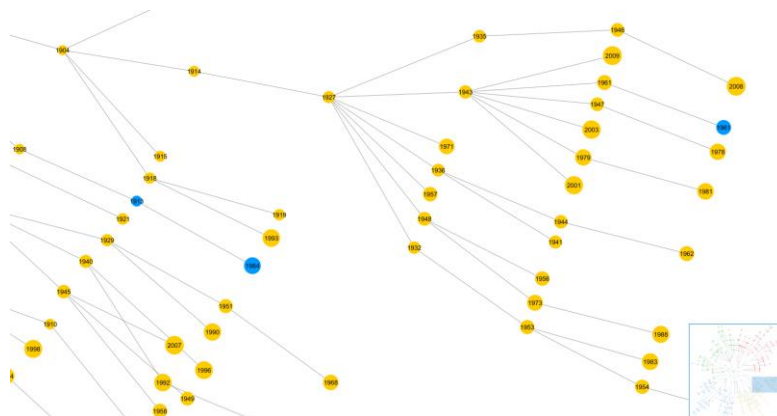


Fig. 2. – Different seasons in a branch (case of Budapest - three winter seasons in autumn branch)

Table 1.

**Displaced seasons.**

CITY	TYPE OF DISPLACEMENTS	YEARS OF DISPLACEMENTS
Budapest	winter in spring branch	1914   <b>2003</b>   <b>2006</b>   <b>2013</b>
	spring in summer branch	2014   <b>2019</b>
	winter in autumn branch	1913   1961   1984
Debrecen	spring in autumn branch	1931   1940   1994   1998   2012
Pécs	spring in summer branch	1934   <b>1990</b>   <b>1994</b>   <b>1998</b>   <b>2012</b>
	winter in spring branch	1965   1988   <b>1997</b>   <b>2018</b>   <b>2020</b>
Szeged	autumn in spring branch	1930   1947   1964
	spring in autumn branch	1967   1989   2007   2014
Szombathely	winter in spring branch	1924   1926   1947   1954   1988   1989   <b>2008</b>
	spring in autumn branch	1989   <b>1996</b>
		1922   1937   1945   1985

If we look at the evolution of the number of displacements over 30-year periods (Fig. 3), we can see a sharp increase. While in the first 30 years (1901-1930) there were only 6 such situations, in the following period there were 8, then 11, and in the last 30 years 17. For Szombathely and Debrecen, the total number of displacements is lower, but the percentage of displacements for the last 30 years is comparable with registered at other locations. For Szombathely, only 17% of the displacement occur in the last 30 years, while for Debrecen the percentage is 60%. Considering the total number of displacements, Budapest is in the middle of range, but proportionally it has more displacements for the last 30 years than Pécs or Szeged, which have higher total displacements (Fig. 4).

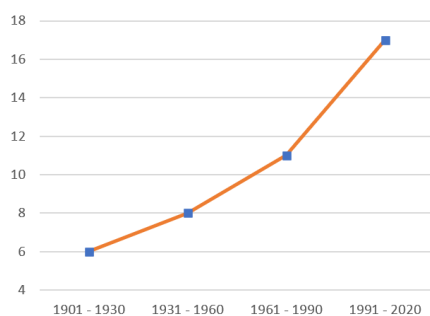


Fig. 3. – Evolution of displaced seasons number

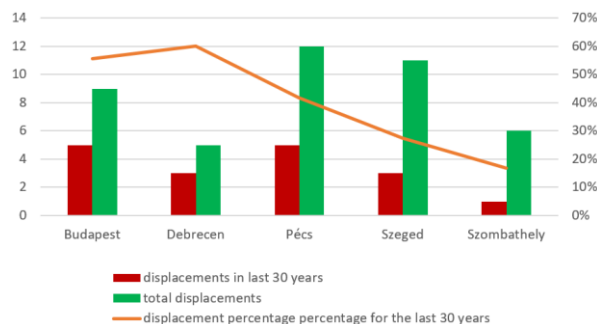
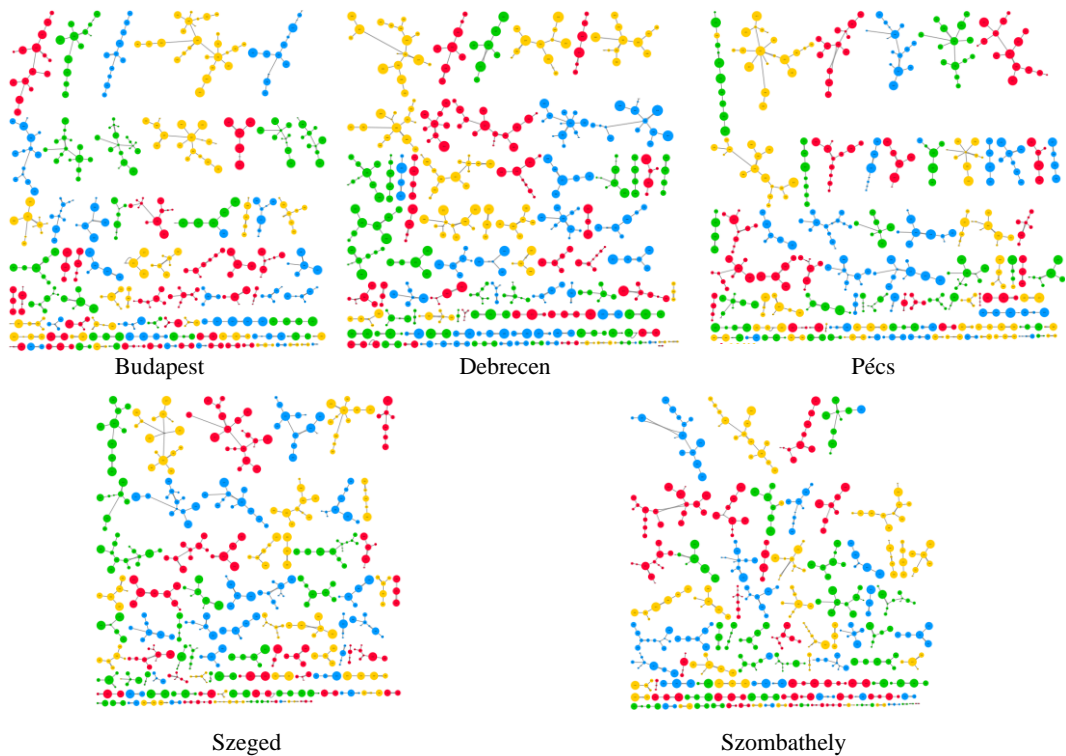


Fig. 4. – Displacement percentage for the last 30 years

The visual content of the second data model is different from the previous one (**Fig. 5**). In this case the number of components and the number of nodes in these components are the most relevant. The more components has a network, the more heterogeneous was the weather in the given municipality. However, not only the number of components is important, but also the number of nodes. The larger components are placed at the beginning of each diagram. Components with at least 10% of the total number of nodes has been named as large components, which characterize the most similar weather conditions.



**Fig. 5.** – Network components based on highest similarity index  
(colors meaning – winter:blue; spring: green; summer: red; autumn: yellow)

Analyzing the resulted network, we can observe that the number of components is relatively stable at different municipalities for different seasons, this is particularly true for Szombathely, while more pronounced differences can be observed for Budapest and Debrecen (**Fig. 6.a**). It is also noticeable that, with the exception of Szombathely, the other municipalities seem to be most coherent in different seasons, Budapest in spring, Debrecen in autumn, Pécs in summer and Szeged in winter. Similarly, the highest fragmentation pattern for different seasons appears at different locations: summer at Budapest, winter at Debrecen, autumn at Pécs and spring at Szeged. The above findings are confirmed by the average number of the components (**Fig. 6.b**).

The number of large components and the ratio of the number of nodes in each of them divided by the total number of nodes shows a similar pattern (**Fig. 6.c,d**). It's important, however, that in the case of Debrecen and Szeged, no large components could be identified for spring season, which means that this season shows the highest degree of heterogeneity, with the fewest number of years with similar weather patterns. Although, with varying degree, autumn shows the greatest cohesion for Budapest, Debrecen and Pécs, as significant number nodes are held by the large components of this season.

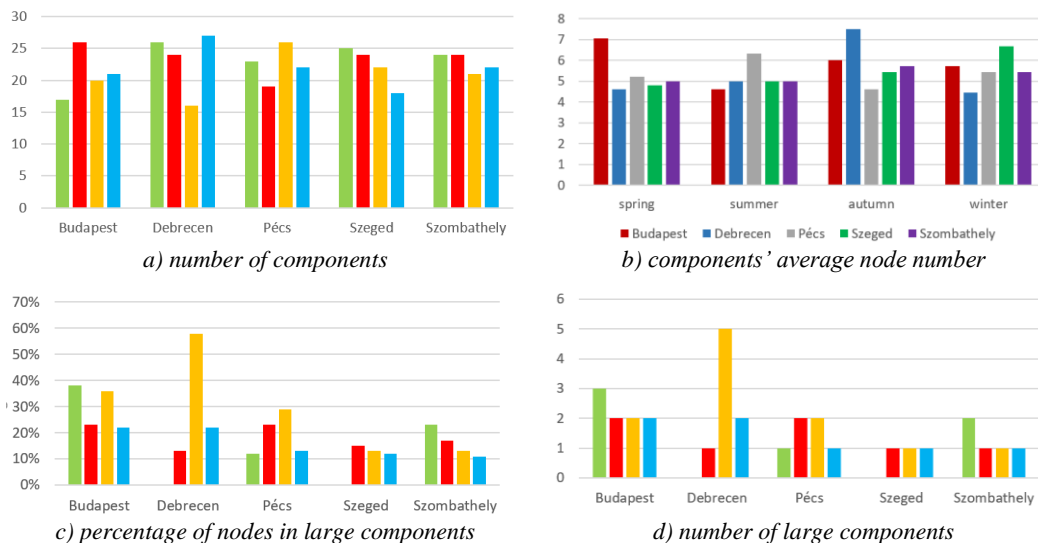


**Fig. 6.** – Evaluation graphs on number of network components and number of nodes (colors meaning – winter:blue; spring: green; summer: red; autumn: yellow)

The visual interpretation of the third data model containing only the edges necessary for all shortest paths is impossible due to the complexity of the network (**Fig. 7**). Its analysis can only be based on network indicators. In this case a separate network model was create for every season and every municipality. Four common characteristics of networks were used in data evaluation (Newman, 2010): the diameter of the network, the weighted diameter of the network, the density of network connections, and the total cost of the network divided by the number of connections.

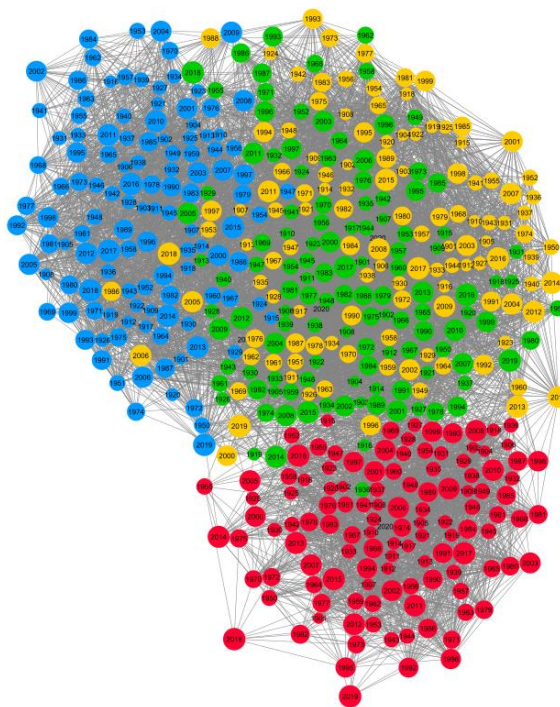


**Fig. 7.** –Result obtained using third network data model – case of Szeged

The diameter of a network is the longest shortest path that connects node pairs. The smaller the diameter value, the node pairs are closer to each other, which means that the global rate of change is smaller. If we look at the weighted diameter, which shows the highest weight of the shortest paths, we can observe that in some cases these values roughly follow the variation in network diameter (**Fig. 8**). For Budapest and Szeged this is the case for all seasons, but in case of Pécs, for example, although the diameter of the summer network model is the smallest, the weighted diameter value is the largest. Similarly, for Pécs, the network diameter of the autumn season is the largest, yet the weighted diameter is the smallest. If the two indicators do not vary in the same direction means that there are routes with intermediate nodes, resulting shorter lengths than those links which connects directly the two nodes. We can conclude that the two nodes are distant in terms of similarity. This is the case for the summer at Pécs and partly Debrecen.

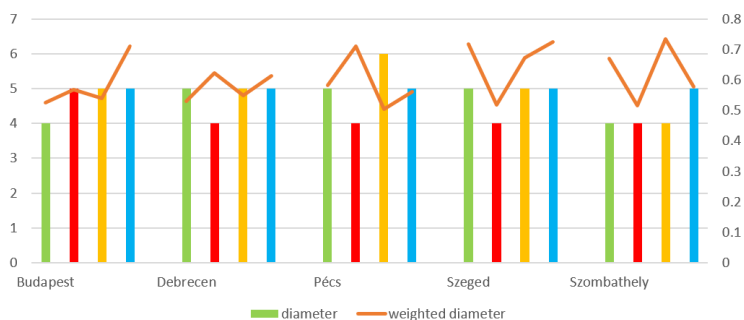


**Fig. 8** – Diameter and weighted diameter of networks based on third network model (colors meaning – winter:blue; spring: green; summer: red; autumn: yellow)

For the same diameter values, if the weighted diameter is higher, this indicates a higher divergence, indicating greater seasonal variability. Thus, for example, in case of summer for Debrecen, Pécs, Szeged and Szombathely (having identical diameter), the highest variability has Debrecen. The diameter of winter is the same for all the municipalities, but the weighted average shows the strongest variation for Budapest and Szeged. Autumn and spring also have highest variation for Szeged than in case of other municipalities.

The connection density of the network model refers to how many of all possible connections was kept in order to have all shortest paths in the structure. The lower this value is, the fewer 'alternative' routes are needed between two nodes, more frequently they can be connected at the lowest cost using direct connections, and hence the lower the variability is within a given season. From **Fig. 9** which plots these densities, we can see that for all five municipalities, winter is the least variable and summer the most variable, even though there is no significant difference between the density indices for spring, summer and autumn at Pécs, Szeged and Szombathely.

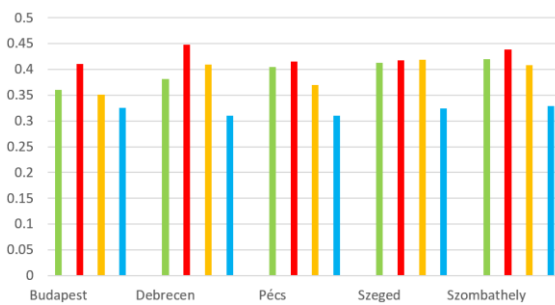


**Fig. 9** – Connection density values (colors meaning – winter:blue; spring: green; summer: red; autumn: yellow)

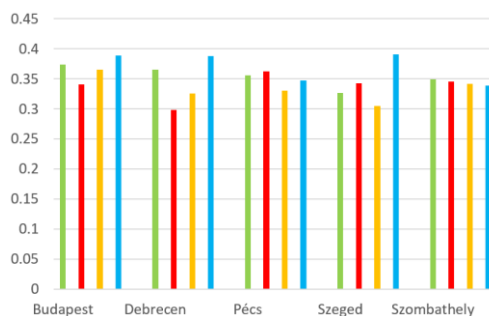


**Fig. 10** – Seasons cohesion based on average cost distance (higher value for lower cohesion) (colors meaning – winter:blue; spring: green; summer: red; autumn: yellow)

The last indicator of the third network model shows the total cost of the network divided by the number of connections. Since the network is constructed based on the differences between the seasons, a higher average value per connection indicates a higher average difference. This shows (**Fig. 10**) that the difference between years is largest for winter, with the lowest average cohesion at Budapest, Debrecen and Szeged. However, the values do not differ that much, that individual comparison can be useful, and the values were included in three cohesion categories. In low cohesion category belongs the spring, autumn and winter in case at Budapest, the spring and winter at Debrecen and the winter at Szeged. The medium category includes the summer at Budapest, all seasons at Pécs and Szombathely, and the autumn at Debrecen. The summer at Debrecen and the autumn at Szeged have high cohesion, they being the most stable seasons.

#### **4. CONCLUSIONS**

The aim of this research was to investigate how different network data models based on weather parameters can be used to model and assess climate changing. Five municipalities from Hungary were selected as test locations. Network modelling is a novel approach to climate studies with no specific methodological literature. This research was an attempt to explore the possibility to link two fields: networks and climate. Through the research several network data models were envisioned, but three of them were actually used. One of the important conclusions of this study is that different data models provide different opportunities for data mining. This opens the possibility of further researches to develop other useful network data models. Different data models, as they use different kind of structure and building rules, can highlight different aspects of the changing climate. Admitting this, it can be seen that the individual results do not always converge in the same direction with the same intensity, but the totality them can still emphasize different changes. Since climate change itself is multifaceted, manifesting itself in different ways in different locations, different data models and their indicators can capture different elements of the change.

One of the results of my research was actually the construction of the models, for which I created several modules and functions developed in R Cran. Finding programming methods that could do this in a time-efficient way was very important in the case of large amounts of data processing.

Interpreting a significant number of results for a single municipality or for a single season is a complex task. Two different examples of it are highlighted for Budapest and Debrecen.

Winter at Budapest is changing in many ways, supported by all three models:

- from the first network model, it can be seen that 78% incorporation into other seasons, with the last 30 years mostly incorporation into spring

- from the second network model, it is observable that it has many components, showing considerable variation, with the proportion of large components being the lowest compared to other seasons at that location

- from the third network model the changing characteristic of the winter is shown by the highest weighted diameter and it has the lowest cohesiveness

Autumn at Debrecen is a stable season, based on the following considerations:

- according to the first network model, the autumn compact does not appear in the branches of other seasons

- the second network model shows a high number of large components but a low number of components compared to other seasons, both indicating a compact situation. This is also confirmed by the average number of component nodes, which is the highest for all municipalities

- the third network model shows a low weighted diameter of the network, with a cohesion value that is the second strongest of the four seasons

The performed research confirms that network data models can play a role in climate change modelling and that they have a place in this field, not necessarily stand-alone, but as a valuable complementary method. It is a novel data mining approach, in which the structural characteristics of the network data models are used in analysis, the weather data being used just in the models building phase.

## ACKNOWLEDGEMENTS

The presented research was supported by the DOMUS scholarship program of the Hungarian Academy of Sciences.

## REFERENCES

- Arquilla and D. Ronfeldt. *Networks and Netwars: The Future of Terror, Crime, and Militancy*. RAND: Santa Monica, CA, 2001.
- Borgs, C., Chayes, J., Daskalakis, C., Roch, S. (2007), First to market is not everything: an analysis of preferential attachment with fitness, *STOC'07 Proceedings of the thirty-ninth annual ACM symposium on Theory of computing*, 135-144, DOI: 10.1145/1250790.1250812
- Bulkeley, H. (2012). *Cities and Climate Change*. Routledge. DOI: 10.4324/9780203077207
- Csardi G, Nepusz T (2006). The igraph software package for complex network research. *InterJournal, Complex Systems*, 1695. <https://igraph.org>.
- Emmert-Streib F., Tripathi S., Yli-Harja O., Dehmer M. (2018), Understanding the World Economy in Terms of Networks: A Survey of Data-Based Network Science Approaches on Economic Networks, *Frontiers in Applied Mathematics and Statistics*, 4, DOI: 10.3389/fams.2018.00037
- Han, J., Kamber, M., Pei, J. (2012), *Data Mining: Concepts and Techniques*, Elsevier, DOI: 10.1016/C2009-0-61819-5
- Hunt, A., Watkiss, P. Climate change impacts and adaptation in cities: a review of the literature. *Climatic Change* 104, 13–49 (2011). DOI: 10.1007/s10584-010-9975-6
- Ihaka, R., Gentleman, R. (1996), R: A Language for Data Analysis and Graphics, *Journal of Computational and Graphical Statistics*. 5 (3): 299–314. DOI:10.2307/1390807.
- Hopkins, L. (2007), Network Pharmacology. *Nature Biotechnology*, 25: 1110-1111,
- Li, C., Maini, P.K. (2005), An evolving network model with community structure, *Journal of Physics: a mathematical and general*, 38 (45), 9741-9749 DOI: 10.1088/0305-4470/38/45/002
- Light, S., Kraulis, P., Elofsson, A. (2005), Preferential attachment in the evolution of metabolic networks, *BMS Genomics*, 6,159, DOI: 10.1186/1471-2164-6-159;
- Magyari-Sáska Zs., Dombay S (2020), Seasons' shifts in some depressions of the Eastern Carpathians, based on daily temperature analysis, *Air and Water Components of the Environment*, Conference proceedings, 213-222
- Magyari-Sáska, Zs. (2019), Road Network Based Community Detection. Case Study for an Eastern Region of Austro-Hungarian Monarchy, *Geographia Technica*, 14(1), 82-91, DOI: 10.21163/GT\_2019.141.06
- Moran, P. A. P. (1950). Notes on Continuous Stochastic Phenomena. *Biometrika*. 37 (1): 17-23. DOI:10.2307/2332142
- Newman, M. (2010), *Networks: an Introduction*, Oxford University Press
- Probáld F. (2014), The urban climate of Budapest: past, present and future, *Hungarian Geographical Bulletin* 63 (1) (2014) 69–79. DOI: 10.15201/hungeobull.63.1.6
- Shannon, P., Markiel, A., Ozier, O., Baliga, N. S., Wang, J. T., Ramage, D., Ideker, T. (2003). Cytoscape: a software environment for integrated models of biomolecular interaction networks. *Genome Research*, 13(11), 2498–2504.
- Stone, B. (2012) *The City and the Coming Climate. Climate Change in the Cities we Live*. Cambridge, Cambridge Univ. Press, 198 p.
- Tan PN, Steinbach M, Kumar V (2005). *Introduction to Data Mining*. ISBN 0-321-32136-7
- Thompson D.J., (2009), Shifts in season, *Nature* 457, p 391-392

## USING WEB GIS FOR MARKETING HISTORICAL DESTINATION CAIRO, EGYPT

*Reda Alkot MOHAMED<sup>1</sup>, Zakaria Yehia ABD EL GAWAD<sup>2</sup> , Mihai VODA<sup>3</sup> *

DOI: 10.21163/GT\_2021.162.16

### **ABSTRACT:**

The article is analyzing the use of WebGIS for tourism development in historic Cairo which is considered as an open-air museum, designing the touristic map and publishing it on the web as an interactive map. ArcGIS Server and WebGIS were used to create and promote a platform guide for tourists enabling them to find the touristic places and services in an easy and quickly manner. Therefore, by using the WebGIS, the digitization of the cultural heritage will create a large quantity of digital images and maps of the study area, leading to an easy and accurate identification, analysis and interpretation of geographical data and touristic places attributes. The research results will contribute to local authorities better planning and decision-making process, having good impacts on the touristic development of Egypt in general.

*Key-words: WebGIS, Hhistoric Cairo, Interactive map, ArcGIS Server, Cultural heritage, Tourism.*

### **1. INTRODUCTION.**

The success of planning for development depends on the availability of accurate information about the existing resources. It is, therefore, essential to conceive the ways and means of organizing computerized information system. These systems have to be capable of handling huge amount of data and represent it in an easy manner (Kumar and Babu, 2016). However, the use of GIS techniques will lead to an easy and accurate identification, measurement, analysis and interpretation of geographical data, all of these helping in good forecasting and aiding the decision- making process in tourism development. According to Amazon Web Services, ArcGIS is used to gain an understanding of the geographical location data and to take better informed decisions (Amazon Web Services, 2012).

The Internet is making the information and knowledge more common to the public, facilitating the desire to share and collaborate the geographic data over the web of many organizations who decided to develop their businesses with GIS resources (Law, 2013).

#### **1.1. Web GIS definition and development**

Web-based GIS (referred to as Web GIS) is a form of GIS that is deployed using an Internet Web browser (Reed and Bodzin, 2016). Maps from GIS applications were restricted to users of the local area network (intranet), but by Sharing these maps with anyone in anywhere by using the web, it will become a webGIS. Therefore, Web GIS is a Geographic Information System for the Internet. By using GIS, data and maps are stored in an infrastructure and can be configured to meet the digital mapping and IT requirements. We can share these spatial data with the users by using the Internet (Web GIS), because Web GIS is a hypertext-based service, allowing the users to browse data and information on networks. Also, the use of Web GIS has been growing in recent years, which is shown by the increasing number of GIS workstations that are distributed across the World Wide Web. It allows the sharing of resources and geographical information online easily and quickly within all over the world. Any user regardless of location and environment can have access to the geospatial data and GIS capabilities using the Web, enabling sharing the app with large number of users easily and quickly (Evic, 2004).

---

<sup>1</sup> Cairo University, Faculty of Arts, Geography department, Giza, Egypt: [redaelkot@cu.edu.eg](mailto:redaelkot@cu.edu.eg)

<sup>2</sup> Thebes Academy, Department of civil engineering, Cairo, Egypt: [z.yehia@thebes.edu.eg](mailto:z.yehia@thebes.edu.eg)

<sup>3</sup> Dimitrie Cantemir University, Targu Mures, Romania: [mihaivoda@cantemir.ro](mailto:mihaivoda@cantemir.ro)



Web GIS offers some of the same functions as a desktop GIS, but does not require the full suite of (often expensive) specialized software or tools that need to be mastered before one may effectively use the software. The utilization of GIS PC-programs may be difficult to public users (Reed and Bodzin, 2016). Web GIS facilitates a non-technical user to access the geographical information due to the friendly interface web-pages and apps which won't require prior specific GIS knowledge. These user-friendly systems, need to be developed continuously and to be kept simple in order to transfer the technology from the scientific community to the ordinary people (Kumar and Babu, 2016).

GIS and a Web GIS development may be expensive, but open source (OS) software, is available to this sector. Therefore, using these technologies is ranging from a free-cost software license to the flexibility of adapting the program to meet actual needs without depending on closed software. ArcGIS Online includes creating web app, and 3D web scenes. So Web GIS represents a considerable cheaper alternative when compared with the cost of building a stand-alone desktop solution which needs separate installation for every user. Moreover, the map can be modified or updated with additional data layers according to the user needs, making Web GIS useful to e-government, e-business, and daily life. ESRI and Amazon Web Services are offering an approach to running GIS applications in the cloud, with an overview of the most relevant individual storage options for geospatial applications building. The individual storage options form the building blocks that can be used to create web-scale geospatial applications (Amazon Web Services, 2012).

### **1.2. Web GIS and tourism**

Tourism is an international activity that needs global publicity, and the map is a good visual advertisement for the attractions in any location. Given the use of GIS to facilitate understanding the relationships, patterns and trends between geo-referenced data (Reed and Bodzen, 2016), the use of GIS in the tourism industry leads to many studies concerned with highlighting the spatial dimensions of tourist sites, as well as planning and marketing them. With the availability of such systems, tourism marketing has become more accurate and flexible (Ahmed, 2011). Since GIS can link the map and descriptive information of these tourist places, and through the GIS on the Internet we can publish these tourism ads globally in an attractive way, by presenting the maps and tourist information in an organized manner to facilitate tourists use. Installing a program to prepare travel plans determines the use of Web GIS, where you can include all the data from online sources. It is automatically collected by connected tourism information systems (Wessel et al, 2006).

The role of GIS in the development of tourism in Historic Cairo will be through designing a tourist map system that contains an interactive tourist map and publishing it on the web by ARC GIS Server (AGS) to be a guide for tourists to find tourist places and their services easily and quickly, which will have good effects on tourism development in Egypt in general. Products are also displayed on the shelf to be marketed and create interest and attract people towards them (Hashmi, 2006). Similarly, any country can present itself as a tourist using the web by digitizing its cultural heritage, which will produce large amounts of digital images, and the creation of web interfaces for the general public will help in the exploration of such images by classifying them across time periods, places, geographical regions, or schemes thematic classification designed by the owners (Yao et al. 2020; Ernawati et al. 2018; Ilies et al. 2017). Also, through network analysis in GIS, tourism GIS technologies can have a role in determining the shortest route to tourist places that will be time-saving and economical (Gumusay 2004; Gupta et al. 2018; Voda and Montes 2018).

### **1.3. Development and benefit of using webGIS for tourism in Cairo.**

By searching on the internet, no result are found about using WebGIS for Cairo. The only thing that is found is just some webpages for general tourism text information about Cairo (Viator, 2021), but without any maps. And also we found some other sites of general maps, but without any attributes data (Mapping Properties, 2021). And another GIS technology (mobile GIS) has been created for just a part in touristic Cairo-El moez street (Orchtech, 2021).

This study is aimed to show how we can create webGIS for historical Cairo. Our intention is to develop a webGIS for tourism marketing in Cairo, because one of the benefits and advantages of using it will be its accessibility at the level of tourist personnel. Easy access to a particular landmark - know the path and know the monuments near its location. Easy to search in specific historical location and easy to update the base map and historical layer. This webGIS application saves the tourist from using paper maps and facilitates the quick and easy access to the historical landmarks. Not all the historical sites of Egypt are including GIS maps, they present only pictures and descriptions of the historical signs. Some other historical sites of Egypt are not including the nearest historical signs or search options. Therefore, tourists can easily access more detailed information about tours of Cairo on the Internet. And by developing webGIS for tourism marketing of Cairo, tourists can locate attractions of interest and check for accessibility equipment and the possibility of access through private or public transportation, improving the planning options of their visits.

The role of GIS in the development of tourism in historic Cairo is to design the tourist map system, which contains an interactive tourist map and post it online by ArcGIS Server, as a guide for tourists to find tourist destinations in an easy and fast way. Building an online GIS for historic Cairo is a good tourist ad, because tourism needs to be advertised globally. This goal can be achieved online. Especially using the map and the GIS capabilities feature by linking tourist sites and metadata to design a geographic information system on the Internet once and for all. Also, historic Cairo represents a unique form of cultural tourism that is now more attractive due to the exquisite history of those ancient places. This paper is useful to the local communities to better regulate and manage tourism activities. Therefore, web-based GIS provides an effective environment for the tourism industry. This may be very efficient in promoting the less known historic Cairo, where tourists planning to visit a particular place can get all the details from the GIS on the Internet. Web GIS has a friendly interface for the presentation of thematic maps, with some basic functionality for various types of content. Web GIS applications are opening new possibilities for planning and management of tourism activities because they allow more contribution to greater socialization of information. It represents a useful tool for planning and analysis of geographical data or distribution of services for tourism managers.

#### **1.4. Previous studies**

Web GIS is used in many fields such as health, economics, management, tourism, and others. In the Zambian Ministry of Health, the Zambian Ministry of Health is seeking to create a web-based GIS architecture with an intuitive and simplified user interface to enable non-specialist users to operate the system without any additional training. Managing a tool for monitoring and evaluating health facilities and developing a portal for public interaction with their spatial information (Mushonga et al, 2017). Web GIS maps were used to investigate malaria disease patterns and prevalence in relation to the environment in the Congo and their relationship to environmental and demographic factors to increase public health literacy through dynamic mapping for timely decision making (Reed and Bodzin, 2016)

In a web-based GIS used for the Chesapeake Bay watershed, clicking on a point of data will display its results. As well as creating simple graphs for it. An efficient standard in this web-based GIS is given by the fact that you can narrow down the investigation of data by specific date and location. This can be useful for comparing a specific site in different years. Also, you can filter the data by filter expression (Chesapeake Bay Foundation 2013). An interactive map of the Richmond-San Pablo, CA, USA area is designed to help visualize air quality monitoring sites, air pollution sources, and health burden data, and is intended to support the Steering Committee as it develops a community plan for air monitoring. The map can be modified or updated with additional data layers (Google Maps Help, 2020). The interactive map is produced by Google Maps that allows viewing and editing of maps for sharing online (Google Maps, 2020).

Web GIS is an essential tool for economic development as it provides continuous monitoring of crops and field activities. These systems are able to handle huge amount of data to set up a web-based

GIS monitoring system for sugarcane, to help non-technical users to access information and take appropriate measures to improve crop production (Kumar and Babu, 2016).

The use of web-based GIS in management is demonstrated in an interactive Melbourne map of cooling and greening covering the city's urban areas. The interactive map provides a visual capture of vegetation data at the local, suburban, and Mesh Block levels. The vegetation data set also includes a layer that compares the change in vegetation cover between 2014 and 2018. These data sets are organized into multiple levels. (Victoria State Government, 2020). Another example is the city of Mesa that has made an interactive GIS map available to the public, to find a subdivision of the site, search the state history and find details about the size and owner of the property (Leeds City Council, 2020). Snohomish County Planning and Development Services also provided an interactive map for clients, partners and stakeholders. It provides quick access to a huge amount of information about unincorporated Snohomish County and using map attributes, navigate through topics, such as zoning, future land use, and capital facilities. It also provides a variety of tools for exploring data layers, as well as tools for searching and querying, creating and editing features, and annotations (Snohomish County, 2020).

Web GIS can be applied in teaching and learning as an innovative approach to enhance students' understanding in any subject. It is not only easy to use but also freely available online in teaching and learning history with map. A Web GIS could become more comprehensive like EnviroAtlas, which provides data, research, and analysis on the relationships between nature, people, health, and the economy. It is designed for use by government, professionals, academics, and community users as well as members of the public interested in ecosystem services. It provides multiple tools and GIS toolboxes, including an interactive map, and provides ready access to more than 400 maps and multiple analysis tools (EPA, 2020).

In tourism, the use of GIS led to building a marketing information system for tourism for the Aqaba Governorate, which resulted in saving time and effort and reaching accurate results in a very short time (Ahmed, 2011). Hyderabad has become a hot spot for international tourists, because it has developed into a global destination for information technology, which has contributed to promoting the tourism sector globally in an innovative and better way, thus increasing the country's economy in foreign currency (Hashmi, 2006). And through the development of Web GIS for Hainan Tourism Geographic Information System, it realizes map browsing, zooming, moving, information querying and marking of travel map, attractions, travel routing on electronic map with internet, and arrangement of travel plans on an interactive interface (Shi and Zhang, 2013).

On some web pages of open-air museums, such as in Belgium, it helps to show how to plan the tourist route and parking either by bike, train, bus or by car (Bokrijk, 2020). With the free app (Your Routing), you can download and print the resulting map in the state of Routing (Routeyou, 2020). Another app is "Self-Guided Tour", an app developed by GPSmyCity. This application turns the mobile device into a personal tour guide (Gpsmycity, 2020). By developing a web based Tourism Information System (TIS) for Eastern Uttar Pradesh, it has been modeled on a GIS platform to make it interactive and also connected to the internet to increase the accessibility of reliable information. Such a system is very useful for knowing the current state of tourism and implementing future tourism development programs. (Tyagi, 2014). Web GIS has also been produced in the field of Croatian nature tourism and mountaineering, to facilitate access to reliable information on mountaineering, visitor planning and thus the development of mountaineering tourism (Špoljarić, 2019), and in the GIS Tourist Network of Langkawi Island, is to allow public participation as a supply of information, such as adding an object or editing the attribute data (Masron et al. 2014).

To understand the different approaches to building GIS applications on the web to make geographic science more global, and having a large number of users, the Open Source Geospatial Foundation (OSGeo) has listed many applications that can support advanced mapping and geographic visualization tools (IFIC, 2004), and apply download the web, many of these applications that promote global adoption of open geospatial technology (Osgeo, 2020). GeoServer application for example is a server software that allows users to view and edit geospatial data, and allows great flexibility in creating maps, exchanging data, and displaying geographic information for the world

(Geoserver, 2020). OpenLayers, GeoServer's integrated mapping library, offers quick and easy map generation. For example, MapServer is a platform for publishing geographic data and interactive map applications on the Internet. (Mapserver, 2020). GeoMoose can perform queries without using a server-side scripting language (Geomoose, 2020). PyWPS was started as part of the "Connecting of GRASS GIS (PyWPS, 2020) project. Other useful applications are represented by Degree Program, Mapbender and OpenLayers (Osgeo, 2020). Another example is the relationship developed between Wikipedia, WebGIS and Open Data Monument (ODM) to study the heritage sites of Emilia-Romagna for a profitable and profitable situation where all partners benefit from working together: ODM and Wikipedia pages related to heritage sites in Emilia-Romagna get access to reliable geo-reference and high-quality cultural data from WebGIS; WebGIS in turn gets free high-quality / usable images from ODM as well as a global view through Wikipedia (Magrini, 2018).

## **2. STUDY AREA**

Cairo (Historic Cairo), the capital of Egypt, is considered a spatial acronym for a group of historical periods as an open-air museum like the open-air museums in Europe (Euro-t-guide 2020). The historic center (about 32 square kilometers) houses no less than 600 classified monuments dating back to the 7th century. It involved many streets and ancient dwellings, and thus retains forms of human settlement dating back to the Middle Ages, and this site is described as a historical tapestry of which large areas are still intact. Historic Cairo according to the appointment of the Egyptian Supreme Council of Antiquities as the only official concerning documents Set Historic Cairo, divided into five regions, and our study area will be limited to Zone 2 and it is the buffer zone that includes the Fatimid nucleus along with the Citadel area and the area around the Ahmed Ibn Tulun Mosque (UNESCO 2012).

Present-day Cairo is a contiguous chain of several successive historical sites over time. Since the Islamic rule of it in the year 640 during the caliphate of Omar ibn al-Khattab, and the construction of the first Islamic city of Fustat. After that, Ahmad ibn Tulun (809-904) built the city of Qatay in the year 870 near the city of Fustat. After that, the al-Khashid dynasty (935- 969), the Fatimid dynasty (969-1171), which founded fatty Cairo. The Ayyubid dynasty (1171-1250) (Mary 2012), the Mamluk period (1250-1517).

From the previous history of Cairo, an unparalleled number of tourist buildings have been found (see **Fig. 1**). The most prominent architectural heritage of medieval Cairo dates back to the Mamluk period, which was characterized by comprehensive architectural projects, where we can find many uses in the same building, such as mosques that can be used as a school at the same time. Because the Mamluk sultans and elites were supporting religious and scientific life by building Religious complexes whose functions include a mosque, a madrasa, a khanqa (for Sufis) and water distribution centers (spills) at the same time. Among the most famous examples of Mamluk antiquities in Cairo that show these comprehensive religious complexes are the huge Sultan Hassan Mosque, the Sultan al-Ghuri complex, and three monuments in the Bayen Kasserine area that includes the Sultan Mansour Qalawun complex, the Al-Nasir Muhammad School, and the Sultan Barkouk School. Therefore, WHC developed Historic Cairo as well as the quantity and quality of historical monuments on the World Heritage List as one of the first historical cities to be included in the World Heritage (UNESCO 1979).

## **3. DATA AND METHODS**

The most important tourist buildings in Historic Cairo, were categorized into Mosque- (Mosques), Madrass(Madrass), Qutab (Koranik Schools), Palaces and Bimaristans (Hospitals). These data are collected from Egyptian Survey authority, (1948), the Map of Cairo Islamic monuments, sheet 1&2, 1:5000, Egypt, with polygon data type and display of the google maps in the back ground, the map scale is 1:5000 in UTM projection.

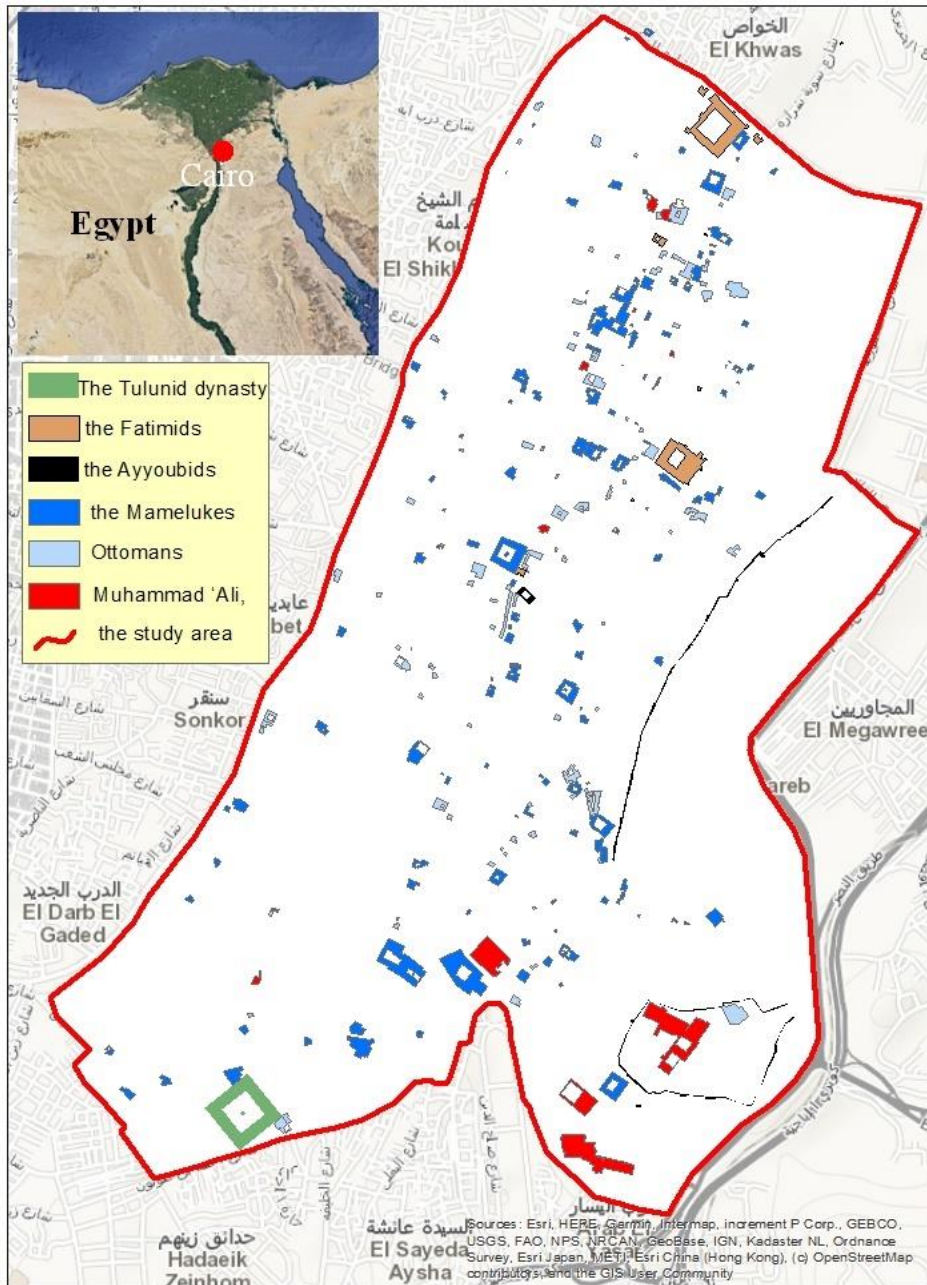


Fig. 1. Study area and density of historical monuments.

Deployed on the site by Arc GIS Web Manager Application, the site is created by selecting "Create Web Application Tool", then locate the data and add service layers using "Add Layer" (Add task) and through this tool add task Create procedural operations such as query attributes, search for attributes, and print and then they are modified to output the service (map). Adjust the map layout (such as map scale, north arrow).

**Mosques:** The first mosque in Egypt and Africa was the Amr Ibn Al-Aas Mosque in Fustat. While the Ibn Tulun Mosque represents the oldest mosque that retains its original shape and is a rare example of Abbasid architecture, from the classical period of Islamic civilization, so we can consider

Historic Cairo to be influenced by the historical architecture of other civilizations such as the state The Abbasid as well as the Ottoman Empire, so it can be considered an open museum for the influences of a number of other civilizations. The Al-Azhar Mosque, which was founded in the Fatimid era, may compete with the Qarawis in Fez for the title of the oldest university in the world. Other monuments dating back to the Fatimid era include the Great Mosque of Al-Hakim Al-Ammar Mosque, and others.

**Sabil-s:** It is free drinking fountains for local communities, constructed by some sponsored by wealthy merchants and some by elites.

**Madrasas (schools):** Historic Cairo had many schools such as: Al-Azhar University, Baybars II Khanaqah, Al-Nasir Muhammad School, Al-Madrasah, the tomb of Al-Salih Najm Al-Din Ayyub, the Mosque-Madrasa of Sultan Barkouk

**Caravanserais:** (also known as wikalas or khanates) The Mamluks, and later Ottomans, built many souks and commercial buildings to house merchants and goods. The most famous example is the rich Wikala. Khan al-Khalili is a famous bazaar (Fahim, 1996), and a trading center. Another example of historical commercial architecture It is the Kasbah in the Gulf of Radwan in the seventeenth century, which is now part of the Khayamiya area whose name comes from the decorative textiles (Khayamiya) that are still sold there.

**Fortifications** (Walls, gates and Citadel): When the Fatimids established Cairo as a palace city in 969, parts of it remain today like walls and gates, for example: Bab Zuweila in the south, Bab al-Futuh and Bab al-Nasr in the north. After that, the walls were extended and modified by the Ayyubids as part of Salah's plan Al-Din to protect both Cairo and Fustat with one set of walls and some Ayyubid gates such as Bab al-Barqiah. Salah al-Din also began building a vast castle in 1176 to be the headquarters of the authority in Egypt.

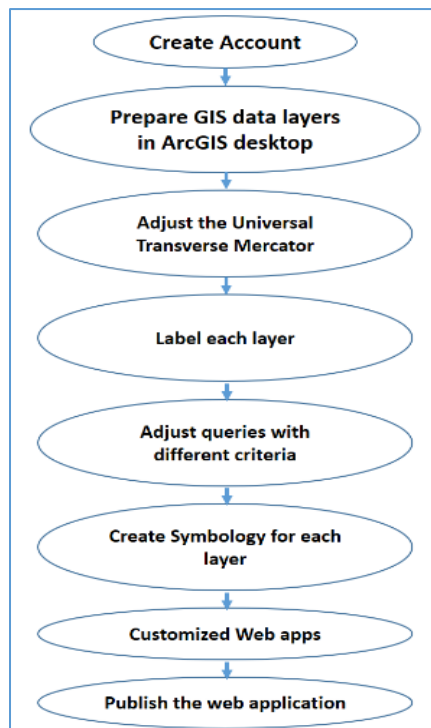


Fig. 2. Steps of creating WebGIS for Historic Cairo.



Therefore, Historic Cairo is the densest in terms of its morphology and layers of history since the middle Ages. Cairo landmarks including public buildings, fortifications, and schools reflect intellectual prowess, and the numerous streets and squares reflect their commercial activities, many of which are seen as masterpieces in terms of the shape of its architecture. Thus, it celebrates the way in which the historic center of Cairo is a physical witness to the international importance of the political, strategic, intellectual and commercial activities of the city that developed during the medieval period as a lively, dynamic and multifunctional city. There were few cities in the world that were as rich at the time as Historic Cairo in terms of the way its ancient buildings display history. It was radically changed by recent developments or conflicts. Today's Historic Cairo is an extraordinary survival, not only as a city Antique or as a museum but as a dynamic city that still easily displays its value (UNESCO, 2014).

The following chart (**Fig. 2**) shows the steps from creating an account in WebGIS till publishing the WebGIS application on the internet. Using ArcGIS to ease the use and prepare GIS maps and customize the WebGIS applications with symbology and different queries.

#### 4. RESULTS AND DISCUSSION

The tourist map of any tourist site can be created through the program (Arc GIS Server) by adding geotourism data, so that this data is in the form of layers designed through the Arc Map program.

Creating the site is the beginning of specifying its primary administrator, as he has full powers to manage it, create users and define their tasks. Then specify the path to save server files and store services in the two folders (directory and configuration-store), and then the server starts uploading files to the two folders to activate the site. Finally create a web tourism application. (See **Fig. 3**).

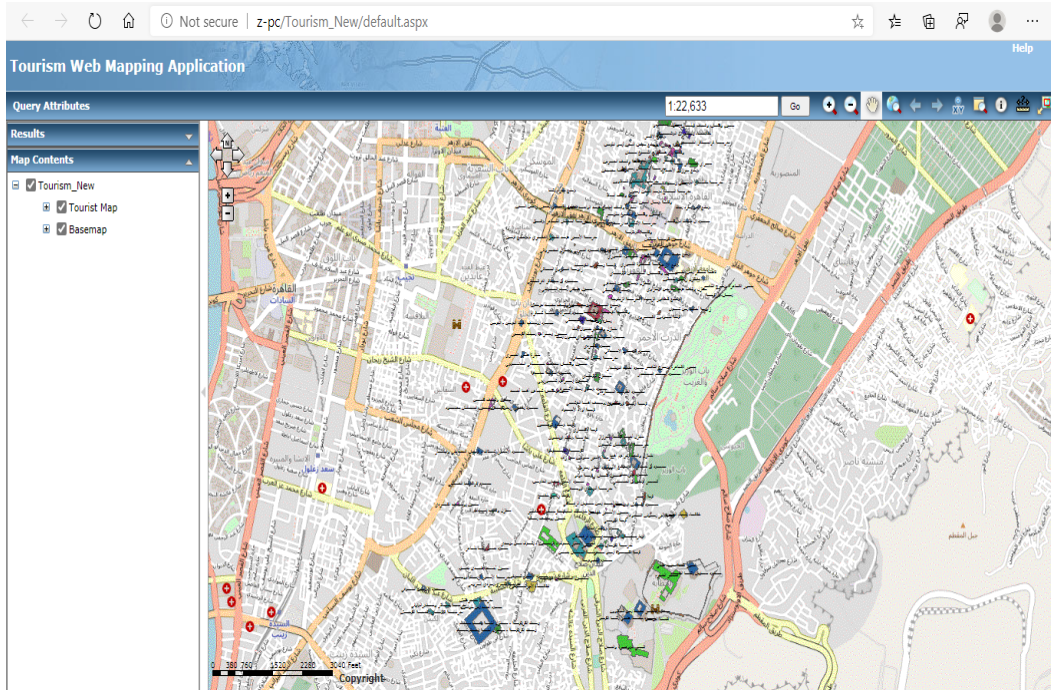


**Fig. 3.** Tourism web application (street map in the back ground).



The tourist map and analytical operations are processed in the program (Arc Map). This is explained in the following steps:

- The interactive tourist map is prepared for the final output before it is published to ArcGIS Server, so that it is suitable in terms of interactive (kinetic) and (technical) output.
- For the interactive map (full range), by choosing the appropriate scale for the appearance of the entire study area, and then the appearance of texts and symbols for the geographical layers.

To display the geographical tourism system, after the completion of the construction stages, the tourist map is displayed in all its layers, procedural and analytical processes as shown in **Fig. 4**. We can also make query about all kind of tourist buildings as shown in **Fig. 5**.

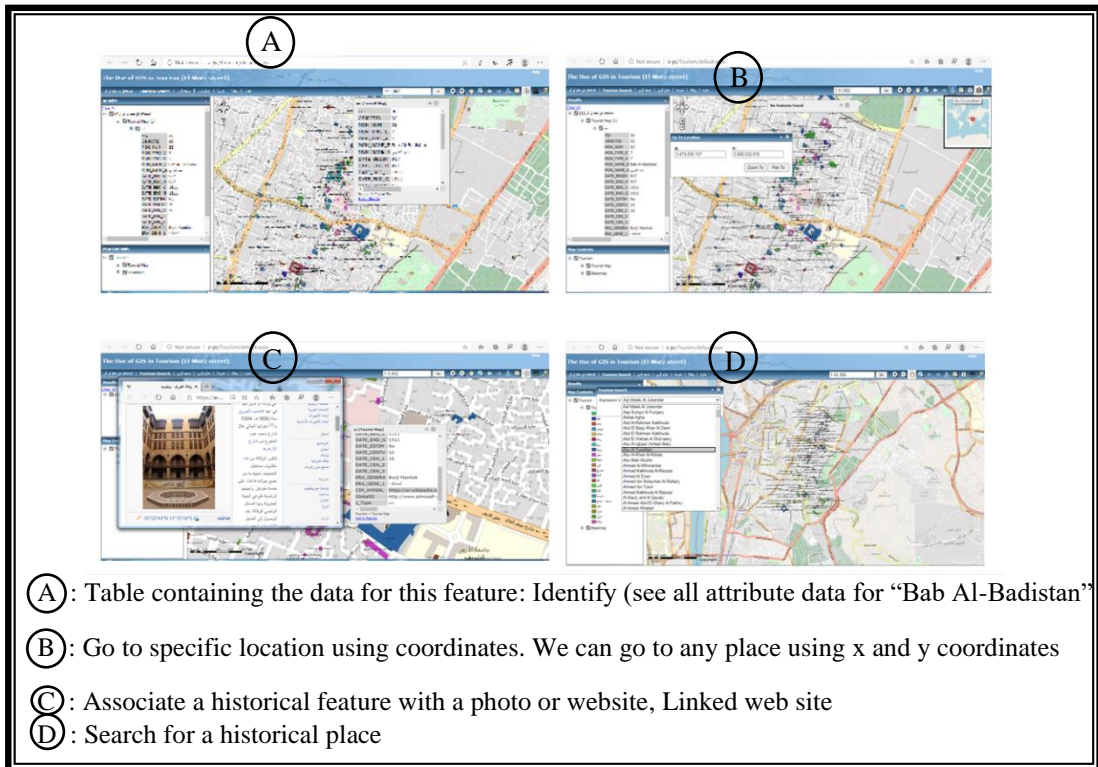


**Fig. 4.** Some advantages of using a GIS on the Internet for Historic Cairo.



**Fig. 5.** Querying for each type of tourist building.

The analysis finds that historical sites of Cairo are not including GIS maps, but only pictures and descriptions of historical signs. Some historical sites of Cairo do not mention the nearest signs and lack in search criteria, therefore, in our future work we aim to improve the WebGIS application by creating better Web/mobile apps to consume the same map and add Graphics and charts for supplementary data statistics in historical data.

## 5. CONCLUSIONS

Contemporary information technology greatly influences the development of tourism on a large-scale, allowing visitors to always stay abreast of the latest tourist details. The role of our webGIS research in Cairo was to promote and stimulate tourism development by designing a tourist map system that contains interactive options and publishing it on the Internet by ARC GIS Server to be a guide that helps visitors to find attractive places in an easy and fast way. Building Web-GIS on the Internet for Historic Cairo represents a better promotion opportunity, because tourism needs to be more globally advertised. This goal can be achieved via the Internet especially using the map and the advantage of GIS capabilities by linking tourist sites and their metadata for the final web design. Historic Cairo might encapsulate a type of exquisite cultural tourism which is now becoming more and more attractive due to the history of the ancient places. This paper is useful for the local communities to better organize and manage their tourism activities. Therefore, a Web-based GIS provides an effective environment for the tourism industry. This article can be very helpful in promoting tourism in Historic Cairo, as tourists planning to visit a particular place can get all the details from the web-based GIS. Web-based GIS constitutes a spatial decision support system based on Geographical visualization approach using GIS technology and a virtual globe browser.

## REFERENCES

- Ahmed, A. (2011) Building a Marketing Information System for Tourism in Al Aqaba Using ARCGIS 9.3 Software. Master thesis-Business Management department. Middle East University.
- Amazon Web Services. (2012) Mapping and Geospatial Analysis in Amazon Web Services Using ArcGIS. [Online]. Available from: [https://media.amazonwebservices.com/AWS\\_ESRI\\_Mapping\\_GeoSpatial\\_Analysis\\_Using\\_ArcGIS.pdf](https://media.amazonwebservices.com/AWS_ESRI_Mapping_GeoSpatial_Analysis_Using_ArcGIS.pdf). [Accessed June 2020].
- Bokrijk. (2020) PLAN YOUR VISIT, Belgium. [Online]. Available from: <https://www.bokrijk.be/nl/plan-je-bezoek/route-parkeren>. [Accessed June 2020].
- Chesapeake Bay Foundation. (2013) Education – Water Quality Collection- Chesapeake Bay Foundation Water Quality Interactive Map. [Online]. Available from: <https://cbforg.maps.arcgis.com/apps/webappviewer>. [Accessed June 2020].
- EPA. (2020) EnviroAtlas Interactive Map, U.S. [Online]. Available from: <https://www.epa.gov/enviroatlas/about-enviroatlas>. [Accessed August 2020].
- Ernawati, N.M., Torpan, A. & Voda, M. (2018) Geomedia role for mountain routes tourism development. Mesehe and PISOIU Waterfall comparative study. *Geographia Technica*, 13 (1), 41-51.
- Euro-t-guide. (2020) European Tourist Guide, Open-Air Museums, [Online]. Available from: [http://www.euro-t-guide.com/See\\_Type/Open\\_Air\\_1.htm](http://www.euro-t-guide.com/See_Type/Open_Air_1.htm). [Accessed August 2020].
- Evic, S. (2004) The potential of Web-based GIS, *Journal of Geographical Systems*. 6(2):79-81.
- Fahim, M. (1996) Urban classification of Cairo between theory and application, analytical study for Cairo- the City and the region. Master thesis in Engineering faculty, Cairo university.
- Geomoose. (2020) Web Client JavaScript Framework, [Online]. Available from: <https://www.geomoose.org>. [Accessed June 2020].

- Geoserver. (2020) What is Geoserver?, [Online]. Available from: <http://geoserver.org/about>. [Accessed July 2020].
- Google Help. (2020) Create or open a map, Google. [Online]. Available from: [https://support.google.com/mymaps/answer/3024454?hl=en&amp%3Bref\\_topic=3188329](https://support.google.com/mymaps/answer/3024454?hl=en&amp%3Bref_topic=3188329). [Accessed June 2020].
- Google Maps. (2020) Create or open a map, [Online]. Available from: [https://support.google.com/mymaps/answer/3024454?hl=en&amp%3Bref\\_topic=3188329](https://support.google.com/mymaps/answer/3024454?hl=en&amp%3Bref_topic=3188329). [Accessed August 2020].
- Google Maps Help. (2020) Create a map in My Maps, Interactive Map for AB-617 Richmond/San Pablo [Online]. Available from: <https://www.google.com/maps/d/viewer?mid=1BQgFqbTLuuAECxpGebhiwzVpK9iIECzH&ll=37.924676943579456%2C-122.4013167072485&z=10>. [Accessed August 2020].
- Gpsmycity. (2020) Cairo's Most Interesting Landmarks Tour (Self Guided), Cairo. [Online]. Available from: <https://www.gpsmycity.com/tours/cairos-most-interesting-landmarks-tour-2479.html>. [Accessed July 2020].
- Gumusay, M. (2004) GIS Design and Application for Tourism. Yildiz Technical University Istanbul, Turkey.
- Gupta, S.K., Negru, R. & Voda, M. (2018) The Indian Himalaya`s unique attributes: Hemkund Sahib and The Valley of Flowers. *Geographia Technica*, 13 (2), 62-73.
- Hashmi, M., (2006) "Explore Hyderabad" An Interactive Web-based GIS Application Prototype. Master`s Thesis in Geoinformatics, Department of Computer and Information Science, Linköpings university, Sweden.
- Ilies, A., Hurley, P.D., Ilies, D.C., & Baias, S. (2017) Tourist animation –a chance adding value to traditional heritage: case studys in the Land of Maramures (Romania). *Rev. de Etnografie și Folclor*, New Series 1-2.
- Kumar, K., & Babu, D. (2016) A Web GIS Based Decision Support System for Agriculture Crop Monitoring System, a case study from Part of Medak District. *Journal of Remote Sensing & GIS*, 5 (4)
- Law, D. (2013) ArcGIS for Server 10.1, Understanding architecture, deployment, and workflows, Special Section, [Online]. Available from: WWW.ESRI.com. [Accessed August 2020].
- Leeds City Council. (2020) [Online]. Available from: <https://southbankleeds.co.uk/map/poi-arts+poi-education+poi-services-structure+poi-leisure-retail+poi-commercial+poi-residential+landmarks-heritage>. [Accessed June 2020].
- Magrini, S. (2018) WebGIS, Cultural Heritage, Preservation, Tourism and the Wiki world: a case study from Emilia Romagna (Italy), *JLIS.it*, 9, 3.
- Mapping Properties. (2021) Egypt Real estate Interactive Map, Cairo Interactive Map, [Online]. Available from: <https://mapping.properties/cairo-map>. [Accessed October 2021].
- Mapserver. (2020) About MapServer [Online]. Available from: <https://mapserver.org>. [Accessed September 2020].
- Marei, L. K. (2012) Revival of Mamluk Architecture in the 19th & 20th centuries, A thesis in Islamic Art and Architecture, Department of Arab and Islamic Civilizations, School of Humanities and Social Sciences, the American university in Cairo.
- Masron, T. Et al. (2014) Conceptualiste Tourism support system through Webgis for collaborative tourism planning, planning Malaysia: *Journal of the Malaysian Institute of planners*, V.XII.
- Masron, T., Marzuki, A., Mohamed, B. & Ayob, N. (2017) Development of a web based GIS for health facilities mapping, monitoring and reporting: A case study of the Zambian Ministry of health. *South African Journal of Geomatics*. 6(3).
- Orchtech. (2021) El-moez, MOBILE APPLICATIONS [Online]. Available from: <https://orchtech.com/case-categories/el-moez>. [Accessed October 2021].
- Osgeo. (2020) Open Source Geospatial Foundation (OSGeo), OSGeo Projects, Web Mapping. [Online]. Available from: <https://www.osgeo.org>[Accessed July 2020].
- PyWPS. (2020) Web Processing Service, [Online]. Available from: <https://pywps.org>. [Accessed August 2020].
- Reed, R. & Bodzin, A. (2016) Using Web GIS for Public Health Education. *international Journal of environmental & science education*, 11 (14).
- Routeyou. (2020) Enjoy the nicest routes. [Online]. Available from: <https://www.routeyou.com/user/planner/81970/limburg-fietsparadijs>. [Accessed July 2020].

- Shi, Y. & Zhang, C. (2013) Tow-dimension display attribute marking of Hainan tourism geographic information based on the web GIS. Presented At: International Conference on Software Engineering and Computer Science (ICSECS).
- Snohomish County. (2020) Planning and Development Services (PDS) Map Portal. [Online]. Available from: <https://snohomishcountywa.gov/3752/PDS-Map-Portal>. [Accessed July 2020].
- Špoljarić, Z. (2019) Web GIS in mountaineering in Croatia, SPECIAL ISSUE – Applied GIS in the context of smart regions and cities. Original paper, *GeoScape* 13(2).
- Tyagi, N. (2014) Web GIS application for customized tourist information system for Eastern U. P., India. *Journal of Geomatics*, 8 (1).
- UNESCO. (1979) International council on monuments and sites (ICOMOS), world heritage list, (cultural Property) ICOMOS technical review Notes, The Secretariat World Heritage Committee, Division of Cultural Heritage, Paris.
- UNESCO. (2012) Urban Regeneration Project for Historic Cairo, UNESCO World Heritage Centre - Management of World Heritage Sites in Egypt, first report of activities, July 2010-June 2012
- UNESCO. (2014) Report of a joint ICOMOS/UNESCO advisory mission to historic Cairo and the pyramid of Djoser, Saqqara, part of the world heritage property of Memphis and its necropolis – the pyramid fields from Giza to Dahshur, Egypt, p.8.
- Viator. (2021) Cairo Tours. [Online]. Available from: <https://www.viator.com/Cairo-tourism>. [Accessed October 2021].
- Victoria State Government. (2020) Cooling and Greening Melbourne Interactive Map, [Online]. Available from: <http://mapshare.maps.vic.gov.au/coolinggreening>. [Accessed July 2020].
- Voda, M. & Montes, Y.S. (2018) Descending mountain routes future: the North Yungas and Fagaras Geosystem`s comparative study. *Geographia Technica*, 13 (2), 152-166.
- Wessel, H., Van, V., Hartleib, J. & Dam, M. (2006) Web-Based GIS-usage in tourism, International Symposium on Geoinformatics for Spatial Infrastructure Development in Earth and Allied Sciences.
- Yao, N., Chen, S., Wang, S. & Yeh, C. (2020) Displaying spatial epistemologies on web GIS: using visual materials from the Chinese local gazetteers as an example, *International Journal of Humanities and Arts Computing*, 14, (1-2), Edinburgh University Press.

## Aims and Scope

**Geographia Technica** is a journal devoted to the publication of all papers on all aspects of the use of technical and quantitative methods in geographical research. It aims at presenting its readers with the latest developments in G.I.S technology, mathematical methods applicable to any field of geography, territorial micro-scalar and laboratory experiments, and the latest developments induced by the measurement techniques to the geographical research.

**Geographia Technica** is dedicated to all those who understand that nowadays every field of geography can only be described by specific numerical values, variables both of time and space which require the sort of numerical analysis only possible with the aid of technical and quantitative methods offered by powerful computers and dedicated software.

Our understanding of **Geographia Technica** expands the concept of technical methods applied to geography to its broadest sense and for that, papers of different interests such as: G.I.S, Spatial Analysis, Remote Sensing, Cartography or Geostatistics as well as papers which, by promoting the above mentioned directions bring a technical approach in the fields of hydrology, climatology, geomorphology, human geography territorial planning are more than welcomed provided they are of sufficient wide interest and relevance.

### Targeted readers:

The publication intends to serve workers in academia, industry and government. Students, teachers, researchers and practitioners should benefit from the ideas in the journal.

## Guide for Authors

### Submission

Articles and proposals for articles are accepted for consideration on the understanding that they are not being submitted elsewhere.

The publication proposals that satisfy the conditions for originality, relevance for the new technical geography domain and editorial requirements, will be sent by email to the address [editorial-secretary@technicalgeography.org](mailto:editorial-secretary@technicalgeography.org).

This page can be accessed to see the requirements for editing an article, and also the articles from the journal archive found on [www.technicalgeography.org](http://www.technicalgeography.org) can be used as a guide.

### Content

In addition to full-length research contributions, the journal also publishes Short Notes, Book reviews, Software Reviews, Letters of the Editor. However the editors wish to point out that the views expressed in the book reviews are the personal opinion of the reviewer and do not necessarily reflect the views of the publishers.

Each year two volumes are scheduled for publication. Papers in English or French are accepted. The articles are printed in full color. A part of the articles are available as full text on the [www.technicalgeography.org](http://www.technicalgeography.org) website. The link between the author and reviewers is mediated by the Editor.

### Peer Review Process

The papers submitted for publication to the Editor undergo an anonymous peer review process, necessary for assessing the quality of scientific information, the relevance to the technical geography field and the publishing requirements of our journal.

The contents are reviewed by two members of the Editorial Board or other reviewers on a simple blind review system. The reviewer's comments for the improvement of the paper will be sent to the corresponding author by the editor. After the author changes the paper according to the comments, the article is published in the next number of the journal.

Eventual paper rejections will have solid arguments, but sending the paper only to receive the comments of the reviewers is discouraged. Authors are notified by e-mail about the status of the submitted articles and the whole process takes about 3-4 months from the date of the article submission.

Indexed by: **CLARIVATE ANALYTICS**  
**SCOPUS**  
**GEOBASE**  
**EBSCO**  
**SJR**  
**CABELL**

**ISSN: 1842 - 5135 (Print)**  
**ISSN: 2065 - 4421 (Online)**

